Neuropeptidergic Inhibition of Pain Transmission

by

Tyler Scott Nelson

Bachelor of Science and Bachelor of Arts, Wofford College, 2016

Submitted to the Graduate Faculty of the

School of Medicine in partial fulfillment

of the requirements for the degree of

Doctor of Philosophy

University of Pittsburgh

2022

UNIVERSITY OF PITTSBURGH

SCHOOL OF MEDICINE

This dissertation was presented

by

Tyler Scott Nelson

It was defended on

August 11, 2022

and approved by

Dr. Rebecca P. Seal, PhD, Associate Professor, Department of Neurobiology, School of Medicine

Dr. Kathryn M. Albers, PhD, Professor, Department of Neurobiology, School of Medicine

Dr. Kimberly Howard-Quijano, MD, MS, FASE, Associate Professor, Department of Anesthesiology and Perioperative Medicine, School of Medicine

Dr. H. Richard Koerber, PhD, Professor, Department of Neurobiology, School of Medicine

Dr. Hanns Ulrich Zeilhofer, MD, Professor, Department of Pharmacology, Institute of Pharmacology and Toxicology

Dissertation Director: Dr. Bradley K. Taylor, PhD, Professor, Department of Anesthesiology and Perioperative Medicine, School of Medicine

Neuropeptidergic Inhibition of Pain Transmission

Tyler Scott Nelson, PhD

University of Pittsburgh, 2022

In the following dissertation, I present data implicating glutamatergic dorsal horn interneurons expressing the inhibitory G protein-coupled neuropeptide Y Y1 receptor (Y1-INs) in the development and maintenance of neuropathic pain. Neuropathic pain is a debilitating form of chronic pain that arises from a lesion or disease affecting the somatosensory system. Many symptoms of neuropathic pain are hypothesized to result from a loss of spinal cord dorsal horn inhibition and/or a gain in dorsal horn excitation that allow innocuous peripheral inputs to be perceived as painful. Thus, promising future pharmacological agents may dampen maladaptive spinal excitatory signaling.

One promising therapeutic candidate is neuropeptide Y (NPY) which exhibits long-lasting inhibitory control of spinal nociceptive transmission after injury, primarily through NPY-Y1 receptor signaling. However, NPY Y1 receptors are found on Y1-INs, and NPY Y1 and Y2 receptors are expressed on the central terminals of primary afferent neurons arising from the dorsal root ganglion. This dual expression complicates the interpretation of the specific site of anti-nociceptive action for NPY. Thus, a major goal of this thesis was to clarify the specific site(s) of intrathecal NPY that mediate anti-hyperalgesia in rodent models of neuropathic pain.

In this dissertation I detail an extensive pre-clinical research history supporting spinally-directed NPY Y1 agonists as a promising therapeutic for chronic pain. I demonstrate that Y1-INs

are necessary and sufficient for the behavioral signs of neuropathic pain. Additionally, I use single cell RNA-sequencing data in combination with fluorescence *in situ* hybridization to segregate Y1-INs into three distinct dorsal horn interneuron subpopulations and I demonstrate the conservation of these subpopulations across the murine, rhesus macaque, and human spinal cord dorsal horns. I also utilize genetic tools in combination with in *vivo* behavior to show that the *Grp*/*Npy1r*-expressing subpopulation specifically is necessary for the manifestation of neuropathic pain. Finally, I present how endogenous spinal NPY Y1 receptor signaling can synergistically work with mu opiate receptor signaling to maintain postoperative pain in remission. Together, these observations increase our understanding of how nerve injury increases the excitability of Y1-INs and provide rationale for targeting spinal Y1-INs as a novel approach to treat neuropathic pain.

Table of Contents

List of Tables

List of Figures

Preface

In the following dissertation, I examine the role of neuropeptides and neuropeptide receptor-expressing neurons and their ability to inhibit the pre-clinical behavioral signs of chronic pain in rodent models. I predominately focus on the endogenous neuropeptide, neuropeptide Y (NPY), and its ability to inhibit the behavioral signs of chronic neuropathic pain when applied to the spinal cord via acting at its' cognate Y1 receptor.

Chapter 1 is largely based on a review article focusing on the extensive pre-clinical research history of spinal neuropeptide Y and Y1 signaling in both pain and itch that I published in *Progress in Neurobiology* in 2021 (Nelson and Taylor, 2021).

Chapter 2 is a research manuscript focusing on the role of spinal Y1 receptor-expressing interneurons (Y1-INs) in the development of neuropathic pain in rats that I published in *Scientific Reports* in 2019 (Nelson et al., 2019).

Chapter 3 is a research manuscript focusing on NPY Y1-selective spinal pharmacology and the characterization/modulation of spinal cord dorsal horn Y1-INs in a mouse model of neuropathic pain that is currently in revision at *Proceedings of the National Academy of Sciences* (Nelson et al., 2022).

Chapter 4 is a research manuscript focusing on the characterization of Y1-IN subtypes, their role in a mouse model of neuropathic pain, and the conservation of Y1-IN subtypes across

higher-order mammalian species that is currently in preparation for submission to *Proceedings of the National Academy of Sciences*.

Chapter 5 is a research manuscript focusing on a potent and long-lasting endogenous synergy between mu opiate receptor and NPY Y1 receptor signaling that persists to maintain chronic postoperative pain in remission that is currently under review at *PNAS NEXUS*.

Appendix A contains a *Journal Club* article that I published in *The Journal of Neuroscience* highlighting a research manuscript focusing on mechanical allodynia (Nelson, 2019).

Appendix B details a collaborative study where I inhibited downstream NPY Y1 signaling pathways to reinstate the behavioral signs of inflammatory pain that is published in *PAIN* (Fu et al., 2019).

Appendix C details a study where I performed NPY Y2-selective spinal pharmacology in a mouse model of neuropathic pain that is part of a larger study in preparation for submission.

Appendix D details a collaborative study where I performed pharmacological and chemogenetic inhibition of the parabrachial nucleus Y1 receptor-expressing neuron population in a mouse model of neuropathic pain.

Acknowledgements

I have many special people to thank for reaching this accomplishment. First and foremost, I would like to express special appreciation and gratitude to my advisor, Dr. Bradley Taylor. He has been an exceptional mentor who has truly fostered and witnessed my growth as a scientist. He created a laboratory environment where any study I wanted to complete (no matter how difficult the mouse/reagent/tissue/technique was to obtain), I could complete the study. He allowed me true freedom to explore my research interests, take new leaps, and pursue my passions; for this I will be forever grateful. Additionally, he helped me tremendously with scientific writing and I believe this has and will continue to enhance my scientific growth. I feel that with what I have learned/gained under his tutelage, I am well-prepared to move forward into the next stage of my scientific journey. I look forward to instilling the same principles that which he has taught me into the future generations of scientists.

I want to extend a special thank you to the members of my dissertation committee: Drs. Rebecca Seal, Kathryn Albers, Kimberly Howard-Quijano, H. Richard Koerber, and Hanns Ulrich Zeilhofer. They all have generously donated significant amounts of time, energy, and guidance to facilitate my scientific growth as well as contribute to the preparation and review of this dissertation. Each of these researchers has facilitated my career development, improved my confidence as a researcher, and improved my conceptual understanding of science, neurobiology, and pain research. Truly, I am extremely grateful of your support, mentorship, and time that you have allotted to me.

In addition to my committee, I would also like to thank my Pittsburgh (and global!) colleagues, friends, mentors, and research collaborators, that without which, this thesis could never have been possible. The Center for Neuroscience and Pittsburgh Center for Pain Research has been an amazing environment to complete my graduate training in and I have made lifelong friends and colleagues. I especially want to thank members of the Taylor Laboratory (past and present!) who have helped me every single day to reach this milestone. In particular, Drs. Diogo Santos, Ghanshyam Sinha, Pranav Prasoon, and Yanmei Qi helped me to reach this milestone through their persistent comradery, willingness to teach, and genuine friendships. I am privileged to have had the opportunity to learn from and work alongside every single one of you. I have also been fortunate to have never-ending friendship, research assistance, and emotional support from Nina Gakii, Sydney Lamerand, and Abigail Hellman. You three are among my closest friends and I will miss all of you so much. I will forever cherish this time we had together in Pittsburgh.

Finally, I want to thank my family for all they have done. Specifically, I want to thank my Grandpap, Ronald Sivak, who has been my biggest cheerleader throughout this academic journey. His persistent curiosity and generosity are qualities I will forever strive to emulate. I also need to extend my deepest gratitude to my partner, Dr. Heather Allen, and our four fur babies, Sophie, Zig, Nadia, and Possum. Heather has had never-wavering encouragement for my academic dreams since we were undergraduate Biology students together at Wofford College in Spartanburg, SC. Somehow, she still isn't tired of me talking about science late into the evening, on a Saturday or Sunday morning, or even during a vacation. She has traveled the world with me, navigated the ups and downs of pursuing higher education in neuroscience with me, and fully supported every project/grant/job/dream that I have wanted to chase. She is my greatest gift, my best friend, and I

am so happy that I was able to complete this dissertation alongside her. Thank you infinitely for your love and support. I look forward to all of the future adventures we have yet to embark upon. Lastly, but most importantly, this thesis could have in no way been accomplished without the undying love of my four fur children. Exploring, around beautiful Western Pennsylvania with Sophie and Possum has helped me maintain my sanity (just a little bit) during this dissertation process. Additionally, our perfect cat children, Nadia and Zig, have both provided countless snuggles and happy purrs during all my late-night writing sessions. These four are always the happiest to see me and I would do anything for each of them.

To all of you, thank you tremendously for **everything** you have done to help me reach this day.

1.0 Introduction and background

1.1 Introduction and overall hypothesis

Nociceptor activation normally provides a protective function that can reduce tissue damage in the face of potentially hazardous stimuli. However, after tissue damage occurs, pathological changes within peripheral or central neurons can lead to chronic pain (Gold and Gebhart, 2010; Kuner, 2010; Latremoliere and Woolf, 2009). Chronic pain conditions place significant burdens on patients, their families, and society by reducing quality of life and creating enormous financial consequences that total more than 630 billion USD annually for the United States of America alone (Gaskin and Richard, 2012; Henschke et al., 2015). One particularly debilitating form of chronic pain is neuropathic pain that arises from a lesion or disease affecting the somatosensory system (Costigan et al., 2009; Finnerup et al., 2021; Jensen and Finnerup, 2014). The median population prevalence rate for neuropathic pain is 9.4% (Van Hecke et al., 2014). Neuropathic pain presents as spontaneous pain (non-stimulus evoked), hyperalgesia (a noxious stimulus evokes more pain than prior applications of the same stimulus), and/or allodynia (a non-noxious stimulus evokes a pain response) (Colloca et al., 2017).

Interneurons in the dorsal horn of the spinal cord receive direct inputs from primary afferents in the periphery that respond to both noxious and innocuous stimuli (Moehring et al., 2018). The incoming afferent information is processed by complex dorsal horn microcircuits involving inhibitory and excitatory interneurons before being transmitted via projection neurons to several higher-order brain areas (Peirs and Seal, 2016; Todd, 2010). The heterogeneous spinal

cord interneuron populations/microcircuits are essential for processing peripheral sensory input, and changes in their integration/signaling result in sensory dysfunctions such as allodynia (Benarroch, 2016; Lolignier et al., 2014; Moehring et al., 2018; Todd, 2010). Thus, maladaptive spinal signaling is hypothesized to be the underlying cause of varying forms of chronic pain and in particular neuropathic pain (Peirs et al., 2021, 2020; Peirs and Seal, 2016; Woolf and Salter, 2000). Consequently, the dorsal horn spinal cord interneurons represent a promising target for the development of novel pain therapeutics.

Excitatory and inhibitory dorsal horn interneurons process somatosensory input and the balance between the two determines the net outflow of pain signals from neurons projecting to the brain (Koch et al., 2018). In neuropathic pain, loss of dorsal horn inhibition allows the propagation of low threshold innocuous touch inputs to be perceived as painful (Lu et al., 2013; Miracourt et al., 2007; Petitjean et al., 2015; Schoffnegger et al., 2008). However, the excitatory interneurons that propagate the innocuous inputs as painful following nerve injury remain to be determined. Multiple populations of excitatory interneurons may mediate neuropathic pain (Peirs et al., 2021, 2020; Todd, 2017), but few represent readily druggable pharmaceutical targets. One promising exception is an excitatory subpopulation that express the G_i protein-coupled Y1 receptor for neuropeptide Y (NPY) (Diaz-delCastillo et al., 2018).

A rich and growing body of preclinical evidence implicates spinal NPY, acting via its cognate Y1 and Y2 receptors, in the potent inhibition of chronic pain (Brumovsky et al., 2007; Diaz-delCastillo et al., 2018; Hökfelt et al., 2007; Smith et al., 2007). *In vitro* quantitative receptor autoradiography demonstrates the highest density of NPY binding sites in superficial laminae I-II

of the dorsal horn (Kar and Quirion, 1992), a key relay of noxious sensations from the periphery to the brain. The antinociceptive actions of NPY may be occurring via targeting Y1 receptor-expressing interneurons (Y1-INs) that are an abundant subpopulation of interneurons in laminae I-II of the dorsal horn (Brumovsky et al., 2007, 2006), the central terminals of Y1 receptor-expressing peptidergic primary afferents (Taylor et al., 2014; Zhang et al., 1994), or the central terminals of Y2 receptor-expressing small-to-medium sized, peptidergic, thinly myelinated, putative A-nociceptor primary afferents (Brumovsky et al., 2005).

This dissertation tests the hypothesis that exogenous or endogenous spinal neuropeptide Y potently inhibits the behavioral signs of chronic pain via inhibiting pain facilitatory Y1 receptor-expressing dorsal horn interneurons.

1.2 Brief overview of spinal pain circuitry implicated in neuropathic pain

A hallmark of pathological pain stemming from nerve injury is pain experienced in response to light mechanical touch, clinically referred to as mechanical allodynia or touch-evoked pain (Lolignier et al., 2014). Changes in the spinal cord dorsal horn microcircuitry are strongly implicated as the underlying cause of mechanical allodynia (Peirs et al., 2020; Peirs and Seal, 2016). Within the dorsal horn, a laminar architecture largely segregates noxious and innocuous sensory inputs (Rexed, 1952). High threshold C and Aδ-fibers that transmit noxious inputs, itch, and temperature synapse in superficial laminae I-II in the dorsal horn. Conversely, low threshold C and Aδ-fibers transmitting aspects of touch largely synapse in inner lamina II-III, while innocuous touch A-fibers largely synapse in inner laminae II-IV. Therefore, superficial dorsal horn is primarily involved in the processing and transmission of noxious inputs, while inner laminae II-IV process innocuous inputs or aspects of touch, denoting this region the low-threshold mechanosensor-recipient zone (LTMR-RZ) (Moehring et al., 2018) (**Figure 1**). However, following peripheral nerve injury, pathological changes within the dorsal horn allow innocuous inputs to the LTMR-RZ to be propagated to the superficial dorsal horn and ultimately be perceived as noxious.

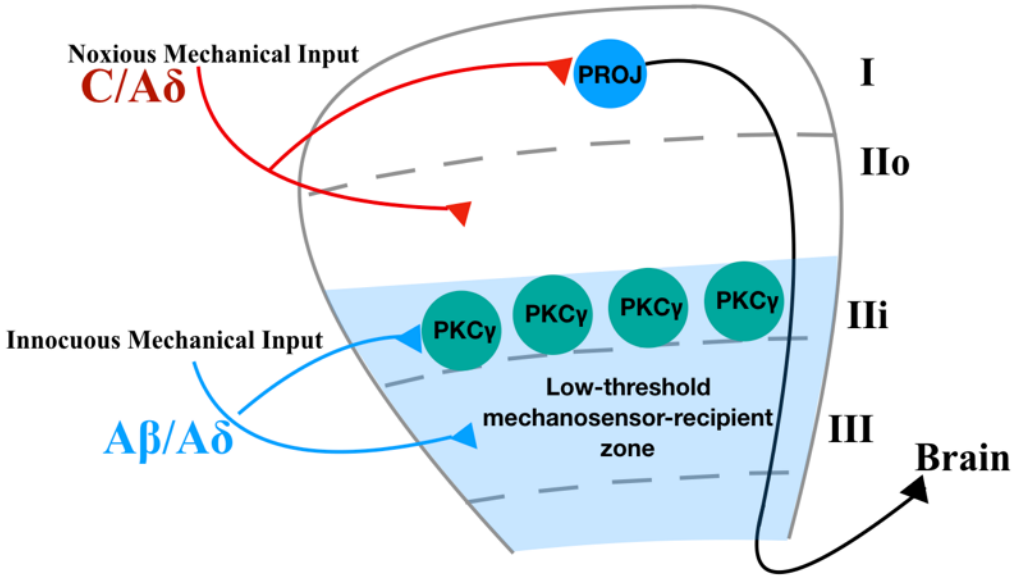

Figure 1. General organization of pain and touch circuitry in the spinal cord

Inner lamina II through lamina IV represents the low-threshold mechanosensory recipient zone (LTMR-RZ) shown in light blue. PKCγ interneurons are found in a dense band in inner lamina II at the boundary between the LTMR-RZ and superficial lamina that receive, modulate, and transmit noxious stimuli.

Input from low threshold mechanoreceptors does not excite nociceptive projection neurons in lamina I. Aβ activation in slices from naïve rats remains confined to the LTMR-RZ, but following spared nerve injury (SNI), excitation spreads to the superficial dorsal horn (Schoffnegger et al., 2008). This spread of innocuous touch input into superficial dorsal horn is believed to be mediated through a loss of inhibition in the spinal cord as bath applications of $GABA_A$ and glycine receptor antagonists in slices from naïve rats is sufficient to reproduce the spread of excitation into superficial dorsal horn (Schoffnegger et al., 2008). Further evidence for the loss of inhibition mediating allodynia stems from ablation or inhibition of dynorphin, glycine, parvalbumin, and neuropeptide Y inhibitory neuron populations in the dorsal horn, all of which are able to induce tactile allodynia (Duan et al., 2014; Foster et al., 2015; Petitjean et al., 2015; Tashima et al., 2021). Pharmacologically-mediated glycinergic disinhibition is also sufficient to

induce spikes and cFos activation in superficial laminae of the dorsal horn in response to Aβ-fiber range stimuli (Miracourt et al., 2007). At the boundary between the LTMR-RZ and the superficial dorsal horn, Fos positive cells colocalize with neurons immunoreactive for protein kinase C γ (PKCγ), implicating PKCγ interneurons in the transmission of innocuous input to nociceptive projection neurons (**Figure 1**) (Neumann et al., 2008; Peirs et al., 2015). Intracisternal administration of a selective PKCγ inhibitor prevents both behavioral mechanical allodynia and superficial Fos activation in animals with glycinergic disinhibition (Miracourt et al., 2007), and intrathecal PKCγ inhibitors also attenuate SNI-induced mechanical allodynia (Peirs et al., 2021; Petitjean et al., 2015).

PKCγ interneurons are primarily found in a dense band within inner lamina II of the dorsal horn and are activated by innocuous but not noxious stimuli (Neumann et al., 2008; Polgár et al., 1999). Paired neural recordings demonstrate that PKCγ interneurons undergo strong glycinergic feedforward inhibition in response to dorsal root stimulation at C, Aδ, and Aβ fiber input ranges (Lu et al., 2013). However, following peripheral nerve injury, this feedforward inhibition is lost and activation at each of C, Aδ, and Aβ fiber inputs produces EPSPs in both PKCγ interneurons as well as in paired transient central cells superficial to the PKCγ interneurons (Lu et al., 2013; Wang et al., 2020). Transient central cells are excitatory neurons in lamina II that receive direct C fiber input and can activate vertical cells, which in turn can activate pain projection neurons in lamina I (Lu and Perl, 2005). One potential source for the loss of feedforward inhibition is the loss of parvalbumin-positive inhibitory synaptic appositions onto PKCγ interneurons that has been found following SNI (Petitjean et al., 2015). Furthermore, pharmacological inhibition of PKCγ attenuates tactile allodynia after SNI as well as the induction of Fos in superficial laminae after

light mechanical stimulation (Peirs et al., 2021; Petitjean et al., 2015). Thus, it is hypothesized that loss of feedforward inhibition onto PKCγ interneurons opens a "gate" and permits innocuous input to be propagated throughout the nociceptive circuitry, and consequently, selective inhibition of PKCγ attenuates both behavioral and immunohistochemical markers of tactile allodynia following nerve injury.

Models of the spinal neural circuit for allodynia include propagation of low threshold mechanosensory information from disinhibited PKCγ interneurons, to transient central cells, to vertical cells, and then to NK1R projection neurons (Peirs and Seal, 2016; Todd, 2017) (**Figure 2**). While the vertical cell population has recently been denoted as interneurons that express the gastrin releasing peptide receptor (Polgár et al., 2022), the identity of transient central cells remains unknown, The transient central cell population likely involves a subset of somatostatin-expressing excitatory interneurons as their ablation causes loss of mechanical pain (Duan et al., 2014). One population of transient central cells has been identified that expresses gastrin releasing peptide but this population is hypothesized to be involved in itch and not pain (Albisetti et al., 2019; Dickie et al., 2019). Peirs et al. have identified the calretenin interneurons as a candidate transient central cell population based on the fact that chemogenetic activation of dorsal horn calretenin interneurons produces mechanical allodynia (Peirs et al., 2015). However, neuronal activity (Fos immunohistochemistry) and behavioral analyses demonstrate that calretenin interneurons play a larger role in inflammatory mechanical allodynia than neuropathic injury-mediated mechanical allodynia (Peirs et al., 2015), and calretenin firing patterns in response to current injection do not match well with the transient firing type (Smith et al., 2015). Excitatory interneurons that express the neuropeptide Y1 receptor are one likely candidate transient central cell population as their

firing pattern in response to current injection closely matches the transient type (Sinha et al., 2021), and we have recently implicated this population as necessary for the manifestation of peripheral nerve injury-induced mechanical allodynia (Nelson et al., 2019). In conclusion, more research is needed to identify the excitatory interneuron populations that connect low threshold mechanoreceptors with lamina I projection neurons to propagate nerve injury-induced allodynia.

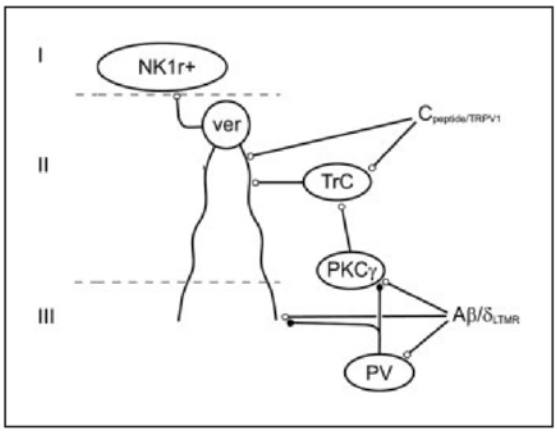

Figure 2. A diagram of the mechanical allodynia circuitry.

Myelinated low-threshold afferent A fibers synapse in the LTMR-RZ. A feedforward circuit involving inhibitory parvalbumin and glycinergic interneurons normally prevents activation of PKCγ interneurons by the A fibers, however, following peripheral nerve injury this feedforward inhibition is lost. A dorsally-directed polysynaptic circuit allows activation of PKCγ interneurons, transient central cells, vertical cells, and lamina I projection neurons by low-threshold mechanosensory afferent input. This schematic is taken from (Todd, 2017) and largely based on the work of (Grudt and Perl, 2002; Lu et al., 2013).

1.3 Neuropeptide Y receptor anatomy and physiology in the dorsal root ganglion and dorsal horn of the spinal cord

Neuropeptide Y (NPY) is a 36 amino acid peptide first described in 1982 (Tatemoto et al., 1982). It is highly expressed throughout the body and regulates a wide variety of physiological processes that include food intake, emotional regulation, and cardiovascular function (Brothers and Wahlestedt, 2010). Most species express at least 4 of the different receptor subtypes that bind NPY: Y1, Y2, Y4, and Y5. All NPY receptor subtypes are G_i protein-coupled receptors, so NPY agonists decrease the production of cyclic adenosine monophosphate (cAMP) thus dampening intracellular signaling (Brothers and Wahlestedt, 2010; Brumovsky et al., 2007). NPY receptors are located in the spinal cord across a wide variety of species, including humans (Allen et al., 1984; Gibson et al., 1984). *In vitro* quantitative receptor autoradiography demonstrates the highest density of NPY binding sites in superficial laminae I-II of the dorsal horn (Kar and Quirion, 1992), a key relay of noxious sensations from the periphery to the brain. Evidence suggests that only Y1 and Y2 receptor expression is found at the spinal level (Brumovsky et al., 2007; Diaz-delCastillo et al., 2018; Hökfelt et al., 2007; Smith et al., 2007).

1.3.1 Expression of NPY receptors in the dorsal root ganglion

Y1 receptor expression is found in the somatic plasmalemma of small, unmyelinated, calcitonin gene-related peptide (CGRP)-expressing, peptidergic neurons in the dorsal root ganglion (DRG) (Taylor et al., 2014; Zhang et al., 1994). Y1 and CGRP are co-expressed extensively in the DRG soma, and it is becoming increasingly apparent that Y1 is trafficked to central terminals in the dorsal horn only to a limited degree. First, CGRP-positive primary afferent terminals rarely (if-ever) co-express Y1 receptor-like immunoreactivity in the substantia

gelatinosa (Brumovsky et al., 2002; Taylor et al., 2014; Zhang et al., 1994); this could be due to extremely sparse expression or limitations in currently available detection tools. Second, despite the clear finding that sciatic nerve ligation robustly downregulates Y1 receptor expression in the DRG and slightly alters Y1 expression in the dorsal horn (proposed to be an effect on Y1-INs and not central terminals) (Brumovsky et al., 2004), other forms of peripheral nerve injury, including dorsal rhizotomy, sciatic nerve transection, or spared nerve injury, cause little to no change in Y1 immunoreactivity in the superficial dorsal horn (Nazli and Morris, 2000; Nelson et al., 2019; Zhang et al., 1994). Thus, it seems that Y1 expression is robust in the soma of CGRP-expressing DRG neurons but minimal at their central terminals. This is consistent with the idea that NPY acts at Y2 rather than Y1 receptors on the central terminals of primary afferents to inhibit SP release (Duggan et al., 1991) and electrical stimulus-evoked EPSCs (Moran et al., 2004).

Y2 receptor-like immunoreactivity is found in approximately 10% of rat lumbar DRG neurons, most of which are small-to-medium sized, peptidergic, thinly myelinated, putative A-nociceptors (Brumovsky et al., 2005). In support of this characterization, an $Npy2r^{ChR2}$ mouse line found the majority (75%) of ChR2 expression in lumbar DRG neurons that co-express neurofilament- heavy polypeptide (Nefh), a marker of myelinated neurons, CGRP, and the nerve growth factor receptor TRKA, a peptidergic nociceptor marker, altogether indicating that Y2 neurons are a population of A-fibers that mediate pain (Arcourt et al., 2017). However, an earlier characterization of an $Npy2r^{eGFP}$ mouse line found eGFP-positive afferents that formed lanceolate endings around hair follicles: this is characteristic of rapidly adapting, low-threshold, Aß-mechanoreceptors that mediate light touch somatosensation (Li et al., 2011). This discrepancy is now partially resolved with a comprehensive analysis of *Npy2r*-expressing DRG neurons from

three separate single-cell RNA sequencing gene expression datasets. These datasets demonstrate that *Npy2r* is expressed in 90% of *Nppb/Sst* neurons (implicated in the transduction of histaminergic itch), 38% of all Aδ-nociceptors, and 17% of all C-nociceptors; less than 10% *Npy2r* expression is detected in other cell types including Aß-mechanoreceptors (Ma et al., 2020). Together, these results indicate that Y2 receptors are most heavily expressed in small, peptidergic, thinly myelinated, A-fiber nociceptors that contribute to pain (Chen et al., 2019) and unmyelinated *Nppb*/*Sst* afferents implicated in itch (Huang et al., 2018; Ma et al., 2020).

1.3.2 Localization of Y1-INs and NPY receptors in the spinal cord

To date, at least seven distinct populations of Y1-INs have been identified in the rat lumbar spinal cord (for a more detailed review see (Brumovsky et al., 2007, 2006)), the most abundant of which are referred to as Type 1 Y1-INs (Brumovsky et al., 2006). Type 1 Y1-INs are densely packed within the superficial dorsal horn, particularly in outer lamina II (Brumovsky et al., 2006; Hökfelt et al., 2007). In rat, Y1-INs do not colocalize with the PKCγ interneurons that demarcate the lamina II-III border but instead lie in a tight band just dorsal to them (Nelson et al., 2019). Brumovsky and Hökfelt's comprehensive analysis of Y1 immunolabeling in the dorsal horn of the rat awaits replication in the mouse.

The vast majority of Y1-INs in outer lamina II are small, fusiform-like shaped, bipolar cells with dendrites extending in the rostral-caudal but not dorsal-ventral axes (Brumovsky et al., 2006). Of the five morphological classes of lamina II interneurons described by Grudt and Perl (Grudt and Perl, 2002), we note that Y1-IN morphology closely matches the "central cell" class. Central cells are restricted to lamina II with a fairly dense dendritic arbor that extends moderately in the

rostral-caudal direction and limited dorsal-ventral branching. Additionally, a central cell (and fusiform)-like morphology was noted for ~2/3 of identified lamina II Y1-Cre lineage neurons in the mouse (Acton et al., 2019). Finally, electrophysiological recordings found the majority of neurons that responded to NPY application exhibited a morphology characteristic of central or radial cells (~77%) and only rarely exhibited the morphological characteristics of vertical cells (~8%) (Melnick, 2012). Taken together, these data indicate that most Y1-INs in lamina II of the dorsal horn demonstrate a central cell-like morphology.

Y2 receptors are rarely detected in spinal cord interneurons, as: 1) Y2 receptor-like immunoreactivity in the dorsal horn is restricted to central terminals and never colocalizes with a somatic marker (Brumovsky et al., 2005); 2) dorsal rhizotomy completely eliminates the expression of Y2 receptor immunoreactivity in the dorsal horn (Brumovsky et al., 2005); 3) $Npy2r^{eGFP}$ BAC transgenic mice express minimal to no adult GFP expression in the dorsal horn (GENSAT, Stock No: 011016-UCD); and 4) a single cell RNAseq analysis of the dorsal horn reported only a very sparse (and possibly insignificant or nonexistent) expression of *Npy2r* in the GABA10 subpopulation of GABAergic interneurons (Häring et al., 2018). This extremely sparse expression of Y2 in dorsal horn neurons is in stark contrast to the robust expression of Y1 on Y1-INs.

1.3.3 Neurophysiological responses of superficial dorsal horn neurons to NPY receptor agonists

Whole cell recordings in the rat spinal cord slice consistently indicate that bath application of NPY inhibits both presynaptic and postsynaptic components of excitatory neurotransmission in the dorsal horn (**Table 1**). Interrogation of presynaptic mechanisms with voltage-clamp recordings revealed that Y2- but not Y1-selective agonists inhibit the frequency but not amplitude of TTX-resistant miniature excitatory postsynaptic currents (mEPSCs) (Moran et al., 2004); likewise, Y2 but not Y1-selective antagonists blocked the ability of NPY itself to inhibit mEPSC frequency (Melnick, 2012; Moran et al., 2004). Also indicative of a presynaptic action was the ability of NPY to change paired-pulse ratio (Moran et al., 2004). However, further studies are needed in molecularly and/or morphologically identified neurons, as one study could not confirm presynaptic effects of NPY on mEPSCs, possibly due to the tremendous heterogeneity of unclassified substantia gelatinosa neurons (Miyakawa et al., 2005). Further studies are needed to profile subsets of Y1-INs based on molecular, morphological, and/or electrophysiological characteristics. One exciting approach uses transgenic reporter mice to better elucidate intrinsic and evoked firing patterns and perhaps reveal functionally distinct subclasses of Y1-INs. Such an approach has been used to study calretinin-, substance P, and GRP -expressing interneuron populations in the dorsal horn, for example ((Dickie et al., 2019; Smith et al., 2015)). Albeit, the current consensus is that Y2 inhibition of presynaptic boutons reduces the release of pronociceptive neurotransmitters (Smith et al., 2007). This is most likely from the central terminals of primary afferent neurons, as Y2 expression has not been found on local interneurons or the terminals of supraspinal neurons (see **1.1.2**).

In stark contrast to the view that Y2 mediates the ability of NPY to presynaptically inhibit central terminals, the prevailing view is that Y1 mediates the ability of NPY to postsynaptically inhibit spinal interneurons. Bath administration of NPY or the Y1 receptor-specific agonist [Leu^{31},Pro^{34}]-NPY consistently produced an outward current and membrane hyperpolarization in spinal interneurons that can be blocked with Y1 but not Y2 antagonists (Melnick, 2012; Miyakawa et al., 2005; Sinha et al., 2021). The NPY-induced outward current was blocked with either barium ions or cesium ions + TEA, consistent with activation of K+ channels (Melnick, 2012; Miyakawa et al., 2005). The NPY current was also blocked with GDP-β-S (Melnick, 2012; Miyakawa et al., 2005), and current-voltage curves revealed that NPY generated inward rectification in some neurons (Miyakawa et al., 2005; Moran et al., 2004), suggesting an NPY-mediated activation of G_i-protein coupled inwardly rectifying K+ (GIRK) channels. However, NPY activated an inwardly rectifying potassium conductance in only a subset (26%) of cells (Moran et al., 2004); the low percentage may reflect the fact that recordings were conducted in unidentified neurons that may or may not express Y1. Therefore, it is through GIRK channels that NPY is thought to hyperpolarize excitatory Y1-INs and thus block action potential discharge, leading to the occlusion of spinal transmission of nociceptive signals from the central terminal of primary afferent neurons. Further evidence for this comes from voltage-clamp studies showing that NPY inhibits eEPSCs and dorsal root stimulation-evoked action potentials (Miyakawa et al., 2005; Moran et al., 2004; Sinha et al., 2021). These data provide the framework for the simplest and most prominent postsynaptic mechanism of NPY analgesia (**Figure 3**).

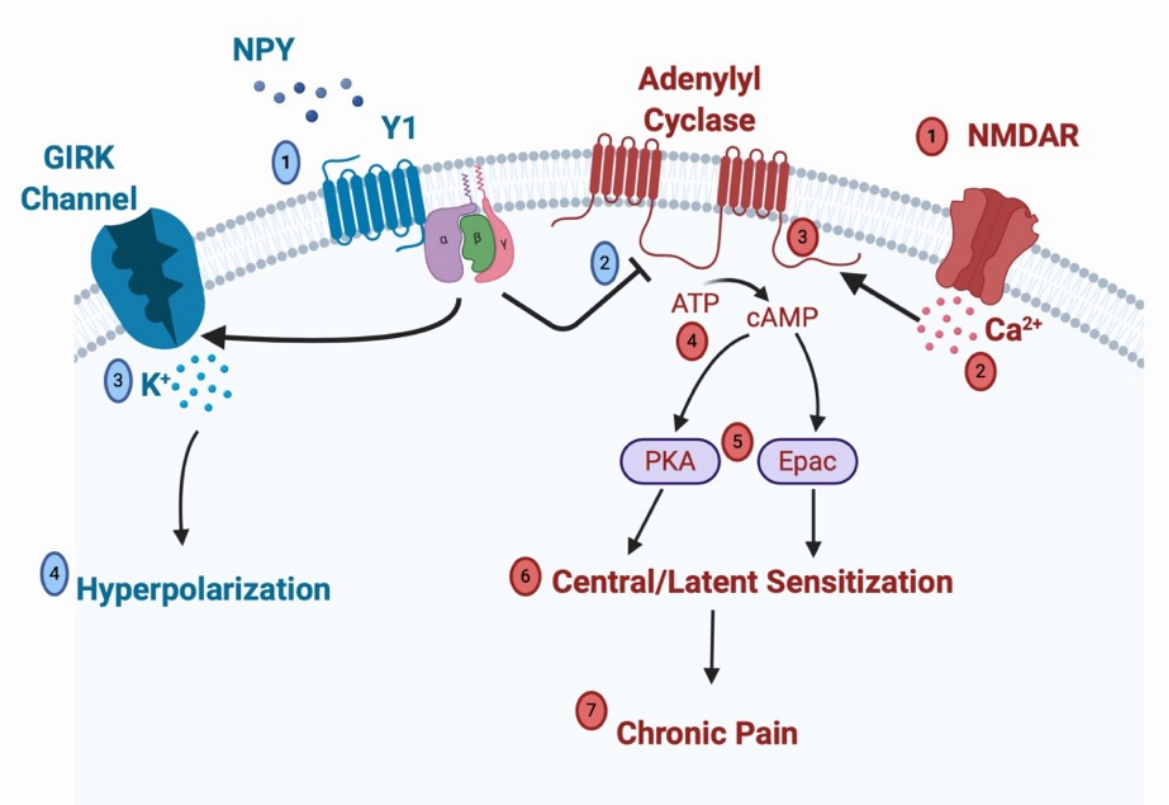

Figure 3. An intracellular signaling mechanism in spinal Y1-INs for the endogenous or pharmacological inhibition of chronic pain by NPY

Injury induced sensitization and pain (denoted in red). Tissue injury leads to the opening of N-methyl-D-aspartate receptors (NMDAR) (1) and subsequent calcium influx into the cell (2). Increased calcium stimulates adenylyl cyclase type 1 (AC1) (3) to catalyze the conversion of adenosine triphosphate (ATP) into cyclic adenosine monophosphate (cAMP) (4). Increased cytosolic cAMP serves as a second messenger that activates protein kinase A (PKA) and exchange protein activated by cAMP (Epac) (5) leading to long term potentiation and increased neuronal responsiveness to nociceptive inputs that are characteristic of central and latent sensitization (6). Central/latent sensitization in Y1-INs leads to the development and maintenance of chronic pain (7). *Endogenous or exogenous NPY inhibition of pain (denoted in blue).* NPY binds to Y1 G_i protein-coupled receptors on Y1-INs (1), and G_i protein activation leads to potent inhibition of AC1 that significantly decreases cytosolic cAMP levels (2). Additionally, activation of G_i promotes the opening of gated inwardly rectifying potassium channels (GIRK) and potassium influx (3) that lead to hyperpolarization of Y1-INs (4). Thus Y1-selective ligand binding acts as a therapeutic in order to promote anti-hyperalgesia and hold chronic pain in a state of remission. Published in (Nelson and Taylor, 2021).

Like mu opioid receptor analgesic drugs, Y1 agonists suppress not only excitatory but also inhibitory synaptic events in substantia gelatinosa neurons. For example, either NPY or the Y1 agonist [F^7,P^{34}]NPY effectively and reversibly attenuated eIPSCs that were evoked by dorsal root stimulation (Moran et al., 2004; Smith et al., 2007). To reconcile this finding with the clear anti-hyperalgesic effects of NPY, we proposed a second mechanism of NPY analgesia: NPY/Y1 inhibits the spinal release of inhibitory neurotransmitters onto inhibitory neurons, e.g. disinhibition of pain inhibition (Smith et al., 2007); however, this hypothesis requires demonstration that Y1 agonists will preferentially decrease eIPSCs in inhibitory neurons. A third and more likely explanation is that Y1 agonists dampen excitatory inputs from Y1-INs to many classes of dorsal horn interneurons, including inhibitory ones. Thus, reducing excitatory Y1-IN inputs to both excitatory and inhibitory neurons dampens net excitatory and inhibitory transmission.

1.4 Immunohistochemical, neurophysiological, and genetic identification of excitatory Y1-IN subpopulations

1.4.1 Immunohistochemical evidence of Y1-INs as a subpopulation of excitatory interneurons

Tomas Hökfelt and colleagues were the first to demonstrate in rat dorsal horn that Y1-INs are predominantly excitatory (Zhang et al., 1999). This was based on the extensive co-expression of Y1 and somatostatin immunoreactivity; somatostatin is almost exclusively expressed in glutamatergic and not GABAergic interneurons (Chamessian et al., 2018; Duan et al., 2014). The large-scale transcriptomic analyses discussed in section **1.2.4** are consistent with the detection of *Npy1r* in excitatory, somatostatinergic interneurons in the superficial dorsal horn, but

immunohistochemical co-labeling had been difficult to interpret due to the intense plexus of dendritic and terminal staining that surrounds Y1-immunopositive cells. Therefore, to enhance Y1 resolution within dorsal horn neurons, we first injected NPY by the intrathecal route to promote receptor internalization, thereby concentrating the Y1 signal within the cell soma. With this new method, we reported that rat Y1-INs colocalize not only with somatostatin, but also with immunoreactivity for calbindin (~36% colocalization) and calretinin (~19% colocalization) (Nelson et al., 2019), two additional markers of excitatory interneuron populations implicated in nociceptive transmission (Craig et al., 2002; Peirs et al., 2015; Petitjean et al., 2019; Smith et al., 2019, 2015). Future immunohistochemical studies with newly established and largely nonoverlapping neurochemical markers of excitatory interneurons in superficial dorsal horn, such as substance P, Neuropeptide FF, and cholecystokinin (Dickie et al., 2019; Gutierrez-Mecinas et al., 2019; Todd, 2017), will enable the further segregation of Y1-INs into distinct subpopulations.

1.4.2 Y1-Cre lineage neurons are a subpopulation of excitatory interneurons

The above findings have been difficult to replicate in the mouse due to the absence of a specific Y1 antibody that robustly stains mouse spinal cord, leading some to turn to Y1-Cre lineage neurons characterized in a Y1-Cre x tdTomato reporter mouse line. This approach reveals colocalization with two markers of excitatory interneurons that have been implicated in the transduction of mechanical stimuli: cMaf^{+} (~35% colocalization): and retinoid-related orphan receptor alpha (RORa) (~10% colocalization), as well as gastrin releasing peptide (GRP)-expressing neurons (~15% colocalization) and neurokinin 1 receptor (NK1R)-expressing interneurons, located in both superficial (lamina I) and deep (lamina III-IV) dorsal horn (~10% colocalization). Colocalization was not detected with either gastrin releasing peptide receptor

(GRPR)-expressing interneurons or cells that express the astrocytic markers s100b or glial fibrillary acidic protein (GFAP) (Acton et al., 2019). A cautionary note with interpretation of this data, however, is that the Y1-Cre lineage captured an extremely large population of dorsal horn neurons (~40% of total $NeuN^+$ dorsal horn neurons). Many of these likely represent neurons that exhibit transient *Npy1r* expression in development, as ~55% of adult Y1-Cre lineage neurons contained *Npy1r* mRNA. A large population of deeper neurons (lamina IIi – lamina III) was also labeled with tdTomato yet found to be *Npy1r* negative (Acton et al., 2019). Against this backdrop, we note that c-Maf is predominately expressed in the interneurons of laminae III-IV (Hu et al., 2012), while Y1 is predominately expressed in superficial dorsal horn (Brumovsky et al., 2007, 2006; Nelson et al., 2019). Furthermore, both single-cell and single-nucleosome transcriptional profiling indicate that the *Npy1r* and *Maf* genes are in distinct clusters of dorsal horn interneurons (Häring et al., 2018; Sathyamurthy et al., 2018). These data suggest that any colocalization of Y1-Cre lineage neurons with c-Maf represents an artifact of transient expression during development. This can be tested with double-label fluorescence *in situ* hybridization in dorsal horn of the adult mouse.

1.4.3 Developmental fate transcription factors indicate that Y1-INs are excitatory interneurons

Tlx1/3 is a transcription factor that determines glutamatergic cell fate in dorsal horn interneurons (Cheng et al., 2005; Guo et al., 2012; Xu et al., 2008). *In situ* hybridization of *Npy1r* mRNA with antibodies against Tlx3 established that the majority of dorsal horn superficial Y1-INs are glutamatergic neurons. Additionally, *Tlx1/3* knockout almost completely abolished *Npy1r* expression in mouse dorsal horn (Guo et al., 2012). Perhaps most convincingly, we show here for the first time that Y1-immunoreactivity densely colocalizes with Tlx3-immunoreactivity in the lumbar dorsal horn of rats (**Figure 4**). Another transcription factor that is downstream from *Tlx1/3, Lmx1b,* is also found almost exclusively in excitatory spinal neurons and is extensively colocalized with Y1-Cre lineage neurons in mice (Acton et al., 2019). Conversely, *Pax2* is a transcription factor that determines inhibitory cell fate in dorsal horn interneurons (Huang et al., 2008), and Pax2 immunoreactivity does not colocalize with Y1-INs in rat (Nelson et al., 2019) (**Figure 4**) or Y1-Cre lineage neurons in mouse (Acton et al., 2019). Together these data indicate that almost all Y1-INs in dorsal horn are glutamatergic.

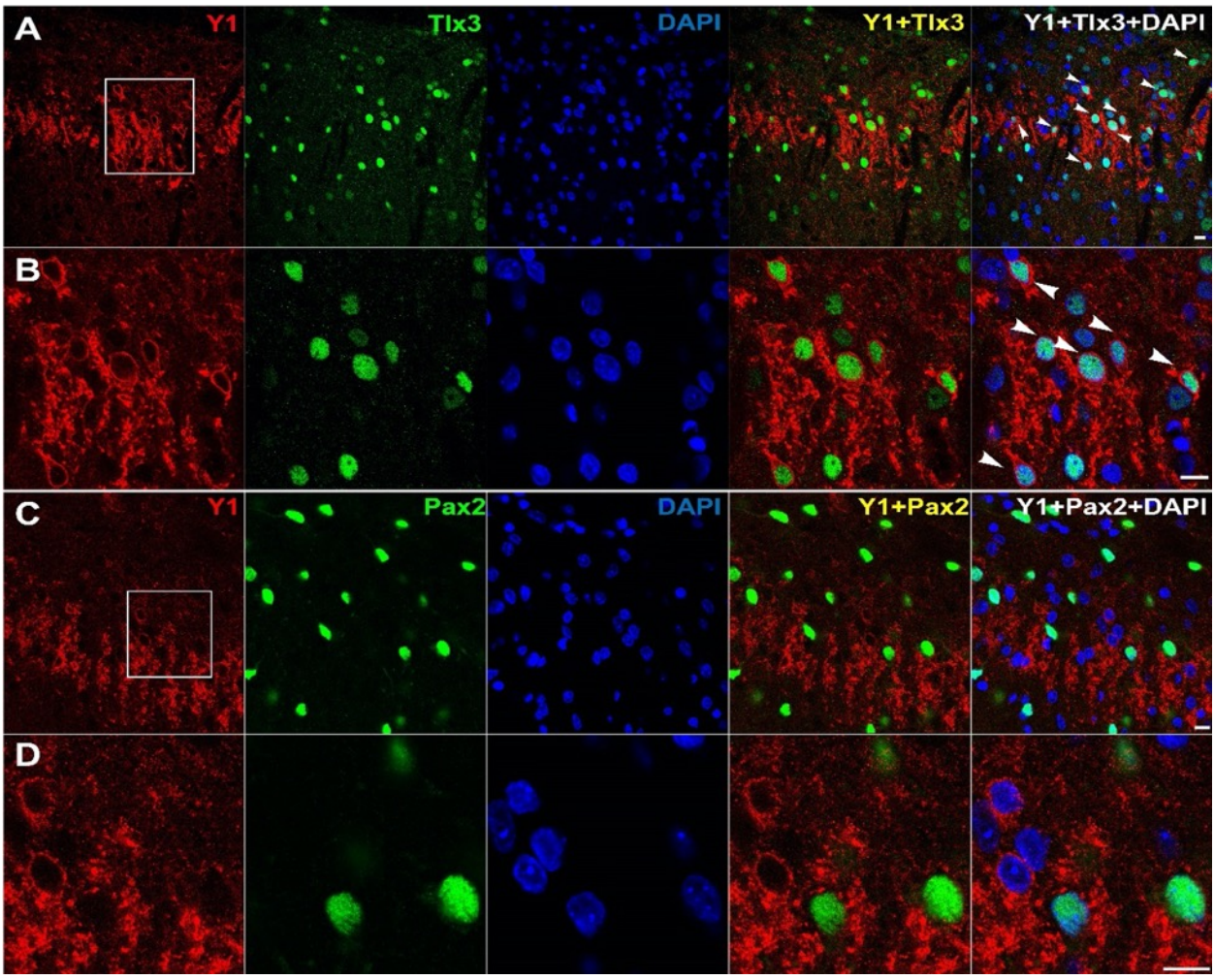

Figure 4 . **Y1-INs colocalize with excitatory Tlx3 but not inhibitory Pax2 immunoreactivity in rat dorsal horn**

98.96% of Y1-INs in lamina II colocalize with the excitatory neuronal marker Tlx3 (**A**, **B**). In contrast, 3.39% of Y1-INs colocalize with the inhibitory neuronal marker Pax2 (**C**, **D**). Panels **B** and **D** show magnified images from their respective regions of interest. Arrows indicate instances of colabeling. Scale bars: 10 µm. All images are courtesy of Dr. Weisi Fu. Images **A** and **B** are published here for the first time in (Nelson and Taylor, 2021). Images **C** and **D** are reproduced with permission from (Nelson et al., 2019). Methods are described in detail in (Nelson et al., 2019). Briefly, male Sprague-Dawley rats (Charles Rivers Laboratories) were perfused and L4-L6 transverse spinal cord sections were collected. Primary antibodies: rabbit anti-NPY Y1 receptor (1: 5,000, courtesy of Janice Urban), and guinea pig anti-Tlx3 (1: 10,000, courtesy of Carmen Birchmeier), goat anti-Pax-2 (R&D systems, 1: 1,000, AF3364). To help with identification of Y1-INs, two successive intrathecal injections of 30µg NPY were performed in naïve rats, separated by 1h to promote Y1 receptor internalization (Nelson et al., 2019). Published in (Nelson and Taylor, 2021).

1.4.4 Transcriptomic sub-classification of Y1-IN subpopulations

High-throughput, unbiased, transcriptomic analyses have revolutionized the characterization of interneuron populations in the dorsal horn, as pioneered by the laboratories of Ariel Levine and Patrik Ernfors. In the first dorsal horn transcriptomics study, Sathyamurthy *et al.* used single-nucleus transcriptional profiling and identified *Npy1r*-expressing neurons as one of the 43 cluster types (DE-2) to be selectively enriched. DE-2 is an excitatory interneuron cluster defined by the expression not only of *Npy1r* but also by the expression of both neuropeptide genes *Grp* (codes for gastrin releasing peptide) and *Sst* (codes for somatostatin) (Sathyamurthy et al., 2018). This is interesting because, as described in **1.2.1**, Y1-INs extensively colocalize with somatostatin-like immunoreactivity in the superficial dorsal horn (Nelson et al., 2019; Zhang et al., 1999). Somatostatin-expressing interneurons (SST-INs) are excitatory dorsal horn neurons predominately found in outer lamina II that receive direct C-fiber inputs (Duan et al., 2014). Transcriptional profiling of SST-INs identified *Npy1r* as a significantly enriched gene (Chamessian et al., 2018). Because of the importance of the somatostatin and gastrin releasing peptides in spinal pain and itch transmission, we felt it was important to rigorously confirm the presence of *Sst* and *Grp* in Y1-INs. To this end, we conducted *in situ* hybridization for *Grp* and *Sst* in the lumbar spinal cord of Npy1r^{eGFP} BAC transgenic mice. As illustrated in **Figure 5,** our results point to Y1^{eGFP} neurons containing extensive *Grp* and *Sst* mRNA, as predicted by the transcriptomic data.

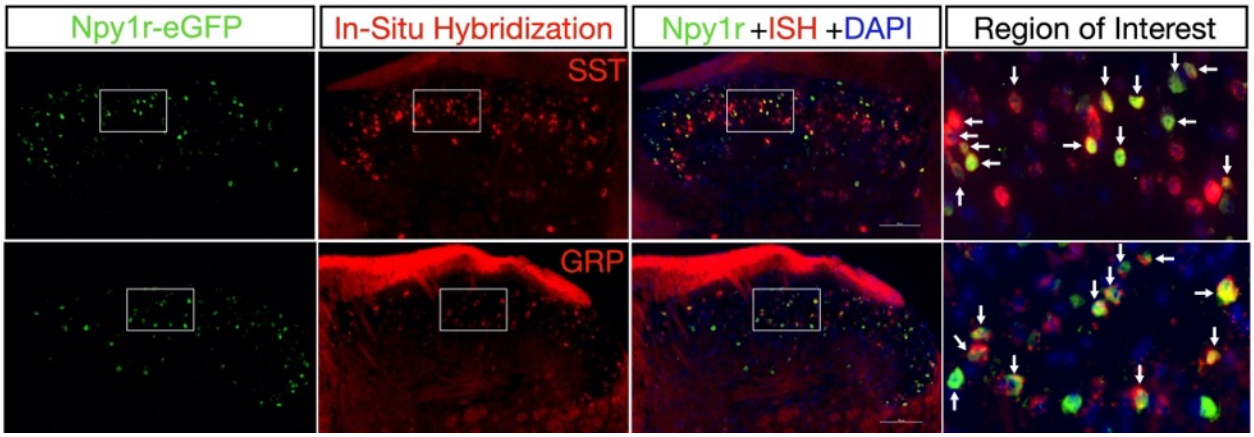

Figure 5. **Npy1r^{eGFP} interneurons colocalize with *Grp* and *Sst* mRNA**

Double staining of Npy1r^{eGFP} interneurons from BAC transgenic mice with *Sst* or *Grp* mRNA by *in situ* hybridization. Right panels show magnified images from their respective insets. Arrows indicate instances of colabeling. Scale bars: 100 µm. Brief description of experimental methods: 8-week-old male Npy1r^{eGFP} mice (MMRRC, 010554-UCD) were transcardially perfused with ice cold 1x PBS followed by 10% buffered formalin and spinal cords were extracted, post-fixed in 10% formalin overnight at 4°C, and then stored in 30% sucrose at 4°C. 20µm thick L3-L4 floating spinal cord sections were obtained on a vibrating microtome and mounted on Superfrost Plus Microscope slides. Slides underwent pretreatment for *in situ* hybridization (ISH) consisting of 10min Xylene bath, 4min 100% ethanol bath, and 2min RNAscope® H_2O_2 treatment. Slides were washed in deionized H_2O and allowed to dry overnight. The following day the ISH protocol for RNAscope Fluorescent v2 Assay (Advanced Cell Diagnostics) was followed for hybridization to marker probes (RNAscope® Probe- Mm-Grp-C2, 317861-C2; RNAscope® Probe- Mm-Sst-C2, 404631-C2). Upon completion of ISH, slides were blocked for 1h with 3% normal goat serum and incubated overnight at 4°C with chicken anti-GFP primary antibody (Abcam, 1:1,000, ab13970) to restore the GFP fluorescence (which had diminished during fixation). The following day slides were incubated in goat anti-chicken Alexa Fluor 488 secondary antibody (Invitrogen, 1:1,000, A-11039) for 1h, and coverslipped with VECTASHIELD HardSet Antifade Mounting Medium with DAPI. All images were captured on a Nikon Eclipse Ti2 microscope using a 40x objective and analyzed using NIS-Elements Advanced Research software v5.02. Data collected by Tyler Scott Nelson and published in (Nelson and Taylor, 2021).

In a second transcriptomics study, Häring *et al* used unbiased single-cell RNA-sequencing of dorsal horn and also found *Npy1r* to be selectively enriched in excitatory neurons, namely the glutamatergic clusters Glut2, Glut8, and Glut9 (Häring et al., 2018). The Glut2 cluster represents *Cck*-expressing neurons that are predicted to participate in allodynia or pathological pain but not acute pain transmission (Häring et al., 2018). The Glut8 and Glut9 clusters were located in the superficial dorsal horn, consistent with the known expression pattern of the Y1 receptor. Noxious heat increased immediate early gene expression within both Glut8 and Glut9 excitatory neurons and noxious cold activated Glut9 neurons, supporting the idea that the NPY-Y1 system contributes to the spinal transmission of noxious heat and cold (Hua et al., 1991; Lemons and Wiley, 2012; Taiwo and Taylor, 2002).

Interestingly, results from both transcriptomics studies found an extremely large overlap between *Npy1r* and *Nmur2*, the gene that encodes the neuromedin U receptor 2. In both electrophysiological and behavioral experiments, neuromedin U via the neuromedin U receptor 2 has been implicated in nociception (Cao et al., 2003; Torres et al., 2007; Yu et al., 2003). This colocalization between *Npy1r* and *Nmur2* is novel, and like other genes that significantly overlap with the Y1-IN population, such as *Car12*, *Reln*, *Npff*, *Grp*, and *Cck* (Häring et al., 2018; Sathyamurthy et al., 2018), remains to be further explored. Together these large-scale transcriptomic analyses indicate that *Npy1r* is detected in excitatory, somatostatinergic interneurons in the superficial dorsal horn. Future studies should investigate the overlap of adult *Npy1r* with candidate gene targets such as *Nmur2*, *Car12*, and *Grp* to uncover potentially distinct Y1-IN subpopulations of dorsal horn interneurons.

1.4.5 Neurophysiological evidence of Y1-INs as an excitatory population

The firing patterns of action potentials are another way to segregate neuronal populations in the superficial dorsal horn (Todd, 2017). A depolarizing current injection may evoke several distinct patterns that are often referred to as initial bursting firing (IBF), phasic firing (PF), tonic firing (TF), or delayed firing (DF). Current injection is typically injected while the cell is held at resting membrane potential; however, detection of the delayed firing pattern often requires current to be injected from hyperpolarized holding potentials (Sinha et al., 2021). A recent study from our laboratory characterized Y1-IN firing patterns from both resting and hyperpolarized membrane potentials. This key study was performed in *ex vivo* lumbar spinal cord slice recordings from a reliable *Npy1r*^{eGFP} mouse line (Sinha et al., 2021). It identified four main firing patterns with the following characteristics: Delayed, Long Latency Firing (DLLF) neurons typically exhibit a clear delay of >180 ms (range, 180-850 ms) in action potential firing that lasts the duration of current injection, Delayed, Short Latency Firing (DSLF) neurons exhibit a short depolarizing delay of 60-180 ms prior to firing the first action potential and mostly terminate before the end of current injection, Initial Burst Firing (IBF) neurons exhibit a short burst of two to four high frequency (~90 Hz) action potentials on top of a long-lasting (~200 ms) Ca^{2+} spike, owing to the presence of low-threshold Ca^{2+} currents, and Phasic Firing (PF) neurons exhibit several action potentials immediately after the onset of current injection but terminate before the end of the current pulse. These firing populations were distinct from randomly sampled interneurons (eGFP-lacking spinal neurons) as the phasic firing type was more common in *Npy1r*^{eGFP} neurons when assessed from resting membrane potential, and the DSLF phenotype was abundantly more prevalent in *Npy1r*^{eGFP} neurons from hyperpolarized conditions. As phasic and delayed firing are more common in spinal cord glutamatergic interneurons, these neurophysiology results suggest that *Npy1r*^{eGFP} neurons are

excitatory interneurons that mainly exhibit phasic firing rather than delayed firing patterns, though delayed firing can be unmasked when current clamp recordings are initiated at hyperpolarized conditions (Sinha et al., 2021).

1.5 Pharmacological or endogenous engagement of NPY-Y1 signaling reduces behavioral signs of chronic pain

The pioneering studies of Yaksh and colleagues found that intrathecal administration of NPY dose-dependently increased noxious hotplate thresholds in rats (Hua et al., 1991). This was confirmed a decade later and found to be specific to the heat modality, as NPY or Y1-selective agonists do not change baseline mechanical withdrawal thresholds in rats (Taiwo and Taylor, 2002). Additionally, early studies from Tomas Hökfelt and colleagues found that intrathecal NPY profoundly decreases the nociceptive flexor reflex in naïve rats and in models of nerve injury and acute inflammation (Xu et al., 1994, 1998, 1999). Since these early behavioral studies, an established body of preclinical evidence across a variety of injury conditions as far ranging as bone cancer-induced pain (Diaz-delCastillo et al., 2018) indicates that intrathecal administration of NPY acts through Y1 receptors to dose-dependently reduce behavioral (and spinal molecular) markers of spinal nociceptive transmission, including not just heat but also cold and mechanical hypersensitivity (**Table 1**).

Table 1 Chronological studies of NPY receptor interventions on spinal cord physiology, pain, and itch

Model	Species	Sex	NPY Receptor Intervention	Outcome Measure	Key Results	Reference
Naïve	Rat	Male	Intrathecal (i.t.) NPY	Mean arterial blood pressure (MAP) and heart rate (HR)	NPY dose-dependently decreased MAP and HR in normotensive and hypotensive rats.	Chen et al., 1988
Naïve	Rat	Male	i.t. NPY	MAP and HR, multiunit activity recordings from exposed renal sympathetic nerve	NPY dose-dependently decreased MAP, slightly decreased HR, and decreased renal sympathetic nerve activity.	Chen et al., 1990
Naïve	Cat	Not Stated (NS)	Microinjection of NPY into the dorsal horn (DH)	Evoked release of immunoreactive substance P upon electrical stimulation of unmyelinated primary afferents of the tibial nerve	NPY reduced the evoked release of immunoreactive substance P.	Duggan et al., 1991
Naïve	Rat	Male	i.t. NPY	Heat: hotplate (HP) withdrawal (w/d) latency, Mechanical: pressure threshold	NPY dose-dependently increased the HP w/d latency but had no effect on mechanical pressure.	Hua et al., 1991
Naïve	Rat	Male	i.t. NPY, Y2 agonistic fragments, or Y1 agonist	MAP	NPY and Y2 agonistic fragments but not Y1 agonist dose-dependently decreased MAP.	Chen and Westfall, 1993

Table 1 Continued

Neuropathic Pain: sciatic nerve transection	Rat	Female	i.t. NPY	Flexor reflex	NPY dose-dependently depressed flexor reflex in naïve and injured rats but the antinociceptive effect was stronger and longer lasting after nerve transection.	Xu et al., 1994
Neuropathic Pain: partial sciatic nerve ligation	Rat	NS	i.t. NPY, Y1 or Y2 agonists, or a nonselective NPY antagonist	Mechanical: pressure threshold	NPY or Y1 agonist but not Y2 agonist increased nerve injury-induced mechanical hypersensitivity. The nonselective NPY antagonist attenuated the nerve injury-induced hyperalgesia.	White, 1997
Naïve	Rat and Cat	Rat: Males; Cat: NS	None	DH release of immunoreactive NPY	Neither electrical stimulation of peripheral nerves nor noxious mechanical or heat stimulation changed the extensive spontaneous NPY release observed in the DH.	Mark et al., 1997
Neuropathic Pain: chronic constriction of the sciatic nerve	Rat	Male	None	DH release of immunoreactive NPY	CCI extended the zone of spontaneous ipsilateral release of NPY into the deep DH. Electrical stimulation of the injured nerves produced widespread NPY release.	Mark et al., 1998

Table 1 Continued

Inflammatory Pain: hindpaw injection of carrageenan	Rat	Male and Female	i.t. NPY	Flexor reflex	NPY dose-dependently produced brief reflex facilitation at low doses and long-lasting depression at high doses in naïve and injured rats. The reflex facilitation was greater in carrageenan injected animals.	Xu et al., 1998
Neuropathic Pain: sciatic nerve transection	Rat	Female	i.t. Y1 or Y2 agonist	Flexor reflex	Y1 agonist dose-dependently produced reflex depression in naïve and injured rats. Y2 agonist did not produce reflex depression in naïve rats but dose-dependently produced reflex depression in sciatic nerve transected rats.	Xu et al., 1999
Neuropathic Pain: chronic constriction of the sciatic nerve	Rat	Male	None	DH release of immunoreactive NPY	Total conduction block of the injured nerve did not change spontaneous NPY release in the ipsilateral DH.	Colvin and Duggan, 2001

Table 1 Continued

Inflammatory Pain: hindpaw injection of formalin, intraperitoneal injection of acetic acid or MgSO4; Neuropathic Pain: partial sciatic nerve ligation	Mouse	Male	Global knockout of *Npy1r*; i.t. NPY	Heat: HP w/d latency, tail flick latency; Mechanical: von Frey (vF) w/d threshold; Inflammatory Pain: number of events (lifting, shaking, licking and biting of the paw), number of abdominal stretches	*Npy1r* knockout increased sensitivity to heat and mechanical stimuli, hyperalgesia in the Phase I but not Phase II response to formalin, visceral hyperalgesia, and peripheral nerve injury-induced mechanical hypersensitivity. *Npy1r* knockout abolished the antinociceptive effect of NPY on heat hypersensitivity.	Naveilhan et al., 2001
Inflammatory Pain: hindpaw injection of carrageenan or CFA	Rat	Male	i.t. NPY or Y1 or Y2 antagonists	Heat: HP w/d latency, radiant heat w/d latency; Motor Coordination: latency to fall on an accelerating rotarod	NPY dose-dependently increased response latency to heat stimuli, inhibited carrageenan- and CFA-induced heat hypersensitivity, and did not alter motor coordination. The antinociceptive effects were abolished by a Y1 but not Y2 antagonist. A Y1 antagonist enhanced CFA-induced heat hypersensitivity.	Taiwo and Taylor, 2002

Table 1 Continued

Naïve	Rat	NS	NPY or Y1 agonist on spinal cord (SC) slices	Electrophysiology: blind whole-cell patch-clamp recordings in voltage clamp, recording eEPSCs and eIPSCs, recording mEPSCs and mIPSCs, paired-pulse stimulation	NPY acts via Y1 to suppress inhibitory transmission by pre- and postsynaptic mechanisms. NPY acts via Y2 to suppress excitatory transmission exclusively by a presynaptic mechanism. NPY activates an inwardly rectifying K^+ conductance in DH neurons.	Moran et al., 2004
Inflammatory Pain: hindpaw injection of formalin	Rat	Male	i.t. NPY or Y1 or Y2 antagonists	Inflammatory Pain: licking duration and the number of flinch events in the formalin assay; MAP and HR	NPY dose-dependently inhibited formalin-induced nocifensive responses that were partially blocked with a Y1 antagonist. NPY dose-dependently increased MAP that was prevented with a Y2 but not Y1 antagonist.	Mahinda et al., 2004
Naive	Rat	Male	NPY, Y1 agonist, or Y1 antagonist on SC slices	Capsaicin-evoked immunoreactive CGRP release from lumbar DH	NPY or Y1 agonist reduced CGRP exocytosis from central terminals of capsaicin sensitive afferent fibers and was partially blocked by a Y1 antagonist.	Gibbs et al., 2004

Table 1 Continued

Naïve	Rat	Male	NPY, Y1 agonist, or Y1 antagonist on SC slices	Electrophysiology: whole-cell patch-clamp recordings in voltage clamp, recording mEPSCs and mIPSCs, recording dorsal root Aδ- or C-fiber-evoked EPSCs	NPY or Y1 agonist induced a potassium-dependent outward current, membrane hyperpolarization, and a suppression of dorsal root stimulation-evoked action potentials. NPY-induced responses were blocked by a Y1 antagonist.	Miyakawa et al., 2005
Naïve	Mouse	Male	Global knockout of *Npy1r*	Mechanical: vF w/d threshold	*Npy1r* knockout mice demonstrated profound mechanical hypersensitivity.	Shi et al., 2006
Inflammatory Pain: hindpaw injection of CFA; Neuropathic Pain: partial sciatic nerve ligation	Mouse	Male	Global knockout of *Npy1r;* i.t. NPY or Y1 antagonist	Heat: HP w/d latency, radiant heat w/d latency; Mechanical: vF w/d threshold; Motor Coordination: latency to fall on an accelerating rotarod	*Npy1r* knockout produced heat hypersensitivity and longer lasting CFA-induced heat hyperalgesia. *Npy1r* knockout or a Y1 antagonist prevented the antinociceptive effect of NPY after CFA or partial sciatic nerve ligation. NPY and Y1 antagonist did not alter motor performance.	Kuphal et al., 2008

Table 1 Continued

Inflammatory Pain: hindpaw injection of formalin; Neuropathic Pain: spared nerve injury (SNI, spared sural nerve)	Rat	Male	i.t. NPY or Y1 or Y2 antagonists	Inflammatory Pain: licking duration and the number of flinch events; Cold: acetone w/d duration; Mechanical: vF w/d threshold, tactile stimulus-evoked Fos expression in superficial DH	NPY reduced formalin-induced behaviors, dose-dependently reduced SNI-induced mechanical and cold hypersensitivities, and reduced both formalin- and SNI-induced tactile stimulus-evoked Fos expression. SNI-induced mechanical hypersensitivity and Fos expression were blocked by a Y1 or Y2 antagonist.	Intondi et al., 2008
Inflammatory Pain: hindpaw injection of formalin	Rat	Male and Female	i.t. NPY-saporin to selectively ablate Y1-INs	Heat: HP w/d latency and time licking and guarding hindpaws; Inflammatory Pain: time licking, lifting and biting, and number and time course of responses	NPY-saporin reduced SC but not DRG Y1 immunoreactivity. NPY-saporin elevated reflex w/d thresholds and reduced time spent licking/guarding paws to only low (44°C) heat. NPY-saporin reduced formalin-induced nocifensive behaviors.	Wiley et al., 2009

Table 1 Continued

Inflammatory Pain: hindpaw injection of CFA, latent sensitization after CFA; Neuropathic Pain: SNI, Cp_xS_x (spared tibial nerve), latent sensitization after Cp_xS_x	Mouse	Male	Conditional doxycycline-induced global knockdown of NPY, or intrathecal Y1 or Y2 antagonists	Heat: HP w/d latency, radiant heat w/d latency; Cold: acetone w/d duration; Mechanical: vF w/d threshold; Motor Coordination: latency to fall on an accelerating rotarod; Ambulatory activity: exploration in an open field	NPY knockdown did not alter baseline sensory thresholds, motor coordination, or ambulatory activity but increased the intensity and duration of SNI-induced mechanical and cold hypersensitivity. After the resolution of CFA- and Cp_xS_x-induced hypersensitivities- NPY knockdown or Y1 or Y2 antagonists reinstated behavioral hypersensitivities. Y2 antagonist increased Fos and pERK in the DH after CFA.	Solway et al., 2011
Inflammatory Pain: hindpaw injection of CFA	Rat	Female	i.t. NPY-saporin to selectively ablate Y1-INs	Cold: 10°C cold plate (CP), thermal preference assay (two chamber 15°C vs. 45°C); Affective: feeding interference (overcome a 10°C floor plate to consume a sweet solution), and an escape task (climb onto a shelf to avoid a 10°C floor plate)	NPY-saporin reduced cold aversion on thermal preference and escape tasks, was analgesic to noxious heat on the escape task, and reduced CFA-induced hypersensitivity to cold temperatures experienced on the CP, thermal preference, feeding interference, and escape tasks.	Lemons and Wiley, 2012

Table 1 Continued

Naïve	Rat	NS	NPY, Y1 or Y2 antagonists, or Y1 or Y2 agonists on SC slices	Electrophysiology: blind whole-cell patch-clamp recordings in voltage clamp, recording mEPSCs and mIPSCs; Morphological Categorization: *post hoc*	NPY or Y1 agonist induced a hyperpolarizing potassium conductance and outward current in primarily central- or radial-like neurons that was abolished by a Y1 but not Y2 antagonist. Y2 agonist had no effect on DH neurons. NPY moderately reduced the frequency of both mEPSCs and mIPSCs via Y1 and Y2.	Melnick, 2012
Inflammatory Pain: hindpaw plantar incision	Rat	Male	i.t. NPY, or Y1 or Y2 antagonists	Hindpaw guarding behavior; Mechanical: vF w/d threshold; Heat: radiant heat w/d latency	NPY reduced incision-induced guarding behavior and heat and mechanical hypersensitivity. The antinociceptive NPY effects were abolished with a Y1 but not Y2 antagonist.	Yalamuri et al., 2013

Table 1 Continued

Inflammatory Pain: hindpaw injection of carrageenan or CFA	Rat and Mouse	Male	Superfusion of slices with Y1 agonist; i.t. NPY or Y1 agonist	NK1R internalization; Y1 agonist stimulated [^{35}S]GTPγS binding; *In vivo* microdialysis of DH substance P release; Mechanical: vF w/d threshold, pin prick w/d duration; Cold: acetone w/d duration; Heat: radiant heat w/d latency	Y1 agonist decreased dorsal root stimulation-evoked NK1R internalization. CFA increased the affinity of coupling between Y1 and activated G-proteins, but its efficacy was reduced by roughly half. NPY reduced capsaicin-evoked substance P release *in vivo*. NPY Y1 agonist inhibited CFA- and carrageenan-induced NK1R internalization and nociception.	Taylor et al., 2014
Inflammatory Pain: hindpaw injection of CFA; Mechanical Itch: touch-evoked itch test; Chemical Itch: intradermal pruritogens	Mouse	NS	Ablation or chemogenetic inhibition of SC NPY-Cre lineage interneurons	Mechanical: vF w/d threshold, response to light brush, pressure; Cold: acetone w/d duration, CP w/d latency; Heat: HP w/d latency, radiant heat w/d latency; Motor Coordination: latency to fall on accelerating rotarod; Mechanical Itch: alloknesis from vF stimulation at nape; Chemical Itch: number of scratching and wiping behaviors and bouts	Ablation or inhibition of SC NPY-Cre lineage neurons induced spontaneous scratching behaviors and skin lesions, increased mechanical but not chemical itch, but did not alter cold, heat, or mechanical sensitivity, motor coordination, or CFA-induced mechanical hypersensitivity.	Bourane et al., 2015

Table 1 Continued

Neuropathic Pain: chronic constriction injury (CCI)	Rat	Male	i.t. Y1 agonist	Mechanical: vF w/d threshold; Cold: acetone w/d duration	Y1 agonist dose-dependently reduced behavioral signs of CCI-induced mechanical and cold hypersensitivity.	Malet et al., 2017
Mechanical Itch: touch-evoked itch test; Chemical Itch: intradermal pruritogens	Mouse	NS	i.t. NPY, Y1 agonist, or Y1 antagonist	Mechanical Itch: scratch and shake episode frequency and duration from vF stimulation at nape; Chemical Itch: scratch and shake episode frequency and duration	Y1 agonist reduced shake episode frequency and duration induced by nape stimulation. NPY and Y1 agonist reduced the duration of compound 48/80- and histamine- but not chloroquine-induced scratching.	Gao et al., 2018
Bone Cancer Pain: intra-tibial infusion of MRMT1 -Luc2 cancer cells	Rat	Male and Female	i.t. NPY, or Y1 or Y2 antagonists	Limb use test and limb weight-bearing assay	NPY restored limb function and weight bearing and these antihyperalgesic effects were blocked by Y1 or Y2 antagonists.	Diaz-delCastillo et al., 2018
Inflammatory Pain: hindpaw plantar incision	Rat	Male	i.t. NPY	Mechanical: vF w/d threshold; hindpaw guarding behavior; Heat: radiant heat w/d latency	NPY reduced incision-induced hindpaw guarding and thermal hyperalgesia.	Gupta et al., 2018

Table 1 Continued

Spontaneous Itch: non-evoked acute scratching behavior	Mouse	Male	i.t. Y1 agonist or Y1 or Y2 antagonists	Mechanical: vF w/d threshold; Heat: radiant heat w/d latency; Motor Coordination: latency to fall on an accelerating rotarod; Spontaneous Itch: number of scratching bouts	Y2 but not Y1 antagonist induced spontaneous pain-related scratching and mechanical but not thermal sensitivity. Y1 antagonist alleviated Y2 antagonist-induced pain behaviors. Y2 antagonist reduced motor coordination at high doses.	Chen et al., 2019
Inflammatory Pain: hindpaw injection of formalin or capsaicin; Spontaneous Itch: non-evoked acute scratching behavior; Mechanical Itch: touch-evoked itch test; Chemical Itch: intradermal pruritogens	Mouse	Male and Female	SC and hindbrain *Npy1r* knockout; Ablation of SC NPY-Cre lineage neurons; Ablation or chemogenetic activation and inhibition of SC Y1-Cre lineage interneurons	Mechanical: vF w/d threshold, responsiveness to light brush, pressure threshold, pin prick w/d duration; Heat: HP w/d latency, radiant heat w/d latency; Inflammatory Pain: time spent licking, flinching, and biting; Spontaneous Itch: number of spontaneous scratching bouts; Mechanical Itch: alloknesis score from vF stimulation at nape; Chemical Itch: scratching bouts, duration, and rate	Y1-Cre lineage neuron ablation prevented NPY-Cre lineage neuron ablation-induced itch, enhanced mechanical itch, and reduced vF thresholds without changing mechanical, heat, or inflammatory pain responses. Activation of Y1-Cre lineage neurons reduced vF thresholds and increased mechanical and spontaneous itch. SC *Npy1r* knockout reduced vF thresholds but did not change mechanical, heat, acute pain, or chemical pruritogen-induced behavioral responses.	Acton et al., 2019

Table 1 Continued

Neuropathic Pain: SNI	Rat	Male	Y1 internalization in SC slices as an *in situ* measure of NPY release	Y1 internalization was quantified by visually counting Y1-INs in laminae I-II and classifying them as either with or without internalization; Mechanical: vF w/d threshold, and non-noxious- or noxious-evoked Y1 internalization.	NPY, capsaicin, NMDA, and high K^+ induced Y1 internalization in DH neurons. Electrical stimulation of the DH frequency-dependently induced NPY release and was decreased by a Y1 antagonist. Dorsal root immersion in capsaicin induced NPY release and it was blocked by CNQX. Nerve injury increased Y1 internalization induced by DH stimulation and *in vivo* internalization induced by noxious and non-noxious stimuli.	Marvizon et al., 2019

Table 1 Continued

Inflammatory Pain: Latent sensitization after intraplantar CFA	Mice	Male	i.t. Y1 antagonist	Mechanical: vF w/d threshold	Y1 antagonist reinstated mechanical hypersensitivity following the resolution of CFA-induced inflammation and this was prevented in AC1 knockout mice or with administration of a pharmacological blocker to the N-methyl-D-aspartate receptor (NMDAR), adenylyl cyclase type 1 (AC1), protein kinase A (PKA), transient receptor potential cation channel A1 (TRPA1), channel V1 (TRPV1), or exchange protein activated by cAMP (Epac1 or Epac2).	Fu et al., 2019

Table 1 Continued

Neuropathic Pain: SNI	Rat	Male	i.t. NPY, or NPY-saporin	Mechanical: vF w/d threshold, pressure threshold, pin prick w/d duration, tactile stimulus-evoked Fos expression in superficial DH; Cold: acetone w/d duration; Heat: HP w/d latency, radiant heat w/d latency; Motor Coordination: latency to fall on an accelerating rotarod; Ambulatory Activity: exploration in an open field	NPY-saporin dose-dependently attenuated the development of SNI-induced mechanical and cold allodynia, but did not change normal mechanical or thermal thresholds, motor coordination, or locomotor activity. NPY reduced SNI-induced mechanical hypersensitivity and light touch-evoked c-Fos expression in DH Y1-INs.	Nelson et al., 2019
Neuropathic Pain: Latent sensitization after Cp_xS_x	Mouse	Male	Doxycycline-induced global knockdown of NPY, or intrathecal Y1 antagonist	Mechanical: vF w/d threshold; Cold: acetone w/d duration; Affective Pain: 3-chamber conditioned place preference and avoidance assay	Y1 antagonist or NPY knockdown induced conditioned place aversion (CPA). Y1 antagonist reinstated mechanical and cold hypersensitivity following the resolution of Cp_xS_x-induced hypersensitivity and reinstatement and CPA were prevented in AC1 knockout mice or with an NMDA receptor antagonist, AC1 inhibitor, or TRPV1 or TRPA1 channel blockers.	Fu et al., 2020

Table 1 Continued

Mechanical Itch: touch-evoked itch test; Chemical Itch: intradermal pruritogens; Atopic Dermatitis-like Itch: application of dust mite extract	Mouse	Male and Female	i.t. Y2 agonist or Y2 antagonist	Mechanical Itch: scratch and shake episode frequency and duration from vF stimulation at nape; Chemical Itch: scratch and shake episode frequency and duration; Atopic Dermatitis-like Itch: scratch and shake episode frequency and duration	Y2 agonist reduced the frequency and duration of compound 48/80-induced scratching and the duration of IL-31- and histamine-induced scratching. Y2 agonist did not reduce scratching induced by SLIGRL, chloroquine, topical dust mite extract, or mechanical itch induced by vF at nape.	Ma et al., 2020
Inflammatory Pain: intra-articular injection of dilute formalin	Rat	Male	i.t. Y1 agonist, Y1 antagonist, or NPY-saporin	Mechanical: Paw Elevation Time (PET)-rats are placed on a revolving cylinder for 1min and scored for the total time that the hindpaw is not in contact with the cylinder surface	NPY-saporin and Y1 agonist reduced formalin-induced PET and conversely Y1 antagonist increased the PET.	Souza-Silva et al., 2020
Neuropathic Pain: ligating and cutting the L5 spinal nerve	Rat	Male	Intaspinal activation, inhibition, or ablation of spinal NPY-INs with an AAV for NPY promoter-dependent gene transduction	Mechanical: vF w/d threshold, Cold: acetone w/d duration; Heat: radiant heat w/d latency	Ablation or silencing of NPY-INs converted Aβ fiber-derived signals to pain-like responses. Activation of NPY-INs in nerve-injured rats reversed Aβ fiber-derived neuropathic pain-like behavior and was shown to be morphine-resistant.	Tashima et al., 2020

Table 1 Continued

Naïve	Mouse	Male and Female	NPY or Y1 agonist on SC slices	Electrophysiology: whole-cell patch-clamp recordings in voltage clamp in a *Npy1r*^{eGFP} mouse line	Under hyperpolarized conditions, most Y1^{eGFP} neurons exhibited fast A-type potassium currents and delayed, short-latency firing (DSLF). Y1^{eGFP} DSLF neurons were almost always rapidly adapting and often exhibited rebound spiking, indicating enrichment of T-type calcium currents.	Sinha et al., 2021
Opioid-induced Itch	Mouse	Male and Female	i.t. NPY	Opioid-induced Itch: Quantification of scratch bouts over time	i.t. NPY substantially suppressed i.t. morphine-induced scratching behavior	Wang et al., 2021
Mechanical Itch: touch-evoked itch test	Mouse	Male and Female	i.t. NPY, i.t. Y1 agonist, or i.t. neutralizing NPY (anti-NPY IgG)	Mechanical Itch: alloknesis score from vF stimulation at nape; Apoptosis: Quantification of NPY Tunel-positive neurons in aged and young mice	Aging produces NPY-IN apoptosis and enhanced mechanical itch. i.t. anti-NPY IgG slightly increases mechanical itch in young mice. Aging-induced itch is alleviated via i.t. NPY or i.t. Y1 agonist.	Cui et al., 2021

1.5.1 Global and selective spinal/hindbrain *Npy1r* knockout

Global germ line *Npy1r* knockout mice display abnormally enhanced behavioral reflex responses to noxious heat, visceral chemical, and non-noxious mechanical stimuli as compared to genetic controls (Naveilhan et al., 2001b; Shi et al., 2006). They also develop a more pronounced hypersensitivity in response to inflammation or peripheral nerve injury (Kuphal et al., 2008; Naveilhan et al., 2001b). However, Y1 receptors are expressed throughout the body and so Goulding and colleagues ablated *Npy1r* specifically in spinal cord and hindbrain neurons (including the medulla, pons, and cerebellum) by crossing *Npy1r*-Flox mice with *Lbx1*-Cre mice (Acton et al., 2019). In contrast to germ line deletion, these mice exhibited hypersensitivity to von Frey hairs but not to other sensory stimuli including light brush, noxious pinprick, noxious pressure, noxious heat, capsaicin, or chemical pruritogens. These studies suggest that spinal/hindbrain Y1 contributes to a tonic inhibition of responsiveness to non-noxious punctate mechanical stimulation, while Y1 receptors located elsewhere contribute to the tonic inhibition of responsiveness to dynamic brush, noxious mechanical stimulation, noxious heat, and chemical pain.

In contrast to the reduced thresholds observed in *Npy1r* deletion mutant mice, intrathecal administration of Y1 antagonists did not change von Frey mechanical withdrawal thresholds in naïve or sham-injured mice (Chen et al., 2019; Fu et al., 2020; Solway et al., 2011). One possible explanation for this discrepancy is that while intrathecal injection likely restricts Y1 antagonism to the spinal cord (and perhaps the DRG), the interruption of Y1 function after *Npy1r* knockout extends to the medulla, where NPY can exert not only pronociceptive but also antinociceptive actions. On one hand, microinjection of NPY into the nucleus gracilis reduced von Frey thresholds

in the uninjured rat (Ossipov et al., 2002), and microinjection of NPY Y1 antagonists into the nucleus gracilis or the cisterna magna reversed mechanical hypersensitivity in rats with spinal nerve ligation (Fukuoka and Noguchi, 2015; Ossipov et al., 2002). On the other hand, injection of NPY into the cisterna magna dose-dependently reversed mechanical hypersensitivity in rats with a variant of the spared nerve injury (SNI) model (Jung et al., 2009). Thus, NPY in the nucleus gracilis is pronociceptive but the pro- or antinociceptive role of NPY in the cisterna magna after peripheral nerve injury remains unclear. Furthermore, injection of NPY into the rostral ventral medulla (RVM) reduced behavioral signs of hypersensitivity in models of chronic neuropathic and inflammatory pain (Cleary et al., 2014; Taylor et al., 2007). The RVM contains two classes of pain modulatory neurons: the pain facilitatory ON-cells, and the pain inhibitory OFF-cells (Chen and Heinricher, 2019). Y1-immunoreactivity is found on both ON- and OFF-cells ((Cleary et al., 2014). Perhaps the loss of *Npy1r* in spinal/hindbrain and global *Npy1r* knockout mice results in an overall net increase in ON-cell activity in the RVM that is responsible for the hyperalgesia to light punctate touch. Future studies could test this hypothesis with conditional knockout of *Npy1r* in specific regions of the CNS, for example with injection of AAV-Cre into the RVM or spinal cord of adult *Npy1r*-Flox mice, followed by the determination of mechanical threshold.

1.5.2 Spinally-directed NPY in models of neuropathic pain

Intrathecal NPY or [Leu^{31},Pro^{34}]-NPY dose-dependently reduced mechanical and cold hypersensitivity in rats with SNI or chronic constriction injury (CCI) (Intondi et al., 2008; Malet et al., 2017), and reduced hind paw withdrawal latency to heat in CD1 mice following partial sciatic nerve ligation (Kuphal et al., 2008). After SNI in rats, NPY reduced the immunohistochemical expression of non-noxious, tactile stimulus-induced Fos, a marker of

neuronal activation, in the superficial dorsal horn. These reductions in neuropathic pain-like behavior and Fos expression were both reversed with BIB03304 (Intondi et al., 2008). Subsequent studies reported that intrathecal NPY reduced Fos expression within Y1-INs, indicating that Y1 retains the capacity to inhibit spinal pain transmission after nerve injury (Nelson et al., 2019). Taken together, these data in both rats and mice promote the spinal Y1 receptor as a compelling target for analgesic drug development to treat traumatic nerve injury-induced neuropathic pain.

1.5.3 Spinally-directed NPY in models of inflammatory pain

Intrathecal NPY or [Leu^{31},Pro^{34}]-NPY produced anti-hyperalgesic effects in rats in the intraplantar CFA model of inflammatory pain (Taiwo and Taylor, 2002; Taylor et al., 2014), the intraplantar formalin model of ongoing pain (Mahinda and Taylor, 2004), the hindpaw plantar incision model of postoperative pain (Gupta et al., 2019; Yalamuri et al., 2013), and the intra-knee joint formalin model of joint inflammation (Souza-Silva et al., 2020)). The Y1 antagonist BIBO3304 prevented these antihyperalgesic effects, and the inhibitory effects of intrathecal NPY on mechanical and heat hyperalgesia in the CFA model of inflammation were lost in *Npy1r* knockout mice (Kuphal et al., 2008). These data promote the spinal Y1 receptor as a compelling target for analgesic drug development to treat inflammatory pain.

1.5.4 Injury engages an endogenous spinal NPY-Y1 signaling cascade that opposes nociception

NPY Y1 receptor antagonists exert minimal if any effect on thermal or mechanical paw withdrawal thresholds in non-injured animals, indicating an absence of a tonic NPY-Y1 inhibitory control of nociception (Chen et al., 2019; Solway et al., 2011). In stark contrast, painful injury induces the development of a robust, compensatory mechanism of NPY antihyperalgesia in the dorsal horn. In the setting of inflammatory pain, for example, intraplantar CFA increased the affinity of functional Y1 receptor-coupling to activated G-proteins in the lumbar dorsal horn (Taylor et al., 2014). This suggests that inflammation augments the functionality of receptor-G protein interactions, leading to the amplification of intracellular signaling. This may explain how after CFA, NPY can effectively reduce the noxious mechanical stimulus-evoked release of substance P from the central terminals of primary afferent neurons, an effect not observed in uninjured controls (Taylor et al., 2014). In the setting of neuropathic pain, peripheral nerve injury induced a massive *de novo* expression of NPY in neurons in the DRG after damage to their axons (Magnussen et al., 2015; Wakisaka et al., 1991). Peripheral nerve injury also increased the spontaneous release of NPY in the dorsal horn (Colvin and Duggan, 2001; Mark et al., 1998) that was not abolished by total anesthesia-induced conduction block of the injured nerve, suggesting that most NPY release is coming from local dorsal horn NPY-inhibitory interneurons and not the injured primary afferents (Colvin and Duggan, 2001). In support of this idea, peripheral nerve injury increased mechanical stimulus-evoked NPY release from dorsal horn neurons *in vivo* (Marvizon et al., 2019); this study overcame the notoriously difficult assessment of spinal NPY concentrations (Mark et al., 1997) with the use of a robust assay of Y1 internalization as a proxy for NPY release (Marvizon et al., 2019). Together these results suggest that NPY release in the

dorsal horn following peripheral nerve injury stems from dorsal horn interneuron release. So then what might the massive injury-induced *de novo* expression of NPY in the DRG be doing? A small body of evidence indicates that NPY causes neurite outgrowth from nerve-injured DRG fibers (White and Mansfield, 1996), suggesting that NPY contributes to the repair and regrowth of damaged neurons. Indeed, NPY-induced repair is commonly observed in the central nervous system (Decressac and Barker, 2012). Future studies in DRG conditional NPY knockout mice may elucidate the contribution of NPY to nerve injury-induced pain and axonal repair and reinnervation in the dorsal horn. Taken together, these results from both inflammatory and neuropathic injury are consistent with a homeostatic process by which injury-induced pronociceptive neurotransmission in the dorsal horn is counterbalanced by: 1) Enhanced NPY release from dorsal horn neurons à 2) Enhanced Y1-G_i protein coupling à 3) Suppressed release of pronociceptive neurotransmitters, including substance P, from the central terminals of primary afferent neurons.

Tissue or nerve injury sensitizes dorsal horn neurons in the spinal cord, leading to an increase in the intensity and duration of pain (Ji et al., 2003; Latremoliere and Woolf, 2009). This central sensitization can facilitate the protective aspects of acute pain, but failure to resolve can lead to chronic pain. With the development of a latent form of central sensitization (latent sensitization or LS), sensitization is kept in remission by an opposing mechanism that typically includes activation of inhibitory G-protein coupled receptors, such as Y1 (B.K. Taylor and Corder, 2014). LS can persist for over a year, even after the appearance of complete recovery from tissue injury and the re-establishment of normal pain thresholds (Basu et al., 2021). LS can be revealed upon disruption of pain inhibitory GPCRs, including spinal NPY signaling. For example, in CFA or peripheral nerve injury models, conditional knockdown of NPY in NPY^{tet} -transgenic mice or

intrathecal administration of BIBO3304 leads to a rapid, robust, and repeatable reinstatement not only of mechanical and thermal hypersensitivity (Fu et al., 2020, 2019; Solway et al., 2011) but also the affective component of pain as determined with conditioned place preference and aversion assays (Fu et al., 2020). These results indicate that the NPY-Y1 system contributes to a powerful endogenous analgesia mechanism whereby animals naturally recover from inflammatory- or nerve injury-induced hyperalgesia. The development of a pathologically high set point in the equilibrium between pronociceptive and antinociceptive processes (an allostatic state) may have important implications: failures in endogenous inhibitory NPY signaling could increase the ratio of excitation/inhibition, thereby unleashing LS to drive the transition from acute to chronic pain states (**Figure 3**).

The pronociceptive signaling pathways associated with LS are being revealed with the use of a four-step approach: 1) induce inflammatory or neuropathic pain, 2) allow pain resolution, 3) interrupt a putative signaling mechanism with pharmacological antagonist or genetic deletion, and 4) test for reinstatement of hyperalgesia and affective pain. With this approach, we could prevent BIBO3304- or genetic NPY knockdown-induced pain reinstatement by spinal blockade of N-methyl-D-aspartate receptors (NMDAR) with intrathecal administration of MK-801, adenylyl cyclase type 1 (AC1) with intrathecal NB001 or in AC1 knockout mice, protein kinase A (PKA) with intrathecal H89, exchange protein activated by cAMP (Epac) with intrathecal ESI-09, TRPA1 with intrathecal HC030031, or TRPV1 with intrathecal AMG9801 (Fu et al., 2020, 2019). As illustrated in the flow diagram of **Figure 3,** we have proposed that injury promotes a pronociceptive NMDARàAC1àcAMP signaling cascade of LS that involves PKA and Epac1/2

and is kept in remission by tonic NPY-Y1 inhibition. New treatments for chronic pain might either mimic endogenous NPY analgesia or inhibit AC1, PKA, or Epac.

1.6 Y1-INs mediate chronic pain

Section **1.3** indicates that spinal nociceptive processing can be inhibited with intrathecal administration of a Y1 agonist or endogenous release of NPY within the dorsal horn. Since Y1 receptors are predominantly located on glutamatergic neurons (Nelson et al., 2019), the consequent activation of inhibitory G-proteins and decreases in intracellular signaling (Brumovsky et al., 2007) and hyperpolarization (Melnick, 2012; Smith et al., 2007) may reduce the net pain excitation:inhibition ratio, tipping the balance towards pain relief. But what is the relative contribution of each of the two key Y1-expressing substrates of excitatory neurotransmission in the dorsal horn, Y1-INs and the central terminals of peptidergic primary afferent neurons? An emerging body of literature has begun to address this question, with an initial focus on two methods to selectively ablate Y1-INs: intrathecal administration of NPY conjugated to the saporin neurotoxin (NPY-saporin) and site-specific conditional knockout of Y1-Cre lineage neurons.

1.6.1 Selective ablation of spinal Y1-INs with NPY-saporin

NPY-saporin is an NPY-conjugated ribosomal toxin that is selectively endocytosed and internalized within Y1-expressing neurons (Lemons and Wiley, 2012; Wiley et al., 2009). As with other peptide-saporin conjugates, intrathecal administration of NPY-saporin selectively ablates dorsal horn Y1-INs, while sparing other subpopulations of neurons (including those expressing

the mu opiate receptor or the neurokinin-1 receptor) as well as Y1-expressing DRG neurons (Nelson et al., 2019; Wiley et al., 2009). There is considerable evidence that intrathecal neuropeptide-saporin conjugates do not produce toxicity in DRG neurons either because they are not internalized into primary afferent terminals, or, if internalized, are not axonally transported to cell bodies in the DRG (Kline IV and Wiley, 2008; Wiley et al., 2009; Wiley and Kline Iv, 2000).

Acute nociceptive reflexes and pain in the absence of injury. When tested in the hotplate test (48-56 °C), a conventional assay of nocifensive reflexive withdrawal, intrathecal NPY saporin did not change paw withdrawal latency (Nelson et al., 2019; Wiley et al., 2009). NPY-saporin also failed to change the hindpaw withdrawal response to noxious radiant heat (Hargreaves' test), noxious pin prick, and von Frey hairs (Nelson et al., 2019). On the other hand, NPY-saporin did decrease nocifensive responses thought to engage supraspinal pain modulatory systems. For example, NPY-saporin reduced hindpaw licking and guarding in a 44 °C hotplate assay of affective pain, reduced ongoing nociception during both phases of the response to intraplantar injection of dilute formalin, and reduced aversion to a 10 °C cold plate (Lemons and Wiley, 2012; Wiley et al., 2009). NPY saporin did not alter motor control in uninjured rats as assessed by time on an accelerating rotarod or general activity measures in an open field arena (Nelson et al., 2019). Taken together, these data indicate that Y1-INs contribute to the affective components of acute pain transmission without impinging upon motor coordination or the protective nocireflexive components of acute pain (**Table 1**).

Ablation of Y1-INs with NPY-saporin did not alter responsiveness to non-noxious von Frey filaments or noxious pinprick (Nelson et al., 2019). In contrast, ablation of excitatory SST-

INs decreased mechanical sensitivity to non-noxious von Frey filaments and abolished responsiveness to noxious pinprick (Duan et al., 2014). Furthermore, hindbrain and spinal cord conditional knockout of *Sst* from SST-INs increased mechanical sensitivity to von Frey filaments (Huang et al., 2018). Somatostatin is well recognized as a pain inhibitory peptide that hyperpolarizes dorsal horn interneurons (Jiang et al., 2003; Kim et al., 2002; Murase et al., 1982). Thus, excitatory SST-INs have a pronociceptive role in mechanosensation and the inhibitory somatostatin peptide has a complimentary antinociceptive role in mechanotransduction, together indicating that SST-INs are critical for baseline mechanosensitivity. This might seem to be inconsistent with the fact that Y1-INs contain extensive somatostatin mRNA (**Figure 5**) and ablation of Y1-INs does not affect mechanical sensitivity at baseline. However, the Y1-IN population is smaller than the SST-IN population (~60% of excitatory interneurons in laminae I-II of dorsal horn) (Gutierrez-Mecinas et al., 2016). The SST-IN population is transcriptomically, immunohistochemically, morphologically, and electrophysiologically heterogenous and overlaps with numerous classes of excitatory dorsal horn interneurons exclusive of the Y1-IN population (Chamessian et al., 2018; Duan et al., 2014; Gutierrez-Mecinas et al., 2016; Häring et al., 2018; Peirs et al., 2020; Todd, 2017). Conversely, Y1-INs are a smaller subclass of excitatory dorsal horn interneurons that often express *Grp* mRNA (**Figure 5**) (Sathyamurthy et al., 2018), and neither ablation nor chemogenetic inhibition of dorsal horn GRP-Cre interneurons altered responsiveness to von Frey filament or pin prick stimulation (Albisetti et al., 2019). We suggest that it is a *Grp*- or *Npy1r*-negative subpopulation of SST-INs that regulates baseline mechanosensitivity. Future work can utilize results from high-throughput transcriptomic datasets to develop refined Flp- and Cre- mouse lines. This will allow more selective targeting of

increasingly smaller dorsal horn neuronal populations to better identify microcircuits responsible for individual behaviors.

Tissue and nerve injury models of persistent pain: Intrathecal administration of NPY-saporin reduced several operant and cognitive measures of CFA-induced allodynia, including responsiveness to cold temperatures in a thermal preference assay (two chamber 15 °C vs. 45 °C) , feeding interference (overcome a 10 °C floor plate to consume a sweet solution), and an escape task (climb onto a shelf to avoid a 10 °C floor plate), but did not interfere with systemic morphine-induced analgesia (Lemons and Wiley, 2012). Similarly in the SNI model of neuropathic pain, NPY-saporin dose-dependently reduced the development of mechanical allodynia (hindpaw withdrawal response to von Frey filaments), mechanical hyperalgesia (response to blunt pin), and cold allodynia (hindpaw withdrawal response duration to acetone droplet evaporation) (Nelson et al., 2019). Together, these directed lesion studies support the idea that the Y1-IN subpopulation of dorsal horn neurons is necessary for the maintenance of both mechanical and cold modalities of nociceptive transmission in chronic pain states.

1.6.2 Selective ablation of spinal Y1-Cre lineage INs with intersectional genetics

Goulding and colleagues restricted the expression of diphtheria toxin receptors or inhibitory designer receptors to Y1-Cre lineage neurons in the spinal cord and then applied diphtheria toxin or clozapine-N-oxide (Acton et al., 2019). The resulting ablation or inhibition of Y1-Cre lineage neurons did not alter responsiveness to noxious stimulation, be it cutaneous heat or mechanical pressure or hindpaw injection of capsaicin or formalin. Contrary to the NPY-saporin studies, however, ablation or silencing of Y1-Cre lineage neurons in the adult mouse reduced

sensitivity to light punctate touch using von Frey filaments (Acton et al., 2019). A probable explanation for this discrepancy is that in addition to the tight band of somatostatin- and Y1-INs in adult superficial dorsal horn (Duan et al., 2014; Nelson et al., 2019), the Y1-Cre lineage captures additional populations of neurons that appear to represent transient developmental expression of Y1 in the low-threshold mechanosensor-recipient zone (LTMR-RZ) in deeper laminae. Because the LTMR-RZ processes input from low-threshold mechanoreceptors (ie. Aß fibers) (Abraira and Ginty, 2013; Moehring et al., 2018), their ablation, rather than those of the Y1-INs expressed in the adult, likely explains the reduced sensitivity to light punctate touch. Still, this study sets the stage for important studies to assess the role of Y1-INs in chronic pain states. One such study could be the intraspinal administration of recombinant adeno-associated viruses (rAAVs) carrying inhibitory chemical- or opsin-gated channels into the spinal cords of Y1-Cre mice (Haenraets et al., 2018, 2017). This approach will allow the selective manipulation of adult Y1-INs and avoids the transient developmental expression of Y1 seen in the Y1-Cre lineage studies. Future studies might then probe inhibition of Y1-INs using chemogenetics or optogenetics in both naïve and chronic pain states. Such studies would complement and extend the NPY-saporin studies in clarifying the role that YI-INs play in the development and maintenance of chronic pain.

1.7 Where do Y1-INs fit within the dorsal horn microcircuitry of chronic pain?

It is becoming increasingly clear that different injury conditions engage distinct dorsal horn spinal microcircuits to mediate allodynia (Peirs et al., 2021, 2015; Peirs and Seal, 2016). Accordingly, Y1 agonists may inhibit pain differently depending on the type of injury, e.g. inflammation vs. nerve injury, as we previously hypothesized (Smith et al., 2007).

Inflammatory pain: In the context of inflammation, Y1 agonists likely prevent C- and Aδ-fiber primary afferent nociceptive transmission from being propagated to lamina I nociceptive projection neurons in the dorsal horn. This effect may occur via both pre- and postsynaptic mechanisms. First, Y1 agonists may hyperpolarize Y1-INs that are the postsynaptic targets of C-fibers (Miyakawa et al., 2005). One such postsynaptic target may be calretinin-positive Y1-INs; dorsal horn interneurons that express calretinin have been increasingly implicated in inflammatory pain (Peirs et al., 2015), and we find that there is ~19% colocalization between calretinin- and Y1-immmunoreactive neurons in the rat dorsal horn (Nelson et al., 2019). Second, Y1 agonists may act presynaptically on peptidergic, capsaicin-sensitive primary afferent terminals that contain Y1 receptors to reduce primary afferent transmitter release (Gibbs et al., 2004; Taylor et al., 2014), although this remains controversial; Moran and Smith reported that unlike Y2 agonists, the Y1 agonist F^7P^{34}NPY did not suppress excitatory transmission at the central terminal of presynaptic primary afferent neurons (Moran et al., 2004). Third, Y1 agonists may act collectively at both pre- and postsynaptic targets to reduce inflammatory hyperalgesia.

Neuropathic pain: The dorsal horn circuitry of mechanical allodynia after peripheral nerve injury is believed to involve the propagation of low-threshold input from Aß-fibers. For example, selective pharmacological inhibition of A-fibers suppressed mechanical allodynia after chemotherapy, nerve injury, and diabetic neuropathy, while inhibition of C-fibers did not (Xu et al., 2015). Because Y1 is exclusively found in small, peptidergic DRG neurons and only sparsely expressed at their central terminals, we suggest that Y1-INs in neuropathic pain circuits are inhibited by Y1 agonists at a site that is downstream of Aß-fiber input. As illustrated in **Figure 6**,

the propagation of low-threshold input from Aß-fibers is thought to activate disinhibited PKCg interneurons in inner lamina II that transmit light touch in a dorsally-directed microcircuit to lamina I projection neurons (Lu et al., 2013; Peirs and Seal, 2016; Petitjean et al., 2015; Todd, 2017). This circuit begins with PKCg interneurons that first synapse onto excitatory transient central cells, which in turn synapse onto excitatory vertical cells, that then target lamina I pain projection neurons (Lu et al., 2013). We hypothesize that Y1-INs are a subset of these transient central cells, based on both their morphology and their firing patterns in response to NPY, as discussed in section **1.1.2**. Furthermore, the only transient central cell population that has been identified to date is the GRP population (Dickie et al., 2019), and both single nucleosome RNA-sequencing (Sathyamurthy et al., 2018) and the *in situ* hybridization results of **Figure 5** demonstrate significant overlap between *Npy1r* and *Grp*. Taken together, these results provide the premise for our hypothesis that spinally-directed Y1 agonists prevent the propagation of light-touch information to spinal projection neurons by inhibiting Y1-IN transient central cells (Nelson et al., 2019).

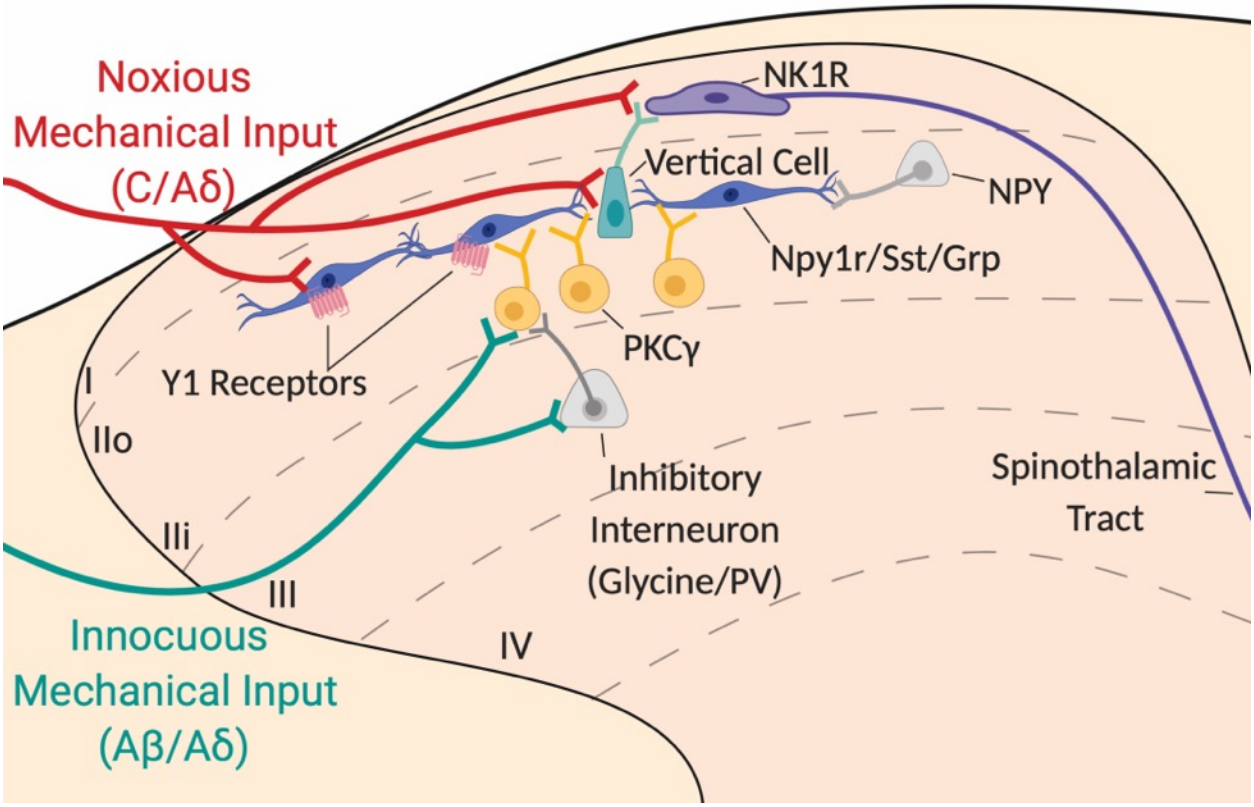

Figure 6. Hypothetical contribution of the Y1-IN in the ascending dorsal horn microcircuit for mechanical pain

Noxious mechanical inputs activate C/Aδ nociceptors (red) that project into the superficial laminae of the dorsal horn and synapse onto Y1-INs (dark blue), projection neurons that express the neurokinin receptor type 1 (NK1R) (purple), and/or vertical cells (green). Inhibitory NPY interneurons (light grey) may "gate" some of these nociceptive inputs at the Y1-IN. Innocuous mechanical inputs activate Aß/Aδ myelinated afferents (green) that project into deeper laminae of the dorsal horn and synapse onto interneurons marked by the expression of protein kinase C γ (PKCγ) (yellow). However, feedforward inhibition via inhibitory glycinergic and parvalbumin (PV) interneurons (light grey) prevents the activation of PKCγ interneurons. In the context of neuropathic pain, feedforward inhibition onto PKCγ interneurons is lost and innocuous light touch inputs are able to activate a dorsally-directed microcircuit from PKCγ interneurons onto transient central cells (Npy1r/SST/GRP neurons) that synapse onto vertical cells, ultimately leading to the activation of ascending NK1R interneurons that travel via the anterolateral tracts in the contralateral spinal cord to be processed via higher order pain centers such as the lateral parabrachial nucleus. Published in (Nelson and Taylor, 2021).

1.8 NPY and Y1-INs in Itch

A rapidly emerging body of literature implicates NPY signaling at Y1-INs in the regulation of both mechanical and chemical itch (**Table 1**).

1.8.1 Intrathecal NPY inhibits mechanical and chemical itch

Mechanical Itch: Bourane *et al.* reported that the application of a 0.07 gram von Frey filament to the shaved nape of the neck in mice produced directed scratching behavior, thus establishing a new mouse model of mechanical itch (thought to represent the tickle-like experience of an insect walking on exposed skin) (Bourane et al., 2015). Intrathecal administration of the Y1-selective agonist [Leu^{31},Pro^{34}]-NPY reduced filament-induced scratching, indicating that exogenous administration of NPY acts at Y1 to dampen mechanical itch (Acton et al., 2019; Gao et al., 2018). Additionally, more recent work from Cui et al. indicates that aging may reduce NPY-IN expression and promote the manifestation of mechanical itch. The number of Tunel-positive NPY-INs is enhanced in aged (24-month-old) mice and they exhibit increased scratching in reponse to nape stimulation. Furthermore, inhibition of NPY (i.t. anti-NPY IgG) in young mice enhances mechanical itch, whereas, i.t. NPY or [Leu^{31},Pro^{34}]-NPY reduced filament-induced scratching in aged mice (Cui et al., 2021).

Chemical Itch: Intradermal injection of pruritogenic compounds, such as histamine or the mast cell degranulator 48/80, increases duration and frequency of scratching bouts. Intrathecal [Leu^{31},Pro^{34}]-NPY reduced the duration of scratching behavior but not the frequency of scratching bouts induced by either 48/80 or histamine (Gao et al., 2018). Similarly, intrathecal administration

of the Y2 agonist, peptide YY (PYY)3–36, also reduced 48/80- and histamine-induced scratching (Ma et al., 2020). These data indicate that exogenous administration of NPY acts at Y1 and Y2 receptors to dampen chemical itch. Additionally, although not exactly chemical itch but similar, intrathecal NPY potently inhibits intrathecal morphine-induced itch behavior (Wang et al., 2021). The chemical itch circuit involves a specialized relay from periphery to spinal cord dorsal horn. Neuropeptide natriuretic polypeptide b (Nppb) is expressed in somatostatin positive DRG neurons that respond to chemical pruritogenic stimuli in the periphery (Huang et al., 2018). NPPB-expressing primary afferents subsequently activate GRP neurons in the spinal cord that in turn activate gastrin releasing peptide receptor-expressing INs (GRPR-INs) and begin the supraspinal transmission of itch (Jakobsson et al., 2019; Mishra and Hoon, 2013; Pagani et al., 2019; Solinski et al., 2019). Y1 agonists may inhibit chemical itch transmission via hyperpolarization of interneurons coexpressing Y1, SST, and GRP in the superficial dorsal horn (Jakobsson et al., 2019; Wang et al., 2021) (**Figure 7**). Additionally, ~90% of NPPB-expressing DRG neurons coexpress Y2 (Ma et al., 2020). We speculate that intrathecal NPY may prevent the release of pruritogenic neurotransmitters from Nppb-expressing central terminals via Y2 activation and suggest that NPY may represent a therapeutic target for chronic itch at both Y1 and Y2 receptors (**Figure 7**).

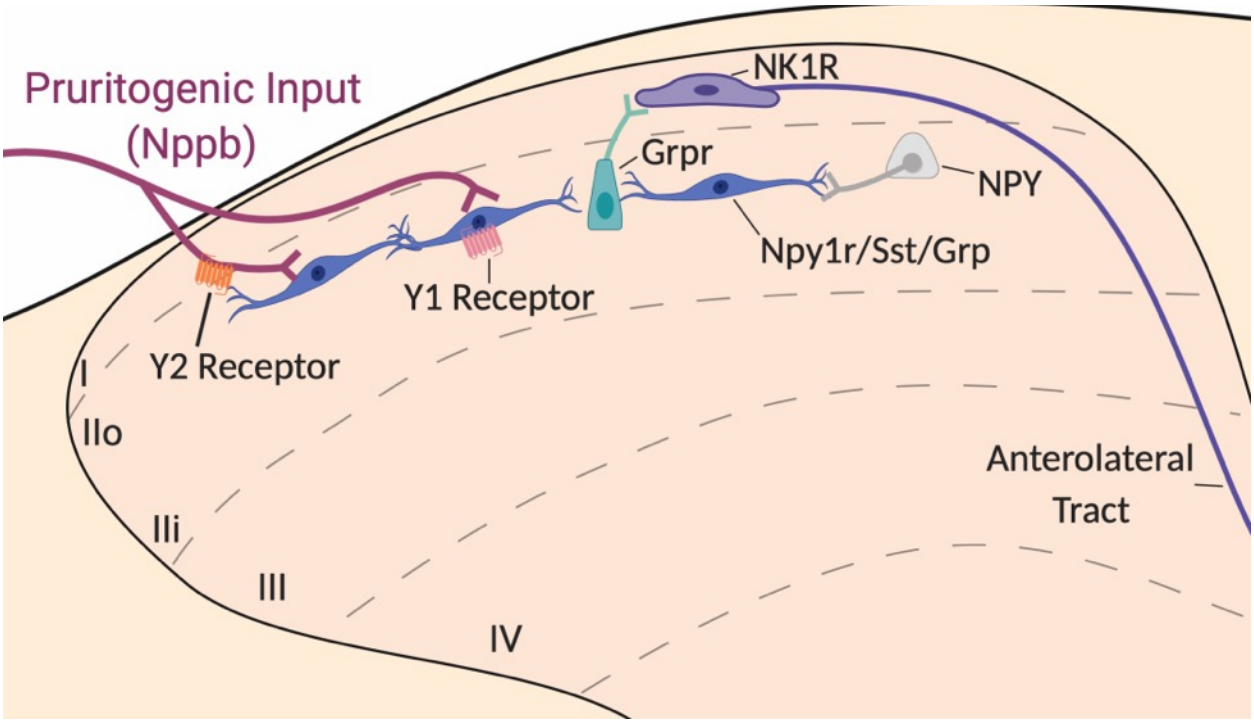

Figure 7. Hypothetical contribution of the NPY Y1 and Y2 receptors in the ascending dorsal horn microcircuit for chemical itch

Natriuretic polypeptide b-expressing (Nppb) pruritogenic inputs (maroon) project into the superficial laminae of the dorsal horn and synapse onto Y1-INs (dark blue) that co-express somatostatin (Sst) and gastrin releasing peptide (Grp). The central terminals of the Nppb-expressing pruritogenic inputs express the Y2 receptor (orange). Y1-INs synapse onto interneurons marked by the expression of gastrin releasing peptide receptor (Grpr) which in turn activate ascending itch projection neurons that express the neurokinin receptor type 1 (NK1R) (purple). NPY interneurons (light grey) may "gate" some of these pruritogenic inputs at Y1-INs or Y2-expressing terminals. Thus, endogenous or exogenous NPY can act at either or both NPY receptors to dampen the transmission of chemical itch. This figure is adapted from (Jakobsson et al., 2019; Ma et al., 2020). Published in (Nelson and Taylor, 2021).

1.8.2 Ablation of spinal NPY-Cre lineage INs induces spontaneous and mechanical itch

NPY-expressing neurons represent approximately one-third of spinal inhibitory interneurons in the superficial dorsal horn (Boyle et al., 2017). Selective ablation of spinal NPY-Cre lineage interneurons induced spontaneous scratching behaviors as well as mechanical (but not chemical) itch (Bourane et al., 2015). These data suggest that NPY-Cre lineage interneurons tonically inhibit spontaneous scratching and mechanically-evoked itch, with the caveat that ablation can lead to confounding compensations that include circuit rearrangements.

1.8.3 Spinal NPY-Cre ablation-induced itch is attenuated by lesion of spinal Y1-Cre or Ucn3-Cre INs

NPY-Cre interneuron ablation-induced scratching could be prevented with concomitant ablation of Y1-Cre lineage neurons (Acton et al., 2019). By contrast, ablation of somatostatin-Cre (SOM-Cre) lineage neurons had no effect (Acton et al., 2019). These disparate results following Y1-Cre and SOM-Cre ablation are surprising because the vast majority of Y1-INs are somatostatin-positive (Nelson et al., 2019; Sathyamurthy et al., 2018; Zhang et al., 1999) (**Figure 5**). As described in Section **1.4.2**, one explanation for this discrepancy may be the transient expression of Y1-Cre in the LTMR-RZ. Further studies are needed to determine whether ablation of Y1-Cre neurons in superficial lamina II, or deeper Y1-Cre neurons in the LTMR-RZ, are responsible for loss of filament-induced itch.

Pan *et al.* reported that NPY-Cre ablation-induced mechanical itch is prevented by concomitant ablation of a small excitatory interneuron population marked by Urocortin 3 expression (Ucn3-INs) (Pan et al., 2019). The Ucn3-INs are found in inner lamina II and outer

lamina III of the dorsal horn and receive direct Aß low-threshold mechanosensory input (Pan et al., 2019). Very few Ucn3-INs exhibit *Npy1r* expression (14.3% colocalization), and in recordings from Ucn3-INs in spinal cord slices, application of [Leu^{31},Pro^{34}]-NPY did not attenuate action potential induction following current injection (Pan et al., 2019). These results imply that Ucn3-INs exhibit little to no functional Y1, and it is a very small population of Ucn3/Y1-INs that gate mechanical itch, or, more likely, Y1-INs are not involved in gating mechanical itch at all. Further studies, including investigations of a possible Y1-Cre lineage/Ucn3-IN overlap, are warranted to determine if a small population of Ucn3/Y1 interneurons are "gated" via NPY-Cre interneurons and mediate mechanical itch.

1.9 Scope of thesis

There is a critical and pressing need to develop safe, nonaddictive, and efficacious analgesic drugs. Thirty years of preclinical research suggest that NPY is potently antihyperalgesic in a myriad of models of chronic pain (**Table 1**). NPY likely acts via the Y1 receptor to hyperpolarize Y1-INs, a subclass of excitatory interneurons in the superficial dorsal horn that are likely to be essential for pain. The present studies were designed to test the overarching hypothesis that *exogenous or endogenous spinal neuropeptide Y potently inhibits the behavioral signs of chronic pain via inhibiting pain facilitatory Y1 receptor-expressing dorsal horn interneurons.* In these studies we determine that the specific anti-nociceptive target for NPY in the setting of neuropathic pain is at Y1-INs. Further, we characterize the histochemical heterogeneity of the dorsal horn Y1-IN population and utilize genetic tools to selectively modulate Y1-INs and Y1-IN subpopulations in *vivo* in both naïve and neuropathic pain

conditions. We extend this work to both macaque and human spinal cord tissue to demonstrate the conservation of Y1-IN expression across higher-order mammalian species. Lastly, we demonstrate that endogenous NPY-Y1 signaling can synergistically work with mu opiate receptor signaling to maintain chronic postsurgical pain in remission. Altogether, these studies provide extensive pre-clinical evidence that spinally-directed Y1 agonists may be a novel therapeutic for the treatment of chronic pain via inhibiting pain facilitatory Y1 receptor-expressing dorsal horn interneurons.

2.0 Facilitation of neuropathic pain by the NPY Y1 receptor-expressing subpopulation of excitatory interneurons in the rat dorsal horn

2.1 Introduction

Peripheral nerve damage can lead to a debilitating neuropathic pain syndrome that persists for years (Jensen et al., 2007). Even the most powerful opioid analgesics lack reliable efficacy, and instead cause an unacceptable set of adverse effects that often includes addiction (Finnerup et al., 2015). To address this problem, distinct populations of excitatory interneurons have been identified within the spinal dorsal horn microcircuitry that are required for the behavioral expression of neuropathic pain (Braz et al., 2014; Duan et al., 2014; Gangadharan and Kuner, 2015; Peirs et al., 2015; D. Wang et al., 2018; Wang et al., 2013). These subpopulations can be defined by the expression of either a small molecule neurotransmitter (e.g. gamma-aminobutyric acid, GABA), a neuropeptide transmitter (e.g. somatostatin) (Duan et al., 2014), transporter protein (e.g. vesicular glutamate transporter 3, VGlut3) (Peirs et al., 2015), or opioid receptor (e.g. DOR) (D. Wang et al., 2018); however, none of these neural population have been found to be readily druggable targets for the development of pharmacological agents directed at non-opioid neurotransmitter receptors.

Both exogenous and endogenous NPY acts at Y1-INs within the dorsal horn to inhibit neuropathic pain. Intrathecal administration of NPY or the Y1 receptor agonist, [Leu^{31}-Pro^{34}]-NPY, dose-dependently reduced mechanical and cold hypersensitivity after spared sural nerve injury or chronic constriction injury to the sciatic nerve (Intondi et al., 2008; Kuphal et al., 2008; Malet et al., 2017). Likewise, either conditional NPY knockdown in NPY^{tet}-transgenic mice or

intrathecal administration of the Y1 antagonist BIBO 3304 elicited a robust and reliable increase in cold and mechanical hypersensitivity (Solway et al., 2011), indicating that neuropathic hyperalgesia is tonically inhibited by NPY that is endogenously released within the dorsal horn.

Y1-INs are highly expressed at the dorsal horn of the spinal cord, including several populations of small interneurons located throughout laminae I–III (Brumovsky et al., 2006, 2004, 2002; Ji et al., 1994). Immunohistochemical studies have localized Y1-INs to the dendrites and somas of somatostatin-positive dorsal horn neurons (Zhang et al., 1999). Since this population expresses VGLUT1 and VGLUT2 (Hökfelt et al., 2007; Todd et al., 2003), Y1-INs have been presumed to be glutamatergic, and thus excitatory (Brumovsky et al., 2007; Wiley et al., 2009). Indeed, we have postulated that Y1-INs are excitatory interneurons under an NPY-mediated inhibitory influence (Smith et al., 2007); however, rigorous immunohistochemical co-labeling of Y1-IN cell bodies in wild-type (non-transgenic) spinal cord tissue with markers of excitatory neurons has been difficult to interpret due to the intense plexus of dendritic and terminal staining that surrounds Y1-INs. To enhance Y1 resolution within dorsal horn neurons, we developed and evaluated a new intrathecal NPY injection strategy to promote receptor internalization, thereby concentrating Y1 from more distal dendritic locations to within the cell soma; the enhanced signal allowed quantification of Y1 co-localization with multiple markers of excitatory and inhibitory interneurons.

Next, to address the functional significance of spinal Y1R-expressing neurons to the development of neuropathic pain, we selectively lesioned Y1R-expressing dorsal horn interneurons using intrathecal administration of the NPY-conjugated ribosomal toxin, NPY-

saporin (Lappi and Wiley, 2012; Lemons and Wiley, 2012; Wiley et al., 2009). NPY-saporin selectively, reliably, and dose-dependently delivers the cytotoxic ribosome inactivating protein, saporin, into Y1R neurons following NPY Y1 receptor-mediated endocytosis saporin (Lemons and Wiley, 2012; Wiley et al., 2009). As with other peptide-saporin conjugates, NPY-saporin is selectively internalized by somatodendritic Y1 receptors on dorsal horn interneurons, while sparing axon terminals including those of $Y1^{+}$ DRG neurons (Wiley et al., 2009). Our approach, which uses NPY-saporin, readily discriminates between targets on cell bodies and axon terminals, and avoids pitfalls associated with the use of Y1-Cre transgenic mice that include germline recombination, transient expression, and aberrant expression at non-targeted sites (Song and Palmiter, 2018).

2.2 Methods

Animals: Male Sprague-Dawley rats (Charles Rivers Laboratories), delivered at 165–205g and weighing 235-260 g at time of surgery were used throughout the study. Animals were housed in a temperature-controlled room on a 12-hr light/dark cycle and were given chow and water ad libitum. All animal use protocols were approved by the IACUC of the University of Kentucky. All experiments and methods were performed in accordance with institutional relevant guidelines and regulations and in accordance with the NIH Guide for the Care and Use of Laboratory Animals.

Intrathecal delivery of NPY and NPY-saporin: *NPY*: Our initial attempts to visualize Y1-IN cell bodies failed due to the high background staining from the dense plexus of central terminals of primary afferent neurons, as noted previously (Brumovsky et al., 2006). To overcome

this problem, Brumovsky *et al* used tyramide signal amplification (TSA) method combined with confocal imaging in thin optical sections to visualize $Y1^+$ cell bodies (Brumovsky et al., 2006). Here, we used an alternative approach to enhance visualization of Y1-INs: we delivered spinal NPY to promote receptor internalization, thereby concentrating Y1 from more distal dendritic locations to within the cell soma. This was achieved following two intrathecal injections of NPY (30 µg) separated by 1 hour. One hour after the second injection, rats were deeply anesthetized with isoflurane and perfused with 0.1 M PBS containing heparin (10,000 USP units/L) followed by 10% buffered formalin.

NPY-Saporin: To selectively ablate spinal Y1-INs, the saporin-conjugated peptide NPY-saporin, or a control blank-saporin (Advanced Targeting Systems, San Diego, CA) was intrathecally injected at the lumbar level in a volume of 10 µl using a 25 µl Hamilton microsyringe attached to a 27-gauge disposable sterile needle under isoflurane anesthesia (5% induction; 1.5 – 2% maintenance). Blank saporin is an 11-amino acid, randomly-mixed version of the sequence of melanocyte-stimulating hormone. Its amino acid residues are typical of peptides that bind to G-protein-coupled receptors although this random peptide has no homologous sequences that which it can bind to *in vivo*. Blank-saporin was delivered at a 1000ng dilution. The needle was inserted into the subarachnoid space through the intervertebral foramen. A tail flick response was used as verification of correct placement of the needle and successful saporin delivery was verified via decreases in Y1 immunoreactivity.

Spared Nerve Injury (SNI) surgery: Fourteen days after intrathecal NPY-saporin or blank-saporin injection, animals underwent SNI surgery. SNI was performed as described

previously(Decosterd and Woolf, 2000; Intondi et al., 2008). Anesthesia was induced and maintained with 5% and 2-3% isoflurane, respectively. After shaving and Betadine wipe of the left hind limb, an incision was made in the skin at the level of the trifurcation of the left sciatic nerve. The overlying biceps femoris muscles were retracted, exposing the tibial, common peroneal, and sural nerve branches. The common peroneal and tibial nerves were ligated with 6-0 silk (Ethicon, Somerville, NJ), and then the knot and adjacent nerve (2 mm) were transected, leaving the sural branch intact. The muscle was sutured with 4-0 silk sutures and the wound was closed with 9-mm metal clips, followed by Neosporin®.

Behavioral Testing: Behavioral testing was conducted at baseline and 3, 8, 11, 14, 17, 21, 28, 35, 42, and 54 days post-SNI. In a separate cohort of rats, spinal cord tissue and dorsal root ganglia tissue were collected at 14 days post SNI surgery for immunohistochemistry. For naïve studies, rats received rotarod training for 2 days, then received intrathecal injection of NPY-saporin or blank-saporin. Testing in these rats was completed 2-3 weeks post intrathecal injection.

Mechanical Hyperalgesia, von Frey: To evaluate sensitivity to a non-noxious mechanical stimulus, we used an incremental series of 8 von Frey filaments of logarithmic stiffness (0.4-15 grams). The 50% withdrawal threshold was determined using the Up-Down method (Chaplan et al., 1994). Each filament was applied perpendicular to the lateral hindpaw surface with sufficient force to cause a slight bending of the filament. A positive response was defined by a rapid withdrawal of the paw within 5 seconds.

Mechanical Hyperalgesia, noxious pin: To evaluate sensitivity to a noxious mechanical stimulus, we gently and rapidly applied the point of a dull pin to the lateral aspect of the hind paw, avoiding damage to the skin. The duration of time with which the animal raised this paw was recorded, with a cut-off of 30 seconds. Three measurements were averaged.

Mechanical hyperalgesia, paw pressure: To assess sensitivity to increasing noxious mechanical pressure, animals were lightly restrained while extending the hind paw. The plantar surface was placed on the plinth between the calipers of the Randall-Selitto device (IITC) and increasing gram force was gradually applied on the surface of the paw until the animal exhibited a withdrawal or vocalization. Three measurements of gram force at time of response were averaged.

Cold Allodynia, acetone drop: To evaluate the response to a cool stimulus, we used a piece of PE-90 tubing, melted at the tip, to apply a drop (10-12 ul) of acetone to the lateral aspect of the ventral hindpaw. The duration of time with which the animal raised this paw was recorded, with a cut-off of 30 sec. Three measurements were averaged.

Heat Hyperalgesia, Hargreaves' irradiant heat: To evaluate the response to a heat stimulus, rats were placed in a clear Plexiglas box on a glass floor. The thermal stimulus consisted of a radiant heat source positioned under the glass floor directly beneath the hind paw. Voltage intensity was adjusted such that paw withdrawal latency was 10 ± 0.5 seconds. If the animal did not respond within 20 seconds, the heat was discontinued to prevent damage to the paw. Withdrawal responses to three stimulus pairs, delivered every five minutes, were averaged.

Heat hyperalgesia, hot plate: To evaluate the response to a heated floor stimulus, a single rat was placed on a 48, 52, or 56 °C surface within an acrylic enclosure (Columbus Instruments). The animal was immediately removed from the enclosure when it jumped, licked, or lifted a hind paw. Response latencies to three trials were averaged.

Motor coordination, rotarod: To evaluate motor coordination, rotarod testing was performed at 7 and 14 days post-saporin injection. Rats were trained on two training days prior to intrathecal injection. The rotarod accelerated 0.5 rpm every 5 sec, with a maximum speed of 40 rpm. Training involved repeated placement on the rotarod until one of the following was achieved: exposure to 20 sessions, or successful performance of at least 150 seconds for three consecutive trials. For experimental testing, rats were placed on the rotarod at one and two weeks post-intrathecal injection. Performance time, recorded in seconds, was determined when the animal fell off of the rotating bar, thus breaking a light beam. Five consecutive trials were averaged for each animal.

Integrated Exploratory Activity: To evaluate innate exploratory behaviors of rats in a dark novel "open field", a single rat was placed in a clear Plexiglas box on a Plexiglas floor. We evaluated activity using the automated Photobeam Activity System (PAS) with Flexfield Animal Activity System (San Diego Instruments, Inc, San Diego), coupled to a computer to eliminate human interaction and bias. Using 32 infrared photobeams, six main parameters were measured in six 5−min intervals: rearing events, active time and resting time, beam breaks, and distance traveled.

Immunohistochemistry: Animals were deeply anesthetized with pentobarbital (Fatal Plus, diluted to 200 mg/kg i.p., Med-Vet International, Mettawa, IL) and perfused transcardially with 200 ml of room temperature (RT), 0.01M phosphate buffered saline (PBS) with heparin (10,000 USP units/L) followed by 300 ml of ice-cold fixative (10% buffered formalin). The cord was removed and post-fixed for 4 hr in 10% buffered formalin (4°C) and then cryoprotected (30% sucrose in 0.01M PBS for 36-96 hr). L4-L6 transverse sections (35-40μm) were cut on a freezing microtome and collected in 0.01M PBS. The sections were washed three times in 0.01M PBS and then pretreated with 3% normal goat or donkey serum serum and 0.3% Triton X-100 to block non-specific binding. Sections were then incubated in a primary antibody, rabbit anti-Fos (1:20,000, Calbiochem), rabbit anti-Y1 (1:5,000, courtesy of Janice Urban), rabbit Anti-CGRP for mouse/rat (1:20,000, Bachem) and rabbit anti-NK1R (1:10,000, Neuromics) overnight at RT on a slow rocker. For fluorescence co-labeling studies, we used a rabbit anti-Y1R antibody (Neuromics) derived from the same antigen as that developed by Janice Urban and colleagues, but at a more concentrated dilution (1:500). Spinal cord sections were then co-incubated with Y1 antibody together with either markers of excitatory interneurons (mouse anti-calbindin, 1:1,000, Sigma; goat anti-calretinin, 1:5,000, Swant; guinea pig anti-PKCγ, 1:10,000, courtesy of Allan Basbaum; mouse anti-somatostatin, 1:500, GeneTex) or a marker of inhibitory interneurons (goat anti-Pax-2, 1:1,000, R&D systems). The tissue was then washed three times in 0.01M PBS, and incubated at RT in secondary antibody for either enzyme (1:200 dilution) or fluorescent (1:700 dilution) labeling. Secondary antibodies used for the co-localization studies were: Alexa 568-conjugated goat anti-rabbit; Alexa 568-conjugated donkey anti-rabbit; Alexa 488-conjugated goat anti-mouse; Alexa 488-conjugated goat anti-guinea pig; Alexa 488-conjugated donkey anti-goat (all 1:1,000;

Invitrogen). For fluorescent IB4 labeling, tissue was incubated in a primary IB4 antibody conjugated to FITC (1:500, Sigma) and cover-slipped with Prolong Gold with DAPI mounting medium (Molecular Probes).

Confocal microscopy, image processing, and quantification of Y1 co-localization: Representative confocal images of $Y1^+$ co-labeling with markers of excitatory or inhibitory interneurons were acquired with a Leica ABOS TCS SP5 inverted laser scanning confocal microscope, fitted with a 100x oil immersion objective (numerical aperture 1.46). The microscope is a Leica DMI 6000 with LAS AF 2.7.2.9586 software. Laser excitation lines and emission windows for the different fluorophores were: Alexa Fluor 488 - excitation 488 nm (Ar laser), emission 505–555 nm; Alexa Fluor 568 - excitation 543 nm (diode laser), emission 565–615 nm; DAPI - excitation 405 nm (HeNe laser), emission 435-485 nm. Line averaging was used to decrease signal to noise ratio. Adobe Illustrator CS6 (Adobe Systems Inc., Mountain View, CA) was used to assemble the multi-panel figures.

Quantification of staining in randomly-selected sections was performed with NIS Elements Advanced Research software. To distinguish immunohistochemical staining patterns of tibial and sural terminals, we selected ROIs spanning the medial-central and central-lateral regions, respectively, of lamina II of the tibial and sural across the mediolateral axis of the dorsal horn. Only DAPI-labeled cells were counted. Three animals per group and three slices per animal were quantified for Y1 and/or calbindin, calretinin, PKCγ, or Pax2.

Fluorescence microscopy, image processing, and quantification of Fos immunohistochemistry: Digital photomicrographs were captured from lumbar segment L4-L5

with a Nikon TE2000-E microscope with Metamorph software (Version 6.1r4, Universal Imaging Corp.). Immunoreactivity was quantified with NIH custom ImageJ software. Integrated density was determined by thresholding the images using the default algorithm within ImageJ to reduce background and include positively stained cells in spinal cord dorsal horns from the L4-L5 lumbar region. Integrated density of the region of interest (ROI) is equal to the product of ROI area and mean gray value. The mean gray value represents the sum of the intensity values for all pixels above the threshold in the ROI divided by the number of pixels above threshold within the ROI. This method controls for differences in background between slices and subjects. For quantification of Fos, an observer blinded to treatment manually counted punctate immunoreactive profiles in lamina I-V. Six animals per group and 4-6 slices per animal were quantified for Y1, CGRP, IB4, or NK1R.

Statistical Analysis: Data were analyzed using Prism software (GraphPad, San Diego CA). All data are expressed as mean ± SEM. Statistical significance was set at $P < 0.05$. Behavioral data were analyzed by two-way ANOVA with treatment as the between-subjects factor and time as the within-subject factor. Other data were analyzed by one-way or two-way ANOVA and Bonferroni or Tukey's post-hoc tests, or unpaired, two-tailed student T-tests.

2.3 Results

2.3.1 Expression of Y1 with markers of excitatory but not inhibitory interneurons in dorsal horn

Y1 immunoreactivity in the dorsal horn presents as a dense plexus of axons and dendrites that complicates analysis of co-labeling. We reduced this problem by pretreating animals with two

intrathecal injections of NPY (30 μg) separated by 1 hour so as to promote receptor internalization, thereby concentrating Y1 from more distal dendritic locations to within the cell soma. As illustrated in **Figure 8**, NPY pretreatment concentrated Y1 immunoreactivity within the cell soma, thereby permitting a more accurate assessment of spinal Y1-INs. We found Y1-INs to co-localize with multiple markers of excitatory neurons in superficial laminae: calbindin (**Figures 8A-B, 9A**), calretinin (**Figures 8C-D, 9B**), and somatostatin (**Figure 8H-I**), but neither PKCγ (which labels a band in inner lamina II) (**Figures 8E-F, 9D**) nor Pax2 (a marker of inhibitory neurons) (**Figures 8G-H, 9C**).

The colocalization of Y1 and somatostatin is consistent with studies utilizing Y1 immunoreactivity (Zhang et al., 1999) and transcriptional profile analyses (Chamessian et al., 2018). Neuronal phenotypes can be classified based upon the transcription factors that regulate the development of their lineage (Del Barrio et al., 2013; Gross et al., 2002; Wildner et al., 2013). Notable is Pax2, which continues to be expressed in mature GABAergic neurons. We found very little co-localization with Pax2 (**Figure 9C**), and therefore our results indicate that Y1-INs represent a large subpopulation of excitatory but not inhibitory interneurons.

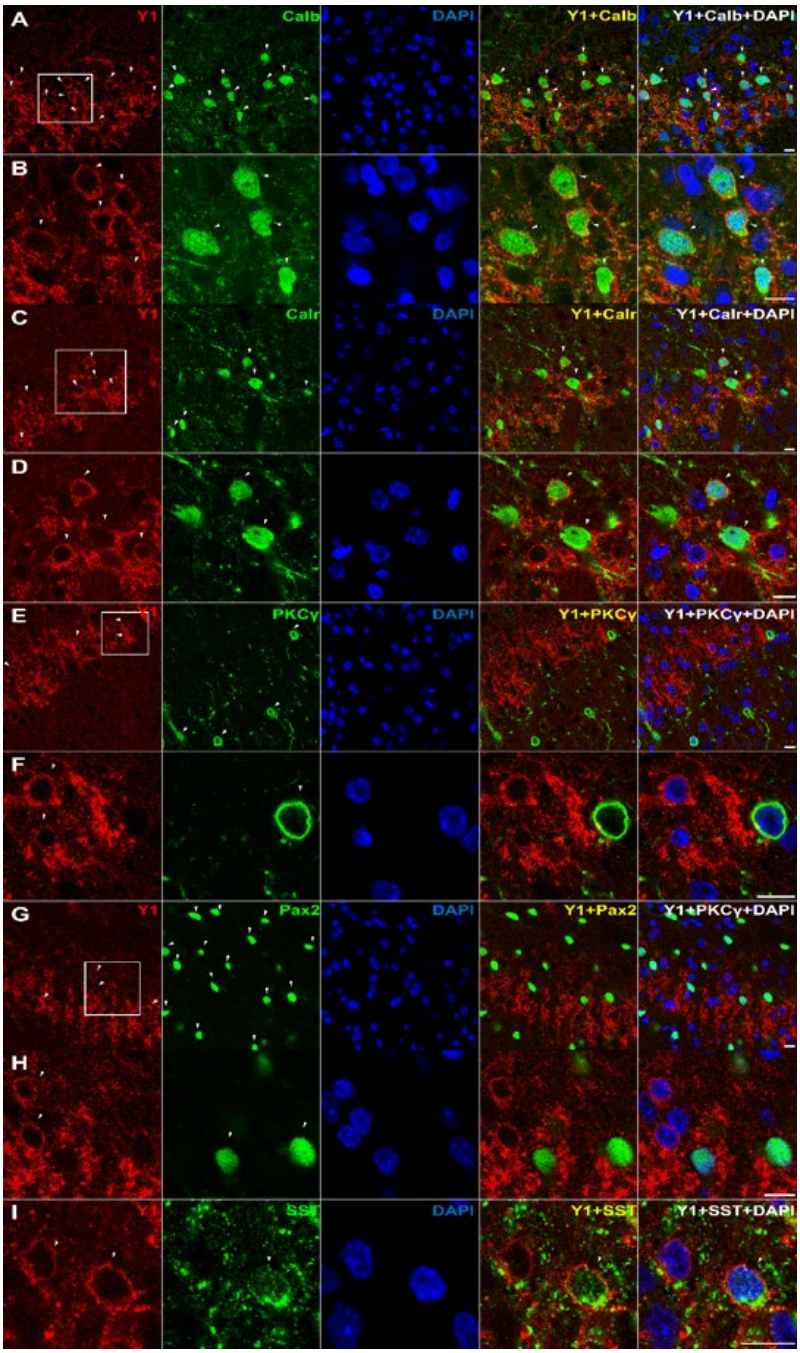

Figure 8. Y1-INs often co-express calbindin, calretinin, and/or somatostatin, but neither PKCγ nor Pax2. Co-staining of Y1 with DAPI and antibodies against **(A,B)** calbindin, **(C,D)** calretinin, **(E,F)** PKCγ, **(G,H)** Pax2, or **(I)** somatostatin. Confocal images of transverse L4-L6 sections from rat dorsal horn were taken with a 100X objective from lamina II. Dorsal side is up. Images in B, D, F, and H are zoomed in from the white square boxes shown in A, C, E, and G, respectively. Arrows indicate instances of Y1 co-labeling. Scale bars: 10µm. (**Confocal images were obtained by Dr. Weisi Fu*)

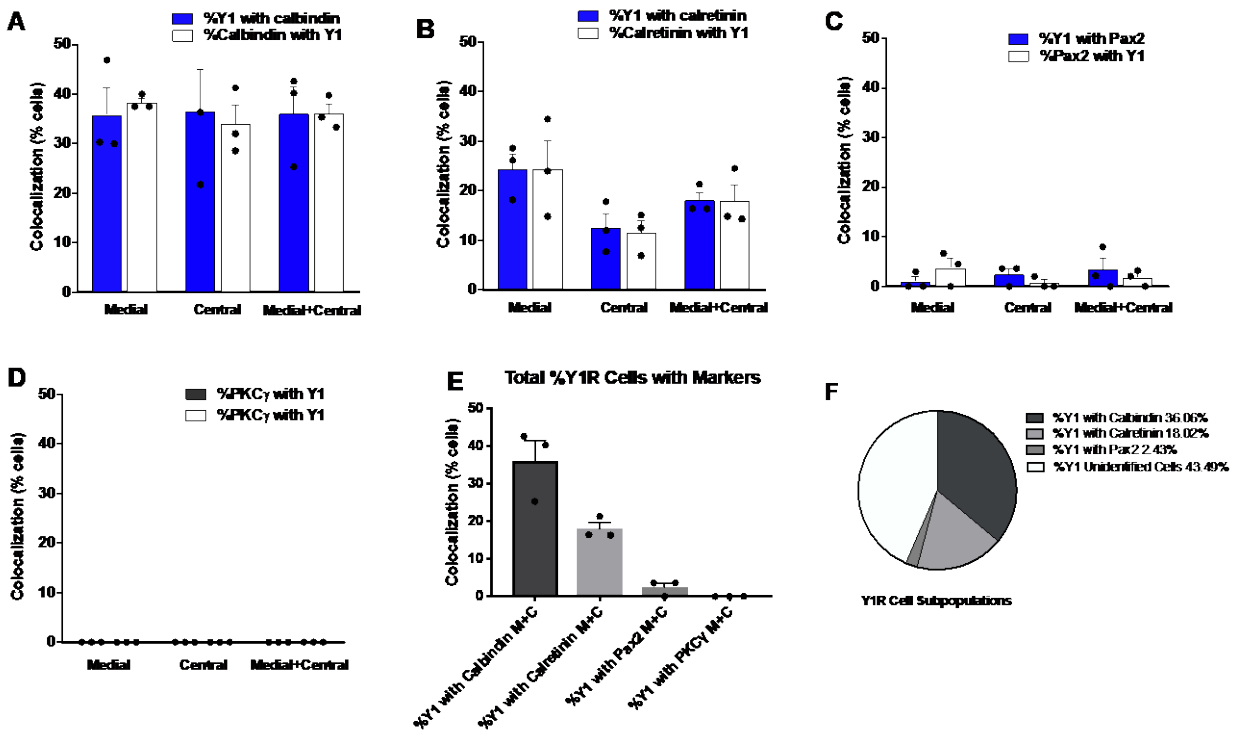

Figure 9. Quantification of Y1 immunoreactivity co-localization

Quantification of colocalization in medial and central dorsal horn of (**A**) Calbindin-, (**B**) Calretenin-, (**C**) Pax2-, and (**D**) PKCγ- with Y1-immunoreactivity. The relative distribution of subpopulations of Y1-INs as determined by % colocalizations can be seen in (**E-F**). N = 3 rats per antibody with N=3 transverse sections averaged per animal.

2.3.2 NPY-saporin selectively ablated Y1-expressing spinal interneurons

The highest dose of NPY-saporin in Wiley et al. (2009) was 750ng. This dose reduced Y1 immunoreactivity in the dorsal horn by approximately 40% (see their Table 1) (Wiley et al., 2009). In an attempt to lesion a greater number of Y1-INs, we used not only the 750 ng dose, but also a higher dose of 1000 ng. As illustrated in **Figure 10 (A-C)**, we found that the 1000 ng dose reduced Y1 staining by approximately 50% as compared to control treatment with an injection of a scrambled peptide conjugated to the saporin toxin. To determine the selectivity of intrathecal NPY-saporin for Y1-INs, we evaluated not only Y1 immunoreactivity, but also immunoreactivity for NK1R (a marker of spinal cord nociception-responsive projection neurons that ascend to the brain), as well as CGRP and IB4 (markers of the central terminals of primary afferent terminals). By contrast, NPY-saporin did not change IB4 staining or NK1R-, or CGRP-immunoreactivity relative to the blank-saporin ($P > 0.05$; **Figure 10D-L**). These findings indicate that Y1-expressing primary afferents and projection neurons were spared by the toxin, and are consistent with Wiley and colleagues who reported that intrathecal NPY-saporin did not change the number of Y1-expressing DRG neurons, nor dorsal horn staining for either NK1R or mu opiate receptor (MOR) as compared to blank-saporin (Wiley et al., 2009).

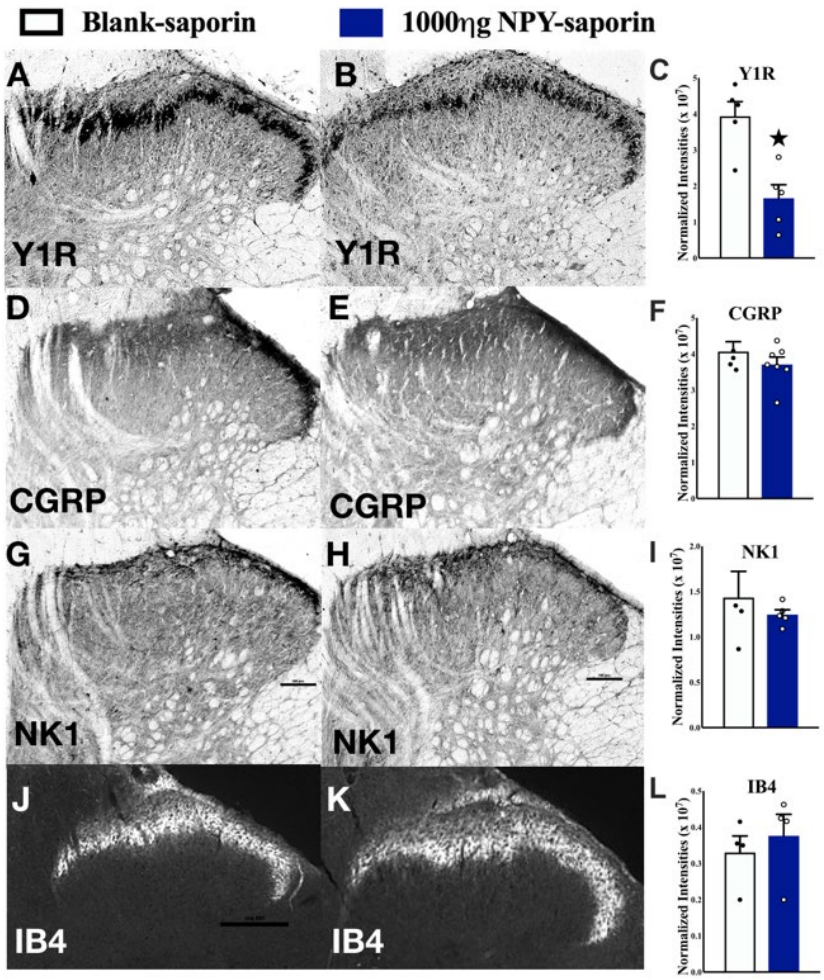

Figure 10. NPY-saporin lesion selectively reduces Y1 immunoreactivity in the dorsal horn

Y1R, CGRP, and NK1 immunoreactivity and IB4 staining in the dorsal horn of naïve rats 14 days after intrathecal injection of **(A,D,G,J*)* blank saporin or **(B,E,H,K)** 1000 ng NPY-saporin. NPY-saporin decreased **(C)** Y1R but did not change staining in the dorsal horn of **(F)** CGRP, **(I)** NK1R or **(L)** IB4 as compared to blank-saporin controls. Values are expressed as integrated density of staining in dorsal horn. ★ $P < 0.05$ compared to blank-saporin. Data represent mean ± SEM. Scale bars: 100µm. (**Images were obtained by Renee Donahue*)

2.3.3 NPY-saporin reduced the development and maintenance of neuropathic pain without changing normal motor behaviors or nociception

Previous studies indicate that NPY-saporin decreased behavioral signs of early inflammatory pain (Lemons and Wiley, 2012), including Phase II of the formalin test, and reduced hotplate reflex responses to low (44°C) intensity heat (Wiley et al., 2009). To determine the contribution of Y1-INs to chronic neuropathic pain, we delivered NPY-saporin 14 days prior to SNI and evaluated the progression of nerve-injury induced hyperalgesia and allodynia over several weeks. SNI produced mechanical hypersensitivity (von Frey), cold hypersensitivity (acetone drop), and mechanical hyperalgesia (blunt pin prick) that peaked at approximately 21 days in blank-saporin-treated control rats (**Figure 11**). While both mechanical and cold hypersensitivities reached a steady-state that was maintained until at least 54 days post-SNI, pin prick mechanical hyperalgesia gradually decreased from Day 28 through Day 54. Relative to rats treated with blank-saporin, NPY-saporin dose-dependently reduced mechanical hypersensitivity (Treatment: $F_{2,20}$ = 6.42, P = 0.007), cold hypersensitivity (Treatment: $F_{2,20}$ = 9.76, P = 0.0011), and mechanical hyperalgesia (Treatment: $F_{2, 20}$ = 13.43, P = 0.0002). Secondary analysis of each NPY-saporin group compared to the blank-saporin control group revealed that the 750 ng did not change behavioral signs of neuropathic pain at earlier (*Days 3 – 17)* timepoints (P > 0.05), but decreased vF mechanical hypersensitivity ($F_{1,13}$ = 12.0, P = 0.0042), cold hypersensitivity ($F_{1,13}$ = 4.53, P = 0.05), and mechanical hyperalgesia ($F_{1, 13}$ = 5.29, P = 0.039) at later timepoints (*Days 21 – 54).* By contrast, the 1000 ng dose of NPY-saporin decreased behavioral signs of neuropathic pain at both earlier timepoints (*Days 3 – 17)*: vF mechanical hypersensitivity ($F_{1,15}$ = 7.93, P = 0.013), cold hypersensitivity ($F_{1,15}$ = 8.20, P = 0.012), pin prick mechanical hyperalgesia ($F_{1, 15}$ = 14.0, P = 0.002), as well as later timepoints (*Days 21 – 54)*: vF mechanical hypersensitivity ($F_{1,15}$ = 14.2, P

= 0.0019), cold hypersensitivity ($F_{1,15}$ = 18.0, P = 0.0007) and mechanical hyperalgesia ($F_{1,13}$ = 25.4, P = 0.0001).

Analysis of area under the curve (AUC) illustrates that effect size depends on the somatosensory modality, time of testing after injury, and dose of NPY-saporin, Thus, while the 750 ng dose did not change mechanical withdrawal thresholds as compared to blank-saporin controls over Days 3-17 (just a 1.6% increase), it produced a quite robust, greater than 3-fold increase in mechanical thresholds over Days 21-54 (360% increase); also the 750 ng dose decreased behavioral signs of noxious mechanical hyperalgesia and cold allodynia by approximately one-third regardless of timepoint (Days 3-17: 30.3% reduction in cold withdrawal response, 32.3% increase in pin prick withdrawal; Days 21-54: 36.3% reduction in cold withdrawal response, 33.7% increase in pin prick withdrawal). The 1000 ng dose produced even greater effects as compared to blank-saporin controls over Days 3-17 (increased mechanical withdrawal thresholds by 114%, reduced cold withdrawal response by 68.5%, and increased pin prick withdrawal by 74.4%) and Days 21-54 (increased mechanical withdrawal thresholds by 458%, reduced cold withdrawal response by 64.6%, and increased pin prick withdrawal by 66.8%). In summary, the effects of NPY-saporin on neuropathic pain behaviors are strongest at later timepoints, and the higher dose recruits an additional effect on mechanical allodynia at early timepoints.

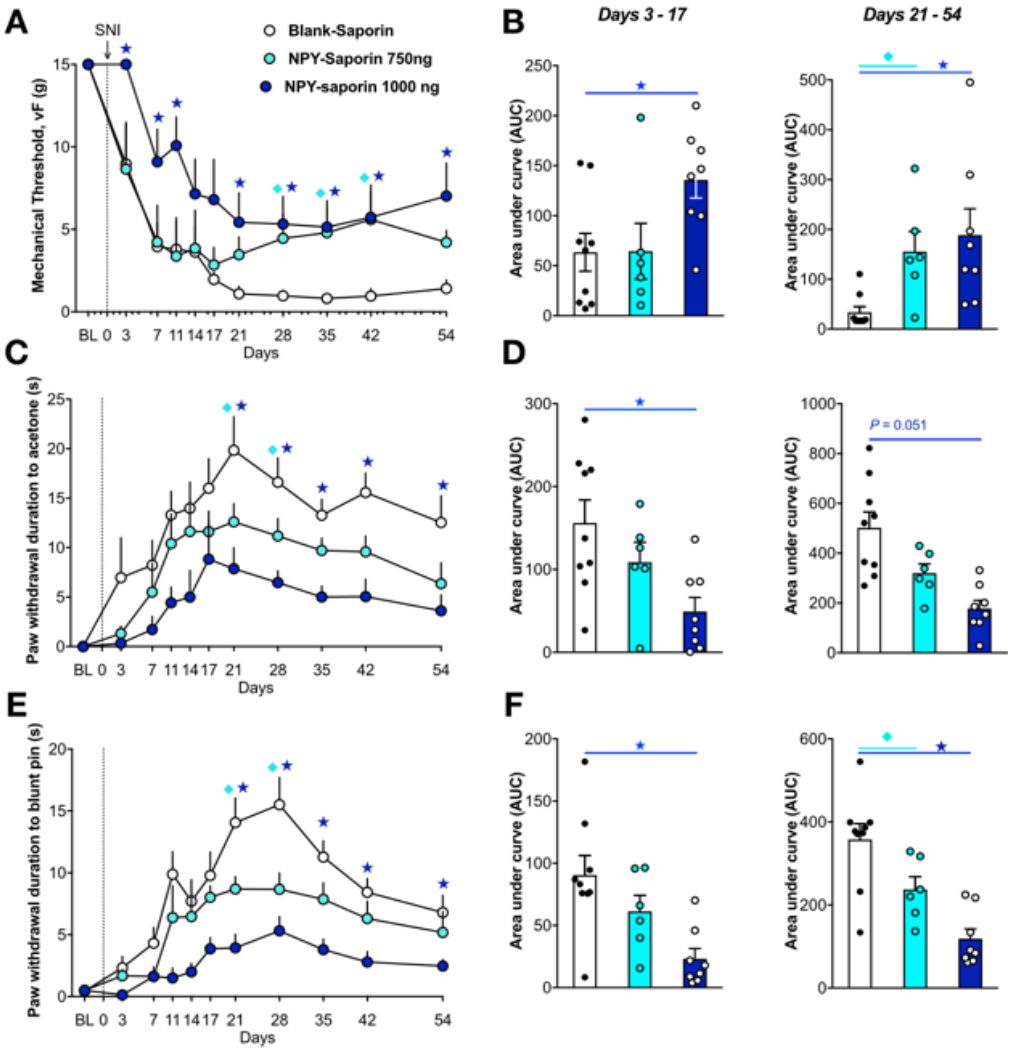

Figure 11. Lesion of spinal Y1-INs reduces the severity of neuropathic pain

(A, C, E) Intrathecal NPY-saporin (750 ng or 1,000 ng) reduced the development of **(A)** mechanical hypersensitivity to von Frey filaments ($F_{2,20} = 5.516$, $P = 0.01$), **(C)** cold response duration during acetone evaporation ($F_{2,20} = 9.889$, $P = 0.001$), and **(E)** mechanical response duration to blunt pin ($F_{2,20} = 13.43$, $P = 0.0002$), compared to intrathecal Blank-saporin. Repeated Measures Two-way ANOVA + Bonferonni. **(B, D, F)** Area Under the Curve (AUC) analyses for days 3-17 ($P < 0.05$ for all panels) and 21-54, respectively. One-way ANOVA + Bonferonni. N = 6 - 9 per group. ★ $P < 0.05$ compared to Blank-saporin. Dots represent individual subjects within the analysis. Data represent mean ± SEM. (**Behavioral experimentation peformed by Renee Donahue*)

We evaluated the effect of NPY-saporin on numerous parameters of acute pain and motor control (**Figure 12**). As compared to blank-saporin, NPY-saporin did not change thermal or mechanical sensitivity, body weight, motor coordination, ambulatory behavior, nor exploratory behaviors in an open field activity box ($P > 0.05$). This data suggests that the anti-hyperalgesia effects of NPY observed in **Figure 11** do not apply to all modalities of acute nociception, and are not confounded by motor side effects. Our results indicate that NPY-saporin did not change hindpaw withdrawal thresholds in response to application of noxious heat at 48°C, 52°C, or 56°C. This is consistent with Wiley et al (2009) who reported no effect in response to 47°C or 52°C (antinociceptive effects were observed only at a much lower temperature of 44°C) (Wiley et al., 2009).

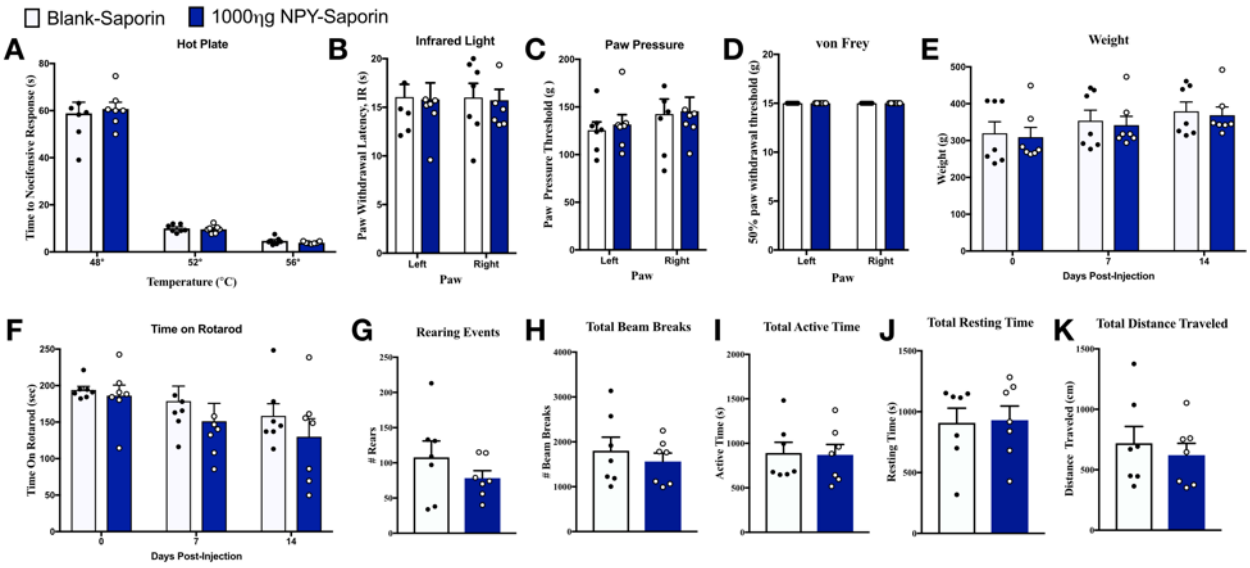

Figure 12. Lesion of spinal Y1-INs does not alter basal nociception or motor control

The effect of intrathecal blank-saporin or NPY-saporin (1000 ng) on rat nociceptive behavior in the **(A)** hotplate assay and **(B)** Hargreave's thermal assay for heat hyperalgesia, and the **(C)** Randel-Siletto paw pressure assay and the **(D)** von Frey filament assay for mechanical sensitivity. (**E**) Neither blank-saporin nor NPY-saporin changed body weight. The effect of intrathecal blank-saporin or NPY-saporin (1000 ng) on rat motor behavior in the **(F)** Rotarod test for motor coordination, and **(G-K)** general activity measures in an open field arena. Dots represent individual subjects within the analysis. Data represent mean ± SEM. (**Behavioral experimentation peformed by Renee Donahue*)

2.3.4 Nerve injury does not decrease NPY-Y1 receptor signaling in the dorsal horn

Peripheral nerve injury decreases the expression of several neuropeptide transmitters and receptors in dorsal root ganglion and spinal cord (Hökfelt et al., 1994), as well as the signal transduction of pain inhibitory GPCRs in in the brain (Hoot et al., 2010). For example, injury-induced decreases in the dorsal horn expression of the mu opioid receptor is accompanied by decreases in capacity for opioid-induced analgesia (Kohno et al., 2005; Zhang et al., 1997), a mechanism that might explain the poor efficacy of opioid analgesics for neuropathic pain (Taylor, 2009). Whether nerve injury produces similar changes in Y1 signaling and responsiveness to NPY antinociception is unknown. To address this question, we evaluated Y1 density and NPY-induced FOS activation of Y1-INs after SNI. We used a polyclonal antibody whose Y1R specificity in rat tissue was confirmed using western analysis, preadsorption of the antibody with peptide, and preimmune serum controls (Wolak et al., 2003).

As previously described (Brumovsky et al., 2006), we observed a pattern of intense Y1 immunoreactivity in laminae I-II comprised of tightly-packed cell bodies, embedded in Y1R-expressing processes, surrounded by CGRP-immunoreactive nerve endings (**Figure 13A**), and overlapping with IB4-positive cells **(Figure 13B)**. As expected, SNI substantially reduced CGRP immunoreactivity and IB4 staining within the innervation territories of the tibial and common peroneal nerves (**Figure 13C, D**). By contrast, SNI only slightly reduced spinal Y1 immunoreactivity density within just the tibial and not the common peroneal innervation territory (**Figure 13E, F**). While this slight immunoreactive reduction likely represents loss of Y1 expressed on the central terminals of primary afferent neurons that terminate in the IB4-positive laminar band, the small effect here is consistent with preliminary reports suggesting that “light” or

“medium” chronic constriction injuries impact 80% or less of the sciatic nerve and, thus, would not substantially reduce spinal Y1 immunoreactivity density (Brumovsky et al., 2004).

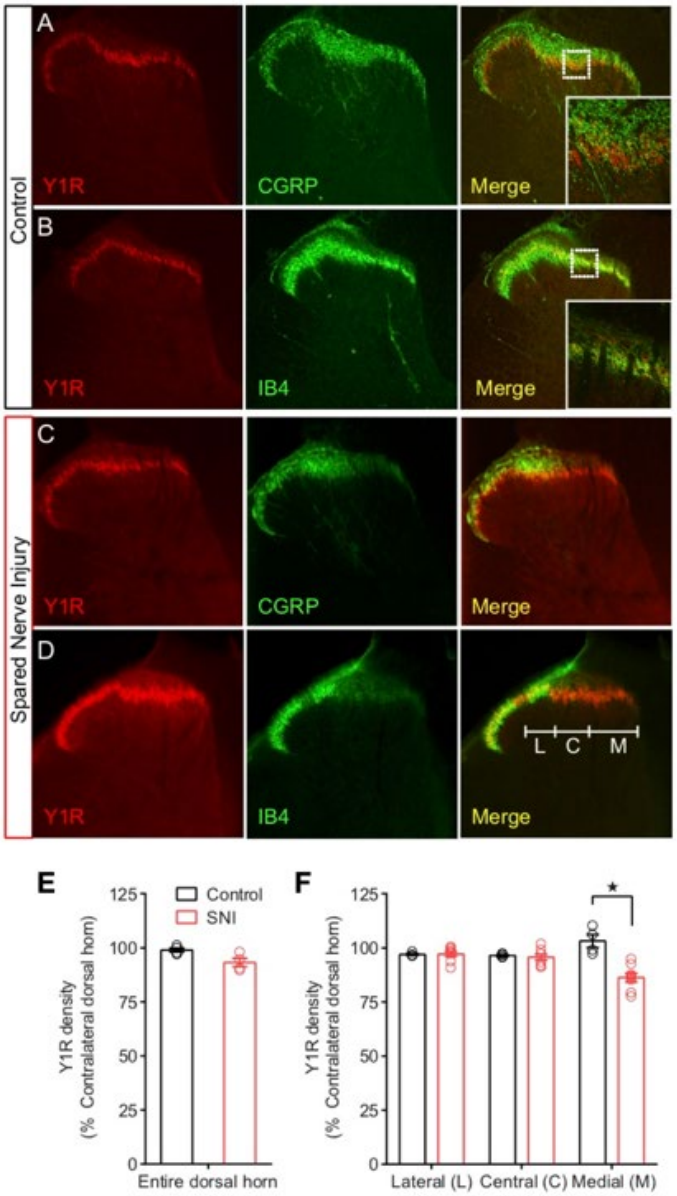

Figure 13. Peripheral nerve injury largely spares Y1 receptor expression in the dorsal horn

(**A-B**) In uninjured rats, Y1 receptor immunostaining of lumbar spinal cord slices shows minimal colocalization with the afferent terminal markers (**A**) CGRP and (**B**) IB4. SNI largely spared Y1 in contrast to large decreases in (**C**) CGRP and (**D**) IB4. (**E**) Quantification of Y1 immunostaining across the entire mediolateral axis of the dorsal horn revealed no significant overall loss of Y1. (**F**) Segregation of the dorsal horn by the innervation zones of the tibial (medial, M), common peroneal (central, C) or sural (lateral, L) branches of the sciatic nerve revealed a slight decrease in Y1 density in the tibial innervation zone relative to controls. Control, N = 4; SNI, N = 8. ★ $P < 0.05$ compared to control. Data represent mean ± SEM. Dots represent individual subjects in the analysis. (**Images obtained by Dr. Gregory Corder*)

We next evaluated the effect of NPY on neuronal activity in Y1-INs during neuropathic conditions. After intrathecal administration of NPY, we quantified the co-expression of Fos and Y1 in dorsal horn neurons. We found that intrathecal NPY increased von Frey thresholds (**Figure 14A**, $P < 0.05$) and reduced the number of Fos-expressing cells in the dorsal horn (**Figure 14B**, $P < 0.01$). Importantly, NPY decreased Fos expression within Y1-INs (**Figure 14C**, $P < 0.05$). In summary, peripheral nerve injury spares spinal Y1 receptor density and responsiveness of Y1-INs to NPY. These studies indicate that the Y1 receptor retains the capacity to inhibit spinal pain transmission after nerve injury.

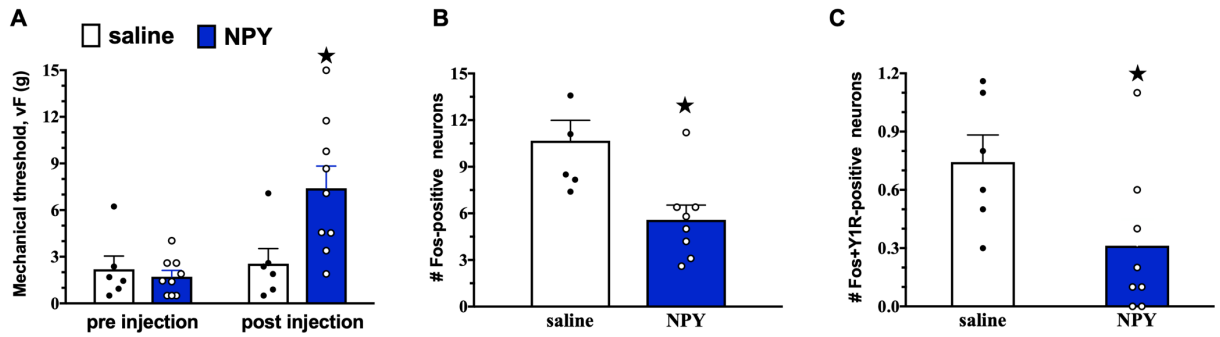

Figure 14. NPY reduces neuropathic mechanical hypersensitivity and light touch-evoked c-Fos expression in Y1-INs.

(**A**) von Frey thresholds 14 days after SNI before (pre-injection) and 60 min after intrathecal injection of saline or NPY (post-injection). Non-noxious mechanical stimulus-evoked expression of Fos-immunoreactivity in laminae I-II **(B)** for all neurons and **(C)** in Y1 receptor-immunoreactive neurons. N = 6 - 9. ★ $P < 0.05$ compared to control. Data represent mean ± SEM. Dots represent individual subjects in the analysis. (**Quantification performed by Dr. Gregory Corder*)

2.4 Discussion

The key finding of the present studies is that selective ablation of Y1R-expressing neurons in the dorsal horn delayed the onset and reduced the intensity of behavioral signs of neuropathic hyperalgesia after peripheral nerve injury. The effect was broad spectrum, impinging upon multiple somatosensory modalities including non-noxious mechanical, noxious mechanical, and cold hypersensitivity. These results further support spinal Y1R as a potential target for the pharmacological treatment of chronic pain.

2.4.1 Y1 receptor-expressing spinal excitatory interneurons contribute to neuropathic pain

Calbindin and calretinin are primarily located in different sub-populations of dorsal horn neurons and are largely (but not exclusively) restricted to glutamatergic cells (Smith et al., 2016, 2015; Todd, 2010). For the first time, we show that both are contained in Y1R-immunoreactive neurons. PKCγ-immunoreactive neurons are present throughout laminae I–III (Malmberg et al., 1997; Polgár et al., 1999), particularly in the inner half of lamina II, where their dendrites form a dense plexus (Hughes et al., 2003; Neumann et al., 2008). Although PKCγ-immunoreactive cell bodies make numerous contacts with NPY-positive boutons and dendrites (Polgar et al., 2011) and thus might appear to be a candidate for co-expression with Y1-INs, this population is largely distinct from the calbindin and calretinin populations and did not colocalize with Y1 in the current study. We conclude that the vast majority of Y1-INs are excitatory interneurons that lie dorsal to the inner lamina II band that is demarcated by PKCγ staining.

We found that Y1-immunoreactive neurons in lamina II typically contain somatostatin (Zhang et al., 1999). Most somatostatin-containing boutons contain the vesicular glutamate

transporter 2, VGLUT2 (Todd et al., 2003), and somatostatin lineage-tdTomato cells extensively co-label with *Vglut2* mRNA (Duan et al., 2014). Because excitatory interneurons and their boutons in the dorsal horn express VGLUT2 (Punnakkal et al., 2014; Todd et al., 2003; Yasaka et al., 2010), it is highly likely that somatostatin-expressing neurons are excitatory. Furthermore, selective ablation of somatostatin lineage neurons, using an intersectional genetic strategy, decreased mechanical allodynia associated with SNI in the mouse, suggesting that spinal somatostatin-expressing excitatory interneurons transmit neuropathic mechanical information (Duan et al., 2014). This is consistent with the present results showing that deletion of Y1-INs, and thus a subset of somatostatin neurons, decreased the neuropathic allodynia in the rat.

In addition to novel immunohistochemical profiling of neuropeptide and neurotransmitter neuron populations of the dorsal horn, significant progress has been made in the past decade in understanding the development of dorsal horn spinal neuron lineages. Of note is the uncovering of specific transcription factors that determine the excitatory (glutamatergic) or inhibitory (GABAergic/glycinergic) cell fate of spinal dorsal horn neurons (Bröhl et al., 2008; Huang et al., 2008; Xu et al., 2008). In support of our studies, *Npy1r* gene expression is almost exclusively found in $Tlx3^+$ glutamatergic neurons, and rarely found in $Pax2^+$ GABAergic neurons (Guo et al., 2012). Further, transcriptomic profiling analysis has determined that *Npy1r* mRNA is significantly enriched in the somatostatin dorsal horn neuron population (Chamessian et al., 2018). Single-nucleus RNA sequencing has clustered *Npy1r* into a dorsal excitatory peptidergic neuron cluster (Sathyamurthy et al., 2018), and single-cell RNA sequencing has classified *Npy1r* neurons as excitatory glutamatergic interneurons (Häring et al., 2018).

2.4.2 Y1 receptor-expressing interneurons contribute to the development and maintenance of neuropathic pain

The effect of NPY-saporin on the development (early timepoints) and maintenance (late timepoints) of allodynia and hyperalgesia varied with dose and somatosensory modality. For example, the 750 ng dose did not change von Frey mechanical threshold at earlier timepoints, but exerted a robust increase in threshold at later timepoints. By contrast, the 1000 ng dose of NPY-saporin reduced mechanical thresholds (and cold and pinprick responses) at all timepoints. The additional efficacy of the higher NPY-saporin dose at earlier timepoints suggest that two subpopulations of Y1 receptor+ interneurons differentially control the early development and the long-term maintenance of nerve injury-induced mechanical allodynia. Thus, in addition to a Y1-IN subpopulation that maintains neuropathic pain and is vulnerable to 750 ng NPY-saporin, there is an additional subpopulation that drives the development of neuropathic pain and is only vulnerable to the 1000 ng dose.

These studies are the first to implicate Y1-INs in the development of neuropathic pain and are consistent with previous studies indicating that Y1 receptors contribute to the maintenance of neuropathic pain. For example, intrathecal administration of neuropeptide Y or the selective Y1 receptor agonist, [Leu^{31} Pro^{34}]-NPY, dose-dependently reversed established markers of neuropathic pain including hyperalgesia and stimulus-evoked Fos expression in the dorsal horn (Intondi et al., 2008; Malet et al., 2017). Further studies are needed to determine whether ablation or inhibition of Y1-INs, with either intrathecal administration of NPY-saporin or optogenetic or chemogenetic inhibition of Y1-INs utilizing cre driver lines, will inhibit established signs of neuropathic pain when administered days to weeks after peripheral nerve injury.

2.4.3 NPY-saporin selectively targets Y1-INs rather than central terminals of primary afferent neurons or spinal projection neurons

Y1 receptors are expressed on small- to medium-sized DRG neurons and spinal cord neurons (Brumovsky et al., 2007, 2006, 2002; Taylor et al., 2014; Zhang et al., 1999). Since intrathecal NPY-saporin could conceivably cross the fibrous sheath that encases the DRG (as observed with GFP-conjugated viral particles), or be taken up by terminals of Y1 receptor-expressing primary afferents, and attack peripheral Y1 receptor-containing cells, one might predict that intrathecal NPY-saporin would kill not only Y1 receptor-containing dorsal horn neurons but also DRG neurons and their unmyelinated afferents that terminate in lamina I / outer part of lamina II (CGRP-containing) or in the inner part of lamina II (isolectin B4-containing). This is unlikely for several reasons. First, the current studies indicate that NPY-saporin did not change CGRP and IB4 staining in the dorsal horn. Second, spinal Y1 immunoreactivity does not readily co-stain with CGRP, SP, or IB4 (Brumovsky et al., 2002; Taylor et al., 2014) and is unchanged following dorsal rhizotomy (Ji et al., 1994), indicating that its existence on the central terminals of primary afferents is sparse at best. Third, Wiley and colleagues reported that intrathecal NPY-saporin had no effect on Y1 receptor-expressing cell counts in DRG of the fourth lumbar spinal segment (Wiley et al., 2009), indicating insufficient penetration into the DRG. Lastly, the vast majority of NPY Y2 receptors in the dorsal horn are found on the central terminals of primary afferents(Brumovsky et al., 2005), but a recent single-cell RNA sequencing analysis suggests the existence of Y2 receptors on a few interneurons (Häring et al., 2018). We cannot exclude that these very few Y2 receptor-expressing neurons were affected by NPY-saporin but consider it highly unlikely that this would affect the conclusions drawn in our study, as has been previously concluded (Wiley et al., 2009). Therefore, we conclude that the vast majority of Y1 receptor immunoreactivity is located on dorsal

horn neurons, and that NPY-saporin selectively ablates this Y1 receptor-containing population of neurons, rather than Y1- or Y2 receptor-positive terminals of primary afferent neurons.

Similar lack of effect on DRG neurons has been reported after intrathecal injection of dermorphin-saporin, a mu opiate receptor-specific toxin (Kline IV and Wiley, 2008). In that study, dermorphin-saporin injections destroyed lamina II MOR-expressing interneurons but had no effect on MOR-expressing DRG neurons. Although immunotoxins, such as OX7-saporin, 192-saporin and anti-dopamine beta-hydroxylase saporin are effective suicide transport agents (killing target neurons after selective uptake into axon terminals, followed by retrograde axonal transport to cell bodies where saporin acts to induce cell death), there is considerable evidence that intrathecal neuropeptide-saporin conjugates do not affect DRG neurons (Kline IV and Wiley, 2008; Wiley et al., 2009; Wiley and Kline Iv, 2000). Thus, there is a key difference between immunotoxins which are effective suicide transport agents and neuropeptide-toxin conjugates which are not.

Y1 receptor-immunoreactive cells exhibited retrograde labeling in lamina I, V, and X after choleratoxin B injection at the level of the 9th thoracic segment, and therefore project, at least, to the lower thoracic levels (Brumovsky et al., 2006) and likely on to the brainstem and diencephalic areas for further processing of nociceptive signals (Braz et al., 2014). The majority of lamina I projection neurons and some in the deeper laminae express the NK1 receptor (Todd et al., 2000, 1998), particularly those with a multipolar or fusiform shape (Almarestani et al., 2007), and it is the latter which are Y1 receptor-expressing (Brumovsky et al., 2006). However, consistent with previous studies (Wiley et al., 2009), we found that NPY-saporin did not change NK1R-immunoreactivity in the superficial dorsal horn, indicating that the mechanism by which NPY-saporin decreases neuropathic pain does not directly implicate NK1 receptor-expressing projection

neurons. Furthermore, we do not believe that NPY-saporin targeted NK1 receptor-negative, large pyramidal-shaped projection neurons in lamina I (Polgár et al., 2008), because those do not express the Y1 receptor (Brumovsky et al., 2006). Although we cannot exclude a contribution of NK1 receptor-negative neurons in deeper laminae, their numbers are small and so we conclude that the mechanism by which NPY-saporin reduces neuropathic pain is most likely due to ablation of Y1-INs, rather than projection neurons, in the dorsal horn.

2.4.4 The Y1 receptor retains its functional responsiveness to the pain inhibitory actions of NPY in the setting of nerve injury

Peripheral nerve injury decreases the expression of opioid receptors (Kohno et al., 2005; Zhang et al., 1997) and the ability of agonists to inhibit synaptic transmission in the dorsal horn (Kohno et al., 2005). Such mechanisms might explain the poor efficacy of opioid analgesics for neuropathic pain (Taylor, 2009). By contrast, we report that nerve injury did not decrease spinal Y1 receptor expression. Instead, intrathecal administration of NPY reduced nerve injury-induced mechanical hyperalgesia as well as stimulus-evoked gene expression (using Fos as a marker) on the Y1-INs, consistent with and extending our previous studies (Intondi et al., 2008). This supports our suggestion that the Y1 receptor, in contrast to the mu opioid receptor, has greater capacity for endogenous pain relief (Solway et al., 2011), and thus may be superior to opioids as a pharmacological target for long-lasting relief from neuropathic pain, particularly when administered at the spinal level (Smith et al., 2007). In summary, our neuroanatomical and behavioral characterization of Y1-INs provides compelling evidence for the development of spinally-directed Y1 receptor agonists to reduce chronic neuropathic pain.

2.4.5 Does endogenous NPY act at Y1-INs to tonically inhibit neuropathic pain?

When administered at the spinal level, NPY Y1 receptor agonists exert a broad-spectrum inhibition of pain (Smith et al., 2007). This action is particularly robust in peripheral nerve injury models of neuropathic pain (Malet et al., 2017), as intrathecal NPY has little effect on thermal thresholds in uninjured animals, but dose-dependently reduces behavioral signs of tactile and thermal hyperalgesia after injury, effects that can be blocked with a Y1 receptor-selective antagonist (Intondi et al., 2008). These pharmacological actions mimic the tonic inhibitory control of neuropathic pain by endogenous NPY (Solway et al., 2011). Indeed, our results are consistent with the hypothesis that NPY-Y1 receptor signaling counters facilitatory mechanisms of neuropathic pain following peripheral nerve damage.

The classic Gate Control Theory (GCT) of pain postulated that the input generated by nociceptive as well as non-nociceptive afferents is regulated by a complex, gated circuit in the dorsal horn. One of the central tenets of GCT is that an inhibitory interneuron in the substantia gelatinosa responds to non-nociceptive input by inhibiting, or closing the gate on, a neuron that transmits pain messages to the brain (Melzack and Wall, 1965). Recent studies indicate that gating might also occur at excitatory interneurons, including those that express somatostatin, VGLUT3, or PKCγ (Duan et al., 2014; Peirs et al., 2015; Petitjean et al., 2015). Based on a large body of anatomical, behavioral, transcriptomic, and electrophysiological evidence, we speculate that the Y1 receptor-expressing excitatory interneurons described here would be gated by inhibitory NPY-expressing interneurons that release NPY (Smith et al., 2007). First, extensive anatomical evidence describes a large subset of GABA-expressing dorsal horn interneurons that co-express NPY (Polgar et al., 2011). Second, we reported that endogenous NPY tonically inhibits neuropathic pain

behavior (Solway et al., 2011). Third, Smith and colleagues described inhibitory actions of NPY on the neurophysiological activity of dorsal horn neurons (Moran et al., 2004).

These results shed further light on the mechanism by which endogenous NPY tonically inhibits peripheral neuropathic pain, and we conclude this likely occurs via the hyperpolarization of Y1 receptor-expressing excitatory interneurons, rather than through disinhibition of Y1 receptor-expressing inhibitory interneurons as we have earlier postulated (Smith et al., 2007). Our results highlight the importance of endogenous NPY-Y1 receptor signaling in chronic pain regulation and provide a foundational mechanism for the targeting of spinal Y1-INs as a promising target for pharmacotherapies to treat clinical neuropathic pain.

3.0 Spinal neuropeptide Y Y1 receptor-expressing neurons are a pharmacotherapeutic target for the alleviation of neuropathic pain

3.1 Introduction

Nociception serves as a danger signal to prevent tissue damage and promote survival (Sherrington, 1906). However, peripheral nerve damage can lead to pathological allodynia (normally innocuous sensory input is amplified and conveyed as painful), debilitating spontaneous pain, and affective comorbidities such as anxiety and depression (Costigan et al., 2009; Finnerup et al., 2021; Taylor, 2009). These features of neuropathic pain are poorly responsive to analgesic drugs (Colloca et al., 2017; Gierthmühlen and Baron, 2016; Jensen and Finnerup, 2014; von Hehn et al., 2012), necessitating the need for new pharmacological targets. Such targets are likely to be found in the spinal cord dorsal horn (DH) (Gong et al., 2019; Moehring et al., 2018; Todd, 2010; West et al., 2015) as peripheral nerve injury increases the intrinsic excitability of DH neurons (Latremoliere and Woolf, 2009; Woolf, 1983) and disinhibits excitatory (glutamatergic) DH neurons (Gradwell et al., 2020; Inquimbert et al., 2018; Sivilotti and Woolf, 1994) to produce allodynia (Boyle et al., 2019; Lu et al., 2013; Peirs et al., 2021; Petitjean et al., 2015; Schoffnegger et al., 2008). Key populations of excitatory neurons that mediate allodynia include those that express protein kinase C gamma (PKCγ) (Lu et al., 2013; Malmberg et al., 1997; Miracourt et al., 2007; Neumann et al., 2008; Peirs et al., 2021; Petitjean et al., 2015; Wang et al., 2020), somatostatin (Sst) (Christensen et al., 2016; Duan et al., 2014), cholecystokinin (CCK) (Liu et al., 2018; Peirs et al., 2021), neurokinin-1 receptor (NK1R) (Maiarù et al., 2018), and transient vesicular glutamate transporter 3 during development (tVGLUT3) (Cheng et al., 2017; Peirs et al., 2015); however, these neural subpopulations do not represent readily druggable pharmaceutical

targets. By contrast, pharmacological agonism at excitatory interneurons that express a neurotransmitter receptor coupled to inhibitory G-proteins ($G_{i/o}$), such as the neuropeptide Y Y1 receptor, should reduce pronociceptive signaling. Indeed, application of NPY Y1-selective agonists to spinal cord slices reduces the excitability of NPY Y1 receptor-expressing interneurons (Y1-INs) and decreases pronociceptive signaling (Melnick, 2012; Miyakawa et al., 2005; Sinha et al., 2021). In this chapter, we use a multi-pronged approach including [^{35}S]GTPγS binding in spinal cord slice, *in vivo* spinal cord pharmacology, optogenetics, chemogenetics, conditional genetic knockout mice, and *ex vivo* slice electrophysiology in the spared nerve injury (SNI) model of neuropathic pain. We demonstrate that spinal Y1-INs facilitate allodynia and mediate the anti-hyperalgesic effects of intrathecally-administered NPY. These results promote Y1-INs as a promising pharmacotherapeutic target for the treatment of neuropathic pain with Y1-selective agonists.

3.2 Methods

Animals

Adult C57Bl/6NCrl (Charles River, #027), *Npy1r*^{Cre} (B6.Cg-*Npy1r*$^{tm1.1(cre/GFP)Rpa}$/J; the Jackson Laboratory, #030544), *Npy1r*^{eGFP} (RRID:MMRRC_010554; UCD), *Npy1r*$^{loxP/loxP}$ (courtesy of Herbert Herzog, (Howell et al., 2003)), *Pirt*^{Cre} (courtesy of Xinzhong Dong, (Kim et al., 2008)), and Lbx1^{Cre} (courtesy of Carmen Birchmeier, (Sieber et al., 2007)) mice were group housed, provided access to food and water ad libitum, and maintained on a 12:12 hour light:dark cycle (lights on at 7:00am) in temperature and humidity controlled rooms. Male and female mice were used in all experiments. No significant sex differences were observed. All procedures were

approved by the Institutional Animal Care and Use Committees of the University of Pittsburgh and University of Kentucky. Additionally, all experiments followed the guidelines for the treatment of animals of the International Association for the Study of Pain.

Intrathecal Injections

Intrathecal injections of [Leu^{31}, Pro^{34}]-NPY (human, rat), BIBO 3304 trifluoroacetate, or BIIE 0246 hydrochloride (TOCRIS) were performed in lightly restrained unanesthetized mice. Briefly, a 30G needle attached to a Hamilton microsyringe was inserted between the L5/L6 vertebrae at the cauda equina, puncturing the dura (confirmed by presence of reflexive tail flick). We then injected a 5µl volume of vehicle or drug. Animals were injected twice using a cross-over design with a 3-7-day separation between two injections. For example, animals receiving vehicle for the first injection received drug for the second, and animals receiving drug for the first injection received vehicle for the second. In all cases, group means of vehicle and drug did not differ on either injection day and were combined for final analysis.

Surgeries

Spared Nerve Injury: SNI was performed as previously described (Nelson et al., 2019; Solway et al., 2011). Briefly, mice were anesthetized with inhaled isoflurane (5% induction and 2% maintenance) and the left hind limb was shaved with trimmers and sterilized with 70% ethanol and 2% chlorhexidine gluconate (ChloraPrep One-Step Applicators). A small incision was made in the skin of the hind left leg and the underlying muscle was spread via blunt dissection to expose the underlying branches of the sciatic nerve. The peroneal and tibial nerves were then ligated with 6-0 silk sutures and transected while carefully avoiding the sural nerve. The muscle tissue was then loosely sutured with 5-0 nylon sutures and the skin was closed with 9mm wound clips. Topical

triple antibiotic ointment (Neosporin) was applied to the wound. Wound clips were removed ~7-10 days post-surgery and behavioral experiments began 14 days after surgery. Sham surgery was performed in an identical manner with nerve exposure but no ligation or transection.

Intraspinal AAV Injections: Mice were anesthetized with inhaled isoflurane (5% induction and 2% maintenance) and the back was shaved with trimmers and sterilized with 70% ethanol and 2% chlorhexidine gluconate (ChloraPrep One-Step Applicators). A midline incision was carefully made until the underlying vertebrae were clearly visible. A partial laminectomy was performed to remove the L1 vertebrae overlying the L4 segment of the spinal cord. A glass microelectrode was inserted into three separate locations in the exposed left lumbar spinal cord along the rostral caudal axis. At each injection site the glass microelectrode was lowered to a depth of 250 μm below the dura using a stereotaxic frame. 333.3 nL of virus was slowly injected into each of the three spots (5 nL/sec) with a 3-minute wait time after completion of each injection to permit adequate infusion. The *lassimus dorsi* was sutured with 5-0 nylon sutures to protect the exposed spinal cord and the overlying skin was closed with 9mm wound clips. Topical triple antibiotic ointment (Neosporin) was applied to the wound. Subcutaneous Buprenorphine HCL (0.05 mg/kg) was utilized for 72 hours as a post-operative analgesic. Behavioral experiments began 21 days after surgery. For the complete list of AAVs used see **Table 2**.

Table 2. List of AAVs Used

AAV8-hSyn-DIO-hM3D(Gq)-mCitrine	Addgene	Cat: 44361-AAV8
AAV8-hSyn-DIO-hM4D(Gi)-mCherry	Addgene	Cat: 44362-AAV8
AAV8-hSyn-DIO-mCherry	Addgene	Cat: 50459-AAV8
AAV8-hSyn-FLEX-Chronos-GFP	UNC	(Klapoetke et al., 2014)

Spinal Optogenetic Neurolux Implant: Intraspinal AAV injections were performed as described above. However, following AAV infusion the *lassimus dorsi* was not sutured and instead Kwil-Sil Silicone Elastomer was applied over the exposed spinal cord to protect the underlying neural tissue. Next, the spinal optogenetic implant (Neurolux Spinal Device- Wavelength 470 nm) was gently placed onto the silicone elastomer with the LED targeting the viral injection sites. Light Super Glue was applied to the implant and muscle to increase the security of the implant. The overlying skin was closed with 9mm wound clips. Topical triple antibiotic ointment (Neosporin) was applied to the wound. Subcutaneous Buprenorphine HCL (0.05 mg/kg) was utilized for 72 hours as a post-operative analgesic. Behavioral experiments began 21 days after surgery.

Behavioral Testing

Mechanical Withdrawal Threshold: Testing was performed as described in (Solway et al., 2011). Mice were habituated to plexiglass chambers with opaque walls (15 × 4 × 4 cm) on a raised wire mesh platform for 30-60 minutes one day before and immediately prior to behavioral testing. Testing was performed using a calibrated set of logarithmically increasing von Frey monofilaments (Stoelting, Illinois) that range in gram force from 0.007 to 6.0 g. Beginning with a 0.4 g filament, these were applied perpendicular to the lateral hindpaw surface with sufficient force

to cause a slight bending of the filament. A positive response was denoted as a rapid withdrawal of the paw within 4 seconds of application. Using the Up-Down method (Chaplan et al., 1994), a positive response was followed by a lower filament and a negative response was followed by a higher filament to calculate the 50% withdrawal threshold for each mouse.

Cold Withdrawal Duration: Immediately following von Frey testing, acetone drop withdrawal testing was performed on mice in the same plexiglass chambers on a raised wire mesh platform. Using a syringe connected to PE-90 tubing, flared at the tip to a diameter of 3 1/2 mm, we applied a drop of acetone to the lateral side of the hind plantar paw. Surface tension maintained the volume of the drop to ~10 μL. The length of time the animal lifted or shook its paw was recorded for 30 s. Three observations were averaged.

Heat Withdrawal Latency: Mice were placed on a heated surface (52.5 ± 1 °C) within an acrylic enclosure (Hotplate; Columbus Instruments, Columbus, OH). The time until hindpaw withdraw response (e.g., jumping, licking, flinching) was recorded. The animal was immediately removed after paw withdraw or a cutoff of 20 s to avoid tissue injury. Three observations were averaged with a between-trial interval of at least 10 min.

Spontaneous Nocifensive Behavior: Following intraperitoneal injection of saline or CNO, we recorded the duration of nocifensive behaviors, defined as hind paw-directed lifting, licking, shaking, or holding of the paw for 10 minutes (30-40 minutes post-injection). These represent commonly described nocifensive behavioral responses in the literature (Chen et al., 2018; Gilding et al., 2020; Grajales-Reyes et al., 2021; Petitjean et al., 2019; Robinson et al., 2018; Smith et al., 2019).

Open Field Testing: The open field exploratory behavioral data were collected in the Preclinical Phenotyping Core of the University of Pittsburgh School of Medicine. Immediately following intraperitoneal CNO injection, spontaneous activity was recorded for 60 minutes in an automated open field apparatus for mice (Omnitech Electronics Incorporated, Columbus, OH). An additional experiment was performed in a separate $hM3D_{(Gq)}$-injected *Npy1r*^{Cre} mouse group in which mice were pretreated with saline or Gabapentin 100 mg/kg i.p., and 30 minutes later injected with CNO 3 mg/kg i.p. before being placed in the open field apparatus for 60 minutes. 24 hours later, the same mice received a crossover injection (saline vs. gabapentin or gabapentin vs. saline) and they were again placed in the open field apparatus for 60 minutes. Movement time, rest time, and stereotypic episode activity counts were measured by infrared photobeams located around the perimeter of the arenas and interfaced to a computer running Fusion v6 software (Omnitech Electronics Incorporated). According to the Omnitech Handbook these three behaviors are defined as: Movement time: "The length of time that the subject spent in activity. Activity is defined as a period in which ambulation or stereotypy occurred.", Rest Time: "The length of time that the subject spent at rest. A resting period is defined as a period of inactivity greater than or equal to 1 second.," and Stereotypic Episode Activity Count: "Number of beam breaks that occur during a period of stereotypic activity. If the animal breaks the same beam (or set of beams) repeatedly then the monitor considers that the animal is exhibiting stereotypy. This typically happens during grooming or head bobbing." An averaged activity plot was generated for all animals of each group using the Fusion Locomotor Activity Plotter analyses module (Omnitech Electronics Incorporated).

Conditioned Place Preference/Avoidance: A three-day conditioning protocol using a biased chamber assignment was used for conditioned place preference (CPP) and conditioned place aversion (CPA). On the acclimation day (Day 1), mice had free access to explore all chambers of a 3-chamber conditioned place testing apparatus (side chambers: 170 x 150 mm; center chamber: 70 x 150 mm; height: 200 mm; San Diego Instruments) for 30 mins. Mice were able to discriminate between chambers using visual (vertical versus horizontal black-and-white striped walls) and sensory (rough versus smooth textured floor) cues. For pre-conditioning (Days 2 and 3), mice were again allowed to freely explore for 15 mins (CPP) or 30 mins (CPA) whilst their position was recorded via a 4 x 16 infra-red photobeam array by associated software (San Diego Instruments). For conditioning (Days 4-6), in CPP each mouse's preferred chamber was paired with saline and the non-preferred chamber with clozapine n' Oxide (CNO), conversely, in CPA each mouse's non-preferred chamber was paired with saline and the preferred chamber CNO. Each morning mice received an i.p. saline injection, were returned to their home cage for 5 min, and were then placed in the designated side chamber for 60 min. 4 hours later, mice received i.p. CNO (3 mg/kg; Tocris), were returned to their home cage for 5 min, and were placed into the CNO-designated chamber for 60 min. On test day (Day 7), mice could freely explore all chambers as their position was recorded as during pre-conditioning for 15 min (CPP) or 30 min (CPA). Difference scores were calculated as the time spent in the chamber on test day minus the time spent during pre-conditioning.

Neurolux testing: We tuned a single von Frey plexiglass chamber with opaque walls (15 × 4 × 4 cm) on a raised wire mesh for optogenetic stimulation and thus ran one single animal at a time. Stimulation frequencies (0-20 Hz, 5 ms pulse width) were wirelessly controlled with a laptop

computer and pre-randomized for each animal to prevent a ramping effect. Upon blue light stimulation at an individual frequency, animals immediately underwent von Frey and acetone withdrawal testing as described above. 5 minutes of light-OFF were provided between each stimulation frequency. Optoelectronic device functionality was verified at the time of perfusion and tissue harvesting.

Hindpaw Brush for pERK: To determine the effect of vehicle or drug on pERK activation in the ipsilateral dorsal horn, a light-touch stimulation protocol was initiated 30 minutes after drug administration (intrathecal agents or i.p. CNO). As previously described (Fu et al., 2019), mice were anesthetized with isoflurane (5% induction, 2% maintenance) and the lateral surface of the left hindpaw was gently stroked in the longitudinal plane with a cotton tipped applicator for 3 seconds of every 5 seconds, for 5 minutes. After an additional 5-minute wait time in their home cage, mice received an intraperitoneal injection of sodium pentobarbital (.100 mg/kg, 0.2 mL, Fatal-Plus) and were transcardially perfused.

Rotarod Motor Coordination Testing: To test for possible effects of spinal LED implantation on motor coordination, naive littermate control mice and mice with spinal LED implants were placed on an accelerating rotarod (Stoelting, Wood Dale, IL). The rotating bar was set to accelerate at a constant rate of 0.5 RPM every 5 seconds beginning at 2 RPM and maxing out at 60 RPM. Mice quickly learn to walk on the rotarod, reaching a plateau within several acceleration trials. Therefore, training trials were repeated until the average latency to fall was approximately 45 s. One day later, we tested the mice for 5 trials and averaged the results.

Immunohistochemistry

Mice received an intraperitoneal injection of sodium pentobarbital (.100 mg/kg, 0.2 mL, Fatal-Plus) and were transcardially perfused with ice-cold phosphate-buffered saline (PBS) followed by ice-cold fixative (10% phosphate-buffered formalin). The lumbar spinal cord and DRGs were removed by blunt dissection, postfixed overnight in 10% phosphate-buffered formalin, and then cryoprotected in 30% sucrose in 0.01-M PBS for several days until the tissue sank. Transverse spinal cord dorsal horn sections (30 μm) centered at L4 were cut on a freezing microtome and collected in antifreeze. L3-L5 dorsal root ganglion sections (12μm) were cut on a cryostat and direct mounted to Superfrost Plus slides. The sections were washed 3 times in PBS and then pretreated with blocking solution (3% normal goat serum and 0.3% Triton X-100 in PBS) for 1 hour. Sections were then incubated in blocking solution containing the primary antibodies overnight at room temperature on a slow rocker. The sections were washed 3 times in 1x PBS and then incubated in secondary antibodies (1:1000) for 60 minutes. Finally, sections were washed in 1x PBS and then 0.01-M phosphate buffer without saline. Spinal cord sections were then mounted onto Superfrost Plus slides, air-dried, and cover-slipped with Hard Set Antifade Mounting Medium with DAPI (VECTASHIELD). All images were captured on a Nikon Eclipse Ti2 microscope using a 20x objective (numerical aperture 0.45) and analyzed using NIS-Elements Advanced Research software. For the complete list of antibodies used see **Table 3**.

Table 3. List of Antibodies Used

Anti-mCherry	Invitrogen	Cat: M11217
Anti-CGRP	Peninsula Laboratories	Cat: T-5027
Phospho-p44/42 MAPK (Erk1/2) (Thr202/Tyr204) (D13.14.4E) XP® Rabbit mAb	Cell Signaling Technology	Cat: 4370
Streptavidin, Alexa Fluor™ 568 conjugate	Invitrogen	Cat: S11226
Anti-GFP	abcam	Cat: ab13970
Anti-PKCγ	Frontier Institute	Cat: PKCg-GP-Af350
Alexa Fluor 488 Goat anti-Rabbit	Invitrogen	Cat: A11008
Alexa Fluor 568 Goat anti-Rat	Invitrogen	Cat: A11077
Alexa Fluor 488 Goat anti-Guinea Pig	Invitrogen	Cat: A11073
Alexa Fluor 568 Goat anti-Guinea Pig	Invitrogen	Cat: A11075

Fluorescence *in situ* Hybridization (FISH) (RNAscope)

Mice were transcardially perfused with ice cold 1x PBS followed by 10% buffered formalin and spinal cords and DRGs were extracted via blunt dissection, postfixed in 10% formalin (2-4 hrs), and then placed in 30% sucrose at 4°C until the tissue sank (~48-72 hrs). 20µm thick L3-L4 floating spinal cord sections were obtained on a vibrating microtome, and 12µm thick L3-L4 DRGs were cut on a cryostat and mounted on Superfrost Plus Microscope slides and air dried overnight at room temperature. Slides underwent pretreatment for fluorescence *in situ* hybridization consisting of 10 min Xylene bath, 4 min 100% ethanol bath, and 2 min RNAscope® H2O2 treatment. Next, the FISH protocol for RNAscope Fluorescent v2 Assay (ACD) was followed for hybridization to marker probes. Slides were either then coverslipped with VECTASHIELD HardSet Antifade Mounting Medium with DAPI or proceeded to immunohistochemistry for GFP labeling. All images were captured on a Nikon Eclipse Ti2 microscope using a 20x or 40x objective

and analyzed using NIS-Elements Advanced Research software v5.02. Cells with at least 3 puncta associated with a DAPI nucleus were considered positive. For the complete list of RNAscope probes used see **Table 4**.

Table 4. List of RNAscope Probes Used

Npy1r probe	ACD	Cat: 427021
Lmx1b probe	ACD	Cat: 412931
Pax2 probe	ACD	Cat: 448981
eGFP probe	ACD	Cat: 400281

[^{35}S]GTPγS binding

14 days post-SNI or sham surgery, the lumbar enlargement of the mouse spinal cord was dissected and snap-frozen in methyl butane. 50µm-thick sections were cut with a cryostat and mounted on gelatin-coated glass slides. Sections were equilibrated at room temperature for 10 min in assay buffer (30 mM MgCl2, 150 mM NaCl, 2.7 mM KCl, and 37.5 mM HEPES, pH 7.4) and for 15 min in 2 mM GDP. Agonist- stimulated binding was then performed with 2 mM GDP and 0.1 nM [^{35}S]GTPγS (GE Healthcare, Little Chalfont, Buckinghamshire, UK) and one of four serial dilutions ranging from 45 nM to 45 µM [Leu^{31}, Pro^{34}]-NPY in water treated with a peptidase inhibitor cocktail containing 0.170 mg/ml bacitracin, 17 µg/ml leupeptin, 17 µg/ml chymostatin, and 0.850 mg/ml bovine serum albumin. Drug was omitted and replaced with either peptidase-treated water for basal determinations or 10 µM unlabeled GTPγS water for nonspecific binding determinations. Slides were incubated at 37 °C for 45 min and then rinsed for 2 min twice with ice-cold 50 mM Tris–Cl, pH 7.4 and twice with deionized water at room temperature. Slides were

exposed to Kodak X-OMAT autoradiographic film (Sigma–Aldrich) for 18–24 hrs. Densitometric analysis of images was performed by measuring the mean density of pixels in the superficial laminae of the left and right lumbar dorsal horn and subtracting the mean dorsal column background value. Percent stimulation over basal was calculated using the following equation:

$$\left[\frac{\text{(DH dose value - column dose value)- nonspecific binding}}{\text{(DH basal value - column basal value)- nonspecific binding}}\right] \text{ x } 100 - 100$$

Electrophysiological Recordings/Biotin Labeling

Slice preparation for electrophysiology: As described previously (Sinha et al., 2021), mice were anesthetized with 5% isoflurane and perfused transcardially with 10 ml of ice-cold, sucrose-containing artificial cerebrospinal fluid (aCSF) (sucrose-aCSF) that contained (in mM): KCl 2.5, KH_2PO_4 1.0, $CaCl_2$ 1, $MgSO_4$ 2.5, $NaHCO_3$ 26, glucose 11, sucrose 235, oxygenated with 95% O_2, 5% CO_2. The lumbar spinal cord was rapidly isolated by laminectomy, placed in oxygenated, ice-cold, sucrose-aCSF, cleaned of dura mater, and nerve roots were cut close to the cord. The spinal cord was immersed in low-melting-point agarose (3% in sucrose-aCSF; Life Technologies, Carlsbad, CA, USA) and parasagittal slices (300–450 μm) were cut in ice-cold, sucrose-aCSF from one lateral side to the other side using a vibrating microtome (7000smz-2; Campden Instruments, Lafayette, IN, USA). All slices were incubated for 15 min at room temperature in recovery solution that contained (in mM): n-methyl-d-glucamine (NMDG) 92, KCl 2.5, NaH_2PO_4 1.2, $NaHCO_3$ 30, HEPES 20, glucose 25, sodium ascorbate 5, thiourea 2, sodium pyruvate 3, $MgSO_4$ 10, $CaCl_2$ 0.5 pH 7.3 (HCl). The slices were then transferred to normal aCSF used for recording, which contained (in mM): NaCl 126, KCl 2.5, NaH_2PO_4 1.25, $CaCl_2$ 2.0, $MgSO_4$ 1.0, $NaHCO_3$ 26, glucose 11, for an hour before beginning any experiment.

Patch-clamp recordings: As described previously (Sinha et al., 2021), a parasagittal spinal cord slice was transferred to a fixed stage mounted under an upright microscope (Olympus BX51 WI), where it was continuously superfused with oxygenated aCSF (see details in(Sinha et al., 2021)). Recordings from neurons were obtained by identification of Y1eGFP-positive cell bodies with epifluorescent microscopy (Sinha et al., 2021). Recording pipettes (3-6 MΩ) containing (in mM): K-gluconate 135, NaCl 1, $MgCl_2$ 2, $CaCl_2$ 1, HEPES 5, EGTA 5, Mg-ATP 2 and Na_4-GTP 0.2, pH 7.3 (~300 mOsm/L). Patch-clamp recordings in current- and voltage-clamp modes were performed on SDH neurons using an Axon Instruments Multiclamp 700B amplifier (Molecular Devices). Signals were low-pass filtered at 4-20 kHz, amplified 1-20 fold, sampled at 5-10 kHz and analyzed offline using pClamp. Series resistance was less than 20 MΩ. No correction was made for the liquid junction potential (calculated value: -13.9 mV). Experimental data were recorded approximately 5-10 min after establishing whole-cell configuration. All recordings were performed at room temperature on neurons selected from the distinctive translucent band in the medial to mediolateral subdivisions of the SDH region, with a depth of roughly 20 to 100 μm representing Lamina II.

Firing during depolarizing ramp currents: Membrane excitability was quantified by examining discharge rates in response to ramp current commands. These were delivered from a set holding voltage of -60 mV at a ramp at 67 pA/s. Number of action potentials, latency to first action potential, initial and average spike frequency and action potential amplitudes were noted. Firing frequency (f) was calculated as the reciprocal of the interspike interval (ISI), rather than average of number of action potential over the duration of current steps, with algorithms written

in MATLAB. The latency to first action potential was measured from the onset of initiation of current ramp to the time of first spike peak.

Firing patterns during steady-state current injection recordings: Firing patterns were determined in response to a series of 3-9 depolarizing steady-state (constant step) current injections (1 s duration) that were delivered every 8 s in increasing steps of 20 pA in neurons held at -80 mV for 500 ms. We elicited firing from hyperpolarized condition to activate the putative partially inactive potassium channels responsible for delayed firing.

We identified four main firing patterns with the following characteristics: Delayed, Long Latency Firing (DLLF) neurons typically exhibit a clear delay of >180 ms (range, 180-850 ms) in action potential firing that lasts the duration of current injection, Delayed, Short Latency Firing (DSLF) neurons exhibit a short depolarizing delay of 60-180 ms prior to firing the first action potential and mostly terminate before the end of current injection, Initial Burst Firing (IBF) neurons exhibit a short burst of two to four high frequency (~90 Hz) action potentials on top of a long-lasting (~200 ms) Ca^{2+} spike, owing to the presence of low-threshold Ca^{2+} currents, and Phasic Firing (PF) neurons exhibit several action potentials immediately after the onset of current injection but terminate before the end of the current pulse

Number of action potentials, latency to first action potential from onset of current injection, initial and average spike frequency and action potential amplitudes at all depolarizing current injections were obtained. Firing frequency (f) was also calculated as the reciprocal of the interspike interval (ISI).

Rheobase: The current required to elicit an action potential threshold (rheobase) was measured by means of a current step protocol that was applied to neurons held at RMP, with 5 ms current steps applied in 2.5 pA increments until the appearance of an action potential.

Current-Voltage relationships: Current-voltage relationships were determined under voltage-clamp using a series of 250 ms voltage commands. Currents were measured just prior to the termination of each voltage pulse.

Spontaneous EPSC recordings: Spontaneous excitatory postsynaptic currents (sEPSCs) were recorded at -60 mV in aCSF. For each neuron, sEPSCs were recorded for a total of 3 min. Mini Analysis Program (Synaptosoft) was used to distinguish sEPSC from baseline noise. Initially spontaneous postsynaptic currents were detected automatically by setting appropriate amplitude and area threshold for each recording. Later, all detected events were re-examined and accepted or rejected based on subjective visual examination. Neurons were classified as silent if they failed to display one or more events during the 3-min sampling period and were omitted from the analysis. Cumulative probability plots were generated to compare the amplitude and inter-event interval in neurons from naive-operated animals and those subjected to SNI. Cumulative probability plots ranked individual amplitudes or interevent intervals in order of increasing size and then plotted this rank value against the amplitude or interevent interval. The Kolmogorov-Smirnov (KS) two-sample test was used to compare distributions of amplitudes and interevent intervals. All accepted events from analyzed data were pooled from neurons separated according to firing patterns separated between naive and SNI animals.

Neurobiotin Labeling: Following electrophysiological characterization, Npy1r^{eGFP} cells were filled with 0.2% neurobiotin added into the pipette solution for morphological classification. Small notches were cut in the ventral tissue at one end of the slice to mark the orientation of the parasagittal slice during recording, and the slice was preserved in 10% formalin at 4°C. Neurobiotin labeling was revealed with a fluorescent marker by means of floating section histochemistry. Sections were rinsed 3 x 10 min in PBS, then incubated in PBS/0.3% Triton X-100 with 1:1000 Streptavidin-Alexa568 for 2.5 hr at RT. Sections were again rinsed with PBS 3 x 10 min, then rinsed in 0.01 M PB 2 x 10 min. Sections were then mounted on microscope slides and allowed to dry, then coverslipped with Prolong Glass mounting media. Neurobiotin-labeled cells were imaged using a Nikon Eclipse Ti2 epifluorescence microscope and/or a Nikon A1R Spectral confocal microscope housed in the Center for Biologic Imaging, University of Pittsburgh, Pittsburgh, PA).

Morphological classification: In concordance with the methods of Grudt and Perl (Grudt and Perl, 2002), we classified the morphology of Npy1r^{eGFP} cells in the dorsal horn based on characteristics of dendritic arborization. Vertical cells generally have multiple dendrites oriented toward the ventral spinal cord, but little or no dendritic arborization in the dorsal direction. Notably, the vertical-like morphologies we noted in this study had small dorsal-ventral dendritic branching (~50 μm) in comparison to the vertical cells noted by Grudt and Perl (~185 μm) and thus might represent a unique morphological class of dorsal horn interneurons. Radial cells extend multiple dendrites from the cell body in any direction, which spread a short distance from the cell. Central cells extend one or two dendrites from each end of the cell oriented in parallel fashion with

the dorsal surface of the spinal cord, with the dendrites often spreading greater distances than in the vertical and radial cell types.

Blinding procedures

In all experiments rigorous experimenter blinding was employed to promote research reproducibility. The experimenter was blinded to drug treatments in all behavioral pharmacology experiments as intrathecal injections were performed by a laboratory colleague thus providing complete anonymity of agent for each animal. For viral experiments a laboratory mate color-coded the tubes for the experimenter. The key for coding was kept hidden in a notebook until the completion of all experiments. The experimenter then obtained the key for data analysis. pERK and spontaneous animal behavior quantification were performed with complete anonymity of animal IDs/treatment.

Statistical Analyses

All data are presented as means ± SEM. Statistical significance was determined as $*P < 0.05$. Statistical tests were the Student's t test (paired and unpaired), χ^2 test, Kolmogorov-Smirnov test, one- way analysis of variance (ANOVA), two-way repeated-measures ANOVA, and three-way repeated measures ANOVA followed by post hoc tests as appropriate. All statistical analyses were performed in GraphPad Prism 9.0 and SigmaPlot 12.0.

3.3 Results

3.3.1 Nerve injury increases the efficiency of coupling between NPY Y1 receptors and G-proteins.

A multitude of G protein-coupled receptors (GPCRs) have been targeted for the development of new analgesic drugs (Che, 2021; Geppetti et al., 2015). However, peripheral injury can alter both the efficacy and potency of GPCR-agonist interactions (Bantel et al., 2002; Chen et al., 2002; Kohno et al., 2005; Taylor et al., 2014; Winter and McCarson, 2005). To determine whether nerve injury changes NPY-Y1-G protein signaling, we assessed guanosine-5′-*O*-(3-[^{35}S]thio)triphosphate ([^{35}S]GTPγS) binding in lumbar spinal cord slices 14 days after spared nerve injury (SNI), a common animal model of neuropathic pain (**Figure 15A**), or sham surgery. SNI has both a development phase (1-7 days post-SNI) and a maintenance phase (8-14 days post-SNI) (Richner et al., 2011); therefore, we performed our studies at the well-established 14 day post-SNI chronic timepoint (Inquimbert et al., 2018; Liu et al., 2018; Solway et al., 2011) to provide evidence for the relevance of Y1 as a potential therapeutic target in the context of established neuropathic pain. As illustrated in **Figure 15B-D** and **Figure 16,** the NPY Y1 receptor-selective agonist, [Leu^{31}, Pro^{34}]-NPY, increased [^{35}S]GTPγS binding with a maximum physiological effect (E_{max}) and effective concentration (EC_{50}) of 37.90 ± 1.32% and 2.80 ± 0.31 nM in the left dorsal horn and 37.40 ± 1.33% and 2.87 ± 0.32 nM in the right dorsal horn of sham-14d mice. In SNI-14d mice, the EC_{50} of [Leu^{31}, Pro^{34}]-NPY was reduced in the left (ipsilateral to injury, 1.84 ± 0.23 nM) but not right (contralateral, 2.56 ± 0.57 nM) dorsal horn compared to sham surgery, respectively. SNI did not change [Leu^{31}, Pro^{34}]-NPY-stimulated E_{max} in the ipsilateral (40.16 ± 1.91%) or contralateral (41.28 ± 2.81%) dorsal horns compared to sham surgery (**Figure 15C-D**). These EC_{50} data indicate that Y1 not only retains its G protein activation capacity in the setting of

nerve injury, but also that nerve injury increases the efficiency of coupling between NPY Y1 receptors and G-proteins, possibly to increase the analgesic potential of NPY-Y1 selective agonists at the dorsal horn.

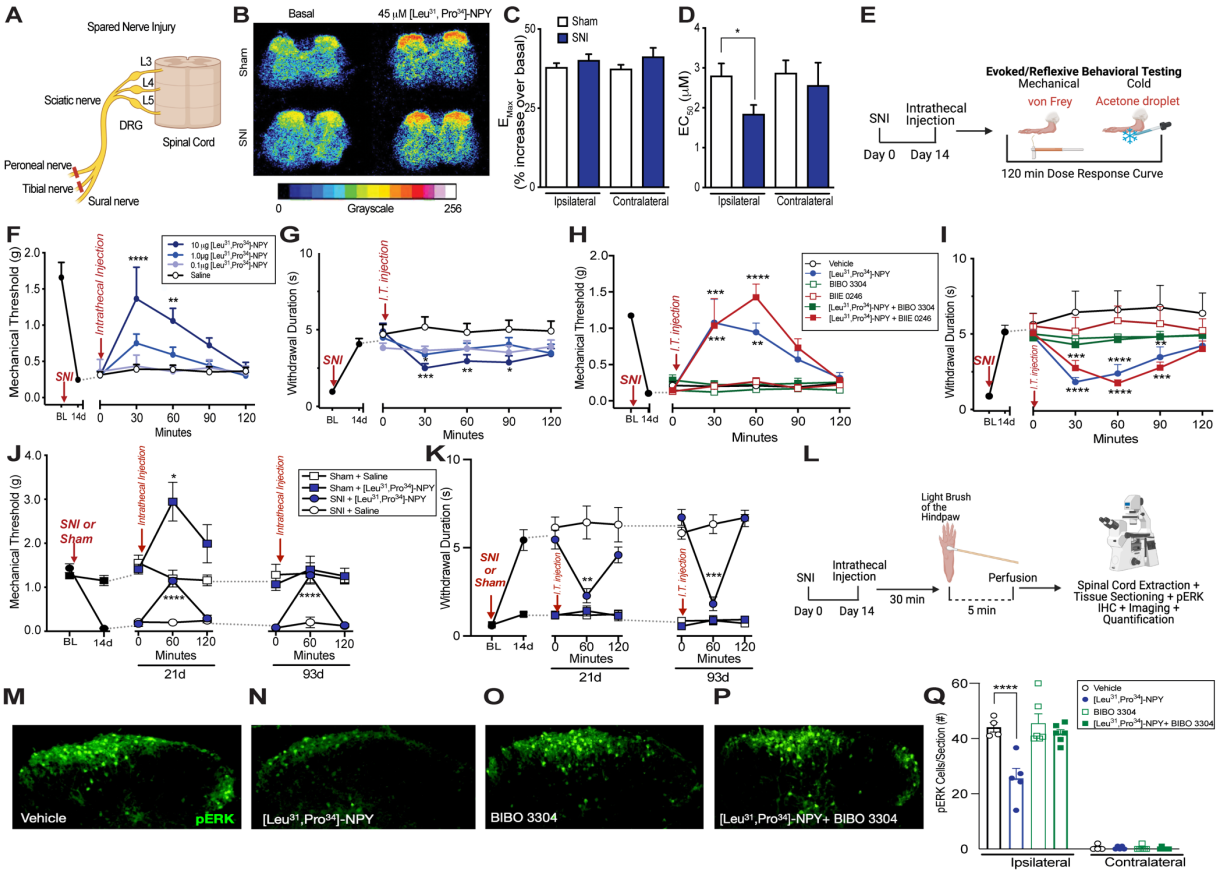

Figure 15. Intrathecal administration of a Y1 agonist alleviates behavioral and immunohistochemical markers of SNI-induced neuropathic nociception.

(**A**) Schematic representation of the spared nerve injury (SNI) model of neuropathic pain. (**B**) Representative pseudo-color images of [^{35}S]GTPγS binding quantitative autoradiography in mouse spinal cord sections. Binding assays were performed in the absence (basal) or presence of 45 μM [Leu^{31}, Pro^{34}]-NPY in sections obtained from mice given sham surgery (nerve exposure but no ligation) or SNI 14 days before the experiment. (**C**) SNI did not change the E_{max} of [Leu^{31}, Pro^{34}]-NPY-stimulated [^{35}S]GTPγS binding (n=5-10 animals/group). Student's unpaired two-tailed t test. (**D**) SNI reduces the EC_{50} of [Leu^{31}, Pro^{34}]-NPY-stimulated [^{35}S]GTPγS binding in the ipsilateral (left) dorsal horn (n=5-10 animals/group). Student's unpaired two-tailed t test. (**E**) Experimental timeline for SNI, intrathecal pharmacology, and evoked/reflexive mechanical (von Frey) and cold (acetone droplet withdrawal) behavioral testing. (**F-G**) Intrathecally administered [Leu^{31}, Pro^{34}]-NPY (0.1 μg, 1.0 μg, or 10.0 μg) dose-dependently reduces SNI-induced mechanical and cold allodynia (n=8-13 mice/group). Two-way RM ANOVA. Holm-Sidak post hoc test. (**H-I**) The Y1 (BIBO 3304, 10.0 μg) but not Y2 receptor (BIIE 0246, 5.0 μg) antagonist abolishes Y1 agonist-induced ([Leu^{31}, Pro^{34}]-NPY, 10.0 μg) mechanical and cold anti-allodynia (n=4-11

mice/group). Two-way RM ANOVA. Holm-Sidak post hoc test. (**J-K**) Intrathecally administered [Leu^{31}, Pro^{34}]-NPY (10.0 μg) can repeatedly abolish SNI-induced mechanical and cold allodynia during the maintenance phase of neuropathic pain (n=6-8 mice/group). Two-way RM ANOVA. Holm-Sidak post hoc test. (**L**) Experimental timeline for SNI, intrathecal pharmacology, light brush of the lateral hindpaw, and immunohistochemical staining for pERK immunoreactivity in the lumbar dorsal horn. (**M-P**) Representative images of ipsilateral dorsal horn light-touched evoked pERK immunoreactivity after intrathecal administration of agents. (**Q**) Intrathecally administered [Leu^{31}, Pro^{34}]-NPY (10.0 μg) reduces light-touched evoked pERK immunoreactivity in the ipsilateral dorsal horn and this effect is abolished with coadministration of the Y1 antagonist, BIBO 3304 (10.0 μg) (n=4-6 mice/group). Two-way ANOVA. Holm-Sidak post hoc test. Data are shown as means ± SEM. *p < 0.05, **p<0.01, ***p<0.001, ****p<0.0001. Dots represent data points from individual animals. (**[^{35}S]GTPγS binding assays were performed by Drs. Michelle K. Winters and Ken E. McCarson*)

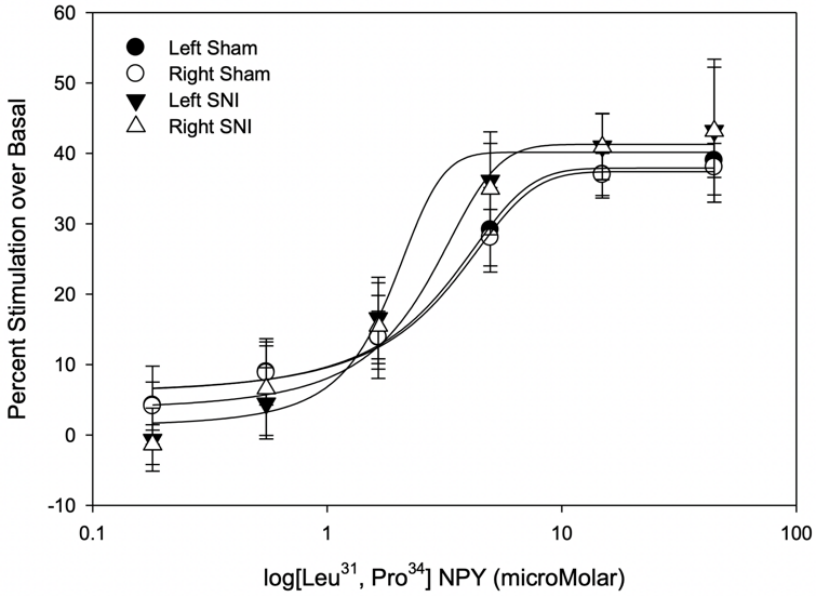

Figure 16. [35S]GTPγS binding stimulated by the Y1 receptor agonist [Leu31,Pro34]-NPY in lumbar spinal cord sections of sham and SNI mice.

Concentration responses of [Leu^{31}, Pro^{34}]-NPY-stimulated [^{35}S]GTPγS binding in right and left dorsal horn of lumbar spinal cords from left leg SNI and sham animals (n=5-10 animals/group). (**[^{35}S]GTPγS binding assays were performed by Drs. Michelle K. Winters and Ken E. McCarson*)

3.3.2 A Y1 selective agonist acts at dorsal horn interneurons, rather than the central terminals of primary afferent neurons, to inhibit mechanical and cold allodynia.

Intrathecal administration of NPY Y1 selective agonists attenuate dorsal horn neuron activation and neuropathic allodynia (Intondi et al., 2008; Kuphal et al., 2008; Malet et al., 2017). However, NPY Y1 receptors are expressed on both excitatory interneurons in the DH and on the central terminals of primary afferent neurons arising from the dorsal root ganglion (DRG) (Brumovsky et al., 2007, 2006; Nelson and Taylor, 2021; Taylor et al., 2014). To resolve the specific site of antihyperalgesic action by intrathecal Y1 agonists, we first extended previous results in the rat (Intondi et al., 2008; Malet et al., 2017), to our mouse SNI model of peripheral nerve injury. 14 days after SNI, rodents exhibit long-lasting mechanical and cold hypersensitivity in the sural innervation territory of the afflicted hindpaw (lateral surface) (Challa, 2015; Decosterd and Woolf, 2000; Intondi et al., 2008; Nelson et al., 2019). At this time point, intrathecal administration of [Leu^{31}, Pro^{34}]-NPY (**Figure 15E**) dose dependently reduced both SNI-induced mechanical and cold hypersensitivity in male and female mice (**Figure 15F-G**). These antihyperalgesic effects were abolished with co-administration of the Y1 receptor antagonist, BIBO 3304, but not the Y2 receptor antagonist, BIIE 0246 (**Figure 15H-I**), suggesting on-target agonist binding at the Y1 receptor. Additionally, we found that intrathecal administration of [Leu^{31}, Pro^{34}]-NPY could repeatedly abolish SNI-induced allodynia long after the induction of nerve injury (**Figure 15J-K**). [Leu^{31}, Pro^{34}]-NPY also reduced light touch-evoked expression of phosphorylated extracellular signal-regulated kinase (pERK) in superficial dorsal horn neurons, a proxy for neuronal activation (Gao and Ji, 2009); this effect was abolished with co-administration of BIBO 3304 (**Figure 15L-Q**). These results indicate that Y1 agonism at the spinal cord potently inhibits behavioral and immunohistochemical markers of neuropathic pain in mice.

Next, we crossed *Npy1r*$^{loxP/loxP}$ mice (Howell et al., 2003) with either *Pirt*^{Cre} (Kim et al., 2016) or *Lbx1*^{Cre} mice (Müller et al., 2002) to selectively knockout *Npy1r* in the DRG, or DH, respectively (**Figure 17A-B**). [Leu^{31}, Pro^{34}]-NPY reduced SNI-induced mechanical and cold hypersensitivity in both control (*Npy1r*$^{loxP/loxP}$) and DRG conditional knockout mice (*Npy1r*$^{loxP/loxP}$;*Pirt*^{Cre}), but not in DH conditional knockout mice (*Npy1r*$^{loxP/loxP}$;*Lbx1*^{Cre}) (**Figure 17C-D**). These results indicate that intrathecal NPY Y1 agonists act at spinal cord interneurons rather than the peripheral terminals of DRG neurons to inhibit behavioral signs of neuropathic pain.

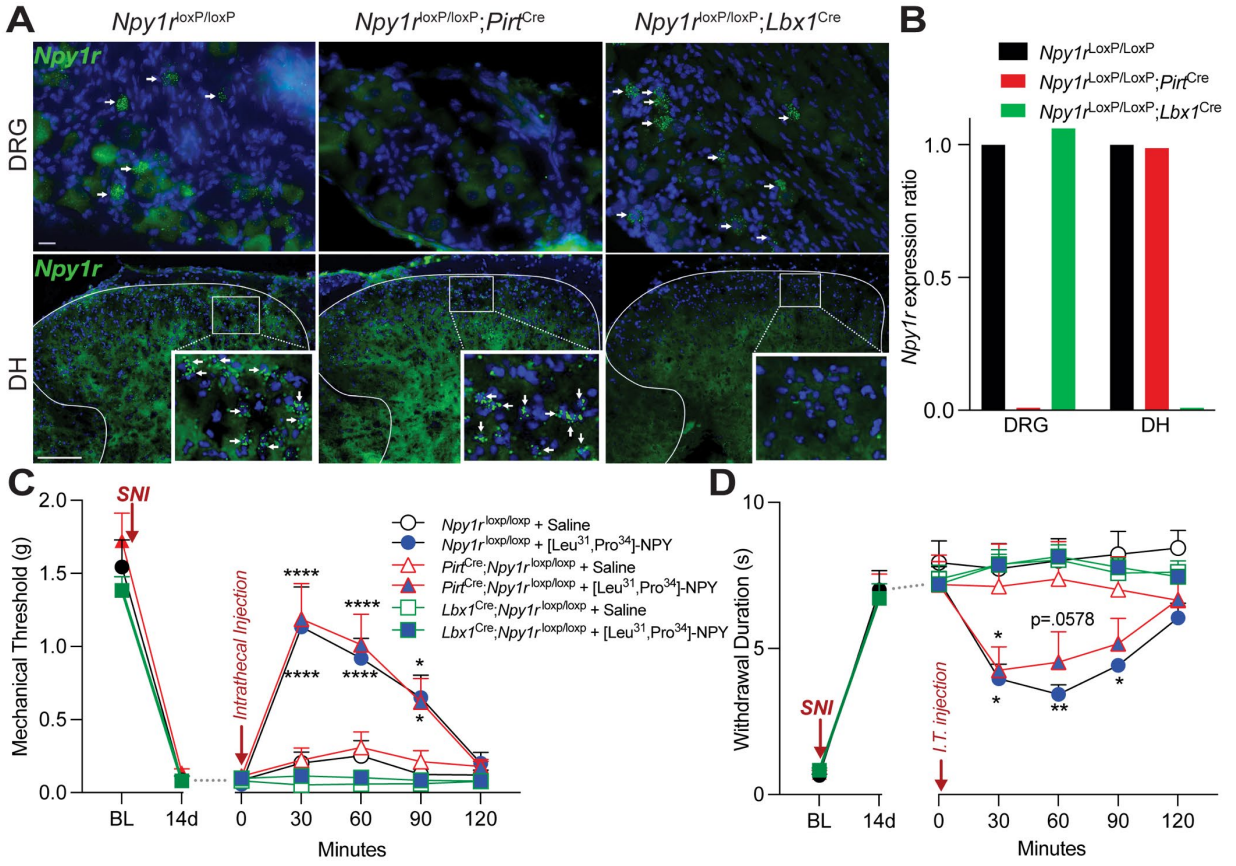

Figure 17. Y1 selective agonist acts at spinal cord interneurons rather than the central terminals of primary afferent neurons to inhibit SNI-induced neuropathic pain.

(**A**) Fluorescence *in situ* hybridization of sections through DRG (top row) and dorsal horn of the spinal cord (bottom row) demonstrate that *Npy1r*$^{loxP/loxP}$ mice express *Npy1r* in DRG and spinal cord, *Npy1r*$^{loxP/loxP}$;*Pirt*^{Cre} mice lack expression of *Npy1r* in the DRG, and *Npy1r*$^{loxP/loxP}$;*Lbx1*^{Cre} mice lack expression of *Npy1r* in the dorsal horn of the spinal cord. (**B**) Quantification of *Npy1r*-expressing cells in L3-L4 DRGs and superficial L4 DH of *Npy1r*$^{loxP/loxP}$, *Npy1r*$^{loxP/loxP}$;*Pirt*^{Cre}, and *Npy1r*$^{loxP/loxP}$;*Lbx1*^{Cre} mice in comparison to *Npy1r*$^{loxP/loxP}$ expression. (**C**) [Leu^{31}, Pro^{34}]-NPY (10.0 µg) abolishes SNI-induced mechanical allodynia in *Npy1r*$^{loxP/loxP}$ and *Npy1r*$^{loxP/loxP}$;*Pirt*^{Cre} mice but not in *Npy1r*$^{loxP/loxP}$;*Lbx1*^{Cre} mice (n=9 mice/group). Three-way RM ANOVA. Holm-Sidak post hoc test. (**D**) Leu^{31}, Pro^{34}]-NPY (10.0 µg) abolishes SNI-induced cold allodynia in *Npy1r*$^{loxP/loxP}$ and *Npy1r*$^{loxP/loxP}$;*Pirt*^{Cre} mice but not in *Npy1r*$^{loxP/loxP}$;*Lbx1*^{Cre} mice (n=9 mice/group). Three-way RM ANOVA. Holm-Sidak post hoc test. Data are shown as means ± SEM. *p < 0.05, **p<0.01, ****p<0.0001. Dots represent data points from individual animals.

3.3.3 Y1-INs are necessary for the sensory and affective components of SNI-induced neuropathic pain.

Our conditional genetic knockout of peripheral and central *Npy1r* data indicate that Y1 receptor agonists act at spinal cord interneurons (Y1-INs) to inhibit SNI-induced neuropathic mechanical and cold hypersensitivities. To directly test the hypothesis that Y1-INs are necessary for the full manifestation of SNI-induced hyperalgesia, we used intraspinal inhibitory chemogenetics to inhibit the adult spinal Y1-IN population. We injected a Cre-dependent inhibitory DREADD (AAV8-hSyn-DIO-hM4D$_{Gi}$) into the left lumbar (targeting L3-L4) dorsal horn of *Npy1r*^{Cre} mice (**Figure 18A**). As described previously (Inquimbert et al., 2018; Peirs et al., 2015), the AAV8-hSyn serotype selectively transfected neurons in the spinal cord but not DRG (**Figure 19**). Immunohistochemical verification of AAV expression was detected ipsilateral to viral injection (left but not right DH) and dorsal to the PKCγ band that delineates lamina IIi, indicating that its expression was restricted to the superficial dorsal horn (laminae I-IIo) (**Figure**

18B). When administered after SNI (but not before), clozapine N-oxide (CNO 3 mg/kg, i.p.) abolished both mechanical and cold hypersensitivity (**Figure 18C-G**) and reduced light-touch evoked pERK in the superficial dorsal horn (**Figure 18H-I**). We selected the 3 mg/kg dose of CNO as this is the lowest suggested dose that enters the CSF to be a suitable DREADD agonist within 15 min of administration while not producing off target effects (Jendryka et al., 2019); additionally, this is a commonly utilized dose for spinal cord chemogenetics (Kiguchi et al., 2021; Petitjean et al., 2015). Further, we used the critical control animals that have the same genetic background (*Npy1r*^{Cre}) and received an injection of a control AAV encoding only a fluorescent tag without DREADDs (mCherry). This control is critical for chemogenetics experiments to assess potential nonspecific effects of the designer ligand.(Vlasov et al., 2018). In addition to stimulus-evoked features of pain such as allodynia, nerve injury also elicits stimulus-independent ongoing affective pain which can be assessed with conditioned place preference (CPP) paradigms (Navratilova et al., 2013). Following SNI and conditioning, mice injected with inhibitory DREADD (hM4D$_{Gi}$) but not control virus (mCherry) spent more time in the CNO-paired chamber (**Figure 18J-K**). These findings indicate that chemogenetic inhibition of spinal Y1-INs reduces stimulus-dependent and -independent components of neuropathic pain.

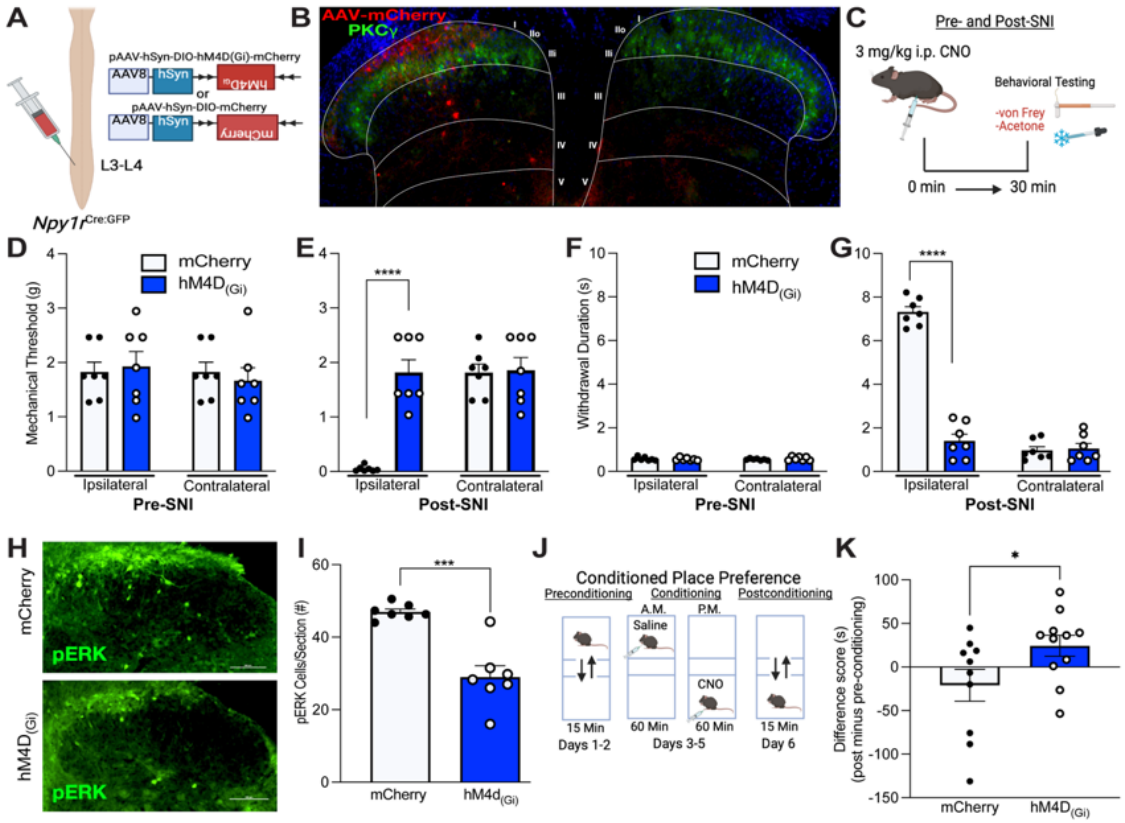

Figure 18. Chemogenetic inhibition of spinal Y1-INs reduces behavioral and immunohistochemical markers of SNI-induced reflexive and affective pain.

(**A**) Strategy for selectively targeting Y1-INs in *Npy1r*^{Cre} mice with intraspinal injections of the Cre-dependent virus AAV8-hSyn-DIO-hM4D$_{Gi}$-mCherry. (**B**) Representative IHC image of the spatial distribution of AAV-hM4D$_{Gi}$-mCherry neurons (red) that is largely restricted to the ipsilateral (left) superficial dorsal horn (laminae I-IIo) and dorsal to the PKCγ band (green). DAPI (blue). (**C**) Experimental timeline of chemogenetic reflexive behavioral testing at both pre- and post-SNI timepoints. (**D-G**) Chemogenetic inhibition of Y1-INs with CNO (3 mg/kg) does not alter mechanical or cold withdrawal thresholds before SNI but dramatically reduces both SNI-induced mechanical and cold allodynia (n=7 mice/group). Two-way ANOVA. Holm-Sidak post hoc tests. (**H**) Representative images of light-touched evoked pERK in the spinal cord dorsal horn following intraperitoneal administration of CNO (3 mg/kg). Scale bars: 100 µm. (**I**) Chemogenetic inhibition of Y1-INs with CNO (3 mg/kg) reduces light-touched evoked pERK in SNI mice (n=7 mice/group). Student's unpaired two-tailed t test. (**J**) Protocol for conditioned place preference. (**K**) Chemogenetic inhibition of Y1-INs induces CPP (increased time in the CNO-paired chamber) in SNI mice (n=10-11 mice/group). Student's unpaired two-tailed t test. Data are shown as means ± SEM. *p < 0.05, ***p<0.001, ****p<0.0001. Dots represent data points from individual animals.

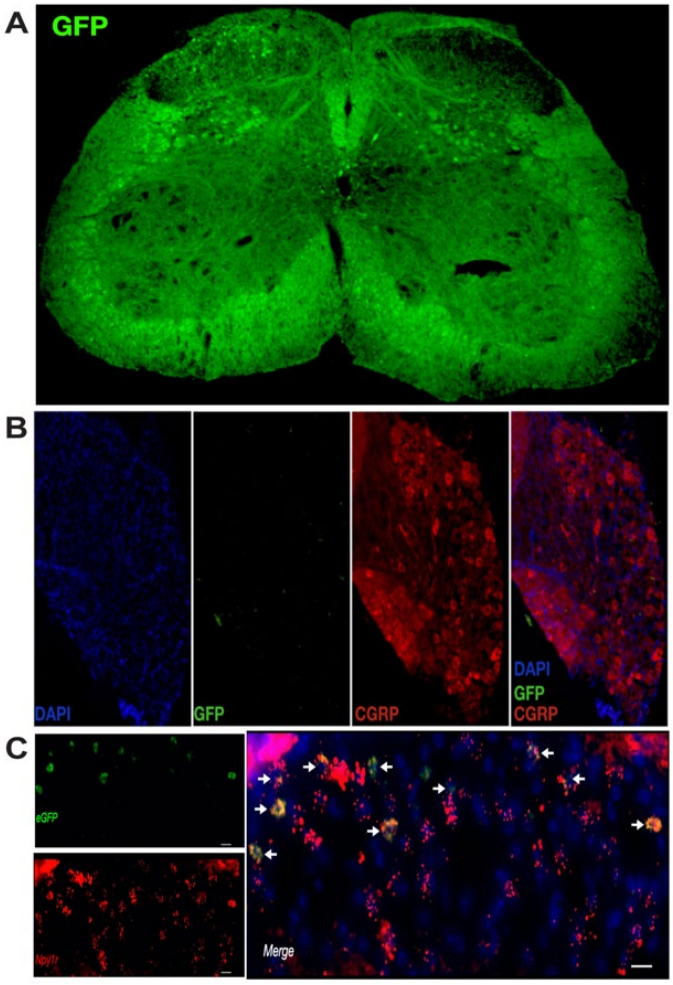

Figure 19. Intraspinal administration of AAV8-hSyn-DIO-mCitrine into Npy1rCre mice selectively transfects Npy1r-expressing cells in the superficial dorsal horn and not primary afferent cells.

(**A**) AAV8-hSyn-DIO-mCitrine was injected into the left spinal cord dorsal horn of *Npy1r*^{Cre} mice and infected superficial cells (green) in the ipsilateral (left) but not contralateral (right) dorsal horn. Post-fixation immunohistochemistry for GFP was utilized to visualize mCitrine fluorescence expression. (**B**) We did not detect any virally infected (GFP-positive) cells in ipsilateral (left) lumbar DRGs. Further, ~100% of *Npy1r*-expressing primary afferent neurons co-express calcitonin gene-related peptide (CGRP) (Brumovsky et al., 2007). For this reason, we co-stained all DRG's for both GFP and CGRP and despite the high prevalence of CGRP-positive cells, we failed to detect a single virally infected primary afferent neuron. (**C**) Dual-label fluorescence *in situ* hybridization for *Npy1r* (red) and *eGFP* (green) shows that all eGFP cells infected by AAV8-hSyn-DIO-mCitrine were *Npy1r*-positive. Scale bar 10 μm.

3.3.4 Nerve injury depolarizes the resting membrane potential and increases the excitability of delayed firing Y1-INs.

3.3.4.1 Neurochemical, neurophysiological, and morphological characterization of Y1-INs.

Spinal cord dorsal horn neurons are classified by neurochemical gene / protein expression, neurophysiological firing pattern, and/or cellular morphology (Peirs et al., 2020; Todd, 2017). Using these criteria, we characterized Y1-INs in lumbar (L3-L4) sections obtained from BAC transgenic mice that express enhanced green fluorescent protein (eGFP) under the control of the *Npy1r* promoter (*Npy1r*^{eGFP}). First, we investigated the neurochemical identity of Y1-INs with fluorescence *in situ* hybridization. Consistent with our previous results in the rat (Nelson et al., 2019; Nelson and Taylor, 2021), we found that almost all *Npy1r*^{eGFP} neurons co-express neurochemical markers of excitatory (*Lmx1b*) but not inhibitory (*Pax2*) neurons (Cheng et al., 2005; Del Barrio et al., 2013; Hernandez-Miranda et al., 2017; Szabo et al., 2015); for the first time we show that this was not altered by nerve injury (**Figure 20**). Second, we characterized superficial DH *Npy1r*^{eGFP} neurons using *ex vivo* slice electrophysiology recordings to evaluate the firing patterns evoked by steady-state current injection as described previously (Sinha et al., 2021) (**Figure 21A**). We identified four main firing patterns in *Npy1r*^{eGFP} neurons: Delayed Long Latency Firing (DLLF) neurons, Delayed Short Latency Firing (DSLF) neurons, Initial Burst Firing (IBF) neurons, and Phasic Firing (PF) neurons (**Figure 21B-C**). Third, with respect to each firing pattern, we used neurobiotin labeling and confocal imaging to characterize the cellular morphology of Y1-INs as described by Grudt and Perl (Grudt and Perl, 2002). As illustrated in **Figure 21D-E**, most Y1-INs, and particularly the DSLF and IBF firing types, exhibited a morphology similar to the central cells described by Grudt and Perl. In summary, most Y1-INs are excitatory neurons that exhibit a DSLF firing pattern and a central cell morphology.

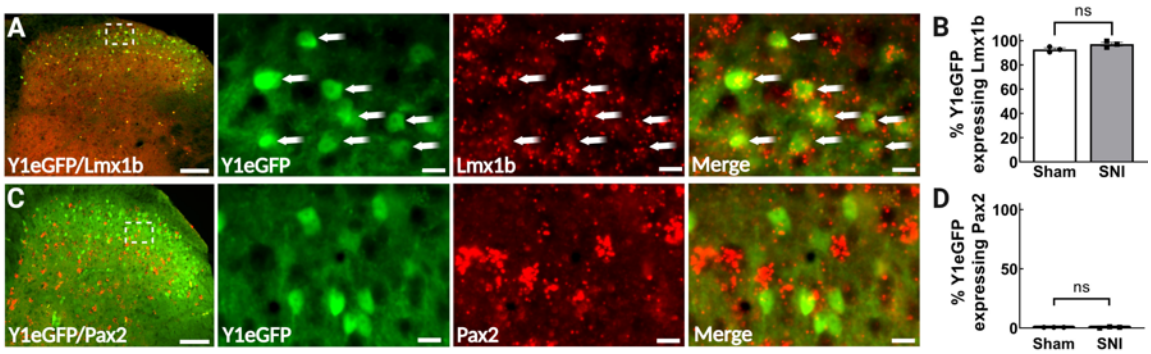

E

mRNA/condition	Y1eGFP (total)	mRNA (total)	Y1eGFP + mRNA	% Y1eGFP that are mRNA	% mRNA that are Y1eGFP
Lmx1b/Sham	57 ± 6.3	74.6 ± 9.5	54.2 ± 6.8	95.0 ± 1.5	72.9 ± 4.8
Lmx1b/SNI	60.5 ± 5.0	79.4 ± 5.5	60.3 ± 4.9	99.6 ± .3	75.9 ± 2.2
Pax2/Sham	40.6 ± 1.7	35.7 ± 5.0	0.3 ± 0.0	0.6 ± 0.07	1.0 ± 0.3
Pax2/SNI	42.8 ± 5.5	27 ± 7.4	0.2 ± 0.001	0.6 ± 0.02	0.6 ± 0.0

Figure 20. SNI does not alter the proportion of superficial dorsal horn Y1^{eGFP} neurons that are excitatory or inhibitory.

(**A**) Representative colocalization of Y1^{eGFP} immunohistochemistry combined with fluorescence *in situ* hybridization for the postnatal excitatory marker *Lmx1b.* Arrows indicate colocalization of Y1^{eGFP} and *Lmx1b.* (**B**) Nearly all superficial Y1^{eGFP} neurons express mRNA for the postnatal excitatory marker *Lmx1b* and this is not altered by SNI. (n= 3 mice/group). Student's unpaired two-tailed t test. (**C**) Representative colocalization of Y1^{eGFP} immunohistochemistry combined with fluorescence *in situ* hybridization for the postnatal inhibitory marker *Pax2*. (**D**) Almost no Y1^{eGFP} neurons express mRNA for the postnatal inhibitory marker *Pax2* and this is not altered by SNI. (n= 3 mice/group). Student's unpaired two-tailed t test. (**E**) A table detailing the quantification from sham and SNI mice shown above (4 sections averaged per mouse). Data are shown as means ± SEM. Images in panels 2-4 represent boxed area. Scale bars = 100 µm and 10 µm for zoomed images. (**Quantification was performed by Dr. Pranav Prasoon*)

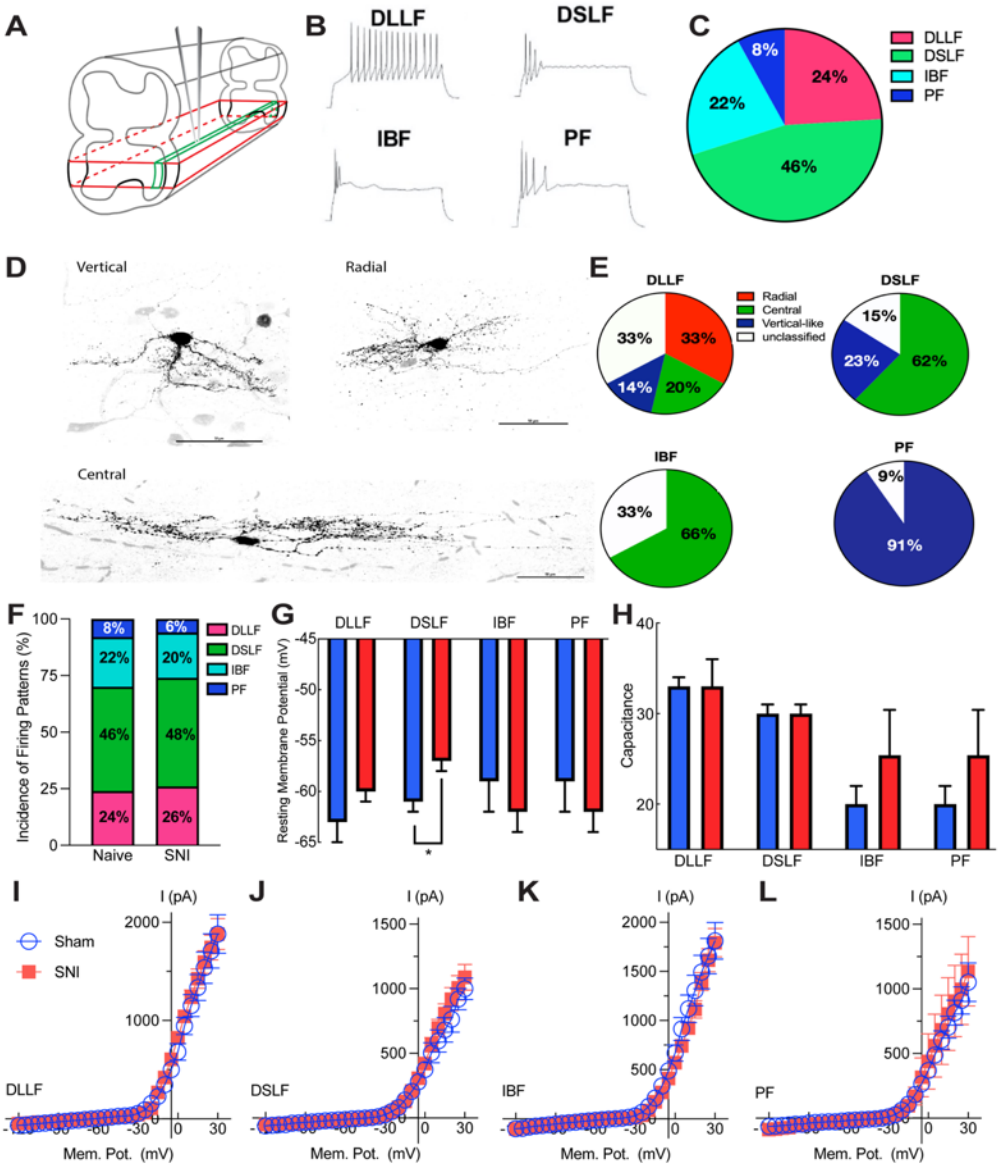

Figure 21. Electrophysiological and Morphological Characterization of Y1-INs.

(**A**) Schematic illustration of para-sagittal slices from the L3/L4 segment of adult mice that were used for electrophysiological recordings in *Npy1r*^{eGFP} neurons. (**B**) Representative examples and (**C**) incidence of firing patterns in *Npy1r*^{eGFP} neurons (delayed long latency firing, DLLF; delayed short latency firing, DSLF; initial burst firing, IBF; or phasic firing, PF) (n=100 neurons from 36 mice). (**D**) Representative examples of biotin filled *Npy1r*^{eGFP} neuron morphologies. Scale bars: 50µm. (**E**) Quantification of morphology incidence within each electrophysiological firing pattern (DLLF (n=15 cells); DSLF (n=13 cells); IBF (n=9 cells); and PF (n=11 cells)). (**F**) Nerve injury did not change the incidence of firing patterns in *Npy1r*^{eGFP} neurons (n= 100 sham neurons and n=100 SNI neurons). χ^2 Test. (**G**) Nerve injury produces a depolarizing shift in the resting membrane potential in

DSLF *Npy1r*^{eGFP} neurons (DLLF (n=10-13); DSLF (n=28-33); IBF (n=4-7); and PF (n=4-7)). χ^2 Test. (**H**) Nerve injury did not change the membrane capacitance of any *Npy1r*^{eGFP} neuron firing types (DLLF (n=14-19 neurons), DSLF (n=41-45 neurons); IBF (n=4-15 neurons), and PF (n=4-15 neurons)). χ^2 Test. (**I-L**) Nerve injury did not change current-voltage (I-V) plots for any *Npy1r*^{eGFP} neuron firing types (DLLF (n=7-11 neurons); DSLF (n=15-23 neurons), IBF (n=4-12 neurons); and PF (n=8-11 neurons)). Two-way ANOVA. Data are shown as means ± SEM. *p < 0.05. (**All slice electrophysiology recordings were performed by Dr. Ghanshyam Sinha, and Biotin Morphological rendering was performed by Dr. Peter Jukkola*)

3.3.4.2 Effect of nerve injury on firing type and passive membrane properties

The response properties of DH neurons are shaped by their passive biophysical membrane properties (Dougherty and Chen, 2016). Interestingly, peripheral nerve injury modestly affects or does not alter the passive membrane properties of randomly sampled interneurons in the rat or GABAergic interneurons in the mouse dorsal horns (Balasubramanyan et al., 2006; Boyle et al., 2019; Chen et al., 2009; Lu et al., 2009, 2013; Schoffnegger et al., 2006; Zhang et al., 2018). For this reason, we hypothesized that SNI would not alter the passive membrane properties of Y1-INs. To test this, we conducted *ex vivo* slice electrophysiology recordings in both naïve and SNI *Npy1r*^{eGFP} mice. As hypothesized, SNI did not change the percentages of DSLF, DLLF, IBF or PF Y1-IN firing patterns (**Figure 21F**). To our surprise, SNI produced a depolarizing shift of the resting membrane potential for specifically DSLF neurons (**Figure 21G**), though did not alter membrane capacitance (**Figure 21H**) nor the current–voltage (I–V) relations (**Figure 21I-L**) in any *Npy1r*^{eGFP} firing populations. In summary, a more positive resting membrane potential in DSLF neurons indicates that SNI increases intrinsic excitability, a key feature of central sensitization (Latremoliere and Woolf, 2009).

3.3.4.3 Effect of nerve injury on active membrane properties

Peripheral nerve injury can enhance the membrane excitability of dorsal horn neurons (Latremoliere and Woolf, 2009). To test the hypothesis that SNI increases the membrane excitability of Y1-INs, we employed depolarizing current ramps to elicit action potential firing (Balasubramanyan et al., 2006; Chen et al., 2009). We focused our analysis on the DSLF subtype for two reasons: 1) DSLF neurons were the only population found to have a depolarizing shift in resting membrane potential after SNI (**Figure 21G**), and 2) the DSLF population is the most

abundant population of Y1-INs when segregated by firing type (**Figure 21F**). Neurons were held at -60 mV and current ramps were applied at 67 pA/s (**Figure 22A**). SNI did not change the number of action potentials in DSLF neurons but decreased the latency to first action potential (**Figure 22B-C**). We then examined the effect of SNI on membrane excitability in DSLF *Npy1r*^{eGFP} neurons using stepped depolarization from hyperpolarized conditions. All DSLF Y1-INs were held at -80 to -85 mV for 500 msec before application of current. Steady-state 1-second, current steps from 0 to 80 pA were used to elicit action potentials. Representative firing patterns in DSLF *Npy1r*^{eGFP} neurons from SNI mice are shown in **Figure 22D**. SNI increased the number of action potentials per step during the 1 second pulse in DSLF Y1-INs (**Figure 22E**), decreased the current threshold needed to elicit first action potentials (**Figure 22F**), increased the number of neurons exhibiting rebound spiking (action potential spike at 0 pA from conditioning hyperpolarized state is used to measure rebound spiking) (**Figure 22G**), and increased the average firing frequency (but not amplitude) at current injecting steps to 40 pA (**Figure 22H-I**). We also found that SNI robustly increased the membrane excitability of DLLF neurons (**Figure 23**). We conclude that SNI increases the membrane excitability of delayed firing Y1-INs.

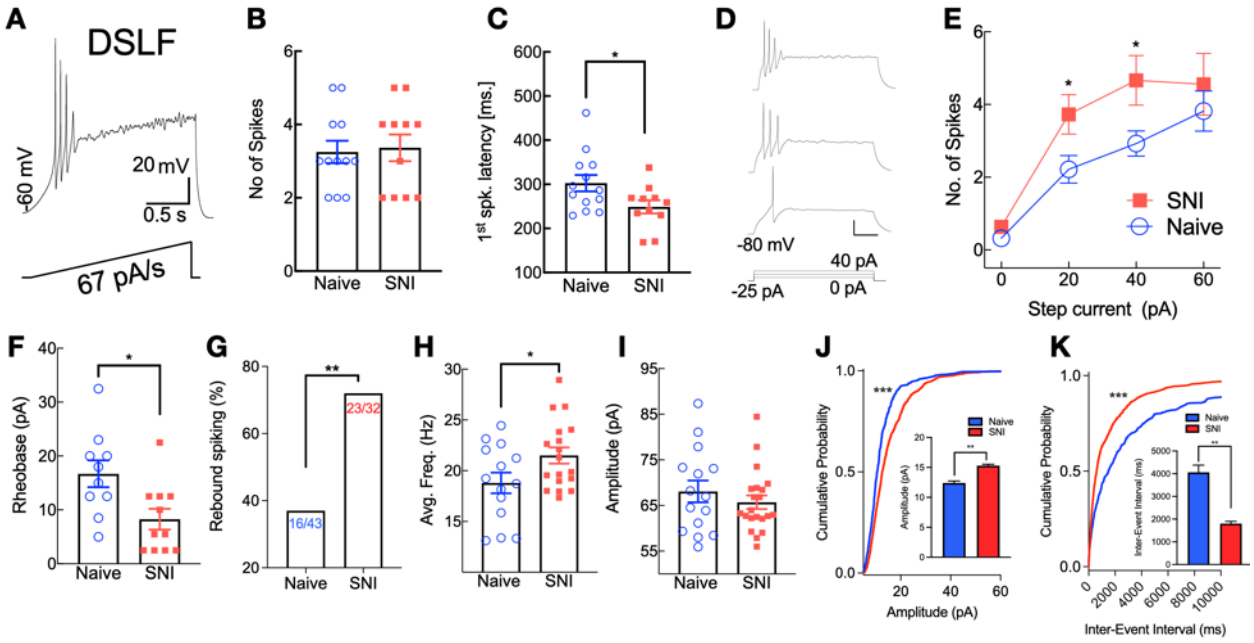

Figure 22. SNI increases the excitability of DSLF Y1-INs in the superficial dorsal horn.

(**A**) Representative example of a DSLF *Npy1r*^{eGFP} neuron firing pattern upon injection of ramped current at 67 pA/s. (**B**) SNI did not alter the number of action potential spikes (**C**) but decreased the latency to first spike elicited by ramp current in DLSF *Npy1r*^{eGFP} neurons (n= 11-13 neurons). Student's unpaired two-tailed t test. (**D**) Representative example of a DSLF *Npy1r*^{eGFP} neuron held at hyperpolarized condition (-80 mV) for 500 msec before application of steady-state 1 second current steps from 0 to 40 pA. SNI (**E**) increased the number of action potential spikes at current injection steps, (**F**) lowered the Rheobase, (**G**) increased the percentage of neurons exhibiting rebound spiking, and increased (**H**) firing frequency but (**I**) not amplitude in DLSF *Npy1r*^{eGFP} neurons (n=10-33 neurons). Student's unpaired two-tailed t test. Cumulative distribution plots (left) and group data (right) show SNI increases the (**J**) average amplitude and (**K**) frequency of sEPSCs in DSLF *Npy1r*^{eGFP} neurons (n= 16 neurons/group). Kolmogorov-Smirnov test and Student's unpaired two-tailed t test. Data are shown as means ± SEM. *p < 0.05, **p<0.01, ***p<0.001, ****p<0.0001. Dots represent data points or averages from individual cells. (**All slice electrophysiology recordings were performed by Dr. Ghanshyam Sinha*)

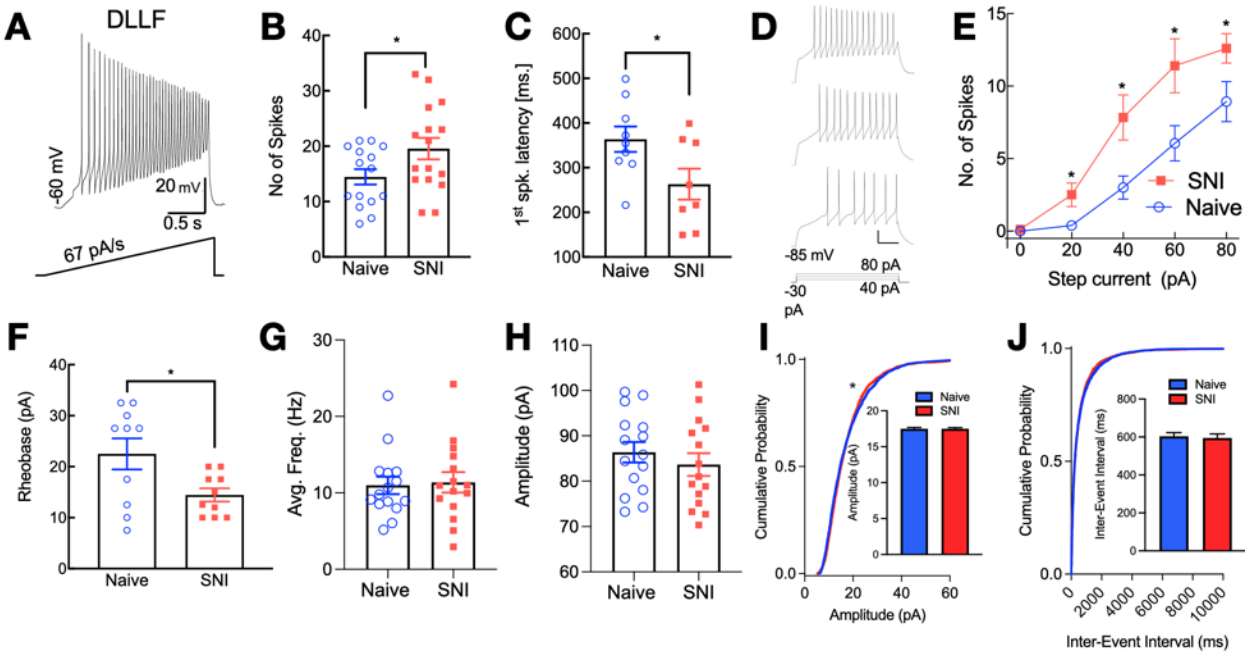

Figure 23. SNI increases the excitability of DLLF Y1-INs in the superficial dorsal horn.

(**A**) Representative example of a DLLF *Npy1r*^{eGFP} neuron firing pattern upon injection of ramped current at 67 pA/s. SNI (**B**) increased the number of action potential spikes (**C**) and decreased the latency to first spike elicited by ramp current in DLLF *Npy1r*^{eGFP} neurons (n= 8-16 neurons). Student's unpaired two-tailed t test. (**D**) Representative example of a DLLF *Npy1r*^{eGFP} neuron held at hyperpolarized condition (-85 mV) for 500 msec before application of steady-state 1 second current steps from 40 to 80 pA. SNI (**E**) increased the number of action potential spikes at current injection steps, (**F**) lowered the Rheobase, (**G**) but did not alter the firing frequency or (**H**) amplitude in DLLF *Npy1r*^{eGFP} neurons (n=10-16 neurons). Student's unpaired two-tailed t test. Cumulative distribution plots (left) and group data (right) show SNI slightly increases the (**I**) average amplitude but (**J**) does not alter the frequency of sEPSCs in DLLF *Npy1r*^{eGFP} neurons (n= 11-12 neurons/group). Kolmogorov-Smirnov test and Student's unpaired two-tailed t test. Data are shown as means ± SEM. *p < 0.05. Dots represent data points or averages from individual cells. (**All slice electrophysiology recordings were performed by Dr. Ghanshyam Sinha*)

3.3.4.4 Effect of nerve injury on synaptic excitability

Peripheral nerve injury dramatically enhances the spontaneous excitatory synaptic activity of excitatory DH neurons (Balasubramanyan et al., 2006; Chen et al., 2009; Inquimbert et al., 2012). To assess changes in excitatory synaptic transmission in Y1-INs, we recorded spontaneous excitatory post-synaptic currents (sEPSCs) from both naïve and SNI *Npy1r*^{eGFP} mice, with the assumption that changes in amplitude and frequency will be attributed to postsynaptic and presynaptic adaptations (Balasubramanyan et al., 2006; Chen et al., 2009), respectively. However, since we recorded sEPSCs and not mEPSCs in the presence of tetrodotoxin, there is the chance of action potential-driven activity and therefore, amplitude changes could also reflect presynaptic release activity. We found that SNI increased both amplitude and frequency (decrease in inter-event interval, IEI) of sEPSCs (**Figure 22 J-K, Figures 24-25**), suggesting that both pre- and postsynaptic adaptations contribute to an increased excitatory drive in DSLF, IBF and PF Y1-INs.

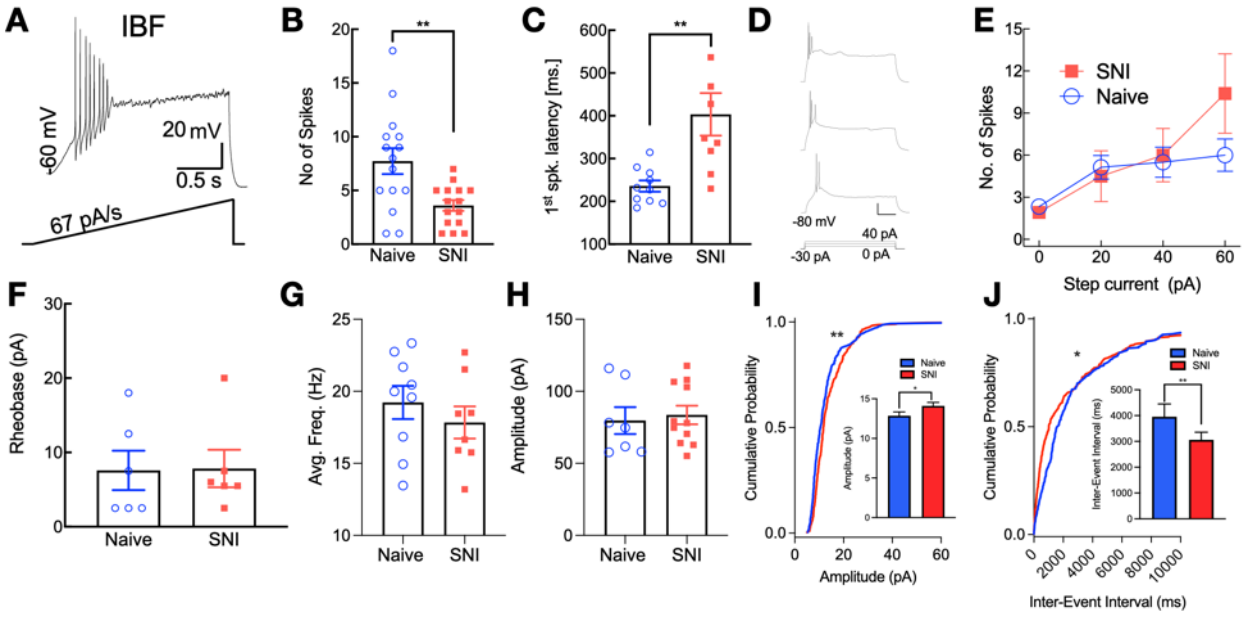

Figure 24. SNI increases the synaptic excitability of IBF Y1-INs in the superficial dorsal horn.

(**A**) Representative example of an IBF *Npy1r*^{eGFP} neuron firing pattern upon injection of ramped current at 67 pA/s. SNI (**B**) decreased the number of action potential spikes (**C**) and increased the latency to first spike elicited by ramp current in IBF *Npy1r*^{eGFP} neurons (n= 8-15 neurons). Student's unpaired two-tailed t test. (**D**) Representative example of an IBF *Npy1r*^{eGFP} neuron held at hyperpolarized condition (-80 mV) for 500 msec before application of steady-state 1 second current steps from 0 to 40 pA. SNI (**E**) did not alter the number of action potential spikes at current injection steps, or affect (**F**) the Rheobase, (**G**) firing frequency, or (**H**) amplitude in IBF *Npy1r*^{eGFP} neurons (n=6-11 neurons). Student's unpaired two-tailed t test. Cumulative distribution plots (left) and group data (right) show SNI increased both the (**I**) average amplitude and (**J**) the frequency of sEPSCs in IBF *Npy1r*^{eGFP} neurons (n= 8-9 neurons/group). Kolmogorov-Smirnov test and Student's unpaired two-tailed t test. Data are shown as means ± SEM. *p < 0.05, **p<0.01. Dots represent data points or averages from individual cells. (**All slice electrophysiology recordings were performed by Dr. Ghanshyam Sinha*)

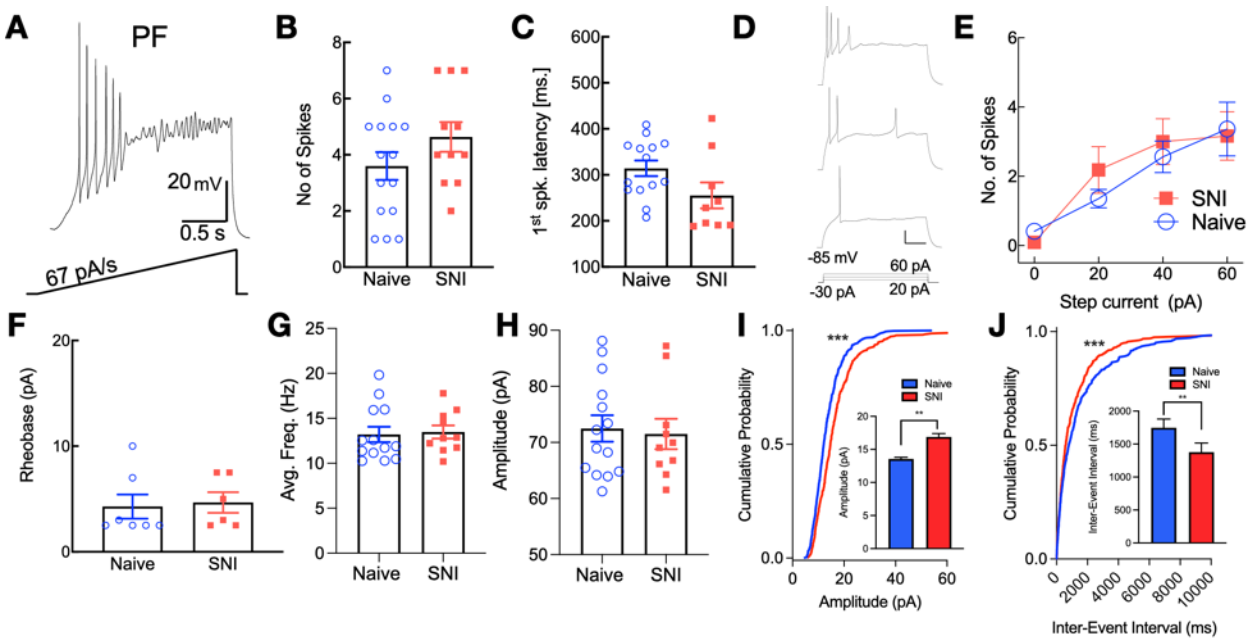

Figure 25. SNI increases the synaptic excitability of PF Y1-INs in the superficial dorsal horn.

(**A**) Representative example of a PF *Npy1r*^{eGFP} neuron firing pattern upon injection of ramped current at 67 pA/s. SNI did not affect the (**B**) number of action potential spikes or the (**C**) latency to first spike elicited by ramp current in PF *Npy1r*^{eGFP} neurons (n= 9-15 neurons). Student's unpaired two-tailed t test. (**D**) Representative example of a PF *Npy1r*^{eGFP} neuron held at hyperpolarized condition (-85 mV) for 500 msec before application of steady-state 1 second current steps from 20 to 60 pA. SNI (**E**) did not alter the number of action potential spikes at current injection steps, or affect (**F**) the Rheobase, (**G**) firing frequency, or (**H**) amplitude in PF *Npy1r*^{eGFP} neurons (n=6-14 neurons). Student's unpaired two-tailed t test. Cumulative distribution plots (left) and group data (right) show SNI increased both the (**I**) average amplitude and (**J**) the frequency of sEPSCs in PF *Npy1r*^{eGFP} neurons (n= 9 neurons/group). Kolmogorov-Smirnov test and Student's unpaired two-tailed t test. Data are shown as means ± SEM. *p < 0.05, **p<0.01, ***p<0.001. Dots represent data points or averages from individual cells. (**All slice electrophysiology recordings were performed by Dr. Ghanshyam Sinha*)

3.3.5 Spinal Y1-INs are sufficient for the behavioral manifestations of pain.

Our intrathecal pharmacology (**Figures 15 and 17**) and inhibitory chemogenetic data (**Figure 18**) indicate that spinal Y1-INs are necessary for the full manifestation of the behavioral symptoms of neuropathic pain. To test the hypothesis that activation of Y1-INs is sufficient to induce pain, we chemogenetically activated Y1-INs and measured both evoked and non-evoked pain-like behaviors in uninjured mice. We injected a Cre-dependent excitatory DREADD (AAV8-hSyn-DIO-hM3D$_{Gq}$) into the left lumbar dorsal horn of *Npy1r*^{Cre} mice (**Figure 26A**), and we measured both CNO-elicited spontaneous and evoked pain-like behaviors (Albisetti et al., 2019) (**Figure 26B**). CNO (3 mg/kg, i.p.), but not saline, induced robust spontaneous nocifensive (lifting, flapping, shaking, licking, guarding) but not itch-like (biting or scratching) behaviors directed to the left ipsilateral hind limb in mice injected with the excitatory DREADD (hM3D$_{Gq}$) but not control (mCherry) virus (**Figure 26C-D**). CNO also elicited both mechanical and thermal hypersensitivities (**Figure 26E-H**). Next, we tested the hypothesis that chemogenetic activation of Y1-INs is sufficient to produce avoidance using a conditioned place aversion paradigm (CPA) (**Figure 26I**). We found that chemogenetic Y1-IN activation produced a robust CPA (**Figure 26J-K**).

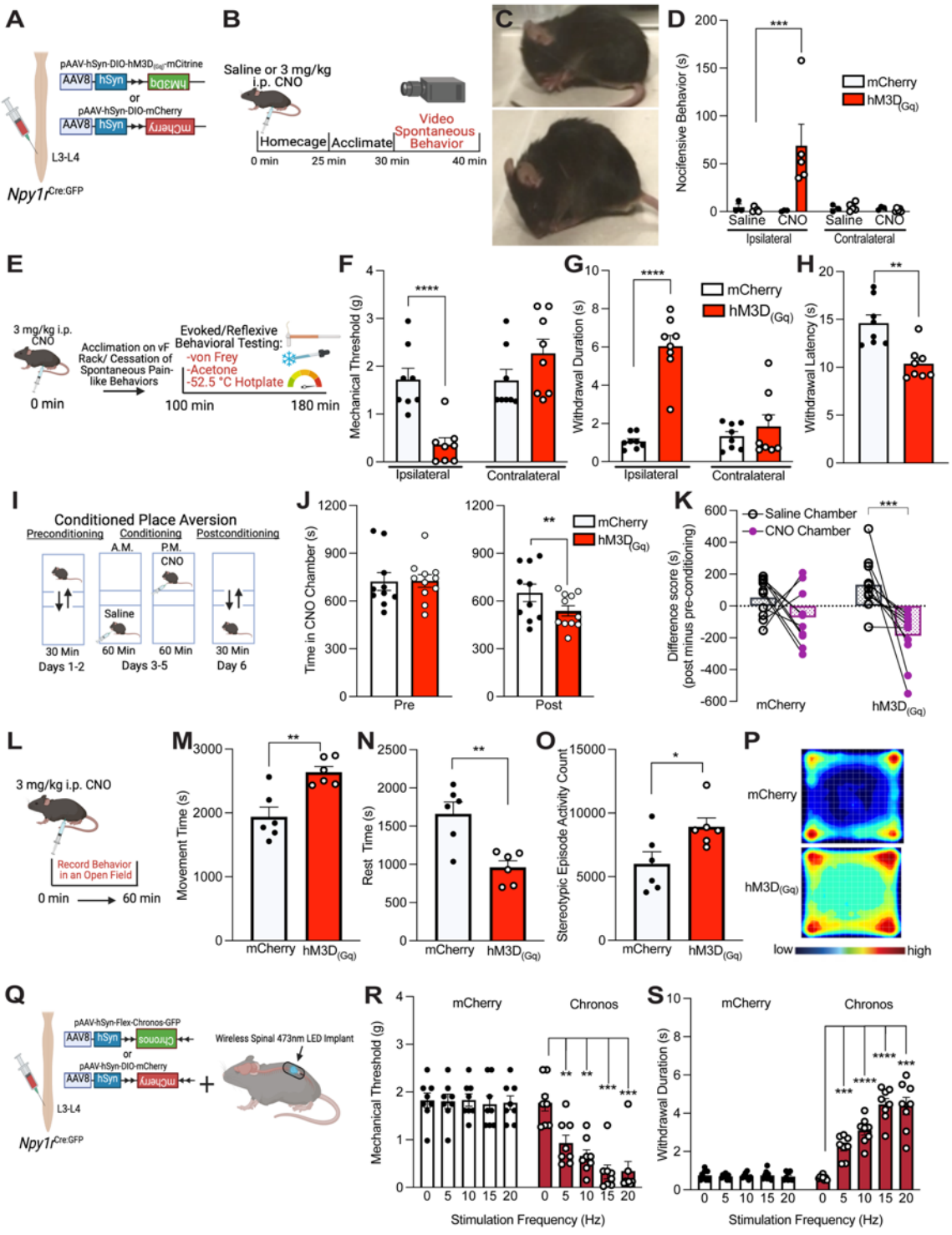

Figure 26. Activation of spinal Y1-INs in uninjured mice is sufficient to induce behavioral nocifensive symptoms correlative of neuropathic pain.

(**A**) Strategy for selectively targeting Y1-INs in *Npy1r*^{Cre} mice with intraspinal injections of the Cre-dependent virus AAV8-hSyn-DIO-hM3D$_{Gq}$-mCitrine. (**B**) Experimental timeline for chemogenetic activation of Y1-INs with CNO

(3 mg/kg) and videoing spontaneous hind left-limb directed nocifensive behaviors. (**C**) Representative example images of mice engaged in ipsilateral hindpaw-specific nocifensive behaviors. (**D**) CNO (3 mg/kg) but not saline induces spontaneous ipsilateral-directed (hind left paw) nocifensive behaviors (lifting, licking, flapping, shaking) in $hM3D_{(Gq)}$- but not mCherry-injected *Npy1r*^{Cre} mice. (n=3-5 mice/group). Three-way RM ANOVA. Holm-Sidak post hoc test. (**E**) Experimental timeline of chemogenetic activation of Y1-INs with CNO (3 mg/kg) and reflexive behavioral testing. Chemogenetic activation of Y1-INs with CNO (3 mg/kg) induces (**F**) mechanical (vF), (**G**) cold (acetone droplet withdrawal), and (**H**) heat (52.5 C hotplate) hypersensitivity (n=8 mice/group). F and G: Two-way ANOVA. Holm-Sidak post hoc tests. H: Student's unpaired two-tailed t test. (**I**) Experimental protocol for conditioned place aversion. (**J-K**) Activation of Y1-INs induces conditioned place aversion (n=10-11 mice/group). J: Student's paired two-tailed t test. K: Two-way ANOVA. Holm-Sidak post hoc test. (**L**) Experimental timeline of chemogenetic activation of Y1-INs with CNO (3 mg/kg) and immediate placement of mice into an open field testing environment. Chemogenetic activation of Y1-INs with CNO (3 mg/kg) produces robust discomfort represented by (**M**) continuous movement, (**N**) lack of rest, and (**O**) increased grooming-like (stereotypic episode activity count) behaviors. (**P**) Heat maps depicting averaged activity for all mice for the entire 60-minute duration of testing (n=6 mice/group). M-O: Student's unpaired two-tailed t test. (**Q**) Strategy for selectively targeting Y1-INs in *Npy1r*^{Cre} mice with intraspinal injections of the Cre-dependent virus AAV8-hSyn-Flex-Chronos-GFP and implantation of a wireless optogenetic 473 nm spinal LED implant. Optogenetic activation of Y1-INs induces a frequency dependent increase in (**R**) mechanical and (**S**) cold hypersensitivity (n=8 mice/group). Two-way RM ANOVA. Holm-Sidak post hoc tests. Data are shown as means ± SEM. *p < 0.05, **p<0.01, ***p<0.001, ****p<0.0001. Dots represent data points from individual animals.

We also evaluated the effect of chemogenetic activation of Y1-INs on non-evoked nocifensive behaviors. Immediately following CNO administration (3 mg/kg, i.p.), mice injected with control virus (mCherry) or excitatory DREADD ($hM3D_{Gq}$) were placed into a novel open field apparatus for 60 minutes (**Figure 26K**). Chemogenetic activation of Y1-INs produced a dramatic increase in ambulation (pain-like agitation), inability to rest, and robust grooming-like behaviors (stereotypic episode activity count) (**Figure 27L-O, Figure 27A-C**). These results are consistent with increased locomotion/agitation and grooming seen following injection of formalin into the hindpaw (Aloisi et al., 1995; Ang et al., 2015; Ibrahim et al., 2021). We do not believe that the increase in movement was attributed to increased anxiety-like behavior as mice demonstrated reduced thigmotaxis (more time in the center and less time in the margin of the open field) following CNO activation (**Figure 27D-E**) (Prut and Belzung, 2003; Simon et al., 1994). Furthermore, the nocifensive chemogenetic Y1-IN activation-induced increases in movement and grooming-like behaviors were reduced by pretreatment with the first-line neuropathic pain analgesic, gabapentin (100 mg/kg, i.p., (Kusunose et al., 2010; Zhang et al., 2021)) (**Figure 27F-I**).

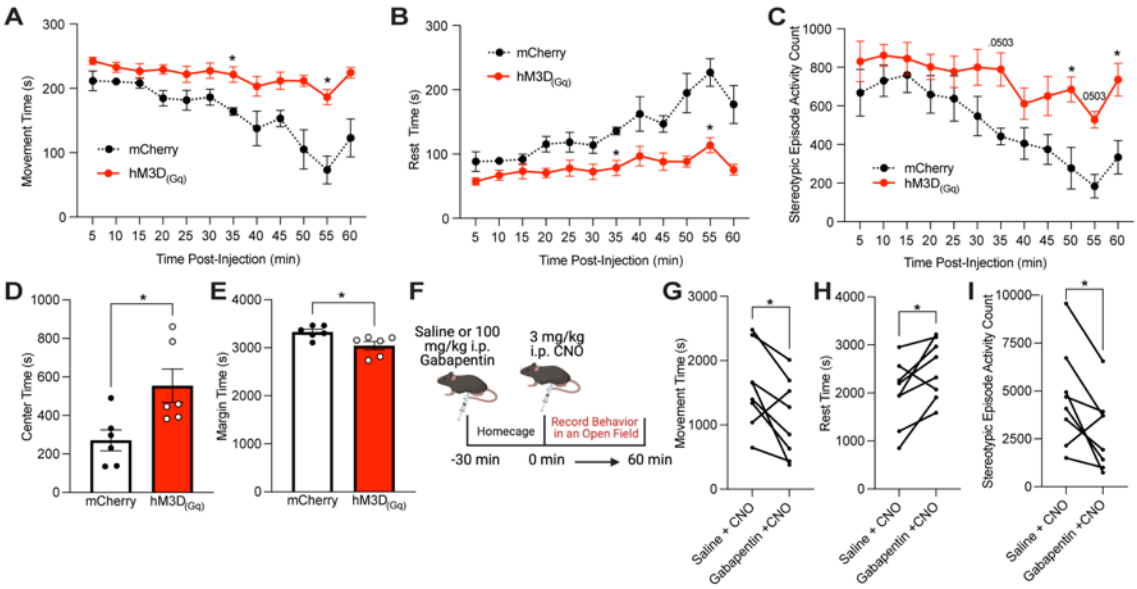

Figure 27. Open field evaluation of chemogenetic activation of Y1-IN-induced nocifensive responses. Chemogenetic activation of Y1-INs with CNO (3 mg/kg) produces robust discomfort represented by (**A**) increased movement time, (**B**) reduced rest time, and (**C**) increased grooming-like behaviors throughout the duration of time in the novel open field-testing chamber. (n=6 mice/group). Student's unpaired two-tailed t test. Two-way RM ANOVA. Holm-Sidak post hoc tests. Chemogenetic activation of Y1-INs with CNO (3 mg/kg) (**D**) increases the time spent in the center of the open field and (**E**) decreases the time spent in the margins of the open field. (n=6 mice/group). Student's unpaired two-tailed t test. (**F**) Experimental timeline of pretreatment with saline or gabapentin (100 mg/kg, i.p.) followed by chemogenetic activation of Y1-INs with CNO (3 mg/kg) and immediate placement of mice into an open field testing environment. Gabapentin (100 mg/kg, i.p.) but not saline reduces chemogenetic activation of Y1-IN-induced nocifensive (**G**) increases in movement time, (**H**) decreases in rest time, and (**I**) increases in grooming-like behaviors. (n=8 mice/group). Student's paired two-tailed t test. Data are shown as means ± SEM. *$p < 0.05$. Dots represent group averages.

Chemogenetic activation provides a powerful tool for excitation of Y1-INs with high spatial resolution, whereas it lacks the frequency-dependent and temporal activation that is afforded by excitatory optogenetic stimulation. To perform *in vivo* spinal optogenetic stimulation of Y1-INs and behavioral testing in awake and freely moving mice, we took advantage of newly developed wireless, lightweight, flexible, and implantable optoelectronic devices (Grajales-Reyes et al., 2021; Samineni et al., 2017). These spinal implants do not alter baseline somatosensation or motor coordination (**Figure 28**). We injected a Cre-dependent excitatory channelrhodopsin with fast kinetics and enhanced light sensitivity (AAV8-hSyn-Flex-Chronos) (Klapoetke et al., 2014) into the left lumbar dorsal horn of *Npy1r*^{Cre} mice before implanting a 473-nm, spinal optoelectronic device overlying the dura mater (**Figure 26P**). Delivery of light to the surface of the dorsal spinal cord in mice injected with the excitatory opsin (Chronos), but not control virus (mCherry), produced a robust and frequency-dependent (0, 5, 10, 20 Hz) increase in mechanical and cold hypersensitivity in the ipsilateral hindpaw (**Figure 26Q-R**). These data indicate that activation of Y1-INs is sufficient to produce pain-like behaviors.

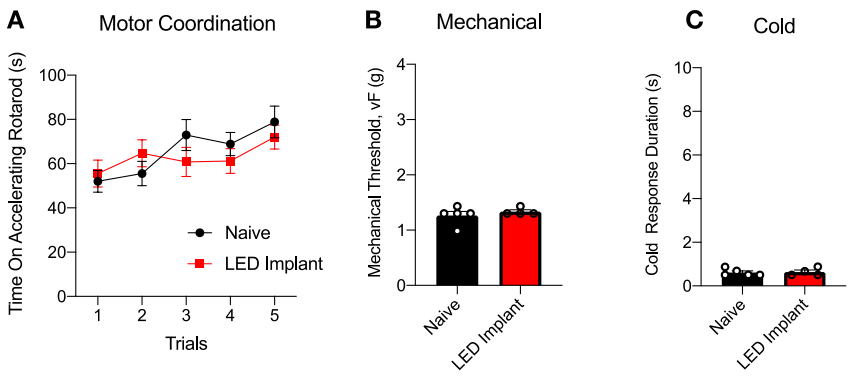

Figure 28. Surgical implantation of the Neurolux spinal LED implant does not alter motor coordination or reflexive baseline sensory withdrawal thresholds.

Implantation of the spinal Neurolux LED implant does not alter (**A**) time to fall on the accelerating rotarod, (**B**) von Frey mechanical withdrawal thresholds, or (**C**) acetone withdrawal response durations compared to naïve littermate controls. (n=4-5 mice/group). Student's unpaired two-tailed t test. Data are shown as means ± SEM. *$p < 0.05$. Dots represent group averages.

3.4 Discussion

We propose that *Npy1r*-expressing neurons in the dorsal horn are fundamental to both the initiation and maintenance of neuropathic pain.

3.4.1 Intrathecal NPY Y1 agonists act at spinal cord interneurons rather than the peripheral terminals of DRG neurons to inhibit behavioral signs of neuropathic pain

Several decades of research have established that intrathecal NPY reduces the behavioral and spinal molecular signs of hyperalgesia in rodent models of chronic pain by targeting Y1 receptors (Brumovsky et al., 2007; Diaz-delCastillo et al., 2018; Hökfelt et al., 2007; Malet et al., 2017; Nelson and Taylor, 2021; Smith et al., 2007). However, the exact target for Y1-mediated anti-nociception has remained elusive due to the dual expression of Y1 at both the central terminals of primary afferents and on spinal interneurons, both of which can be engaged following intrathecal injection. To resolve the Y1 site of action, we utilized the Cre-lox recombination system to conditionally knockout *Npy1r* in either the DRG or the DH (**Figure 17**). The resulting data demonstrate that intrathecal [Leu^{31}, Pro^{34}]-NPY acts exclusively at Y1 on DH neurons to inhibit allodynia. In future studies this same methodology can be utilized to resolve the Y1 agonist target for analgesia in other pain models. In particular, models of peripheral inflammation should be explored as *Npy1r* in the DRG is abundantly expressed within peptidergic C fibers (Brumovsky et al., 2007, 2002; Nelson and Taylor, 2021; Taylor et al., 2014), thus, peripheral Y1 may have more analgesic efficacy in these models.

Additionally, we demonstrate that the Y1 receptor can be repeatably targeted pharmacologically to alleviate behavioral signs of allodynia, up to at least 13 weeks post-SNI (**Figure 15**). These results support earlier chronic administration studies in the rat spinal cord that also found Y1 could be repeatedly engaged to alleviate neuropathic allodynia (Malet et al., 2017). Further, we build on a rich pre-clinical history demonstrating that NPY produces comparable analgesic effects to morphine when administered at the spinal level (Intondi et al., 2008; Nelson and Taylor, 2021; Smith et al., 2007; Taiwo and Taylor, 2002). Contrary to opioids however, which fail to alleviate neuropathic pain due to downregulation of receptors in neuropathic pain states (Chen et al., 2002; Martínez-Navarro et al., 2019), our results suggest that spinally administered Y1 agonists continue to be highly efficacious in chronic neuropathic pain states, a critical result for future clinical translation.

3.4.2 SNI enhances the potency of intrathecal [Leu^{31}, Pro^{34}]-NPY

GPCRs play fundamental roles in regulating biophysical functions and are pharmacological targets for many classes of drugs. [^{35}S]GTPγS binding assays measure the level of G protein activation following the occupation of a GPCR by an agonist to provide pharmacological values of potency, efficacy, and affinity (Harrison and Traynor, 2003). We used [Leu^{31}, Pro^{34}]-NPY-stimulated [^{35}S]GTPγS binding to analyze the functional coupling of Y1 receptors to G proteins in the dorsal horn after SNI. The E_{max} of NPY-stimulated G protein activation through Y1 receptors was unaffected following SNI. This is a positive finding that demonstrated that the magnitude of spinal Y1-coupled effects is not diminished or desensitized following long-term nociceptive activation of the system. We found that SNI increased the potency (decreased the EC_{50} ipsilateral to SNI) of [Leu^{31}, Pro^{34}]-NPY as compared to sham surgery (**Figure**

15). The lowered EC_{50} of NPY after SNI demonstrates that lower concentrations of NPY would be required to activate or maintain Y1-driven antinociceptive signaling during neuropathic pain. This increase in NPY potency after SNI reveals an enhanced affinity of Y1 coupling to G protein activation. The molecular mechanisms underlying this phenomenon are not well-defined, but could reflect the regulation of $Y1/G_{i/o}$ coupling dynamics via altered accessory protein partnering, modified stoichiometry of Y1 receptors to available G protein pools, receptor phosphorylation states, movement between membrane lipid domains, or even oligomerization of receptor proteins (Parker et al., 2008). We propose that the increased activation of G-proteins will amplify the effect of [Leu^{31}, Pro^{34}]-NPY in the setting of peripheral nerve injury, profoundly increasing the anti-hyperalgesic efficacy of [Leu^{31}, Pro^{34}]-NPY. In summary, our findings promote spinal Y1 as an extremely promising $G_{i/o}$ therapeutic target for intervention with intrathecal Y1 selective agonists to treat neuropathic pain.

3.4.3 SNI increases the excitability of Y1-INs

The balance between excitation and inhibition in the DH determines the setpoint of somatosensory processing (Todd, 2010). A shift in this balance towards an enduring increase in excitability can be denoted as “central sensitization" (Latremoliere and Woolf, 2009). Our neurophysiological recordings of passive membrane, active membrane, and synaptic properties demonstrate that SNI increases excitability in Y1-INs. First, we note that SNI increased the resting membrane potential of DSLF Y1-INs (**Figure 21**), suggesting that Y1-INs are more likely to fire an action potential following synaptic input. Second, we note that SNI increased the membrane excitability of DSLF and DLLF Y1-INs (**Figures 22-23**). These results are consistent with peripheral nerve injury-induced hyperexcitability/ central sensitization/ long term potentiation of

DH neurons (Boadas-Vaello et al., 2016; Jiang et al., 2010; Laird and Bennett, 1993; Latremoliere and Woolf, 2009). Third, we note that SNI robustly increased both the frequency and amplitude of sEPSCs in DSLF, IBF, and PF Y1-INs (**Figure 22, Figures 24-25**). The SNI-induced increase in sEPSC frequency is likely a result of an increased frequency of presynaptic action potentials (Okamoto et al., 2001). The SNI-induced increase in amplitude of sEPSCs may be a result of increased postsynaptic effectiveness of glutamate, perhaps due to central sensitization and the upregulation of ionotropic glutamate receptors (Latremoliere and Woolf, 2009). These results are consistent with increased synaptic excitability (indicated by both increases in frequency and amplitude of sEPSCs/mEPSCs) of excitatory DH neurons following peripheral nerve injury (including SNI, chronic constriction injury, and sciatic nerve axotomy) or application of brain derived neurotrophic factor (BDNF) (Balasubramanyan et al., 2006; Chen et al., 2009; Inquimbert et al., 2012; Smith, 2014). Interestingly, gabapentin, the first-line analgesic prescribed for neuropathic pain, acts by reducing both the frequency and amplitude of sEPSCs to spinal cord transient firing neurons (Alles et al., 2017). Although not tested, perhaps one of the mechanisms by which gabapentin is effective in neuropathic pain patients is via reducing the excitability of Y1-INs. This hypothesis is moderately supported by pretreatment of gabapentin preventing Y1-IN chemogenetic activation-induced nocifensive behaviors (Supplemental Figure 7). Together, our results indicate that nerve injury robustly enhances the excitability of Y1-INs. We propose that the hyperexcitability of Y1-INs produces an abnormal amplification of innocuous inputs that drives the manifestation/facilitation of allodynia (Costigan et al., 2009; Woolf and Salter, 2000).

3.4.4 The first investigation of adult dorsal horn *Npy1r*-expressing neurons

In this study we took advantage of NPY Y1 receptor-selective pharmacological agents, conditional genetic knockouts, intraspinal administration of Cre-dependent AAV constructs into the spinal cords of adult mice, and electrophysiological recordings in a reliable *Npy1r*^{eGFP} mouse line (Sinha et al., 2021), to rigorously characterize spinal interneurons that genuinely express the NPY Y1 receptor or *Npy1r* mRNA in adulthood. This is the first rigorous characterization of this population in the mouse. One previous study characterized *Npy1r*^{Cre}-lineage neurons, however, *Npy1r* is transiently expressed robustly during DH development these genetic crosses labeled most of the excitatory neurons in the DH, many of which that were *Npy1r*-lacking (Acton et al., 2019). Thus, we circumvent this developmental issue and draw conclusions about authentic spinal interneurons that express the NPY Y1 receptor. Further, through the use of cell type-specific inhibition tools we build upon prior results lesioning the spinal Y1-INs with NPY-saporin conjugates in rats (Lemons and Wiley, 2012; Nelson et al., 2019; Wiley et al., 2009), however, we avoid the negative pitfalls of lesion studies that include toxicity and circuit rearrangements. Our findings reveal the critical importance of DH Y1-INs to the manifestation and maintenance of neuropathic pain-like behaviors. We conclude that Y1-INs function like a pain rheostat: noxious stimuli increase the activity of Y1-INs to promote pain, whereas their inhibition reduces pain-like behaviors.

4.0 Spinal interneurons co-expressing *Npy1r* and *Grp* are necessary for the manifestation of neuropathic pain

4.1 Introduction

Pain and itch protect organisms from potentially harmful stimuli. Neurons in the superficial spinal cord dorsal horn (DH) are fundamental for the processing of nociceptive and pruritoceptive input (Merighi, 2018). Neurons in the DH are predominately interneurons (not projection neurons) and can be subdivided into two major classes: excitatory or inhibitory interneurons (Braz et al., 2014; Todd, 2010). Most superficial DH interneurons are glutamatergic with marked functional and histochemical heterogeneity (Todd, 2017). Excitatory DH interneurons are required for the appropriate expression of pain and itch behavior (Wang et al., 2013). However, in the setting of peripheral nerve injury, maladaptive hyperexcitation of excitatory DH interneurons can drive chronic neuropathic pain (Finnerup et al., 2021; Todd, 2010; Zeilhofer et al., 2012b). Specifically, peripheral nerve damage can lead to pathological allodynia in which normally innocuous sensory input is amplified and conveyed as painful (Finnerup et al., 2021; Jensen and Finnerup, 2014; Lolignier et al., 2014; Peirs et al., 2020). Multiple excitatory DH neurons are implicated in mediating peripheral nerve injury-induced allodynia, including those that express protein kinase C gamma (PKCγ) (Lu et al., 2013; Malmberg et al., 1997; Miracourt et al., 2007; Neumann et al., 2008; Peirs et al., 2021; Petitjean et al., 2015; Wang et al., 2020), somatostatin (Sst) (Christensen et al., 2016; Duan et al., 2014), cholecystokinin (CCK) (Liu et al., 2018; Peirs et al., 2021), neurokinin-1 receptor (NK1R) (Maiarù et al., 2018), and neuropeptide Y Y1 receptor (NPY1R) (Nelson et al., 2022, 2019). Nonetheless, despite the identification of numerous excitatory DH neurons involved in pathological allodynia, therapeutic intervention remains lacking.

Of the critical neuronal populations implicated in pathological allodynia, the neuropeptide Y Y1 receptor-expressing interneurons represent a promising, druggable, pharmacotherapeutic target for the treatment of neuropathic pain (Nelson and Taylor, 2021). The Y1 receptor is coupled to inhibitory G-proteins ($G_{i/o}$) and application of NPY Y1-selective agonists to spinal cord slices reduces the excitability of NPY Y1 receptor-expressing interneurons (Y1-INs) and decreases pronociceptive signaling (Melnick, 2012; Miyakawa et al., 2005; Sinha et al., 2021). Intrathecal administration of NPY Y1 selective agonists potently reduces the behavioral signs of neuropathic pain (Intondi et al., 2008; Kuphal et al., 2008; Malet et al., 2017; Nelson et al., 2022), and cell-type specific modulation/ablation studies demonstrate that Y1-INs are both necessary and sufficient for the manifestation of neuropathic pain-like behavior (Nelson et al., 2022, 2019). However, this critical interneuron population is histochemically ill-defined. The aims of this study were threefold: 1. use multi-label fluorescence *in situ* hybridization (FISH) to rigorously characterize spinal Y1-INs, 2. define Y1-IN subpopulations and investigate their role(s) in neuropathic pain-like behavior, and 3. evaluate the conservation of Y1-IN subpopulations across higher-order mammalian species to consider the translatability of this work for future pharmacotherapeutic development.

4.2 Methods

Animals

Adult C57Bl/6NCrl (Charles River, #027), *Npy1r*$^{loxP/loxP}$ (courtesy of Herbert Herzog (Howell et al., 2003)), *Grp*^{Cre} (courtesy of Zhou-Feng Chen (Kim et al., 2008)), *Cck*^{Cre} (Jackson Laboratory, #012706), and *Npff*^{Cre} (see below) mice were group housed, provided access to food and water *ad libitum*, and maintained on a 12:12 hour light:dark cycle (lights on at 7:00am) in temperature and humidity controlled rooms. Male and female mice were used in all experiments. Although we were not powered to detect significant sex differences, no major/obvious trends in sex differences were observed and means from both sexes were pooled. The Institutional Animal Care and Use Committees of the University of Pittsburgh approved all procedures. Additionally, all experiments followed the guidelines for the treatment of animals of the International Association for the Study of Pain.

The *Npff*^{Cre} knockin mouse line was generated by Taconic Biosciences GmbH (Leverkusen, Germany), using a conventional ES cell targeting strategy and homologous recombination. Briefly, the sequence for the T2A peptide and the open reading frame of improved Cre recombinase (iCr) were inserted between the last amino acid and the translation termination codon in exon 3 of the NPFF gene. A positive selection marker (Puromycin resistance) flanked by FRT sites was removed by crossing *Npff*^{Cre} mice with germline Flpe mice. The presence of the T2A sequence should result in co-translational cleavage between the NPFF and iCre proteins, resulting in coexpression of both proteins, under control of the Npff promoter.

Intrathecal Injections

Intrathecal injections of [Leu^{31}, Pro^{34}]-NPY (human, rat) were performed in lightly restrained unanesthetized mice. Briefly, a 30G needle attached to a Hamilton microsyringe was inserted between the L5/L6 vertebrae at the cauda equina, puncturing the dura (confirmed by presence of reflexive tail flick). We then injected a 5 μl volume of saline or [Leu^{31}, Pro^{34}]-NPY. Animals were injected twice using a cross-over design with a 3-7-day separation between the two injections. For example, animals receiving saline for the first injection received [Leu^{31}, Pro^{34}]-NPY for the second, and animals receiving [Leu^{31}, Pro^{34}]-NPY for the first injection received saline for the second. In all cases, group means of saline and [Leu^{31}, Pro^{34}]-NPY did not differ on either injection day and were combined for final analysis.

Surgeries

Spared Nerve Injury: SNI was performed as previously described (Nelson et al., 2019; Solway et al., 2011). Briefly, mice were anesthetized with inhaled isoflurane (5% induction and 2% maintenance) and the left hind limb was shaved with trimmers and sterilized with 70% ethanol and 2% chlorhexidine gluconate (ChloraPrep One-Step Applicators). A small incision was made in the skin of the hind left leg and the underlying muscle was spread via blunt dissection to expose the underlying branches of the sciatic nerve. The peroneal and tibial nerves were then ligated with 6-0 silk sutures and transected while carefully avoiding the sural nerve. The muscle tissue was then loosely sutured with 5-0 nylon sutures and the skin was closed with 9 mm wound clips. Topical triple antibiotic ointment (Neosporin) was applied to the wound. Wound clips were removed ~7-10 days post-surgery and behavioral experiments began 14 days after surgery.

Intraspinal AAV Injections: Mice were anesthetized with inhaled isoflurane (5% induction and 2% maintenance) and the back was shaved with trimmers and sterilized with 70% ethanol and 2% chlorhexidine gluconate (ChloraPrep One-Step Applicators). A midline incision was carefully made until the underlying vertebrae were clearly visible. A partial laminectomy was performed to remove the L1 vertebrae overlying the L4 segment of the spinal cord. A glass microelectrode was inserted into three separate locations in the exposed left lumbar spinal cord along the rostral caudal axis. At each injection site the glass microelectrode was lowered to a depth of 250 μm below the dura using a stereotaxic frame (David Kopf Instruments). 333.3 nL of virus (AAV8-hSyn-DIO-mCherry or AAV8-hSyn-DIO-hM4Di-mCherry, University of Pennsylvania Vector Core) was slowly injected into each of the three spots (5 nL/sec) using a Nanoject III (Drummond) with a 3-minute wait time after completion of each injection to permit adequate infusion. The *lassimus dorsi* was sutured with 5-0 nylon sutures to protect the exposed spinal cord and the overlying skin was closed with 9 mm wound clips. Topical triple antibiotic ointment (Neosporin) was applied to the wound. Subcutaneous Buprenorphine HCL (0.05 mg/kg) was utilized for 72 hours as a post-operative analgesic. Behavioral experiments began 21 days after surgery.

Behavioral Testing

Mechanical Withdrawal Threshold: Testing was performed as described in (Solway et al., 2011). Mice were habituated to plexiglass chambers with opaque walls (15 × 4 × 4 cm) on a raised wire mesh platform for 30-60 minutes one day before and immediately prior to behavioral testing. Testing was performed using a calibrated set of logarithmically increasing von Frey monofilaments (Stoelting, Illinois) that range in gram force from 0.007 to 6.0 g. Beginning with a

0.4 g filament, these were applied perpendicular to the lateral hindpaw surface with sufficient force to cause a slight bending of the filament. A positive response was denoted as a rapid withdrawal of the paw within 4 seconds of application. Using the Up-Down method (Chaplan et al., 1994), a positive response was followed by a lower filament and a negative response was followed by a higher filament to calculate the 50% withdrawal threshold for each mouse.

Cold Withdrawal Duration: Immediately following von Frey testing, acetone drop withdrawal testing was performed on mice in the same plexiglass chambers on a raised wire mesh platform. Using a syringe connected to PE-90 tubing, flared at the tip to a diameter of 3 1/2 mm, we applied a drop of acetone to the lateral side of the hind plantar paw. Surface tension maintained the volume of the drop to ~10 μL. The length of time the animal lifted or shook its paw was recorded for 30 s. Three observations were averaged.

Hindpaw Brush for Fos: To produce *Fos* activation, a light-touch stimulation protocol was initiated on the ipsilateral hindpaw of SNI mice 14 days after nerve injury. Mice were anesthetized with isoflurane (5% induction, 2% maintenance) and the lateral surface of the left hindpaw was gently stroked in the longitudinal plane with a cotton tipped applicator for 3 seconds of every 5 seconds, for 5 minutes. After an additional 60-minute awake and freely moving wait time in their home cage, mice received an intraperitoneal injection of sodium pentobarbital (.100 mg/kg, 0.2 mL, Fatal-Plus) and were transcardially perfused.

Fluorescence *in situ* Hybridization (FISH) (RNAscope)

Mice: Mice were transcardially perfused with ice cold 1x PBS followed by 10% buffered formalin and spinal cords were extracted via blunt dissection, postfixed in 10% formalin (2-4 hrs), and then placed in 30% sucrose at 4°C until the tissue sank (~48-72 hrs). 20 μm thick L3-L4 floating spinal cord sections were obtained on a vibrating microtome and mounted on Superfrost Plus Microscope slides and air dried overnight at room temperature. Slides underwent pretreatment for fluorescence *in situ* hybridization consisting of 10 min Xylene bath, 4 min 100% ethanol bath, and 2 min RNAscope® H2O2 treatment. Next, the FISH protocol for RNAscope Fluorescent v2 Assay (Advanced Cell Diagnostics) was followed for hybridization to marker probes. Signal amplification was carried out using the TSA Fluorescein, Cyanine 3, and Cyanine 5 reagents (1:1000; Perkin Elmer or Akoya Biosciences). Slides were either then coverslipped with VECTASHIELD HardSet Antifade Mounting Medium with DAPI or proceeded to immunohistochemistry for mCherry labeling.

Rhesus Macaques: Two rhesus macaques (Male, 4 years at time of death; and Female, 4 years at time of death) were provided by Dr. David Lewis and cared for under the guidelines of the National Institute of Health. No prior manipulations to the spinal cord were conducted in the macaques. At the time of tissue harvest, the macaques were perfused with aCSF and the L5-L7 spinal cord tissue was removed, placed in OCT, and immediately frozen on dry ice. Tissue sections were cut 20 μm thick using a cryostat and mounted on to Superfrost-charged slides and stored at -80 °C until the start of the assay. The fresh frozen FISH protocol for RNAscope Fluorescent v2 Assay (Advanced Cell Diagnostics) was followed for hybridization to marker probes. after a 30-minute fixation step with cold 4% PFA. Signal amplification was carried out

using the TSA Fluorescein, Cyanine 3, and Cyanine 5 reagents (1:1500; Akoya Biosciences). All sections were co-stained for DAPI and coverslipped at the end of the assay.

Human Donor Spinal Cord Tissue: Two human spinal cord fresh-frozen cervical spinal cord tissues were obtained from the NeuroBioBank, National Institutes of Health (project no. 063772) and provided by J. Glausier, Department of Psychiatry, University of Pittsburgh (Male, 45 years at time of accidental death; Female, 44 years at time of natural death). All available evidence indicated that these subjects did not have any major psychiatric illness nor any neuropathological illness at the time of death. All procedures were approved by the Committee for the Oversight of Research and Clinical Training Involving Decedents at University of Pittsburgh, Pittsburgh, Pennsylvania. The fresh frozen FISH protocol for RNAscope Fluorescent Assay (Advanced Cell Diagnostics) was followed for hybridization to marker probes. Briefly, 16 μm thick fresh frozen sections containing human spinal cord were fixed in 4% paraformaldehyde, dehydrated, treated with protease for 15 minutes, and hybridized with gene- and species-specific probes.

Table 5. RNAscope probes used in this study.

Probe	Target Species	Protein/Peptide	Channel Numbers	Catalogue Number	Z-pair number	Target Region
Npy1r	Mouse	Neuropeptide Y receptor 1	1, 3	427021	20	227 - 1169
Grp	Mouse	Gastrin-releasing peptide	2	317861	15	22 - 825
Cck	Mouse	Cholecystokinin	2	402271	12	23 - 679
Npff	Mouse	Neuropeptide FF	2	479901	9	47 - 433
Grpr	Mouse	Gastrin-releasing peptide receptor	2	317871	20	463 - 1596
Tac1	Mouse	Tachykinin precursor 1 (Substance P)	2	410351	15	20 - 1034
Tacr1	Mouse	Tachykinin receptor 1 (Neurokinin 1 receptor)	2	428781	20	845 - 1775
Sst	Mouse	Somatostatin	2	404631	6	18 - 407
Nmur2	Mouse	Neuromedin U receptor 2	3	314111	20	69 - 1085
Prkcg	Mouse	Protein kinase C gamma	3	417911	20	685 - 2438
Fos	Mouse	Fos proto-oncogene (C-Fos)	3	316921	20	407 - 1427
Lmx1b	Mouse	LIM homeobox transcription factor 1-beta	1	412931	16	125 - 1188
Pax2	Mouse	Paired box 2	2	448981	20	2 - 1256
Car12	Mouse	Carbonic anhydrase 12	1	429991	20	552 - 1660
Npy1r	Monkey	Neuropeptide Y receptor 1	2	838471	20	2 - 1023

Grp	Monkey	Gastrin-releasing peptide	2	1079131	20	7-992
Cck	Monkey	Cholecystokinin	1	461721	20	202 - 1297
Npff	Monkey	Neuropeptide FF	3	1089001	20	78 - 1145
Npy1r	Human	Neuropeptide Y receptor 1	1	414511	20	401 - 1493
Grp	Human	Gastrin-releasing peptide	2	465261	14	35 - 851
Cck	Human	Cholecystokinin	2	539041	20	100 - 1486
Npff	Human	Neuropeptide FF	2	1082871	6	55 - 345

Immunohistochemistry

Immediately following the RNAscope V2 protocol, mouse spinal cord sections were washed 3 times in PBS and then pretreated with blocking solution (3% normal goat serum and 0.3% Triton X-100 in PBS) for 1 hour. Sections were then incubated in blocking solution containing the primary antibody overnight (1:2000, Anti-mCherry; Invitrogen, Cat: M11217) at -4 °C on a slow rocker. The sections were washed 3 times in 1x PBS and then incubated in secondary antibody (1:1000, Alexa Fluor 568 Goat anti-Rat; Invitrogen, Cat: A11077) for 60 minutes. Finally, sections were washed in 1x PBS and then 0.01-M phosphate buffer without saline.

Microscopy and Quantification

All images were captured on a Nikon Eclipse Ti2 microscope using a 20x or 40x objective and analyzed using NIS-Elements Advanced Research software v5.02. Cells with at least 3 puncta associated with a DAPI nucleus were considered positive. Mouse quantification exclusively was limited to the superficial 100 µm of the dorsal horn. Each individual data point for a mouse

indicates one animal and the average of 3-5 quantified dorsal horn sections. Macaque quantification occurred in the substantia gelatinosa which appears as a translucent area in the superficial dorsal horn. Each individual data point for a rhesus macaque indicates one individual spinal cord dorsal horn. Intense lipofuscin hindered the ability to accurately quantify expression in the human dorsal horn.

Blinding procedures

In all experiments rigorous experimenter blinding was employed to promote research reproducibility. The experimenter was blinded to drug treatments in all behavioral pharmacology experiments as intrathecal injections were performed by a laboratory colleague thus providing complete anonymity of agent for each animal. For viral experiments a laboratory mate color-coded the virus tubes for the experimenter at the time of surgery as well as clozapine N' oxide (Tocris Bisociences) vs. saline at the time of behavior. The key for coding was kept hidden in a notebook until the completion of all experiments. The experimenter then obtained the key for data analysis.

Statistical Analyses and Data Representation

All data are presented as means ± SEM. Statistical significance was determined as $*P < 0.05$. Statistical tests were two-way repeated-measures ANOVA or three-way repeated measures ANOVA followed by post hoc tests as appropriate. All statistical analyses were performed in GraphPad Prism 9.0. Graphs and Images were created in GraphPad Prism 9.0., Adobe Illustrator 26.3.1., and Biorender.com.

4.3 Results

4.3.1 Characterization of murine *Npy1r*-expressing interneurons using fluorescence *in situ* hybridization

We used multi-label FISH to histochemically characterize L4 superficial Y1-INs. First, we found that *Npy1r* extensively co-localized with the DH excitatory gene, *Lmx1b* (96.91 ± 0.49%), but not the inhibitory marker, *Pax2* (1.39 ± 0.47%) (**Figure 29A-E**) (Cheng et al., 2005; Del Barrio et al., 2013; Hernandez-Miranda et al., 2017; Szabo et al., 2015). This result indicates that Y1-INs are an excitatory DH interneuron population. Recent data from immunohistochemistry, *in situ* hybridization, and unbiased single cell/nucleosome RNA-sequencing of DH interneurons, together, identify several largely non-overlapping excitatory interneuron subpopulations based on the expression of neuropeptides/receptors (Bell et al., 2020; Gutierrez-Mecinas et al., 2019, 2016; Häring et al., 2018; Polgár et al., 2022; Russ et al., 2021; Sathyamurthy et al., 2018). Specifically, these populations are defined by their expression of cholecystokinin (CCK), neurotensin, neurokinin B (NKB), neuropeptide FF (NPFF), substance P (SP), enhanced green fluorescent protein (eGFP) or Cre recombinase under control of the gastrin releasing peptide (*Grp*) promoter in BAC transgenic mice from the GENSAT project (Grp^{eGFP} and Grp^{Cre}), and gastrin releasing peptide receptor (GRPR) (**Figure 29F**). Together, these largely non-overlapping populations account for ~90% of superficial DH excitatory interneurons (Polgár et al., 2022). Thus, we used these markers of largely non-overlapping excitatory DH interneurons to identify putative Y1-IN subpopulation(s). We found that *Npy1r* co-localized with superficial *Cck* (16.60 ± 0.63%), *Grp* (60.61 ± 3.78%), and *Npff* (24.55 ± 1.75%), but little with *Grpr* (6.85 ± 0.45%), *Prkcg* (4.55 ± 0.55%), or *Tac1* (5.13 ± 0.68%) (**Figure 29G-R**). Note that *Prkcg* was used as a marker to broadly encompass both the neurotensin and NKB subpopulations (**Figure 29F**). Together, these results

indicate that Y1-INs are excitatory DH interneurons and largely segregate into three non-overlapping subpopulations demarcated by co-expression of *Npy1r* with the genes *Cck*, *Npff*, or *Grp*.

In addition to markers of largely non-overlapping excitatory interneurons, we also histochemically characterized DH *Npy1r* expression with canonical markers implicated in nociception as well as novel genes of predicted overlap from single-cell RNA sequencing datasets. Specifically, we found that *Npy1r* co-localized extensively with *Sst* (49.26 ± 0.98%) and *Calb2* (33.96 ± 2.42%) but little with *Tacr1* (6.94 ± 1.11%) (**Fig. 29S-X**), three genes implicated in neuropathic and inflammatory mechanical allodynia (Christensen et al., 2016; Duan et al., 2014; Maiarù et al., 2018; Peirs et al., 2021, 2020, 2015). Lastly, we confirmed the co-localization of *Npy1r* with *Nmur2* (37.04 ± 0.94%) and *Car12* (32.83 ± 6.33%), as predicted by single-cell RNA sequencing datasets (**Figure 29Y-AB**) (Häring et al., 2018; Russ et al., 2021).

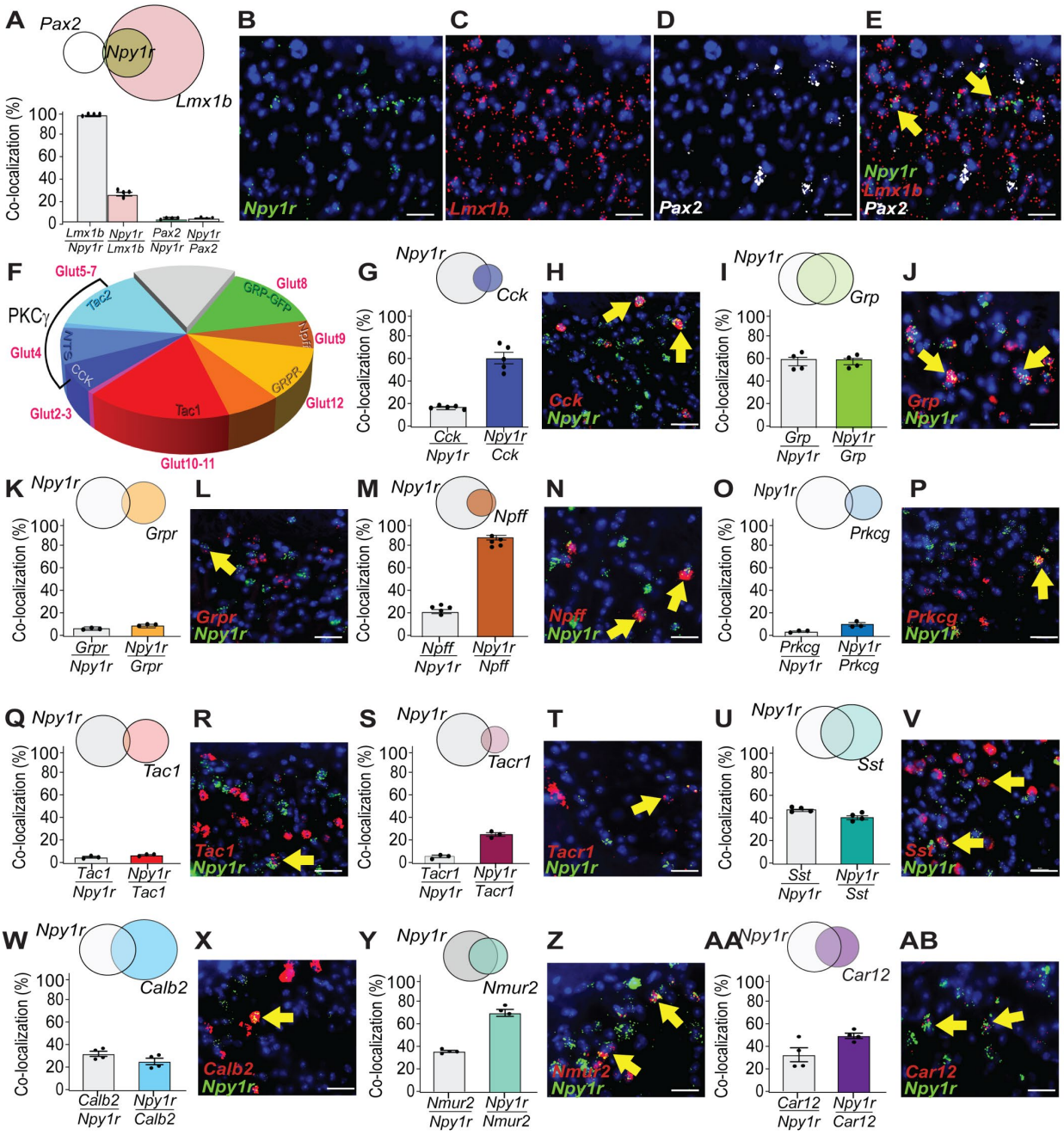

Figure 29. Fluorescence *in situ* characterization of Y1-INs.

(**A-E**) *Npy1r* extensively co-localizes with *Lmx1b* but not *Pax2* (n=4-5 mice/group). (**F**) Excitatory interneurons can be segregated into largely non-overlapping subpopulations. (**G-R**) *Npy1r* co-localizes with superficial *Cck*, *Grp*, and *Npff* but not *Grpr*, *Prkcg*, or *Tac1* (n=3-5 mice/group). (**S-AB**) *Npy1r* co-localizes with *Tacr1*, *Sst*, *Calb2*, *Nmur2*, and *Car12* (n=3-5 mice/group). Each data point indicates the average of 2-4 quantified sections/mouse. Scale bars: 25 µm. Yellow arrows indicate co-localization. Data shown as means ± SEM.

4.3.2 Evaluation of the Y1-IN subpopulation(s) necessary for the manifestation of the behavioral signs of neuropathic pain

Next, we examined the Y1-IN subpopulation(s) activated by a dynamic mechanical light touch stimulation in mice with neuropathic pain. First, we performed spared nerve injury (SNI), a model of peripheral nerve injury-induced neuropathic pain (Decosterd and Woolf, 2000). In the SNI model, the common peroneal and tibial branches of the sciatic nerve are ligated and cut while leaving the sural nerve intact Following SNI, mice develop robust mechanical and cold hypersensitivity in the sural innervation territory (lateral aspect) of the injured hindpaw (Nelson et al., 2022, 2019). Two weeks after spared nerve injury (SNI), we performed light dynamic brush stimulation of the injured hindpaw under anesthesia or no stimulation (isoflurane exposure control) (**Figure 30A**). As predicted, we found that light brush stimulation increased *Fos* expression in the ipsilateral superficial DH. In particular, extensive *Fos* was noted in *Npy1r*-expressing neurons (**Figure 30B**). Further, *Fos* was enriched in the superficial *Grp*/*Npy1r* but not the *Npff*/*Npy1r* or *Cck*/*Npy1r* subpopulations (**Figure 30B-C**). These results suggest that in the context of peripheral nerve injury, dynamic mechanical stimulation activates DH interneurons that co-express *Npy1r* and *Grp* but not those that co-express *Npy1r* and *Cck* or *Npy1r* and *Npff*.

We next tested the hypothesis that one or more Y1-IN subpopulation(s) is necessary for the behavioral manifestation of SNI-induced mechanical and cold allodynia. First, we took advantage of the fact that virtually all *Npff*-expressing DH interneurons co-express *Npy1r* (**Figure 29M-N**). This feature of NPFF-INs allowed us to intraspinally administer Cre-dependent inhibitory DREADDs into the left lumbar (targeting L3-L4) dorsal horn of our newly developed *Npff*^{Cre} mouse line to modulate *Npff*/*Npy1r*-INs. As predicted, immunohistochemical/FISH verification of AAV-mCherry transfection expression was detected ipsilateral to viral injection

(left but not right DH) in superficial DH cells that co-expressed *Npff* and *Npy1r* (**Figure 30D**). To our surprise, chemogenetic inhibition of *Npff*/*Npy1r*-INs with clozapine N-oxide (CNO, 3 mg/kg, i.p.) did not alter mechanical or cold responses before or after SNI (**Figure 3E-I**). We used a 3 mg/kg dose of CNO as this is the lowest recommended dose to be a DREADD agonist without producing off target effects (Jendryka et al., 2019); additionally, this is a commonly utilized dose for spinal cord chemogenetics (Kiguchi et al., 2021; Petitjean et al., 2015). These findings indicate that the spinal *Npff*/*Npy1r*-INs are not necessary for the behavioral manifestation of static mechanical or cold neuropathic allodynia.

In contrast to the DH NPFF-INs, many CCK- and GRP-INs do not co-express *Npy1r*. As a result, we could not use the same chemogenetic approach we used with our $Npff^{Cre}$ mice to also inhibit the Grp^{Cre} or Cck^{Cre} interneuron populations without also modulating neurons that do not express *Npy1r*. Therefore, we crossed $Npy1r^{loxP/loxP}$ mice (Howell et al., 2003) with either Grp^{Cre} (Barry et al., 2020) or Cck^{Cre} (Taniguchi et al., 2011) mice to selectively knockout *Npy1r* from Grp^{Cre} or Cck^{Cre} neurons, respectively (**Figure 30J-M**). Next, we performed SNI that produced mechanical and cold hypersensitivity in all three genetic crosses (**Figure 30N-O**). Two weeks after SNI, we intrathecally administered the Y1-selective agonist, [Leu^{31}, Pro^{34}]-NPY, to inhibit spinal Y1-INs. [Leu^{31}, Pro^{34}]-NPY reduced SNI-induced allodynia in both control $Npy1r^{loxP/loxP}$ and $Npy1r^{loxP/loxP}$;Cck^{Cre} mice, but not in $Npy1r^{loxP/loxP}$;Grp^{Cre} mice (**Figure 30N-O**). These results indicate that intrathecal NPY Y1 agonists act at spinal cord *Npy1r*-expressing interneurons that co-express *Grp* to inhibit the behavioral signs of neuropathic pain. Together, these results reveal that *Grp*/*Npy1r*-INs but not *Npff*/*Npy1r*-INs or *Cck*/*Npy1r*-INs are necessary for the behavioral manifestation of peripheral nerve injury-induced mechanical and cold allodynia.

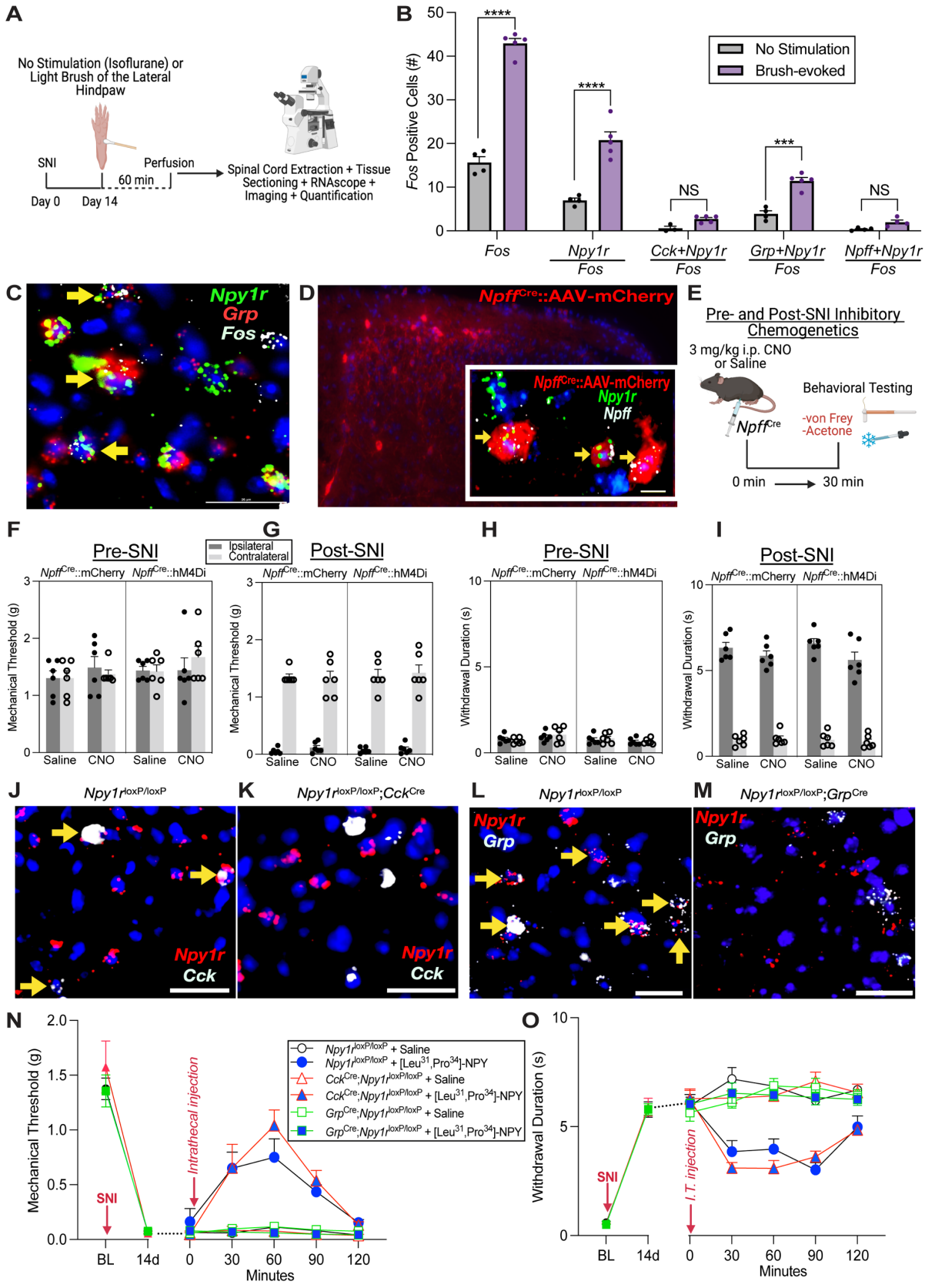
A
No Stimulation (Isoflurane) or Light Brush of the Lateral Hindpaw
SNI
Perfusion
60 min
Day 0
Day 14
Spinal Cord Extraction + Tissue Sectioning + RNAscope + Imaging + Quantification
B
Fos Positive Cells (#)
No Stimulation
Brush-evoked
****
****
NS
***
NS
Fos
Npy1r Fos
Cck+Npy1r Fos
Grp+Npy1r Fos
Npff+Npy1r Fos
C
Npy1r
Grp
Fos
D
Npff^Cre::AAV-mCherry
Npff^Cre::AAV-mCherry
Npy1r
Npff
E
Pre- and Post-SNI Inhibitory Chemogenetics
3 mg/kg i.p. CNO or Saline
Npff^Cre
Behavioral Testing
-von Frey
-Acetone
0 min
30 min
F
Pre-SNI
G
Ipsilateral
Contralateral
Post-SNI
Npff^Cre::mCherry
Npff^Cre::hM4Di
Mechanical Threshold (g)
Saline
CNO
H
Pre-SNI
I
Post-SNI
Withdrawal Duration (s)
J
Npy1r^loxP/loxP
K
Npy1r^loxP/loxP;Cck^Cre
L
Npy1r^loxP/loxP
M
Npy1r^loxP/loxP;Grp^Cre
Npy1r
Cck
Grp
N
Mechanical Threshold (g)
SNI
Intrathecal injection
Npy1r^loxP/loxP + Saline
Npy1r^loxP/loxP + [Leu31,Pro34]-NPY
Cck^Cre;Npy1r^loxP/loxP + Saline
Cck^Cre;Npy1r^loxP/loxP + [Leu31,Pro34]-NPY
Grp^Cre;Npy1r^loxP/loxP + Saline
Grp^Cre;Npy1r^loxP/loxP + [Leu31,Pro34]-NPY
BL
14d
Minutes
O
Withdrawal Duration (s)
SNI
I.T. injection

Figure 30. Evaluation of Y1-IN subtypes in neuropathic pain.

(**A**) Protocol for light-brush evoked *Fos*. (**B**) Quantification of *Fos*-positive cells in superficial DH. Two-Way ANOVA. n=3-5 mice/group. (**C**) Example of *Grp*/*Npy1r*-INs with light brush-evoked *Fos*. (**D**) AAV transfection in $Npff^{Cre}$ mice and FISH confirmation of *Npy1r* and *Npff* expression in transfected cells. Scale bar 10 µm. (**E**) Schematic of $Npff^{Cre}$ chemogenetic behavior. Chemogenetic inhibition of $Npff^{Cre}$ cells did not alter (**F-G**) mechanical thresholds nor (**H-I**) cold sensitivity before or after SNI. Three Way RM ANOVA. n=6 mice/group (**J-M**) Representative conditional deletion of *Npy1r* from Cck^{Cre} and Grp^{Cre} mice. Scale bars 25 µm. (**N-O**). [Leu^{31}, Pro^{34}]-NPY abolishes SNI-induced allodynia in $Npy1r^{loxP/loxP}$ and $Npy1r^{loxP/loxP}$;Cck^{Cre} mice but not in $Npy1r^{loxP/loxP}$;Grp^{Cre} mice (n=8-9 mice/group). Three-way RM ANOVA. Holm-Sidak post hoc tests if applicable. Yellow arrows indicate co-localization. Data are shown as means ± SEM.

4.3.3 Conservation of *Npy1r*-expressing subpopulations in the rhesus macaque and human spinal cord dorsal horns

Finally, we asked if Y1-INs and Y1-IN subpopulations are evolutionarily conserved across the non-human primate and human spinal cord dorsal horns. Analogous to our mouse studies, we performed FISH for *Npy1r*, *Cck*, *Npff*, and *Grp* in spinal cord tissue from both male and female rhesus macaques and humans. First, we found that *Npy1r*-expressing cells were abundantly expressed in the DH of monkey tissue. In the rhesus macaque tissue, we found that superficial *Npy1r* extensively co-localized with *Cck* (22.49 ± 3.08%), *Grp* (27.26 ± 1.63%), and *Npff* (41.98 ± 2.20%) (**Figure 31A-F**). We also found numerous *Npy1r*-expressing cells in the superficial dorsal horn of human spinal cord tissue. Further, *Npy1r* co-expression with *Cck*, *Grp*, and *Npff* was conserved in the human dorsal horn (albeit *Npff* expression is sparse in human DH) (**Figure 31G-I**). Note, that we detected an abundance of the autofluorescent age-related pigment, lipofuscin (Steiner et al., 1989), in the human spinal cord DH that hindered accurate co-localization quantification. Nevertheless, our FISH results demonstrate that Y1-IN subpopulations are conserved across the rhesus macaque and human DHs, and importantly, the *Grp*/*Npy1r*-IN population is abundant in both the macaque and human spinal cord DHs.

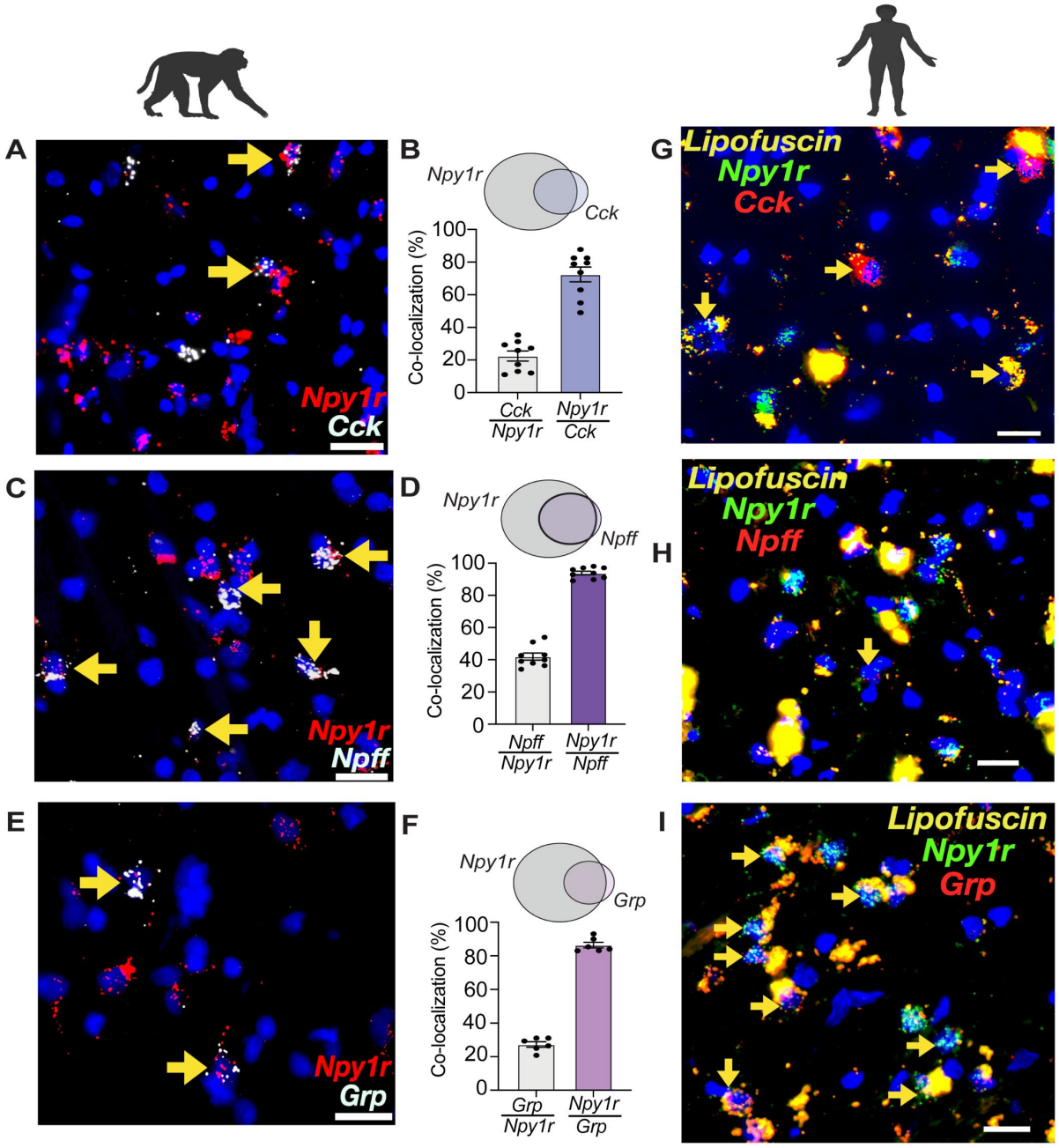

Figure 31. Conservation of Y1-IN subtypes across higher-order mammalian species

(**A-F**) *Npy1r* extensively co-localizes with Cck, *Grp,* and Npff in the rhesus macaque (n=2 macaques). Individual data points represent one single quantified section. Scale bars: 25 µm. (**G-I**) *Npy1r* co-localizes with Cck, *Grp,* and Npff in the human spinal cord DHs (n=2 human organ donors). Scale bars: 20 µm. Yellow arrows indicate co-localization. Data shown as means ± SEM.

4.4 Discussion

Spinal cord DH interneuron populations are fundamental for the appropriate processing of nociceptive and pruritoceptive inputs. In this study, we demonstrate that excitatory *Npy1r*-expressing DH interneurons that co-express *Grp* are fundamental for the behavioral manifestation of peripheral nerve injury-induced mechanical and cold allodynia. Further, we reveal that the expression of this critical neuronal subpopulation is evolutionarily conserved across the murine, monkey, and human spinal cord dorsal horns.

4.4.1 Y1-INs segregate into three glutamatergic subpopulations

In this study, for the first time we rigorously characterized dorsal horn interneurons that express *Npy1r*, an advance that has long-remained challenging due to the lack of an antibody that reliably stains the NPY Y1 receptor in mouse tissue. Previously, a characterization was performed for mouse *Npy1r*^{Cre}-lineage neurons (an important caveat is that approximately half of the neurons in this lineage were *Npy1r* lacking) (Acton et al., 2019) and rat Y1-immunoreactive interneurons (Nelson et al., 2019), but this is the first extensive characterization of adult *Npy1r*-expressing cells in the mouse superficial spinal cord DH. Our results confirm that Y1-INs are an excitatory DH interneuron population in support of previous immunohistochemistry, FISH, and single-cell transcriptomic data (Acton et al., 2019; Häring et al., 2018; Nelson et al., 2019; Nelson and Taylor, 2021; Sathyamurthy et al., 2018). Additionally, our results indicate that superficial DH Y1-INs segregate into three largely non-overlapping excitatory subpopulations demarcated by the co-expression of *Npy1r* with either *Grp*, *Npff*, or *Cck*. This result is consistent with single-cell RNA sequencing, which also identified three excitatory Y1-IN subpopulations (Glut2, Glut8, and Glut9)

that match our characterization (Häring et al., 2018). In comparison of our results with these single cell RNA-sequencing results, we believe that the Glut2, Glut8, and Glut9 clusters correlate to the *Cck*-, *Grp*-, and *Npff*-expressing Y1-IN subpopulations, respectively (Häring et al., 2018). While the significant co-expression of *Npy1r* and *Grp* has been previously reported with both FISH (Nelson and Taylor, 2021; Wang et al., 2021) and transcriptomics (Sathyamurthy et al., 2018), we believe this is the first report of *Npy1r* co-expression with *Npff* and *Cck*.

4.4.2 *Grp*/*Npy1r*-expressing DH interneurons drive neuropathic pain

We reveal for the first time that spinal DH *Npy1r*-expressing interneurons that co-express *Grp* are necessary for the behavioral manifestation of SNI-induced mechanical and cold allodynia. As the function of Y1-INs and GRP-INs are typically considered to drive either chronic pain (Lemons and Wiley, 2012; Nelson et al., 2022, 2019; Nelson and Taylor, 2021) or pruritus (Albisetti et al., 2019; Chen, 2021; Kiguchi et al., 2021; Pagani et al., 2019), respectively, the current results address a decades-long debate about the coding of pain vs. itch in the somatosensory system. Our results contrast with a theorized "labeled line" in which neurons specifically code for either pain or itch (Ma, 2010). Rather, our results support an integrated organization of second-order spinal cord interneurons within sensory circuits. This more complex viewpoint fits well with recent data implicating both Y1-INs (Jakobsson et al., 2019; Nelson and Taylor, 2021) and GRP-INs (Saeki et al., 2022; Sun et al., 2017) as polymodal interneuron populations implicated in both pain and pruritus.

In this study, we demonstrate a novel role for GRP-INs in neuropathic pain. We believe that two key advances allowed us to uncover this novel function. First, we utilized a high-fidelity *Grp*^{Cre} mouse line which labels ~90% of the DH GRP-INs (Barry et al., 2020). Previous *Grp* work used GENSAT's BAC transgenic *Grp*^{Cre} mouse line which only labels ~25% of DH GRP-INs (Albisetti et al., 2019; Bell et al., 2020), and prevented the functional interrogation of the entire GRP-IN population. Second, we probed the role of GRP-INs in a chronic pain model (SNI) rather than acute pain modalities (i.e. heat, von Frey, pinprick) (Albisetti et al., 2019; Barry et al., 2020). To our knowledge this is the first functional interrogation of GRP-INs in a chronic pain model. Thus, with these key advances, we revealed that *Grp*/*Npy1r*-INs are necessary for the manifestation of neuropathic pain. However, these results are not entirely unexpected. Mechanical allodynia is hypothesized to occur via a polysynaptic DH microcircuit that allows A-fibers to transmit innocuous mechanical input to "pain circuits" (Lu et al., 2013). One key neuronal population in this proposed circuit is the "transient central cell" (neurons in lamina II outer with a central morphology that discharge action potentials transiently during a depolarizing step (Grudt and Perl, 2002)). Y1-INs and GRP-INs have both been characterized as transient central cells (Albisetti et al., 2019; Dickie et al., 2019; Nelson et al., 2022). Thus, in the context of nerve injury, we suggest that GRP/Y1-INs (transient central cells) activate GRPR-INs (vertical cells (Polgár et al., 2022)) to drive mechanical allodynia, corresponding to a circuit proposed by Lu et al. (Lu et al., 2013). This may also explain how peripheral nerve injury often leads to the presentation of a neuropathic pain condition that is associated with a neuropathic itch component (Meixiong et al., 2020; Misery et al., 2014; Steinhoff et al., 2018): sensitization of GRP/Y1-INs may give rise not only to allodynia, but also the analogous alloknesis (innocuous touch causes itch) (Hachisuka et al., 2018). Indeed, intrathecal administration of NPY inhibits not only the behavioral signs of

neuropathic pain but also chemical and mechanical itch (Gao et al., 2018; Jakobsson et al., 2019; Nelson and Taylor, 2021). Therefore, we propose that both neuropathic pain and itch share redundant spinal circuitry. Further interrogation of how specific temporal neuronal activation can drive specific transmitter/peptide release to produce differing behaviors (Pagani et al., 2019) will be fundamental to our understanding of this biological redundancy in future studies.

The *Sst*/*Grp*/*Npy1r* neuron population necessary for the manifestation of neuropathic pain likely corresponds to the Glut8 cluster from Häring et al.'s single-cell RNA sequencing database (Häring et al., 2018). Therefore, future studies should further evaluate the Glut8 cluster ($Reln^{+}$, $Nmur2^{+}$, $Npff^{-}$ neurons) and its role in neuropathic pain. For example, the synthesis of an $Nmur2^{Cre}$ mouse line, or perhaps an intersectional approach that develops and utilizes a $Npy1r^{Flp}$ mouse crossed with a Grp^{Cre} mouse, will allow future investigators to perform more advanced analyses of the Glut8 subpopulation in order to better define its role in neuropathic pain.

Another alternative interpretation of our results is that we are not seeing a subpopulation specific effect, but rather the effect of inhibiting a large number of Y1-INs. The *Grp*-expressing subpopulation is the largest subpopulation of Y1-INs and accounts for ~60% of the total superficial Y1-INs. Thus, perhaps SNI is producing a large excitation/inhibition (E/I) imbalance in the DH and it is the total number of excitatory neurons that is needed to be inhibited that is important for a reduction in pain-like behavior- not the specific subpopulation. Unfortunately, the methods I have used cannot readily refute this alternative interpretation. However, inhibition of another large and predominately excitatory interneuron population, the calretinin interneuron population (~30% of all superficial dorsal horn neurons are calretinin-immunoreactive (Smith et al., 2016)- as

opposed to ~25% expressing *Npy1r*), does not affect peripheral nerve injury-induced allodynia (Peirs et al., 2021). This suggests that neuronal specificity does affect specific behavioral phenotypes in the context of peripheral nerve injury-induced allodynia. As discussed above, the development and utilization of an *Npy1r*^{Flp} mouse and intersectional genetic cell type-specific modulation studies can further address this alternative hypothesis. Specifically, one may begin to inhibit multiple Cre lines (increasing larger numbers of transfected cells) in combination with *Npy1r*^{Flp} to test the total numbers vs. cell type hypothesis.

4.4.3 Y1-INs may modulate neuropathic pain in humans

NPY binding sites have been noted in the superficial laminae of the mouse, rat, and monkey spinal cord DHs (Brumovsky et al., 2006; Ji et al., 1994; Kar and Quirion, 1992; Kopp et al., 2010; Sinha et al., 2021; Zhang et al., 1995, 1994). A growing body of preclinical evidence implicates spinal NPY as a potent inhibitor of a variety of preclinical models of pain, particularly neuropathic pain (Nelson and Taylor, 2021), however, it remains unclear if this will one day translate to a potential therapeutic for human chronic pain patients. Unfortunately, the field of pain is facing a preclinical-to-clinical translation crisis that is often driven by species variation from preclinical rodent models to humans (Mogil, 2019). Consequently, we began the first steps of addressing if Y1 agonism may be a viable future drug candidate for the bedside by examining evolutionary conservation of neuropeptide Y Y1 receptors across higher order mammalian species. Using FISH, we found that both Y1-INs and Y1-IN subpopulations are extensively conserved across the rhesus macaque and human spinal cord DHs (although *Npff* expression is sparse in human DH) (**Figure 4**). Importantly, the *Grp*/*Npy1r*-IN population, the subpopulation that we believe is fundamental

to the manifestation of neuropathic pain, is abundant in the macaque and human spinal cords. The evolutionary conservation of *Npy1r* expression may demonstrate its functional importance across species. Further, we propose that *Grp*/*Npy1r*-INs are well positioned in the spinal cord of non-human primates and humans to modulate neuropathic pain, and thus, represent a favorable pharmacotherapeutic target for future drug development. One caveat is that the human spinal cord tissue used in this study was from the cervical spinal cord (due to supply limitation) and the mouse and macaque tissue was lumbar spinal cord. However, in preliminary studies no differences were noted in expression of markers between cervical and lumbar tissue in the mouse (analysis performed by the Andrew Todd lab in Glasgow). Thus, while being a limitation we do not think the human results will greatly change in lumbar tissue. Another important point is that the human tissue had significant lipofuscin build up. It is unclear if lipofuscin alters the total expression of spinal mRNAs (as opposed to masking/hiding during microscopy). The use of younger human tissue would be ideal to avoid this aging-related pigment as much as possible (Moreno-García et al., 2018), however, alternatively we could repeat the macaque and mouse staining in aged tissue for direct comparison.

5.0 Endogenous μ-opioid – neuropeptide Y Y1 receptor synergy silences chronic postoperative pain in mice

5.1 Introduction

Chronic postsurgical pain (CPSP) is a significant healthcare burden that afflicts millions of patients each year (Richebé et al., 2018; Thapa and Euasobhon, 2018). Despite this high prevalence, the biological mechanisms that underlie the transition from acute pain to CPSP remain poorly understood (Glare et al., 2019; Kehlet et al., 2006). The dorsal horn of the spinal cord (DH) processes somatosensory information and is a key driver of pathological pain states (Todd, 2010). Tissue injury sensitizes pro-nociceptive neurons in the DH, contributing to allodynia and hyperalgesia (Jensen and Finnerup, 2014; Kuner, 2010; Latremoliere and Woolf, 2009). However, accumulating evidence from human and animal studies suggest that after tissue injury-induced hyperalgesia resolves, sensitization in the DH persists within a long-lasting silent state of remission, termed "latent sensitization" (LS) (Gerum and Simonin, 2021; Bradley K. Taylor and Corder, 2014).

Following tissue injury and the subsequent resolution of hyperalgesia, intrathecal administration (i.t.) of selective antagonists at inhibitory $G\alpha_{i/o}$ G protein-coupled receptors (GPCRs), including μ-opioid receptors (MOR), kappa opioid receptors (KOR), neuropeptide Y Y1 receptors (Y1R), or several other receptors, unmask LS and reinstate hyperalgesia (Basu et al., 2021; Corder et al., 2013; Fu et al., 2020, 2019; Solway et al., 2011; Walwyn et al., 2016). Remarkably, each antagonist was sufficient to produce a complete, not partial, reinstatement of hyperalgesia. This suggested to us that GPCRs interact in a complex manner, not just additively,

to maintain LS in remission. Indeed, individual cells express many GPCRs whose intracellular second messengers can interact to co-alter signaling (Cordeaux and Hill, 2002; Gupte et al., 2017; Hur and Kim, 2002; Selbie and Hill, 1998). For example, different GPCRs can activate the same G proteins (Alt et al., 2002; Yao et al., 2006). Thus, coincidental activation of second messenger pathways by co-activation of multiple GPCRs can elicit supra-additive (synergistic) amplification of the responses and produce a greater than additive leftward shift in the response curve (Aira et al., 2014; Bourne and Nicoll, 1993; Horioka et al., 2021; Philip et al., 2010).

Examples of spinal analgesic synergy between $G\alpha_{i/o}$ GPCR agonists exist in the pharmacology literature, including mu and kappa-selective or mu and delta-selective opiates (Schuster et al., 2015; Sutters et al., 1990), opiates and cannabinoids (Cichewicz, 2004; Grenald et al., 2017; Kazantzis et al., 2016), and opiates and α2-adrenergic receptor agonists (Chabot-Doré et al., 2015; Overland et al., 2009; Stone et al., 1997). The aim of this chapter is to test the hypothesis that surgical incision produces a tonic and long-lasting synergistic dependence on MOR and Y1R endogenous signaling to oppose the development of CPSP.

5.2 Methods

Animals

Adult C57Bl/6NCrl (Charles River, #027), $Npy1r^{loxP/loxP}$ (courtesy of Herbert Herzog, (Howell et al., 2003)), $Pirt^{Cre}$ (courtesy of Xinzhong Dong, (Kim et al., 2008)), and $Lbx1^{Cre}$ (courtesy of Carmen Birchmeier, (Sieber et al., 2007)) mice were group housed, provided access to food and water *ad libitum*, and maintained on a 12:12 hour light:dark cycle (lights on at 7:00am)

in temperature and humidity controlled rooms. Male and female mice were used in all experiments. No significant sex differences were observed. All experiments were carried out in accordance with guidelines from the International Association for the Study of Pain and with the approval of the Institutional Animal Care and Use Committees of the University of Pittsburgh.

Drugs

Table 6. Pharmacological agents used in this study

Chemical	Source	Dilutant Information
BIBO 3304 trifluoroacetate	TOCRIS – Cat:2412	Diluted in a vehicle solution of ETOH, castor oil and saline in a 1:1:8 ratio
CTOP	TOCRIS – Cat:1578	Diluted in saline
PEAQX tetrasodium salt	TOCRIS – Cat:5018	Diluted in saline

Intrathecal injections

As previously described (Corder et al., 2013; Fu et al., 2019; Solway et al., 2011), the mouse was lightly restrained in a towel and a 30G ½ inch needle attached to a 25-µl Hamilton microsyringe was inserted into the subarachnoid space between the L5/L6 vertebrae at an angle of 30–45° to the horizontal plane. The needle was advanced until a reflexive tail flick was observed, at which time 5 µl of drug or vehicle was slowly administered. The needle was held in place for 10 seconds, withdrawn, and then the mouse was returned to its testing chamber.

Synergistic Interaction/Isobologram Analysis

Drug interactions were evaluated by a statistical method known as isobolographic analysis in which the actual potency of two drugs in combination is compared to that predicted in the absence of an interaction (Tallarida, 2002). Isobolograms were constructed using the values obtained at the concentrations of the compounds administered alone and in combination that produced 50% of the possible maximum antinociceptive effect (ED_{50}) in the Von Frey test. The theoretical dose required for a purely additive interaction (Z_{add}) with the S.E.M. for each combination at a 30:1 ratio was computed from the ED_{50} values of the single drugs as previously described (Tallarida, 1992). The area under the curve (AUC) of mechanical withdrawal testing was calculated using the trapezoidal rule (Tallarida et al., 1989). Concentration-dependent curves for each of the tested compounds were established according to the percentage of antinociceptive effect that was calculated from the AUCs. The antinociceptive effect (%) was obtained from the AUCs of the different treatments relative to the AUC for vehicle. Isobolographics were generated using JFlashCalc (http://www.u.arizona.edu/~michaelo/jflashcalc.html) and reconstructed in GraphPad Prism 9.

The interaction index was calculated as follows:

A = ED_{50} from drug A alone (CTOP)

B = ED_{50} from drug B alone (BIBO 3304)

"a" and "b" = combination doses from the respective drugs based on the ED_{50} of the combination

$$\frac{a}{A} + \frac{b}{B} = y$$

$$\frac{0.006}{260} + \frac{0.193}{8} = y$$

$$0.00002308 + 0.024125 = y$$

$$0.02 = y$$

*Note that $\gamma = 1$ is additive, $\gamma < 1$ is supra-additive (synergistic), and $\gamma > 1$ is sub-additive (antagonistic)

Plantar Incision Model

Post-operative hyperalgesia was induced by longitudinal incision of the plantaris muscle as previously described (Basu et al., 2021; Pogatzki and Raja, 2003). Following antisepsis of the left hind paw with Chlorascrub® and 70% ethanol, a #11 scalpel blade was used to make a 5mm incision through the skin and fascia, beginning 2mm from the proximal edge of the heel and extending towards the digits. The underlying muscle was raised with a curved forceps, extended 4

mm, and then incised longitudinally with the #11 scalpel blade, all while leaving the origin and insertion of the muscle intact. The overlying skin was closed with synthetic 5-0 sutures (PDS*II, Ethicon). Surgery was typically completed within 5-10min. Surgeries were conducted under isoflurane anesthesia (5% induction followed by 1.5% - 2.0% maintenance). After suturing of the skin, triple antibiotic ointment (Neosporin, Johnson and Johnson) was applied to the surgical area. The sutures were removed 10 days after surgery.

Behavioral Testing

Mechanical hypersensitivity: Sensitivity to a non-noxious mechanical stimulus was tested with an incremental series of 8 von Frey monofilaments of logarithmic stiffness (Stoelting, Wood Dale, IL) that ranged in gram force from 0.008g to 6g. The stimulation was applied lateral to the suture line. Filaments were applied to the skin with a slight bending of the filament for a maximum of 5 seconds. A clear withdrawal of the paw from the application of the stimulus was recorded as a positive response. The 50% withdrawal threshold was determined using the up-down method (Chaplan et al., 1994). Before commencement of each von Frey session, we acclimated the animals within individual Plexiglas boxes placed on the top of a stainless-steel mesh platform for 45 min.

Conditioned place aversion: A two-day conditioning protocol using a biased chamber assignment was used for conditioned place aversion (CPA). On the acclimation day (Day 0), mice had free access to explore all chambers of a 3-chamber conditioned place testing apparatus (side chambers: 170 x 150 mm; center chamber: 70 x 150 mm; height: 200 mm; San Diego Instruments) for 30 mins. Mice were able to discriminate between chambers using visual (vertical versus horizontal black-and-white striped walls) and sensory (rough versus smooth textured floor) cues.

For pre-conditioning (Days 1 and 2), mice were again allowed to freely explore for 30 mins during which their position was recorded via a 4 x 16 infra-red photobeam array and associated software (San Diego Instruments). For conditioning (Days 3-4), each mouse's non-preferred chamber was paired with a vehicle i.t. injection and the preferred chamber with a BIBO:CTOP combo i.t. injection. Each morning mice received an i.t. vehicle injection, were returned to their home cage for 5 min (to disassociate the injection with the chamber), and were then placed in the designated side chamber for 60 min. 6 hours later, mice received BIBO:CTOP combo (10ng, i.t.), were returned to their home cage for 5 min, and were placed into the BIBO:CTOP combo-designated chamber for 60 min. On test day (Day 5), mice could freely explore all chambers and their position was recorded as during pre-conditioning for 30 min. Difference scores were calculated as the time spent in the chamber on test day minus the time spent in the same chamber during pre-conditioning.

Touch-evoked phosphorylated extracellular signal-regulated kinase (pERK): pERK was evoked by touch stimulation as previously described (Fu et al., 2019). 21 days after PIM, mice received either i.t. injections of vehicle, BIBO 3304 9.7ng, CTOP 0.3ng, or COMBO 10ng (BIBO 9.7ng + CTOP 0.3ng). One hour later, mice were lightly anesthetized with isoflurane (1.5%), and the ventral surface of the ipsilateral hindpaw was mechanically stimulated with a gentle 3-s stroke with a cotton swab from heel to toe. This was repeated every 5s for 5min. After an additional 5 min pause, mice were more deeply anesthetized with isoflurane and transcardially perfused with ice cold 0.01M phosphate buffered saline (PBS, Fischer Scientific), followed by 10% phosphate formalin buffer. Lumbar spinal cords were harvested and post-fixed in the same fixative overnight at 4 °C and then cryoprotected with 30% sucrose until total submersion (1–3 days).

Immunohistochemistry

Transverse spinal cord sections (30 μm) from L3-L5 were cut on a sliding microtome (Leica, SM, 2000R). A series of sections, each 240 μm apart, were washed in 0.01M PBS, blocked in 3% normal serum (goat; Gemini Bioproducts) containing 0.3% Triton X-100 (Sigma Aldrich) in 0.01M PBS for 1 h, and then incubated with primary rabbit antibody anti-phosphorylated-ERK1/2 antiserum (1:1000, Cell Signaling) at 4 °C for 24h on a shaker. The following day, sections were again washed in 0.01M PBS and incubated for 1 h at room temperature with the secondary conjugated antibody (1:1000, Invitrogen: goat anti-rabbit Alexa Fluor 488). The sections were washed in 0.01M phosphate buffer, mounted and coverslipped with VECTASHIELD HardSet Antifade Mounting Medium with DAPI. At least six good quality sections from segment L4 were selected from each subject for microscopy.

Fluorescence in situ Hybridization (FISH) (RNAscope)

Mice were transcardially perfused with ice cold 1x PBS followed by 10% buffered formalin and spinal cords and DRGs were extracted via blunt dissection, postfixed in 10% formalin (2-4 hrs), and then placed in 30% sucrose at 4°C until the tissue sank (~48-72 hrs). 20μm thick L3-L4 floating spinal cord sections were obtained on a vibrating microtome, and 12μm thick L3-L4 DRGs were cut on a cryostat and mounted on Superfrost Plus Microscope slides and air dried overnight at room temperature. Slides underwent pretreatment for fluorescence *in situ* hybridization consisting of 10 min Xylene bath, 4 min 100% ethanol bath, and 2 min RNAscope® H2O2 treatment. Next, the FISH protocol for RNAscope Fluorescent v2 Assay (ACD) was followed for hybridization to marker probes. Slides were then coverslipped with VECTASHIELD HardSet Antifade Mounting Medium with DAPI.

Microscopy

All images were captured on a Nikon Eclipse Ti2 microscope using a 20x or 40x objective and analyzed using NIS-Elements Advanced Research software v5.02. An examiner blinded to treatment and sex counted the number of positive pERK cells in laminae I-II. Cells with at least 3 puncta associated with a DAPI nucleus were considered positive for fluorescence *in situ* hybridization.

Statistical Analyses

All data are presented as means ± SEM. Statistical significance was determined as $*P < 0.05$. The effects of Drug and Time were analyzed by two-way analysis of variance (ANOVA), followed by Sidak`s multiple comparison tests. Data from dose-response curves were also analyzed as area under the curve using the trapezoidal method and used to produce the non-linear regression analyses of Maximum Possible Effect (% MPE). MPE were used to determine the ED50 for each drug. %MPE was calculated as follows: % MPE = 100 * (post-injection threshold – pre-injection threshold)/(post-injury threshold – pre-injection threshold). All statistical analyses were performed in GraphPad Prism 9.0. GraphPad Prism and Biorender.com were used to make the graphics.

5.3 Results

5.3.1 MOR and Y1R are co-expressed in DRG and DH

Synergistic interactions between MOR and Y1R may be mediated by either 1) intracellular mechanisms in which receptors located on the same cell produce interactions at the level of intracellular signaling cascades, or 2) via intercellular mechanisms which involve coincident inhibition of two neurons in series in the same anatomical pathway or a retrograde feedback mechanism (Chabot-Doré et al., 2015). First, we examined MOR and Y1R localization using fluorescence *in situ* hybridization for *Oprm1* and *Npy1r* and we found colocalization in cells in the lumbar dorsal root ganglion (DRG) (**Figure 32A-B**) and DH (**Figure 32C-D**). Thus, MOR and Y1R intracellular cross-talk in neurons in both DRG and DH is plausible to produce synergistic intracellular signaling.

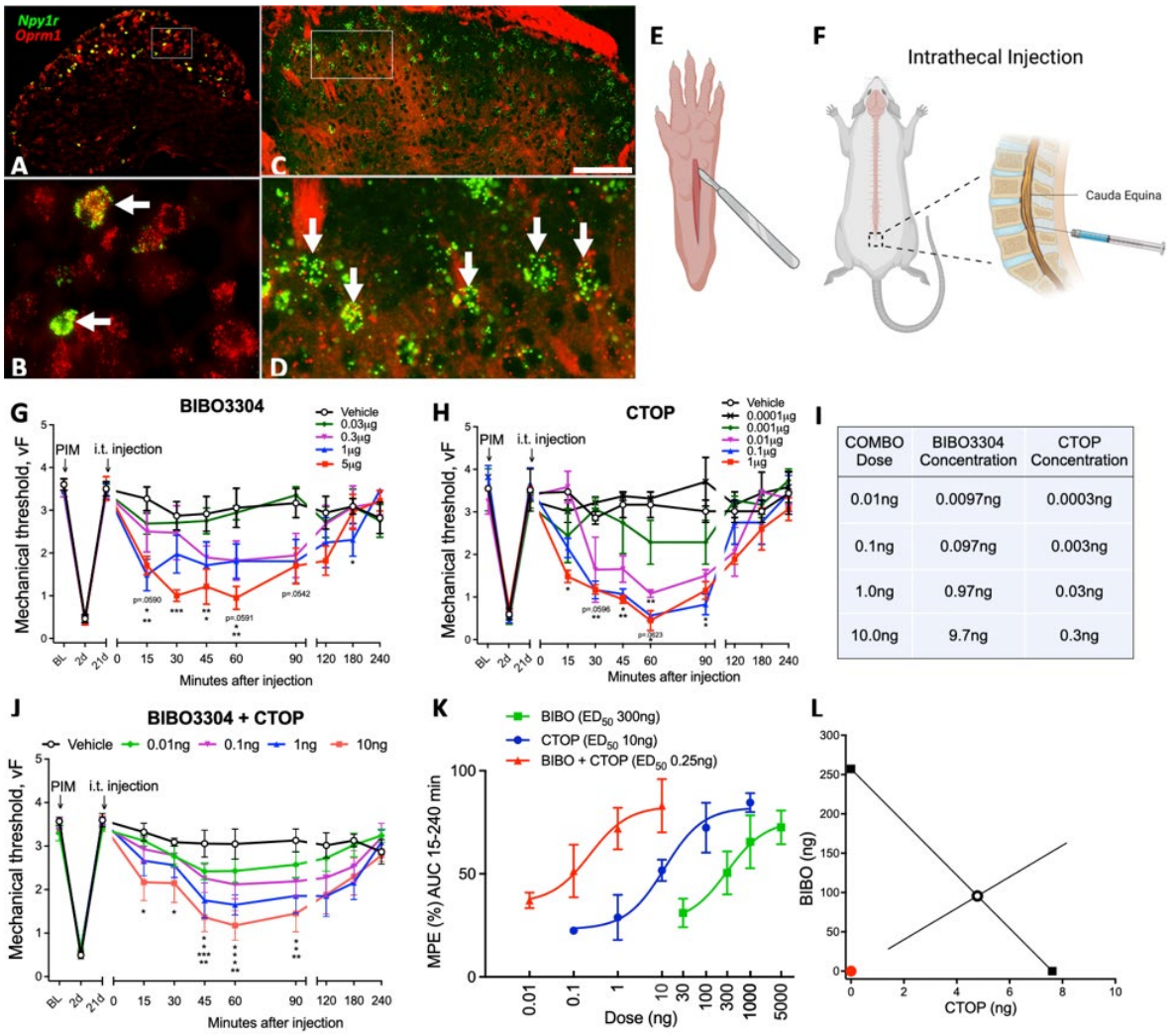

COMBO Dose	BIBO3304 Concentration	CTOP Concentration
0.01ng	0.0097ng	0.0003ng
0.1ng	0.097ng	0.003ng
1.0ng	0.97ng	0.03ng
10.0ng	9.7ng	0.3ng

Figure 32. Y1R and MOR synergistically oppose LS.

Fluorescence *in situ* hybridization demonstrating colocalization of *Oprm1* and *Npy1r* in the same cells in both lumbar DRG (**A-B**) and DH (**C-D**). **B** and **D** represent zoomed in box insets for **A** and **C**, respectively. Schematic depictions of plantar incision (**E**) and intrathecal injections into the mouse to target the spinal cord (**F**). Dose-response time courses of reinstatement of hyperalgesia after intrathecal (i.t.) administration of BIBO3304 (**G**), CTOP (**H**), or BIBO3304 and CTOP in combination (**I-J**) (n=3-8/group). Dose response effects of antagonist-induced reinstatement. MPE: maximum possible effect. AUC: area under curve (**K**). Isobolographic analysis of interaction between BIBO3304 and CTOP and red dot indicating interaction index of 0.02, a measure of drug synergism by which a value < 1.0 is determined to be synergistic (**L**). Data presented as mean ± SEM. Significance determined with two-way RM ANOVAs followed by post hoc if applicable with *P<0.05, **P<0.01, and ***P<0.001.

5.3.2 MOR and Y1R signaling work synergistically to oppose CPSP

Next, we performed plantar incision of the hindpaw (PIM), a model of postoperative pain (**Figure 32E**) that produces robust mechanical hyperalgesia that resolves within 21 days. Following resolution of hyperalgesia, i.t. administration (**Figure 32F**) of a MOR antagonist (CTOP) or a Y1R antagonist (BIBO3304) dose-dependently reinstated mechanical hypersensitivity with an ED_{50} of 260ng and 8ng, respectively (**Figure 32G-H**). Thus, CTOP exhibits a 30-fold difference in potency compared to BIBO3304, and we assessed synergistic interactions with a fixed ratio (30:1) isobologram method (Tallarida, 2016, 1992) (**Figure 32I**). BIBO3304 and CTOP combination (BIBO:CTOP) reinstated mechanical hypersensitivity with robust effects at even a remarkably low 100pg dose (**Figure 32J**). BIBO:CTOP produced a large leftward shift in the dose-response curve as compared to either BIBO3304 or CTOP administered alone (**Figure 32K**), and the isobolographic analysis revealed a synergistic interaction (**Figure 32L**). Additionally, BIBO:CTOP (10ng, i.t.) dramatically increased the light touch-evoked expression of phosphorylated extracellular signal-regulated kinase (pERK) in superficial DH neurons, a proxy for neuronal activation (**Figure 33A-E**), and produced a robust conditioned place aversion in mice with plantar but not sham incision (**Figure 33F-G**).

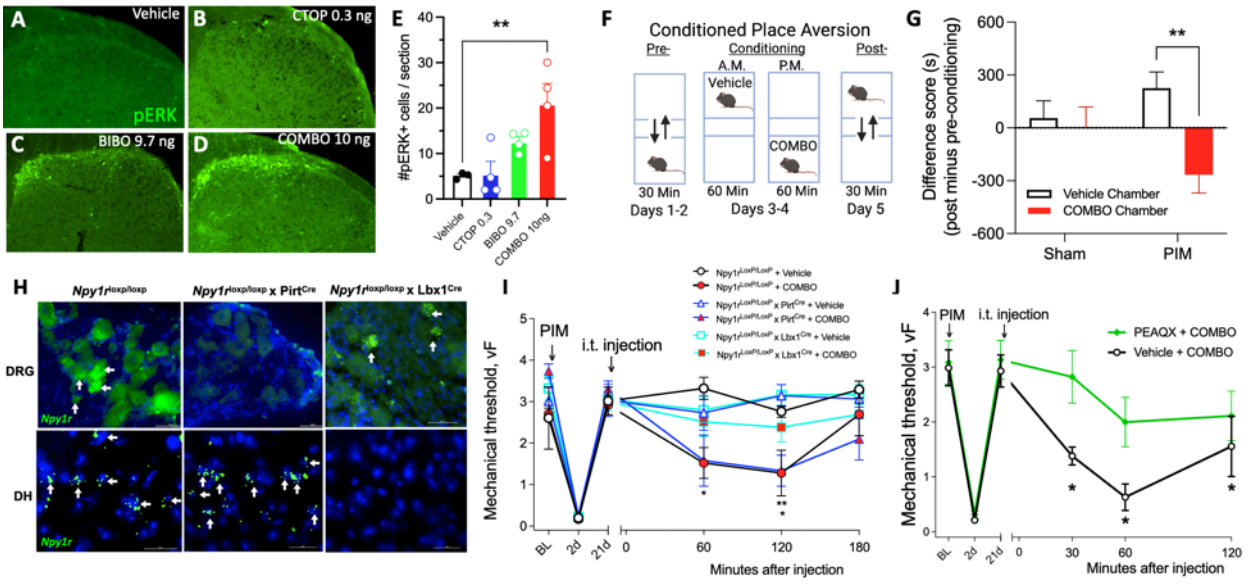

Figure 33. DH but not DRG Y1R and MOR synergy opposes a GluN2-driven LS.

Representative images (**A-D**) and DH laminae I-II quantification of light touch-evoked pERK after intrathecal drug administration (**E**) (n=3-4). Experimental timeline (**F**) and quantification for conditioned place aversion testing (**G**) (n=11-12/group). Fluorescence *in situ* hybridization demonstrating loss of *Npy1r* expression in the DRG of Npy1r$^{loxP/loxP}$ x Pirt^{Cre} mice and SC of Npy1r$^{loxP/loxP}$;Lbx1^{Cre} mice (**H**). BIBO:CTOP reinstated PIM-induced mechanical hyperalgesia in Npy1r$^{loxP/loxP}$ and Npy1r$^{loxP/loxP}$;Pirt^{Cre} mice but not in Npy1r$^{loxP/loxP}$;Lbx1^{Cre} mice (**I**) (n=6-9/group). GluN2a NMDAR subtype antagonist, PEAQX (100ng, i.t.) prevented BIBO:CTOP-induced reinstatement of mechanical hyperalgesia (**J**) (n=7-8). Data presented as mean ± SEM. Significance determined using three- (H) or two-way RM ANOVAs (G, I) followed by post hoc if applicable with *P<0.05, and **P<0.01.

5.3.3 MOR and Y1R signaling within DH rather than DRG neurons works synergistically to oppose LS

Intrathecally administered chemicals can engage both DH and DRG neurons. To resolve the specific site of action for BIBO:CTOP, we crossed $Npy1r^{loxP/loxP}$ mice with either $Pirt^{Cre}$ or $Lbx1^{Cre}$ mice to conditionally knockout *Npy1r* in the DRG or DH, respectively (**Figure 33H**). BIBO3304:CTOP (10 ng, i.t.) reinstated PIM-induced mechanical hypersensitivity in both control ($Npy1r^{loxP/loxP}$) and DRG conditional knockout mice ($Npy1r^{loxP/loxP}$;$Pirt^{Cre}$), but not in DH conditional knockout mice ($Npy1r^{loxP/loxP}$;$Lbx1^{Cre}$) (**Figure 33I**). These data suggest that MOR and Y1R signal within DH neurons, rather than DRG neurons, to synergistically oppose LS and maintain postoperative pain in remission.

5.3.4 Spinal LS is dependent on GluN2A NMDA receptors.

Previously, we demonstrated that a N-methyl-D-aspartate receptor (NMDAR) blocker, MK-801 (dizocilipine), prevented either Y1R (Fu et al., 2019) or MOR (Corder et al., 2013) antagonist-induced reinstatement of peripheral inflammatory pain. Thus, we hypothesized that NMDARs, in particular the GluN2A subunit, also mediate the LS that is unmasked by BIBO:CTOP. To test this, we co-administered the GluN2A-preferring NMDAR antagonist, PEAQX (100ng, i.t.), with BIBO:CTOP (10ng, i.t.). PEAQX, but not vehicle, abolished the BIBO:CTOP-induced reinstatement of mechanical hypersensitivity (**Figure 33J**). These data suggest that MOR and Y1R signaling synergistically opposes a GluN2A-mediated latent postoperative pain sensitization and thus maintains postoperative pain in remission (**Figure 34**).

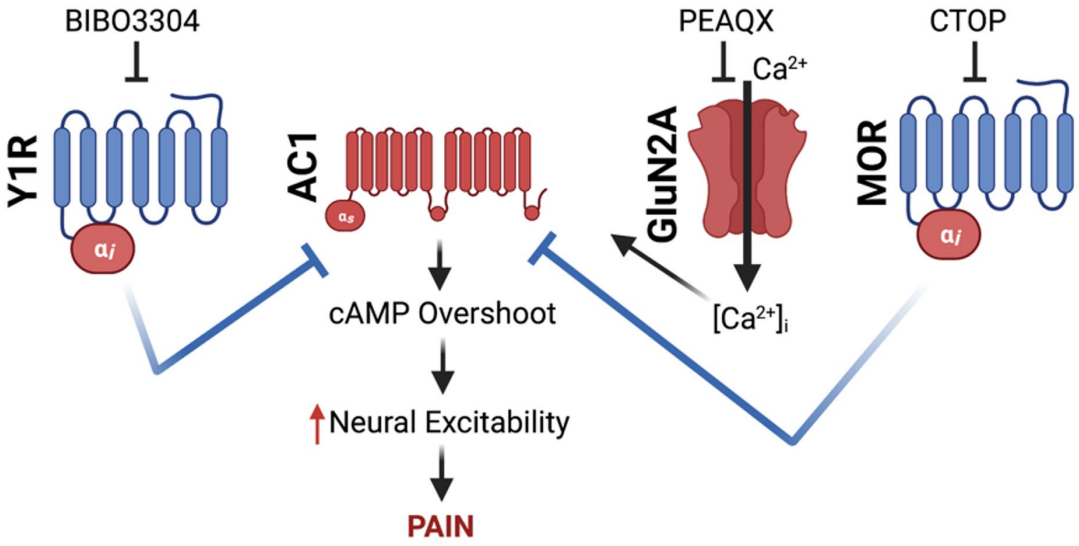

Figure 34. Proposed schematic of cellular pathways involved in endogenous NPY and opioid synergistic pain inhibition.

We propose that following the resolution of injury, endogenous anti-nociceptive peptides (e.g. enkephalins, endorphins, NPY) interact with MOR and Y1R in a synergistic manner to maintain LS in remission. However, this long-lasting $G\alpha_{i/o}$-coupled GPCR activity produces heterologous sensitization of adenylyl cyclase 1 (AC1). We hypothesize that both MOR and Y1R share a common pool of AC1, thus, potent activation or blockade of either MOR or Y1R can prevent or produce a cAMP overshoot and the reinstatement of hyperalgesia, respectively. This idea largely is proposed from the work of (Levitt et al., 2011).

5.4 Discussion

Cells must integrate multiple signals from an array of receptors at any given moment. One of the most fundamental and evolutionarily conserved signaling mechanisms is GPCR activation, which is classically viewed as a compartmentalized cellular event in which a ligand binds a receptor to activate a specific signaling pathway distinct from other GPCRs. (Gurevich and Gurevich, 2020; Hur and Kim, 2002; W. Wang et al., 2018). However, researchers are uncovering examples of how GPCRs and their intracellular second messengers might interact within a cell to supra-additively co-alter signaling (Cordeaux and Hill, 2002; Gupte et al., 2017; Horioka et al., 2021; Hur and Kim, 2002; Overland et al., 2009; Schuster et al., 2015; Selbie and Hill, 1998). For the first time, we report an endogenous analgesic synergy between MOR and Y1R signaling that persists beyond the resolution of hyperalgesia and injury to maintain CPSP in remission. Modest failure in either Y1R or MOR compensatory signaling may underlie the physiological vulnerability to remission and the development of CPSP.

MOR and Y1R are *Pertussis* toxin-sensitive $G\alpha_{i/o}$-coupled GPCRs; thus, upon initial receptor activation, the $G\alpha_{i/o}$ subunit potently inhibits adenylyl cyclase to reduce the production of cAMP. The free $G\beta\gamma$ counterpart acts as a signaling molecule to activate downstream signaling pathways that include activation of G protein-coupled inwardly-rectifying K^+ channels (GIRKs) and inhibition of voltage-gated Ca^{2+} channels to reduce the excitability of neurons (Yudin and Rohacs, 2018). Paradoxically, prolonged activation of $G\alpha_{i/o}$ GPCRs enhances the activity of adenylyl cyclase and markedly increases cAMP production. This cellular phenomenon is referred to as heterologous sensitization (otherwise referred to as supersensitization, cAMP overshoot, cAMP superactivation) and is readily apparent upon removal of the agonist (Brust et al., 2015;

Sharma et al., 1975; Watts, 2002). Interestingly, blockade of MOR constitutive activity in the setting of LS produces heterologous sensitization of adenylyl cyclase 1 (AC1) (Corder et al., 2013). This likely occurs for spinal Y1Rs as well, as the endogenous ligand, NPY, also produces heterologous sensitization (Drakulich et al., 2003), and Y1R antagonism-induced reinstatement of pain-like behavior is lost in AC1 knockout mice (Fu et al., 2020, 2019). Our current results suggest that endogenous anti-nociceptive peptides (e.g. enkephalins, endorphine, NPY) interact with MOR and Y1R in a synergistic manner to maintain LS in remission. $G\alpha_{i/o}$-coupled GPCRs share a common pool of adenylyl cyclase, thus, when one $G\alpha_{i/o}$-coupled GPCR produces heterologous sensitization, administration of a different $G\alpha_{i/o}$ GPCR agonist can prevent subsequent cAMP overshoot (Levitt et al., 2011). As schematized in **Figure 34**, we suggest that endogenous MOR and Y1R activity synergistically inhibit AC1 while counter adaptively also producing a heterologous sensitization of AC1. Antagonism of the synergistically interacting, LS-inhibiting, $G\alpha_{i/o}$-coupled GPCRs is therefore sufficient to evoke a cAMP overshoot and unmask LS to produce a complete reinstatement of hyperalgesia.

The molecular mechanisms underlying the endogenous MOR and Y1R synergy remain unknown, but several possible mechanisms exist. First, MOR and Y1R may form receptor-receptor interactions, such as the formation of heterodimers (Cordeaux and Hill, 2002; Selbie and Hill, 1998). The formation of heterodimers or oligomerization between GPCR receptors can markedly potentiate signal transduction (Jordan and Devi, 1999; Levac et al., 2002). Second, MOR and Y1R may undergo signal transduction interactions. The assumption is that Y1R and MOR coexist on neurons and share a common pool of G proteins; therefore, activation of one receptor may cause redistribution of its G proteins and increase the sensitivity of the other receptor. For example,

binding of an endogenous ligand, such as NPY to Y1R, may shift the affinity of endogenous ligand binding to the separate GPCR MOR (Djellas et al., 2000). Additionally, both MOR and Y1R may synergistically work through downstream effectors. The free Gβγ released from the agonist-induced dissociation of both the MOR and Y1R G_i heterotrimers may co-activate protein kinase C (PKC), phospholipase C (PLC) (Overland et al., 2009; Yao et al., 2003), or protein kinase C epsilon (PKCε) (Schuster et al., 2015) to synergistically oppose LS. Third, peptide hormones like NPY can modulate neurotransmission by recruiting other GPCRs from the interior of the cell to the cell membrane (Holtbäck et al., 1999). Coincident activation of Y1R and MOR may allow recruitment of MORs to the cell membrane and a sensitization of MOR signal transduction (Achour et al., 2008; Cahill et al., 2007; Holtbäck et al., 1999). Future experiments should further evaluate how Y1R and MOR interact mechanistically to promote endogenous synergy.

The current study establishes the existence of supra-additive endogenous MOR and Y1R signaling in the spinal cord DH that maintains LS in remission. Further, we provide a strong basis for future investigations of the mechanisms involved in MOR-Y1R endogenous synergistic signaling and the cellular subpopulations in the DH that drive LS.

6.0 Final Discussion

The aim of this thesis was to test the overarching hypothesis that *exogenous or endogenous spinal neuropeptide Y potently inhibits the behavioral signs of chronic pain via inhibiting pain facilitatory Y1 receptor-expressing dorsal horn interneurons.* We designed and implemented studies that implicate spinal Y1-INs as both necessary and sufficient for the manifestation of neuropathic pain. Additionally, we determined that the specific spinal receptor site for NPY-induced anti-allodynia in pre-clinical models of neuropathic pain is at Y1 on Y1-INs. Further, we present how endogenous NPY-Y1 signaling at Y1-INs can synergistically interact with mu opiate receptor signaling to maintain chronic postsurgical pain in remission. In our proposed model, Y1-INs become hyperexcitable following peripheral injury and promote pain-like behavior. Consequently, endogenous or exogenous NPY, acting via the G_i-coupled Y1 receptors on Y1-INs, can dampen central and/or latent sensitization (**Figure 3**) to potently inhibit the behavioral signs of chronic pain (**Figure 35A**).

6.1 Evolutionary considerations: what is the neurobiological role of Y1-INs and is there an advantage of "maladaptive" pain plasticity?

Npy1r-expressing interneurons account for ~25% of the total excitatory interneurons in the superficial spinal cord DH (**Figure 29**). One would predict that such a large neural population is biologically/evolutionarily important for survival. Specifically, I theorize that Y1-INs were selected for through evolution as they allow the fine-tuned sensory processing of thermal and cold stimuli in the spinal cord dorsal horn. In a healthy (non-injured) setting, Y1-INs are necessary for responding to acute nociceptive stimuli and the accurate perception of both cold and heat stimuli.

Specifically, this is demonstrated with ablation of Y1-INs with NPY-saporin. NPY-saporin reduces hindpaw licking and guarding in a 44 °C hotplate assay of affective pain, reduces ongoing nociception during both phases of the response to intraplantar injection of dilute formalin, and reduces aversion to a 10 °C cold plate (Lemons and Wiley, 2012; Wiley et al., 2009). Further, intrathecal administration of NPY reduces formalin-evoked pain responses and increases the latency to withdrawal on a hot plate equivalent to morphine administration (Hua et al., 1991; Mahinda and Taylor, 2004; Taiwo and Taylor, 2002). These behavioral phenotypes match well with both Y1-INs' location in the superficial dorsal horn (found throughout superficial laminae I-II) as well as the histochemical characterization of Y1-INs. First, heat- and cool-responsive stimuli are transmitted primarily via primary afferents expressing TRPV1(Caterina et al., 1997) and TRPM8 (Peier et al., 2002), respectively. The central terminals of these primary afferent neurons primarily terminate with superficial laminae I-II (Cavanaugh et al., 2011; Dhaka et al., 2008; Wrigley et al., 2009). Additionally, within the spinal cord dorsal horn, heat-responsive (Tsubaki and Yokota, 1983) and cool-responsive (Wrigley et al., 2009) neurons are found in superficial laminae I-II. Recently, histochemical identities of dorsal horn heat and cold response neurons have been uncovered (Horwitz et al., 2022; Wang et al., 2022). Specifically, heat-responsive dorsal horn neurons express ERBb4 (Wang et al., 2022) and cold-responsive neurons express calbindin (while also being somatostatin lacking) (Horwitz et al., 2022). In this dissertation I present that Y1-INs in the rat dorsal horn extensively colocalize with calbindin (36.06% overlap), but I do not know if this is the somatostatin-negative population. I predict that Y1-INs will extensively colocalize with both heat- and cold-responsive markers, and future studies can address this hypothesis.

Y1-INs are involved in the acute response to noxious pain and nociceptive sensitization. Nociceptive sensitization produced by non-lethal injury is an evolutionarily conserved phenomena across most species, and while inconvenient/uncomfortable, this sensitization is actually an adaptive response that enhances responsiveness to threats and increases rates of survival (Crook et al., 2014). Unfortunately, this adaptive sensory responsiveness can become maladaptive in the context of chronic pain. Numerous theories exist about how acute pain becomes pathological including: hyperalgesic priming of nociceptors (Reichling and Levine, 2009), failure in endogenous inhibitory G protein signaling (Gerum and Simonin, 2021; B.K. Taylor and Corder, 2014), loss of descending inhibition from the rostral ventral medulla to the spinal cord (Chen and Heinricher, 2019; De Felice et al., 2011; Ossipov et al., 2014), and long-term net excitation/inhibition balances in somatosensory processing at both the spinal (Kopach et al., 2017; Lee et al., 2019; Zeilhofer et al., 2012a) and supraspinal levels (Cheriyan and Sheets, 2020; Petrou et al., 2012; Potter et al., 2016). The work in this dissertation demonstrates that Y1-IN activation is sufficient to drive robust pain-like responses and that peripheral nerve injury increases the excitability of Y1-INs. However, further work is required to understand exactly how Y1-INs transition from the processing of acute pain responses to driving chronic pain. In summary, Y1-INs normally respond to acute nociceptive stimuli to enhance responsiveness to threats/ increase survival, however, in the context of peripheral nerve injury, Y1-INs become hyperexcitable and engage in maladaptive pain signaling.

6.2 Neuropeptide Y1 receptor-expressing neuron hyperexcitability as a mechanism for the manifestation of chronic neuropathic pain?

The balance between excitation and inhibition in the spinal cord DH is central to normal somatosensory function (Todd, 2010). Our neurophysiological recordings demonstrate that SNI dramatically increases the excitability of Y1-INs. This increased excitability following peripheral nerve injury is consistent with an enduring increase in the excitability found within sensory circuits in chronic pain states often denoted as “central sensitization" (Latremoliere and Woolf, 2009). In our neurophysiological recordings from Y1-INs, we found both an increase in the frequency and amplitude of sEPSCs. These results mirror the effects of chronic constriction injury (CCI) or sciatic nerve axotomy, two other models of peripheral nerve injury, and also the effects of brain derived neurotrophic factor (BDNF) application in uninjured animals on the excitatory neurotransmission to excitatory interneurons in the DH (Balasubramanyan et al., 2006; Chen et al., 2009; Smith, 2014). Conversely, we show that artificial chemogenetic or optogenetic excitation of Y1-INs in uninjured mice is sufficient to induce a neuropathic pain-like phenotype.

Therefore, we suggest that Y1-INs function like a pain rheostat: noxious stimuli increase the activity of Y1-INs to promote pain, whereas their subsequent inhibition reduces pain-like behaviors (**Figure 35A**). SNI represents a severe/persistent pain model in which the rheobase is permanently shifted to a pro-pain state. However, transient/less severe/short-lived injuries, such as complete Freund’s adjuvant-induced inflammation (Fu et al., 2019), plantar incision (**Figure 32**), or spared tibial peripheral nerve injury (a milder form of peripheral nerve injury (Fu et al., 2020; Solway et al., 2011)) shift the rheobase to nociception temporarily, but the hypersensitivity eventually resolves and the rheostat is returned to the original set point. This reset point is achieved

through the endogenous release of NPY to inhibit hyperexcitable Y1-IN activity (perhaps achieved with the synergistic assistance of other pain inhibitory GPCRs as shown in **Chapter 5**). Indeed, we have repeatably demonstrated that intrathecal administration of NPY Y1 receptor antagonists, or conditional NPY knockdown, reinstates mechanical, cold, and affective hypersensitivity following peripheral inflammation, incision, or a milder form of peripheral nerve injury (Fu et al., 2020, 2019; Solway et al., 2011) (**Figure 32**). This suggests an endogenous, tonic inhibition of pain facilitatory Y1-INs via NPY-INs. In the context of mild injury, when dorsal horn inhibition is reduced, NPY-INs can release NPY to inhibit hyperexcitable Y1-INs and return the DH to a homeostatic set point. However, if major injury occurs and chronic pain does not resolve, alternatively, our results suggest that exogenous administration of NPY Y1 agonists at the spinal cord can inhibit Y1-INs to potently reduce pain-like behavior.

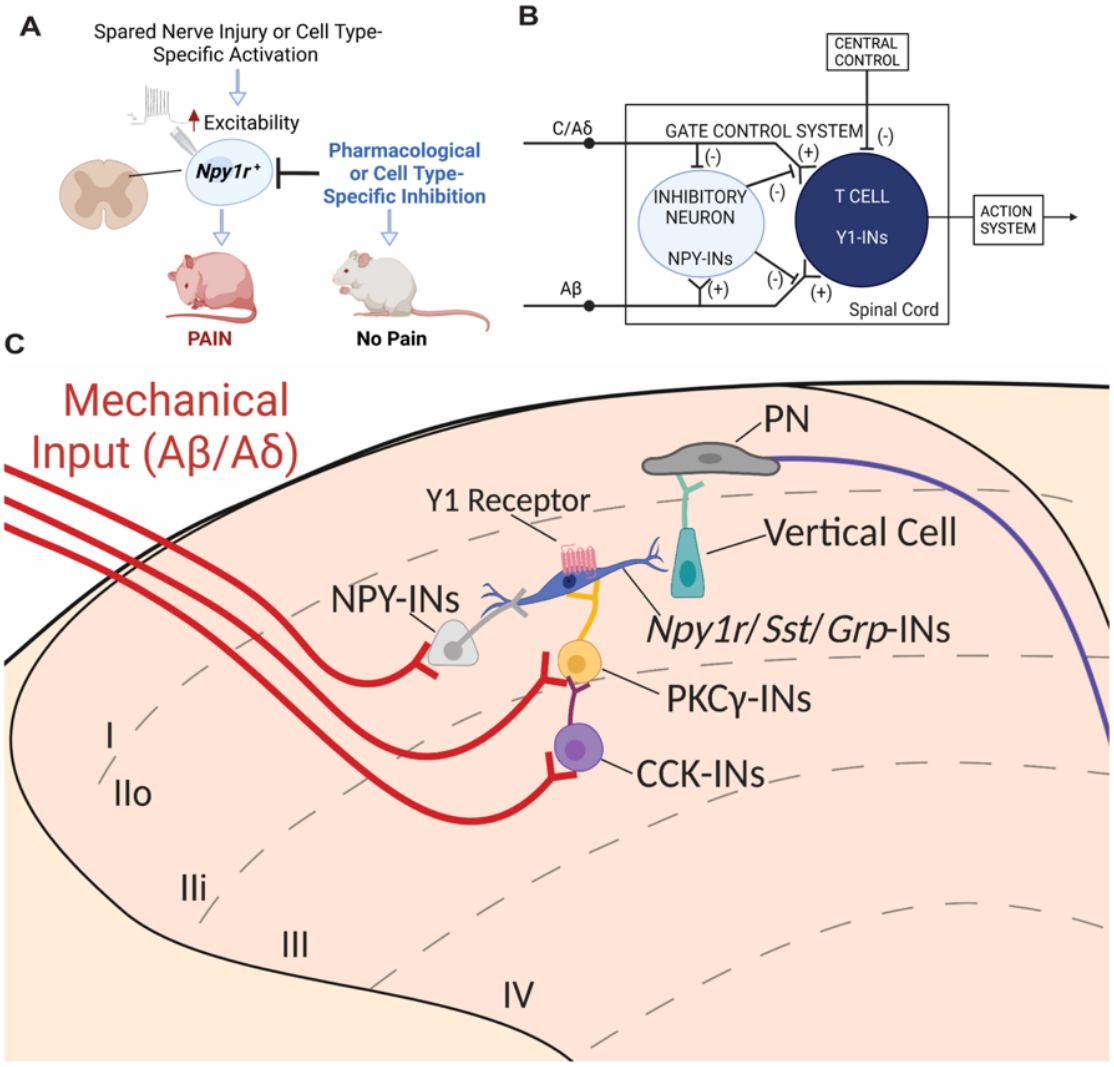

Figure 35. The proposed contribution of Y1-INs to the gate control theory of pain and the ascending peripheral nerve injury-induced mechanical allodynia model in the dorsal horn.

(**A**) Graphical abstract summarizing key data from this manuscript implicating Npy1r-expressing interneuron excitability in the manifestation of pain. (**B**) Schematic showing the modified gate control theory of pain. ‘‘T CELL’’ represents a spinal pain transmission neuron that we speculate is a Y1-IN. ‘‘INHIBITORY NEURON’’ is an inhibitory neuron that we speculate is a NPY-IN. ‘‘(+)’’ and ‘‘(-)‘‘ represent excitatory and inhibitory inputs, respectively. The “ACTION SYSTEM” denotes a behavioral response to a T cell activation. The CENTRAL CONTRAL describes descending modulation from the brain that was not studied here. (**C**) Innocuous mechanical inputs activate Aß/Aδ myelinated afferents (red) that project into deeper laminae of the dorsal horn and synapse onto interneurons marked by the expression of cholecystokinin (CCK) (purple) and protein kinase C γ (PKCγ) (yellow). Normally, feedforward inhibition prevents the activation of these interneurons and as a result light touch is

perceived as non-painful. However, in the context of neuropathic pain, feedforward inhibition onto PKCγ interneurons is lost and innocuous light touch inputs activate a theorized dorsally-directed microcircuit to allow innocuous light touch sensory information to be perceived as painful. In this theorized circuit, activated PKCγ interneurons excite transient central cells (speculated as Y1-INs), that in turn synapse onto vertical cells, which then activate ascending projection neurons (PNs) that travel via the spinothalamic and spinoparabrachial tracts to be processed via higher order pain centers such as the lateral parabrachial nucleus. Inhibitory NPY interneurons (light grey) may "gate" some of these nociceptive inputs at the Y1-IN and normally prevent these neurons from being activated and driving pain-like behaviors. Exogenous NPY or Y1 agonist binding to the Gi-coupled NPY Y1 receptor results in inhibition of Y1-INs and thus the abolishment of peripheral nerve injury-induced mechanical allodynia.

6.3 Cell type-specific interrogation of *in vivo* Y1-INs finds a key role in the manifestation of pain

One of the most influential circuit models in the substantia gelatinosa (lamina II) of the DH is the "Gate Control Theory of Pain" posited by Melzack and Wall in 1965 (Melzack and Wall, 1965). In this model, innocuous mechanosensory inputs to the spinal cord are unable to activate a pain transmission neuron (T cell) due to activation of a feedforward inhibitory neuron (a "gate"). However, reduced inhibition allows innocuous inputs to activate the T cell during chronic pain states. With modern genetic technologies, researchers can now permanently or transiently activate/inhibit/ablate spinal excitatory interneuron populations *in vivo* to test predications about the identity of the pain-transmitting T cells (Duan et al., 2018). To this end, we found that cell type-specific activation of excitatory Y1-INs elicited spontaneous nocifensive behaviors, mechanical and thermal hypersensitivities, and conditioned place aversion. Conversely,

chemogenetic inhibition of Y1-INs reduced pain-like behavior. These data indicate that Y1-INs function much like a pain-transmitting T cell as envisioned by Melzack and Wall.

Previously it was conjectured that DH SST-INs represent the T cell in the gate control theory of pain as their ablation prevented the induction of both neuropathic and inflammatory allodynia (Duan et al., 2014). Subsequently, it was shown that chemogenetic or optogenetic activation of SST-INs induced spontaneous nocifensive behaviors, mechanical and thermal hypersensitivities, and conditioned place aversion (Christensen et al., 2016). These functional results are markedly similar to our Y1-IN chemogenetic and optogenetic activation data, likely due to the extensive overlap of Y1-INs with SST-INs (Chamessian et al., 2018; Nelson et al., 2019; Nelson and Taylor, 2021). These results are also consistent with NPY-saporin lesion studies which find a primary role for Y1-INs in the development and maintenance of both neuropathic and inflammatory pain (Lemons and Wiley, 2012; Nelson et al., 2019). Thus, Y1-INs are likely a subset of the SST population that is sufficient for nocifensive behaviors and fundamental to the manifestation of peripheral nerve injury-induced mechanical pain.

High-throughput, unbiased, transcriptomic analyses have revolutionized the characterization of interneuron populations in the dorsal horn (Häring et al., 2018; Russ et al., 2021). For example, Häring *et al* used unbiased single-cell RNA-sequencing of dorsal horn and found *Npy1r* to be selectively enriched in excitatory neurons, namely the glutamatergic clusters Glut2, Glut8, and Glut9 (**Fig 36A**) (Häring et al., 2018). Similarly, we find that spinal Y1-INs segregate into three predominate glutamatergic neural subpopulations demarcated by the co-expression of *Npy1r* with the genes *Cck*, *Npff*, or *Grp*. Further, we demonstrate that Y1-INs that

co-express *Npy1r* and *Grp* are fundamental for the manifestation of the behavioral signs of neuropathic pain. These neurons likely correspond to the Glut8 cluster from Häring et al.'s single-cell RNA sequencing database. Thus, future studies should further analyze the Glut8 cluster (*Reln*$^{+}$, *Nmur2*$^{+}$, *Npff*$^{+}$ neurons (**Figure 36B**)) in neuropathic pain which likely is the *Sst*/*Grp*/*Npy1r* population necessary for the manifestation of neuropathic pain. For instance, the synthesis of an *Nmur2*^{Cre} mouse or perhaps an intersectional approach that develops and utilizes a *Npy1r*^{Flp} mouse crossed with a *Grp*^{Cre} mouse will allow future investigators to perform more advanced analyses in the Glut8 subpopulation to better define its' role in neuropathic pain.

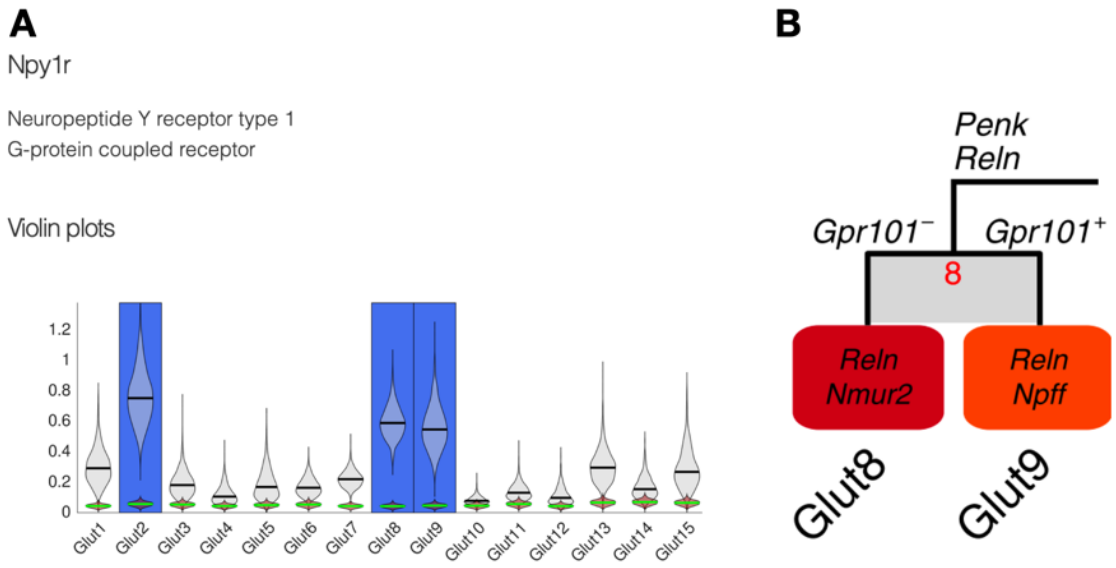

Figure 36. Häring et al. detected *Npy1r* in the Glut2, Glut8, and Glut9 subpopulations.

(**A**) Single-cell RNA sequencing detected Npy1r in three dorsal horn glutamatergic subpopulations: Glut2, Glut8, and Glut9. (**B**) The Glut8 cluster is *Reln*$^{+}$, *Nmur2*$^{+}$, *Npff*$^{+}$ neurons.

One limitation of our work is that it does not address the identity of the inhibitory neuron that "gates" Y1-INs. However, we propose that Y1-INs are normally under strong inhibition from NPY-expressing inhibitory interneurons. Indeed, Y1-INs receive direct and functional synaptic

contacts from inhibitory NPY-expressing interneurons (Acton et al., 2019). We believe that pharmacological lesioning (**Figure 12**) or chemogenetic inhibition of Y1-INs does not alter baseline responsiveness to mechanical or cold stimuli for this reason (**Figure 18**) because inhibition of an already silenced interneuron population has no net effect. However, following peripheral injury, Y1-INs lose their inhibition, become hyperexcitable, and drive pain; consequently, their chemogenetic inhibition potently reduces pain-like behavior. Further support of the idea for NPY-expressing neurons as the gate comes from recent work chemogenetically activating inhibitory NPY-expressing neurons and potently reducing both neuropathic behavioral and spinal molecular signs of hyperalgesia (Tashima et al., 2021). We propose that the chemogenetic activation of NPY-inhibitory interneurons results in indirect Y1-IN inhibition (gating) to prevent allodynia. In summary, our study indicates that *Npy1r*-expressing neurons in the DH are the T cells in the model put forward by Melzack and Wall (Melzack and Wall, 1965) (**Figure 35B**).

6.4 Proposed model of Y1-INs within an ascending dorsal horn microcircuit that develops after nerve injury

Our understanding of the chronic pain circuits underlying mechanical allodynia are limited and as a result therapeutic intervention remains ineffective. Because of this gap in knowledge and the large unmet therapeutic demand, numerous investigators are actively working to unravel the neural populations and circuits that underlie mechanical allodynia (Alba-Delgado et al., 2018, 2015; Artola et al., 2020; Duan et al., 2014; Liu et al., 2018; Lu et al., 2013; Miracourt et al., 2007; Moehring et al., 2018; Nelson et al., 2019; Peirs et al., 2021, 2020, 2015; Peirs and Seal, 2016; Petitjean et al., 2015; Schoffnegger et al., 2008; Tashima et al., 2021; Watanabe et al., 2017). Our

work implicates Y1-INs as a key neuron population in the manifestation of peripheral nerve injury-induced mechanical allodynia. Currently, mechanical allodynia is hypothesized to occur via a polysynaptic DH microcircuit that allows A-fibers to transmit innocuous mechanical input as painful (Lu et al., 2013) (**Figure 2**). Within this model, CCK and PKCγ interneurons have been readily identified/labeled as key neuron populations (Lu et al., 2013; Peirs et al., 2021). However, as this model was first discovered with random patch-clamp recordings in unlabeled DH cells, excitatory transient central cells (neurons in lamina II outer with a central morphology that discharge action potentials transiently during a depolarizing step (Grudt and Perl, 2002)) remain unclassified by neurochemical gene / protein expression. We find that Y1-INs mainly exhibit a central morphology and exhibit a DSLF firing type that closely mirrors the transient firing type (**Figure 21**) (Grudt and Perl, 2002; Sinha et al., 2021). Further, Y1-INs densely overlap with the *Grp*-expressing population of spinal cord interneurons (Nelson and Taylor, 2021; Sathyamurthy et al., 2018) which to date is the only identified class of transient central cells (Dickie et al., 2019). Lastly, we show that *Grp*/*Npy1r*-expressing dorsal horn interneurons are necessary for the manifestation of neuropathic pain. These data suggest that Y1-INs may be the transient central cell population in the peripheral nerve injury-induced mechanical allodynia model (**Figure 35C**). Future research endeavors can focus on the specific anatomical connectivity of Y1-INs in the complicated dorsal horn allodynia circuitry. We predict that many Y1-INs will be downstream of PKCγ interneurons and upstream of both GRPR-INs (vertical cells; (Polgár et al., 2022)) and spinal pain projection neurons to supraspinal regions implicated in pain processing. It is for this reason that activation/inhibition of Y1-INs is sufficient/necessary for the manifestation of the behavioral signs of neuropathic pain.

6.5 Technical considerations in this dissertation

6.5.1 Acetone evaporation as a method to assess "cold allodynia?"

In this dissertation, I used the SNI model of peripheral nerve injury because it is a highly reproducible injury that produces long-lasting chronic neuropathic pain-like behavior including mechanical and cold hypersensitivity (Decosterd and Woolf, 2000). Specifically, this model produces hyperexcitability in the sural innervation territory; the sural nerve innervates the lateral aspect of the rodent hindpaw (Kambiz et al., 2014). For this reason, I applied von Frey filaments and acetone to the lateral surface of the hindpaw to assess behavioral hypersensitivity. In von Frey testing I apply the filament to the lateral surface of the paw (the outer side). I administer acetone using a syringe connected to PE-90 tubing, flared at the tip to a diameter of 3 1/2 mm. I then apply a drop of acetone to the lateral side of the hind plantar paw (surface tension maintains the volume of the drop to ~10 μL) which quickly spreads over the skin covering the lateral surface (some spread may occur beyond the lateral surface but it is largely restricted due to the small volume). While von Frey filaments are a well-established method for assessing punctate static mechanical allodynia, the use of acetone is semi-controversial. The reason acetone is semi-controversial is that the rapid evaporation of acetone may not be producing a behavioral response due to cooling, but rather via activating mechanoreceptors. Thus, acetone may merely be another indicator of SNI-induced mechanical allodynia. While I agree that primary afferents exist that do respond to both acetone and mechanical stimulation (MacDonald et al., 2021), I also believe there is convincing evidence to indicate that acetone produces an innocuous cooling behavioral response. First, acetone produces a behavioral phenotype different to that of application of cold water (Vissers and Meert, 2005). Second, the interpretation that acetone exclusively activates mechanoreceptors (via rapid evaporation) is contradicted by the fact that acetone-evoked responses are almost completely

abolished in TRPM8 knockout mice (Colburn et al., 2007) or via pharmacological blockade of TRPM8 channels with capsazepine (Xing et al., 2007). Additionally, application of acetone to the paw produces both surface and subsurface skin cooling (Leith et al., 2010). With this evidence, particularly the TRPM8 specific data, I believe that the acetone data can be interpreted as cold allodynia.

6.5.2 Cell-type specific modulation of Y1-INs- was it necessary?

In this dissertation, I used multiple complex and time-consuming experimental techniques to address the hypothesis that Y1-INs are necessary and sufficient for the behavioral signs of mechanical and cold allodynia. However, the initial pharmacology data I collected indicated that intrathecal administration of a NPY Y1 receptor-selective agonist was exclusively acting at dorsal horn neurons to reduce SNI-induced allodynia. Thus, was it necessary to exert significant time, energy, and resources to extend this pharmacology work into the cell-type specific modulation of Y1-INs? I absolutely believe that it was, and I will defend this position.

First, chemogenetic inhibition provided several advances to my work that could not be achieved via intrathecal pharmacology. Yes, both approaches function via canonical G_i protein signaling following Y1 agonist or CNO binding to the Y1 or hM4Di receptor: 1. The G_i α-subunit inhibits adenylyl cyclase and decreases cAMP levels and protein kinase A (PKA) activity, and 2. The βγ subunit opens G protein-coupled inwardly rectifying potassium channels (GIRKs) to allow outward movement of potassium ions to hyperpolarize the cell. However, AAV transfection and amplification of viral DNA produces significantly more DREADD receptors on a cell than physiologically relevant Y1 receptors. Thus, CNO inhibition is

significantly more efficacious than pharmacological inhibition and the two methods address separate points: NPY-Y1 signaling vs efficacious Y1-IN inhibition. Intrathecal pharmacology may not hyperpolarize all cells and rather dampen intracellular signaling dependent on the membrane trafficking/internalization and desensitization of the NPY Y1 receptors, whereas CNO will always hyperpolarize the transfected Y1-INs. However, intrathecal pharmacology allows me to target more Y1-INs than intraspinal chemogenetics as I am limited by viral spread/tropism, whereas intrathecal pharmacological agents diffuse widely throughout the spinal cerebrospinal fluid. With these thoughts in mind, inhibitory chemogenetics provided several important advances to my thesis/our understanding of Y1-INs: 1. I was able to use a complementary approach to indicate that chemogenetic inhibition of specifically the spinal dorsal horn Y1-INs completely abolished SNI-induced allodynia to further confirm my hypothesis that Y1-INs are necessary for neuropathic pain-like behavior (importantly, this avoided possible confounds of off target binding via the Y1 agonist on other receptors and/or nervous system regions following intrathecal administration of the agonist into the spinal CSF in my previous pharmacology studies), 2. I was able to efficaciously hyperpolarize a subset of lumbar Y1-INs in naïve (non-injured) conditions (First, this was a significant improvement on previous NPY-saporin lesion studies that may produce circuit rearrangements and second, I could inhibit many Y1-INs in a non-injured setting as the lack of injury may limit the effectiveness of Y1 agonists at this time point because we hypothesize Y1 receptor signaling is minimal in a non-injured setting and upregulated after injury), 3. I was able to perform affective conditioned place preference testing as i.p. injection of CNO was significantly less invasive to repeatedly perform than intrathecal Y1 agonist administration (CPP testing with spinal Y1 inhibition had never been performed before this). However, I did not feel that optogenetic inhibition of Y1-INs was necessary after the

chemogenetic inhibition studies. Both the intrathecal pharmacology and inhibitory chemogenetics addressed my questions about the necessity of Y1-INs and further optogenetic inhibition studies would not have provided additional/valuable information.

I believe that cell-type specific activation of Y1-INs was absolutely worth my time and effort as this was completely novel and uncharted territory. When I first began my chemogenetic activation studies no one had ever activated a Y1-IN largely due to two reasons: 1. A *Npy1r*^{Cre} mouse was only just developed before I began this work, and 2. An inverse agonist for the NPY Y1 receptor does not exist (this is because Y1 receptors are not believed to be constitutively active). Thus, this was a very exciting study that only provided new information. In this work, I learned that activation of Y1-INs was sufficient to produce robust spontaneous and polymodal pain-like behaviors. In addition to chemogenetic activation of Y1-INs, I also performed optogenetic activation of the spinal Y1-IN population. First, this allowed me to demonstrate similar results with two complementary methods (much like intrathecal pharmacology and inhibitory chemogenetic studies before), and second, this allowed me to perform temporal and frequency-specific activation of the cellular population. Together, I think these studies demonstrated that Y1-INs are sufficient for the behavioral signs of neuropathic pain-like behavior. Additionally, using the information I have revealed through this work, future studies can extend this to evaluate the upstream/downstream neurons from Y1-INs and further unravel the spinal circuits underlying allodynia.

6.6 Possible translation of intrathecal administration of NPY for the treatment of chronic pain in humans

Our studies, alongside a rich history of spinal NPY in pre-clinical models of chronic pain, indicate a strong basic science rationale for the development of spinally-directed Y1-selective agonists for the treatment of chronic pain. However, would they be safe in a therapeutic setting? On the one hand, intrathecal administration of antihyperalgesic doses of NPY or Y1-selective agonists disrupts neither motor locomotion nor major touch sensitivity in non-injured rodents (Chen et al., 2019; Kuphal et al., 2008; Malet et al., 2017; Solway et al., 2011; Taiwo and Taylor, 2002). On the other hand, NPY contributes to cardiovascular regulation (Tan et al., 2018), and surface application of NPY to the spinal cord changes blood flow (Chen et al., 1990, 1988). Similarly, intrathecal NPY induces vasoconstriction that results in a transient decrease in blood flow to the spinal cord and increases in mean arterial pressure and heart rate (Mahinda and Taylor, 2004; Xu et al., 1999). Thus, this is a critical physiological feature to better understand as blood pressure and pain are intricately and inversely related. Specifically, increases in blood pressure correlate with reduced acute pain-like behaviors and conversely, decreases in blood pressure relate to increased pain-like behavior (Saccò et al., 2013). Thus, it is important to rule out cardiovascular modulation as a direct effector of pain-like behavior from i.t. NPY. However, the NPY-induced increase in blood pressure was transient and was prevented via the use of a Y1 agonist (rather than NPY) (Chen and Westfall, 1993) or pre-administration of a selective Y2 antagonist before NPY administration (Mahinda and Taylor, 2004). Thus, it seems Y2 but not Y1 agonism promotes the cardiovascular side effects. If Y2 is indeed the primary mediator of cardiovascular side effects following intrathecal NPY, then the potential risks for adverse cardiovascular effects may be avoided with the use of analgesic doses of intrathecal Y1-selective agonists. Additionally, I believe

my chemogenetic inhibition results demonstrate that it is the specific inhibition of Y1-INs in the DH that reduces pain-like behavior and not changes to blood pressure.

Target specificity will be key in the development of a spinally-directed Y1-selective analgesic for chronic pain. In contrast to the clear antihyperalgesic actions of NPY when targeted to the spinal cord (**Table 1**) or multiple brain areas (Alhadeff et al., 2018; Mellado et al., 1996), other studies indicate that Y1 receptor activation in the nucleus gracilus (Fukuoka and Noguchi, 2015; Ossipov et al., 2002) and Y2 receptor activation in the DRG (Sapunar et al., 2011; Tracey et al., 1995) produce hyperalgesia. These pronociceptive actions of NPY in the DRG and nucleus gracilis can be avoided with targeted administration of Y1 agonists to the spinal cord with the implantation of chronic intrathecal catheters, a method commonly engaged for the management of chronic pain (Knight et al., 2007).

A limitation of this work is that it was performed exclusively in rodent models of pain. We have begun to address the translational divide between mouse and human by performing rigorous *in situ* characterization of Y1-IN subpopulations in the rhesus macaque and human spinal cord dorsal horns. This important work suggests that NPY Y1 receptor expression is heavily conserved across species and may be a promising therapeutic target (**Figure 31**). Nevertheless, the next important steps will involve translation of this pre-clinical pharmacology work to increasingly more translatable animal models (i.e. porcine (Hellman et al., 2021b, 2021a) and macaque (Hama et al., 2021)). In these translational animal models, we can perform extensive pain behavioral testing as well as multiple side effect profiling analyses. Specifically, it will be fundamental to assess Y1 agonist contra-indicative activity on feeding behavior/weight gain (Mullins et al., 2001),

hyperinsulinemia (Gao et al., 2004), gut inflammation (Holzer et al., 2012), gastric motility (Chen et al., 1997), cardiovascular regulation (McDermott and Bell, 2007), and sedation (Naveilhan et al., 2001a). However, against this backdrop, intranasal NPY has been recently used in human clinical trials for the treatment of post-traumatic stress disorder and major depression (Mathé et al., 2020; Sayed et al., 2018). These exciting intranasal studies have found NPY to be safe, extremely well tolerated, and efficacious (Mathé et al., 2020; Sayed et al., 2018). Thus, Specifically, our next steps will be the intrathecal administration of a NPY-Y1 agonist in a porcine model of peripheral nerve injury (Hellman et al., 2021b, 2021a). We will assess the effect of intrathecal Y1 agonists on pain-like behavior as well as cardiovascular regulation. We hypothesize that Y1 agonist administration (and by avoiding Y2) will not alter blood pressure/heart rate and will potently inhibit pain-like behavior. We are optimistic that these translational NPY pain studies will begin in the near future and that Y1 agonism will safely and potently reduce the behavioral signs of neuropathic pain in larger mammalian species, and ultimately, human chronic pain patients.

Appendix A Dorsal Horn PKCγ Interneurons Mediate Mechanical Allodynia through 5-HT_{2A}R-dependent Structural Reorganization

Nociceptors function to protect tissue from potential damage by thermal, mechanical, and chemical stimuli. The central terminals of primary nociceptive mechanical and thermal afferents (C/Aδ fibers) converge in superficial laminae I and II in the dorsal horn of the spinal cord. Nociceptive information is processed by excitatory and inhibitory interneurons in the dorsal horn of the spinal cord before being relayed to projection neurons in lamina I that transmit the information to higher brain centers that mediate the experience of pain (Koch et al., 2018) (**Figure 34**).

Light touch does not normally evoke pain, but after nerve injury, innocuous light touch can evoke a pain-like response called allodynia. Information about light touch is carried by low-threshold mechanical primary afferents (Aβ fibers) that synapse in laminae II-IV in the dorsal horn (**Figure 36)**. In inner lamina II, Aβ fibers synapse directly onto excitatory interneurons that express the γ isoform of protein kinase C (PKCγ) (Lu et al., 2013, Neumann et al., 2008). Although PKCγ interneurons do not receive direct input from mechanical nociceptors, they are strongly implicated in mediating mechanical allodynia (Lu et al., 2013, Petitjean et al., 2015). Allodynia is thought to stem from the loss of strong feedforward inhibition by inhibitory interneurons that prevent innocuous input from being transmitted as painful (**Figure 36**). After nerve injury, these inhibitory synapses onto PKCγ interneurons are lost, and normally innocuous mechanical input from deep ventral laminae is transmitted to superficial lamina I to evoke pain (Lu et al., 2013, Miraucourt et al., 2007, Petitjean et al., 2015). Thus, the merging of the innocuous and noxious pathways promotes mechanical allodynia. Spinal nociceptive transmission is also modulated via descending

supraspinal projections which are responsible for the top-down processing of pain. Many of these descending projections contain the neuromodulator serotonin which may play a role in mechanical allodynia as epidural $5HT_{2A}R$ antagonists dose-dependently attenuate mechanical allodynia after nerve injury (Van Steenwinckel et al., 2008).

Mechanical allodynia is a hallmark of inflammatory, as well as neuropathic pain, but the underlying circuitry remains incompletely understood. In particular, whether inflammatory pain also involves disinhibition of PKCγ interneurons and $5HT_{2A}Rs$ has not been clearly shown. Nonetheless, intrathecal administration of a PKCγ inhibitor attenuates capsaicin-induced inflammatory mechanical allodynia in mice, suggesting PKCγ interneurons contribute to inflammatory allodynia (Petitjean et al., 2015). Because both PKCγ (Neumann et al., 2008) and $5HT_{2A}Rs$ (Fay and Kubin, 2000) are found predominately in excitatory interneurons of inner lamina II of the dorsal horn, Alba-Delgado et al. (2018) hypothesized that PKCγ and $5HT_{2A}Rs$ interact in PKCγ interneurons to facilitate inflammation-induced mechanical allodynia.

To test this hypothesis, the authors first tested the effects of $5HT_{2A}R$ agonists and antagonists on mechanical withdrawal thresholds in rats treated with Complete Freund's Adjuvant (CFA) to induce inflammation. Pharmacological blockade of $5HT_{2A}Rs$ prevented CFA-induced mechanical facial allodynia in rats, and activation of $5HT_{2A}Rs$ was sufficient to induce facial mechanical allodynia in naïve rats. In addition, the authors showed that PKCγ interneurons co-express $5HT_{2A}Rs$ and that activation of $5HT_{2A}Rs$ increased levels of phosphorylated extracellular signal-regulated kinases 1/2 (pERK1/2), a marker of neuronal activation, in PKCγ-expressing

neurons. These results suggest that activation of dorsal horn $5HT_{2A}$Rs on PKCγ interneurons leads to mechanical facial allodynia.

Alba Delgado et al. (2018) also probed the electrophysiological and morphological effects of CFA-induced inflammation and $5HT_{2A}$R blockade on lamina II interneurons. Intrinsic electrophysiological properties (resting membrane potential and slope in current-voltage plots) of lamina II excitatory interneurons differed between CFA-treated and sham animals, but these changes occurred independently of 5-HT_{2A}R activation. In contrast morphological changes (reduction in the number of tertiary branches of the dendritic arbor, increase in spine density) induced by CFA occurred selectively in lamina II PKCγ-expressing interneurons, and these changes were partially prevented by blocking 5-HT_{2A}Rs. Finally, specific activation of 5-HT_{2A}Rs in naïve rats replicated CFA-induced morphological changes in PKCγ interneurons. Taken together, these results indicate that activation of 5-HT_{2A}Rs on medullary dorsal horn PKCγ interneurons induces rapid morphological remodeling of the dendritic arbor, which may lead to the development of facial mechanical allodynia.

The 5-HT_{2A}R-dependent morphological reorganization of PKCγ interneuron dendrites is a key finding that expands our understanding of the circuit underlying mechanical allodynia (**Figure 36**). PKCγ interneurons lose inhibitory connections after neuropathic injury (Lu et al., 2013, Petitjean et al., 2015), and this loss might result from apoptosis of inhibitory interneurons or simply a loss of inhibitory contacts onto the PKCγ soma (Iquimbert et al., 2018, Petitjean et al., 2015). The results of Alba-Delgado et al. (2018) suggest that 5-HT_{2A}R-mediated morphological reorganization reduces the dendritic arbor of PKCγ interneurons during inflammation. This

reduced dendritic arbor might lead to decreases in the number of inhibitory synapses onto these neurons, causing a loss of the feedforward inhibition that normally prevents innocuous touch stimuli from exciting PKCγ interneurons. PKCγ interneurons would then be able to excite yet unknown postsynaptic neurons, allowing innocuous stimuli to reach pain projection neurons in the superficial lamina I of the dorsal horn (**see Figure 36**).

Alba-Delgado et al. (2018) raise an important question: what are the postsynaptic targets of the PKCγ interneurons that transmit innocuous mechanical input to superficial pain projection neurons? PKCγ interneurons synapse directly onto excitatory transient central cells in lamina II, and these synapse onto vertical cells, which then target lamina I pain projection neurons (Lu and Perl, 2005, Todd, 2017). The identity of transient central cells remains unknown, and researchers are trying to uncover these neural populations (Piers and Seal, 2016). The most likely candidate is a subset of somatostatin-expressing excitatory interneurons in outer lamina II, as these neurons are necessary for mechanical pain (Duan et al., 2014) (**Figure 36)**. Calretinin interneurons are another probable candidate, as they are implicated in the development of mechanical allodynia (Piers et al., 2015) (**Figure 36**). The excitatory interneurons expressing neuropeptide Y1 receptors (Y1R), which are involved in both mechanical and thermal allodynia that arises after inflammatory and neuropathic injury, may also be a target of PKCγ interneurons as Y1Rs do not colocalize with PKCγ and are found superficial to PKCγ interneurons (Diaz-delCastillo et al., 2017, Nelson et al., 2019) (**Figure 36**).

While Alba-Delgado et al. (2018) focus on PKCγ interneurons in mechanical allodynia, this is only a piece of the circuit. In deeper lamina III, interneurons that transiently express

vesicular glutamate transporter 3 (VGLUT3) are upstream of PKCγ interneurons and also receive information about innocuous touch from Aβ fibers (Peirs and Seal, 2016) (**Figure 36**). Most importantly, VGLUT3 interneurons in the spinal dorsal horn are both necessary and sufficient for mechanical allodynia (Peirs et al., 2015). Perhaps 5-HT_{2A}R activation in PKCγ interneurons and the subsequent reorganization of the dendritic arbor permits them to be excited by VGLUT3 interneurons to induce mechanical allodynia.

The final questions Alba-Delgado et al. (2018) raise concerning the inflammation-induced mechanical allodynia circuitry pertain to the origin and cause of 5-HT release into the dorsal horn to act on PKCγ interneurons. Existing anatomical evidence indicates that 5-HT in the dorsal horn originates almost entirely from descending projections from the rostral ventral-medial medulla (RVM) and is not released from local dorsal horn interneurons (Bannister and Dickenson, 2016). Inflammation may drive ascending pain signals from projection neurons that monosynaptically activate neurons in the RVM. The RVM's descending nociceptive projections, which likely include 5-HT fibers, release 5-HT to act on 5-HT_{2A}R-expressing PKCγ interneurons and drive morphological reorganization and subsequent mechanical allodynia. Another possible circuit involves ascending pain projection neurons that activate neurons in the periaqueductal gray, which in turn can activate RVM descending nociceptive 5-HT fibers to the dorsal horn (Ossipov et al., 2014). In summary, the mechanical allodynia circuit includes not only projections from local dorsal horn excitatory and inhibitory interneurons but also descending 5-HT fibers from the RVM (**Figure 36**).

Alba-Delgado et al. (2018) implicate descending 5-HT projections as mediators of morphological rearrangement in PKCγ interneurons that are both necessary and sufficient for inflammation-induced facial mechanical allodynia. This work is an important addition to the mechanical allodynia circuit summarized in **Figure 36**. In future studies it will be important to uncover the cause of 5-HT release into the dorsal horn and the post-synaptic targets of the PKCγ^{+} interneurons that lead to the development of mechanical allodynia.

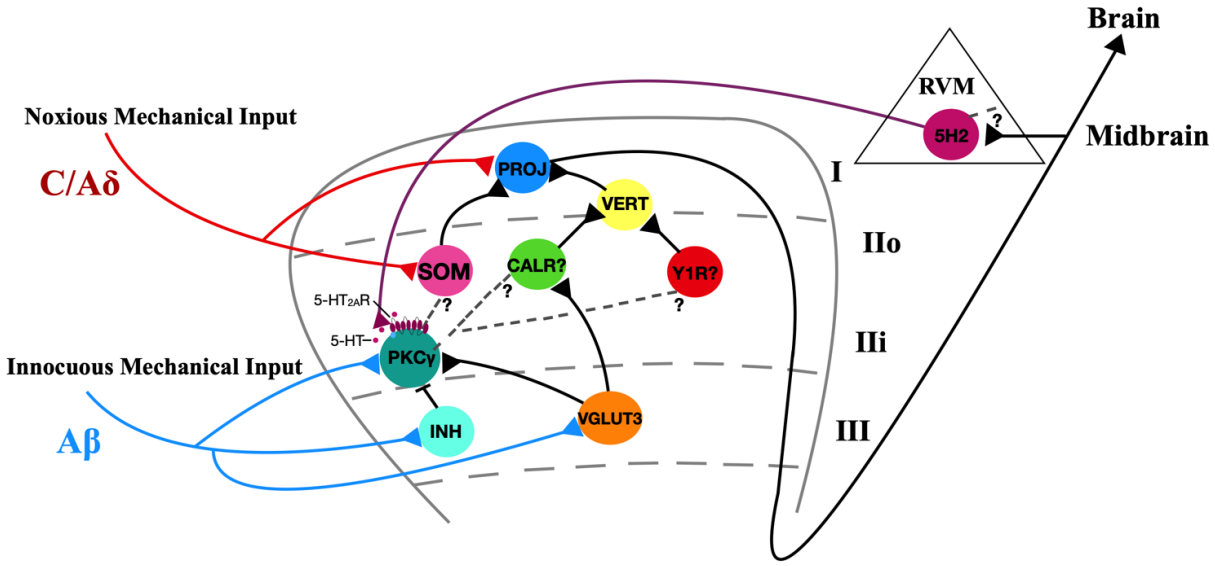

Figure 37. A dorsal horn model for circuits mediating mechanical allodynia.

5-HT, serotonergic descending projections; PROJ, lamina I pain projection neurons; VERT, vertical cells; SOM, somatostatin; CALR, calretinin; Y1R, neuropeptide Y1-receptor expressing; PKCγ, protein kinase C γ; INH, inhibitory interneurons; VGLUT3, vesicular glutamate transporter 3; RVM, rostral ventral-medial medulla.

Appendix B PKA and Epac activation are sufficient to reveal phosphorylated extracellular signal regulated kinase (pERK) induction of central sensitization

Appendix B.1 Introduction

It has been reported that pERK activation in dorsal horn neurons is specifically induced by noxious stimulation and is necessary for the induction of central sensitization (Gao and Ji, 2009). Our previous behavioral results indicate that both PKA and Epac activation are sufficient to reinstate complete Freund's adjuvant (CFA)-induced hyperalgesia following the resolution of pain-like behavior (Fu et al., 2019). To directly implicate both PKA and Epac in the mediation of endogenous latent sensitization, we hypothesized that administration of either a PKA or Epac activator would increase the expression of pERK in the ipsilateral dorsal horn following the resolution of CFA-induced hyperalgesia, directly implicating reinstatement of central sensitization.

Appendix B.2 Methods

Animals

Male C57Bl/6NCrl (Charles River, #027) mice were housed 2 to 4 per cage, with littermates, in a light- (12-hour light/dark cycle), temperature- (68-72˚F), and humidity-controlled room with food and water provided *ad libitum*. Animals were allowed a minimum of 1 week to habituate to the facility before their entrance into the study. All procedures were approved by the Institutional Animal Care and Use Committee of the University of Pittsburgh, followed the

guidelines for the treatment of animals of the International Association for the Study of Pain, and were conducted in full compliance with the Association for Assessment and Accreditation of Laboratory Animal Care.

Complete Freund's adjuvant model of inflammatory pain

Mice were injected subcutaneously with 10 μL complete Freund's adjuvant (CFA) (1 mg/mL; Sigma-Aldrich, St. Louis, MO) into the midplantar region of the left hindpaw with a 30-G needle. Sham treatment involved restraint, with the left hindpaw extended for 1 minute.

Mechanical threshold testing

Animals were acclimated to a stainless-steel grid within individual Plexiglas tubes for at least 60 minutes before behavioral testing. To evaluate sensitivity to a non-noxious mechanical stimulus, we used an incremental series of 8 von Frey filaments (Stoelting, Inc, Wood Dale, IL) of logarithmic stiffness (0.008-6 g). The 50% withdrawal threshold was determined using the up–down method(Chaplan et al., 1994). Each filament was applied perpendicular to the central plantar surface of the hindpaw skin with sufficient force to cause a slight bending of the filament. A positive response was defined as a rapid withdrawal of the paw within a count of 5 seconds.

Intrathecal drug administration

Intrathecal injection was performed in lightly restrained unanesthetized mice. Briefly, a 30G needle attached to a Hamilton microsyringe was inserted between the L5/L6 vertebrae, puncturing the dura (confirmed by presence of reflexive tail flick). We then injected a 5 μL volume of vehicle or drug.

Drug dosing

The following drugs and doses were used for intrathecal injections: N6-benzoyladenosine-39,59-cyclic monophosphate (6- Bnz-cAMP), sodium salt membrane–permeant (6Bnz; BIOLOG Life Science Institute, Bremen, Germany), 10 nmol/5 mL; 8-(4-chlorophenylthio)-29-O-methyladenosine 39,59-cyclic monophosphate sodium salt (8cpt; Enzo Life Sciences, Exeter, United Kingdom), 3 nmol/5 mL; Vehicle was saline.

pERK Behavior and Immunohistochemistry

Separate cohorts of mice were tested for baseline mechanical sensitivity and exposed to CFA or sham treatment. Mechanical thresholds were reassessed 3 days and/or 21 days later, followed by intrathecal injection of 6Bnz (10 nmol), 8cpt (3 nmol), or vehicle (saline) (5 μL). To determine the effect of vehicle or drug on pERK activation in the ipsilateral dorsal horn, a light-touch stimulation protocol was initiated 30 minutes after the end of behavioral testing. Mice were anesthetized with isoflurane (5% induction, 2% maintenance) and the plantar surface of the left hindpaw was gently stroked in the longitudinal plane with a cotton tip for 3 seconds of every 5 seconds, for 5 minutes. After an additional 5-minute wait time, mice received an intraperitoneal injection of sodium pentobarbital (.100 mg/kg, 0.2 mL, Fatal Plus) and were transcardially perfused with ice-cold 13 phosphate-buffered saline (PBS) with heparin (10,000 USP units/L) followed by ice-cold fixative (10% phosphate-buffered formalin). The lumbar spinal cord was removed and postfixed overnight in 10% phosphate-buffered formalin and then cryo- protected in 30% sucrose in 0.1-M PBS for several days. Transverse sections (30 mm) centered at L4 were cut on a freezing microtome or cryostat and collected in antifreeze. The sections were washed 3 times

in PBS and then pretreated with blocking solution (3% normal goat serum and 0.3% Triton X-100 in PBS) for 1 hour. Sections were then incubated in blocking solution containing the primary antibody rabbit anti-pERK (1:1000, Phospho-p44/42 MAPK, Cell Signaling Technology #4370, RRID:AB_2315112) overnight at room temperature on a slow rocker. The sections were washed 3 times in PBS and incubated in goat anti-rabbit secondary antibody (1:1000, Alexa Fluor 488, Invitrogen A11008, RRID:AB_143165) for 60 minutes, washed in PBS then 0.01-M phosphate buffer without saline, mounted onto Superfrost Plus slides, air-dried, and cover-slipped with Hard Set Antifade Mounting Medium with DAPI (VECTASHIELD).

Imaging/Quantification of pERK

All images were captured on a Nikon Eclipse Ti2 microscope using a 103 objective (numerical aperture 0.45) and analyzed using NIS-Elements Advanced Research software v5.02. We focused our quantification of the number of pERK immunopositive cell profiles within lamina I-II, where most nociceptive peripheral afferents terminate within the dorsal horn (Corder et al., 2010), in left (ipsilateral to light touch stimulation) L4 spinal cord segments. Two observers who did not know the identity of the slides/sections (eg, blinded to treatment) manually counted punctate immunoreactive profiles in 3 to 5 high-quality randomly selected sections of L4 spinal cord from each animal. The manual counts for each L4 section were averaged between the 2 blinded quantifiers. These averaged section counts for each individual animal were then averaged for an overall animal mean of punctate immunoreactive profiles.

Statistics

Differences between mean values after intrathecal drug treatment were analyzed with a 1-way ANOVA followed by Holm–Sidak post hoc tests using GraphPad Prism v7.

Appendix B.3 Results

As indicated by the timeline in **Figure 37A**, after the resolution (21 days) of CFA-induced hyperalgesia (**Figure 37D**) we intrathecally administered Vehicle, the selective PKA activator 6Bnz (10 nmol), or the Epac activator 8cpt (3 nmol) to mice. 60 minutes after intrathecal administration (peak timepoint of drug activation) we performed light mechanical stimulation (paw brushing) followed 5-minutes later by perfusion of the animals. Subsequent quantification of pERK-immunoreactivity in the ipsilateral L4 superficial (lamina I-II) dorsal horn found that both 6Bnz and 8cpt administration produced a significant increase in pERK expression compared to animals that received intrathecal Vehicle administration 21 days after CFA-induced hyperalgesia (**Figure 37 E, G, I, J**). Importantly, intrathecal administration of 6Bnz and 8cpt increased pERK expression in 21 day CFA animals but not 21 day sham animals (**Figure 37F-J**). These results indicate that endogenous latent sensitization is mediated by both PKA and Epac, and therefore activation of either signaling mechanism is sufficient to reinstate central sensitization.

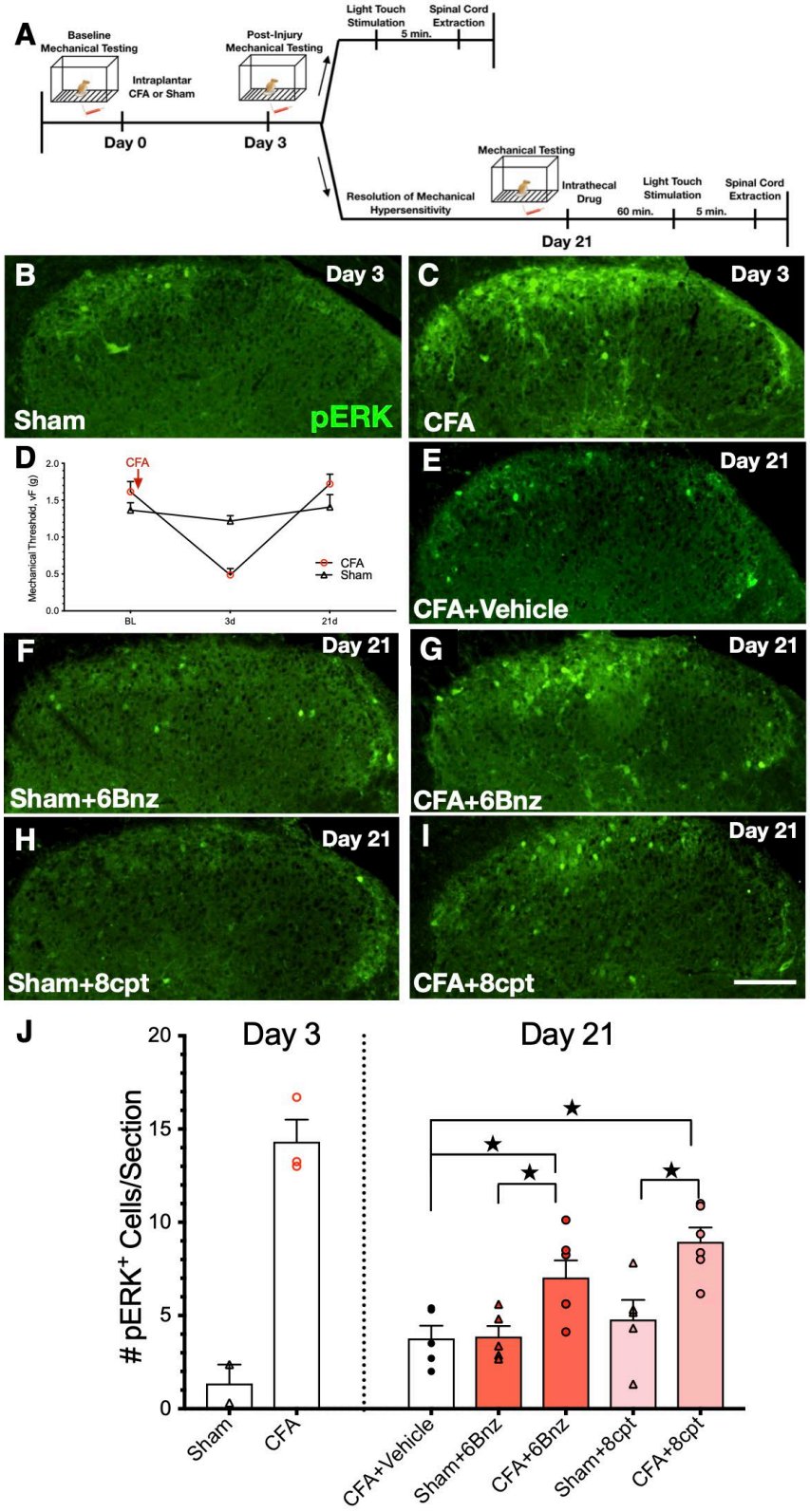

Figure 38. Expression of pERK in the ipsilateral L4 dorsal horn after PKA and Epac activation reveals latent sensitization.

(A) Timeline of experimental design for mechanical stimulation-induced pERK immunoreactivity. (**B- C)** Representative transverse sections of L4 dorsal horn on mice 3 days after CFA or sham injury following light mechanical stimulation. (**D)** CFA (n=20) but not sham injection (n=10) produced a mechanical hyperalgesia that peaked at 3 days and resolved within 21 days. Values represent mean ± SEM. (**E-I)** Representative transverse sections of L4 dorsal horn on mice 21 days after CFA or sham injury, following intrathecal administration of Vehicle, 6Bnz (10 nmol), or 8cpt (3nmol), and light mechanical stimulation. (**J)** After the induction (3 days) and resolution (21 days) of CFA-induced hyperalgesia, intrathecal administration of 6Bnz or 8cpt increased the number of pERK-immunoreactive profiles in lamina I-II as compared to intrathecal administration of vehicle, ★$P < 0.05$ (CFA-vehicle vs. CFA-6Bnz), ★$P < 0.05$ (CFA-vehicle vs. CFA-8cpt), and compared to sham controls, ★$P < 0.05$ (Sham-6Bnz vs. CFA-6Bnz), ★$P < 0.05$ (Sham-8cpt vs. CFA-8cpt). Post-intrathecal injection n=5-6. Individual symbols represent mean pERK-immunoreactivity of 3-5 L4 transverse sections/animal and bars represent group mean ± SEM. Scale bars 100 μm. CFA: Complete Freund's Adjuvant.

Appendix B.4 Discussion

The current pERK immunohistochemical results show that intrathecal injection of either a selective PKA (6Bnz) or Epac activator (8cpt) reinstated hyperalgesia and touch-evoked neuronal activation when given 21 days after CFA induction. These data indicate that inflammation induces a latent sensitization of dorsal horn neurons, such that less PKA or Epac agonist is required to induce allodynia and, ultimately, a state of vulnerability to the transition from acute to chronic pain. Possible underlying mechanisms could be (1) Sensitization of PKA and/or Epac, such that less-robust activation of PKA or Epac is sufficient to produce hyperalgesia; or (2) increased affinity of PKA or Epac for agonist. Although G-protein–coupled receptor pain inhibitory systems (MORCA and NPY-Y1R) are active 21 days after CFA induction, PKA and Epac activators are of sufficient power to override them. Our results are reminiscent of previous studies showing that direct activation of spinal NMDARs (with intrathecal NMDA) or AC (with intrathecal forskolin) produced enhanced spontaneous nocifensive behaviors when given 21 days after CFA induction (Corder et al., 2013).

In conclusion, inflammation produces latent sensitization, which includes not only sensitization of neurons in the dorsal horn, but also a concomitant strengthening of endogenous inhibition. Together, these opposing systems underlie a vulnerability to episodic pain that is manifested when inhibitory controls fail. We identified a novel molecular signaling pathway that drives latent sensitization at the spinal level, after inflammation: NMDAR→AC1→Epac1/2. We argue that this pathway is silently supersensitive during latent sensitization: silent because of tonic inhibitory control by the spinal NPY-Y1R axis.

Appendix C Exploration of spinal NPY Y2-selective agonism in a mouse model of neuropathic pain

Appendix C.1 Introduction

Neuropeptide Y (NPY) in the spinal cord dorsal horn exhibits long-lasting inhibitory control of nociceptive transmission after injury. While the anti-nociceptive actions of NPY at the Y1 receptor have been well characterized, the actions of selective agonism at its' cognate Y2 receptor remain largely unexplored, particularly in the setting of neuropathic pain. The neuropeptide Y2 receptor is a G_i-coupled receptor that is highly expressed in primary afferent but not spinal cord neurons, with the greatest distribution on thinly myelinated afferent neurons (both Aδ- and C-nociceptors) (Nelson and Taylor, 2021). The function of these Y2-expressing dorsal root ganglion neurons has been proposed to be pronociceptive (Arcourt et al., 2017; Chen et al., 2019). The aim of this study was to test if Y2-selective agonism at the spinal cord dorsal horn reduces the manifestation of peripheral nerve injury-induced mechanical and cold hypersensitivity in a mouse model of neuropathic pain.

Appendix C.2 Methods

Animals

Adult C57Bl/6NCrl (Charles River, #027) mice were group housed, provided access to food and water *ad libitum*, and maintained on a 12:12 hour light:dark cycle (lights on at 7:00am) in temperature and humidity controlled rooms. Male and female mice were used in all experiments.

No significant sex differences were observed. All procedures were approved by the Institutional Animal Care and Use Committees of the University of Pittsburgh and University of Kentucky. Additionally, all experiments followed the guidelines for the treatment of animals of the International Association for the Study of Pain.

Intrathecal Injections

Intrathecal injections of PYY_{3-36} (TOCRIS) Were performed in lightly restrained unanesthetized mice. Briefly, a 30G needle attached to a Hamilton microsyringe was inserted between the L5/L6 vertebrae at the cauda equina, puncturing the dura (confirmed by presence of reflexive tail flick). We then injected a 5µl volume of vehicle or drug. Animals were injected twice using a cross-over design with a 3-7-day separation between two injections. For example, animals receiving vehicle for the first injection received drug for the second, and animals receiving drug for the first injection received vehicle for the second. In all cases, group means of vehicle and drug did not differ on either injection day and were combined for final analysis.

Surgery

Spared Nerve Injury: SNI was performed as previously described (Nelson et al., 2019; Solway et al., 2011). Briefly, mice were anesthetized with inhaled isoflurane (5% induction and 2% maintenance) and the left hind limb was shaved with trimmers and sterilized with 70% ethanol and 2% chlorhexidine gluconate (ChloraPrep One-Step Applicators). A small incision was made in the skin of the hind left leg and the underlying muscle was spread via blunt dissection to expose the underlying branches of the sciatic nerve. The peroneal and tibial nerves were then ligated with 6-0 silk sutures and transected while carefully avoiding the sural nerve. The muscle tissue was then loosely sutured with 5-0 nylon sutures and the skin was closed with 9mm wound clips. Topical

triple antibiotic ointment (Neosporin) was applied to the wound. Wound clips were removed ~7-10 days post-surgery and behavioral experiments began 14 days after surgery.

Behavioral Testing

Mechanical Withdrawal Threshold: Testing was performed as described in (Solway et al., 2011). Mice were habituated to plexiglass chambers with opaque walls (15 × 4 × 4 cm) on a raised wire mesh platform for 30-60 minutes one day before and immediately prior to behavioral testing. Testing was performed using a calibrated set of logarithmically increasing von Frey monofilaments (Stoelting, Illinois) that range in gram force from 0.007 to 6.0 g. Beginning with a 0.4 g filament, these were applied perpendicular to the lateral hindpaw surface with sufficient force to cause a slight bending of the filament. A positive response was denoted as a rapid withdrawal of the paw within 4 seconds of application. Using the Up-Down method (Chaplan et al., 1994), a positive response was followed by a lower filament and a negative response was followed by a higher filament to calculate the 50% withdrawal threshold for each mouse.

Cold Withdrawal Duration: Immediately following von Frey testing, acetone drop withdrawal testing was performed on mice in the same plexiglass chambers on a raised wire mesh platform. Using a syringe connected to PE-90 tubing, flared at the tip to a diameter of 3 1/2 mm, we applied a drop of acetone to the lateral side of the hind plantar paw. Surface tension maintained the volume of the drop to ~10 μL. The length of time the animal lifted or shook its paw was recorded for 30 s. Three observations were averaged.

Appendix C.3 Results

Intrathecal administration of $PYY_{(3-36)}$ (0.01-3 µg/5 µl) did not alleviate SNI-induced mechanical or cold hypersensitivity at 14 days post-surgery (**Figure 38**). Higher doses of intrathecal Y2 agonist could not be tested due to a complete paralysis/anesthesia effect at 5 µg.

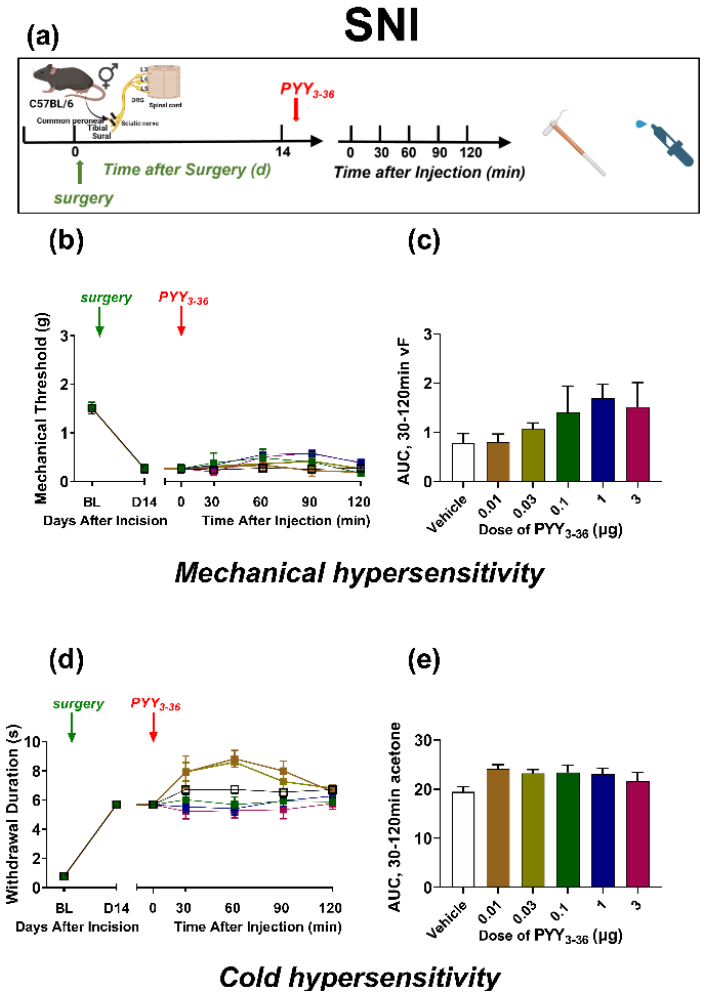

Figure 39. The neuropeptide Y2 receptor agonist PYY_{3-36} does not alleviate nerve injury-induced mechanical or cold hypersensitivity.

(**a**) Experimental timelines in C57BL/6 mice. Line graphs describing mechanical (vF) (**b**) and cold (acetone) (**d**) hypersensitivity at the hindpaw after the administration of Y2 agonist $PYY_{(3-36)}$. (**c**, **e**) Data averaged across timepoints 30-120 illustrate that $PYY_{(3-36)}$ (0.1-3µg, i.t.) did not change mechanical (c) or cold (e) hypersensitivity.. n = 6-8 per group/sex. Two way RM ANOVA. Data represented as mean ± SEM.

Appendix C.4 Discussion

Intrathecal administration of exogenous NPY or the Y1 selective agonist, [Leu^{31}, Pro^{34}]-NPY, dose-dependently reduces peripheral nerve injury-induced mechanical and cold hypersensitivity in rats (Intondi et al., 2008; Malet et al., 2017). Furthermore, intrathecal administration of the Y2 antagonist, BIIE0246, reversed the anti-allodynic actions of intrathecal NPY (Intondi et al., 2008). Thus, we hypothesized that a NPY Y2 agonist would also alleviate SNI-induced mechanical and cold hypersensitivity. Surprisingly, this did not occur. However, recently Chen et al. reported that intrathecal administration of the Y2 antagonist, BIIE0246, is sufficient to induce robust mechanical pain in uninjured mice (Chen et al., 2019). This suggests that tonic endogenous NPY release suppresses mechanical pain. Intondi *et al.* did not test the effect of Y2 antagonist in a sham animal (all SNI-afflicted rats) and thus likely missed this effect (Intondi et al., 2008). Therefore, the anti-nociceptive effects of intrathecal NPY in SNI mice were masked by the induction of mechanical pain from endogenous NPY Y2 receptor blockade, giving the false interpretation that Y2 antagonism abolishes the antinociceptive effect of NPY. Thus, these results indicate that exogenous intrathecal Y2 agonism does not alleviate the behavioral signs of neuropathic pain in stark contrast to Y1 agonism.

Appendix D Parabrachial *Npy1r*-expressing neurons modulate neuropathic pain in mice

Appendix D.1 Introduction

Pain is a complex phenomenon that elicits somatosensory and motor reflexive responses together with marked and long-lasting changes in emotional and autonomic states. Noxious stimuli activate peripheral nociceptors with axons that converge in the superficial dorsal horn of the spinal cord. Inhibitory and excitatory neurons in the spinal cord dorsal horn process the somatosensory information before transmitting it to multiple supraspinal brain regions, ultimately leading to pain perception. The axons of dorsal horn projection neurons terminate within multiple brain regions; however, a major target of projection neurons is the parabrachial nucleus (PBN) (Todd, 2010). The PBN is a small, bilateral, pontine brain structure that has long been known to receive alarming, noxious, or threatening homeostatic information such as taste aversion, nociception, or danger cues. PBN neurons then relay these aversive signals to brain regions such as the central nucleus of the amygdala (CeA), bed nucleus of the stria terminalis (BNST), periaqueductal gray (PAG), and ventromedial hypothalamus (VMH) to facilitate appropriate learning and avoidance responses. A renaissance in the PBN has produced a recent wave of high-profile publications that denote this nucleus of only a few thousand neurons as a "sensory hub for pain and aversion (Chiang et al., 2019)."

Activation of glutamatergic PBN neurons produces pain-like behaviors in naïve mice, and inhibition of glutamatergic PBN neurons reverses nerve injury-induced neuropathic pain-like behaviors (Sun et al., 2020). Additionally, preliminary data from our laboratory finds that *Npy1r*

mRNA is robustly expressed in the PBN, and pharmacological evidence indicates that NPY signaling in the PBN decreases acute inflammatory nociception (Alhadeff et al., 2018). Based on these findings, we used functional *in situ* hybridization, mouse behavioral pharmacology, and cell type-specific chemogenetics to test the hypothesis that *Npy1r* -expressing neurons of the PBN contribute to neuropathic pain.

Appendix D.2 Methods

Animals

Adult C57Bl/6NCrl (Charles River, #027) and *Npy1r*^{Cre} (B6.Cg-*Npy1r*$^{tm1.1(cre/GFP)Rpa}$/J; the Jackson Laboratory, #030544) mice were group housed, provided access to food and water *ad libitum*, and maintained on a 12:12 hour light:dark cycle (lights on at 7:00am) in temperature and humidity controlled rooms. Male and female mice were used in all experiments. No significant sex differences were observed. All procedures were approved by the Institutional Animal Care and Use Committees of the University of Pittsburgh and University of Kentucky. Additionally, all experiments followed the guidelines for the treatment of animals of the International Association for the Study of Pain.

Intra-parabrachial Injections

Intra-parabrachial injections of [Leu^{31}, Pro^{34}]-NPY (human, rat) were performed in lightly anesthetized mice. Briefly, a microinjector connected to a Hamilton microsyringe was inserted into the guide cannula and a volume of 200nL was slowly infused with a syringe driver. Animals were injected three-four times using a cross-over design with a 24-48 hour separation between

injections. In all cases, group means of vehicle and drug did not differ on either injection day and were combined for final analysis.

Surgeries

Spared Nerve Injury: SNI was performed as previously described (Nelson et al., 2019; Solway et al., 2011). Briefly, mice were anesthetized with inhaled isoflurane (5% induction and 2% maintenance) and the left hind limb was shaved with trimmers and sterilized with 70% ethanol and 2% chlorhexidine gluconate (ChloraPrep One-Step Applicators). A small incision was made in the skin of the hind left leg and the underlying muscle was spread via blunt dissection to expose the underlying branches of the sciatic nerve. The peroneal and tibial nerves were then ligated with 6-0 silk sutures and transected while carefully avoiding the sural nerve. The muscle tissue was then loosely sutured with 5-0 nylon sutures and the skin was closed with 9mm wound clips. Topical triple antibiotic ointment (Neosporin) was applied to the wound. Wound clips were removed ~7-10 days post-surgery and behavioral experiments began 14 days after surgery.

Cannulations: 7 days after spared nerve injury, mice were anesthetized with inhaled isoflurane (5% induction and 2% maintenance) and the head was shaved with trimmers and sterilized with 70% ethanol and 2% chlorhexidine gluconate (ChloraPrep One-Step Applicators). The head was fixed into a stereotaxic frame and a midline incision was carefully made before the scalp was retracted and the dura was removed with cotton tipped applicators. Two burr holes were drilled and bone screws were placed over the left and anterior right cortices. A third burr hole was drilled and a cannula was placed overlying the right PBN (Ap-5.15, m/l +1.40, d/v -5.15). The cannula was secured with dental cement the skin was sutured with 6-0 silk sutures. Topical triple

antibiotic ointment (Neosporin) was applied to the wound. Subcutaneous Buprenorphine HCL (0.05 mg/kg) was utilized for 72 hours as a post-operative analgesic. Behavioral experiments began 7 days after surgery.

Intra-parabrachial AAV administration: Mice were anesthetized with inhaled isoflurane (5% induction and 2% maintenance) and the head was shaved with trimmers and sterilized with 70% ethanol and 2% chlorhexidine gluconate (ChloraPrep One-Step Applicators). The head was fixed into a stereotaxic frame and a midline incision was carefully made before the scalp was retracted and the dura was removed with cotton tipped applicators. Two burr holes were drilled and 200nL of AAV virus (AAV8-hSyn-DIO-hM4D(Gi)-mCherry or AAV8-hSyn-DIO-mCherry) was injected into both PBNs (Ap-5.15, m/l+/-1.40, d/v -5.15). The skin was sutured with 6-0 silk sutures. Topical triple antibiotic ointment (Neosporin) was applied to the wound. Subcutaneous Buprenorphine HCL (0.05 mg/kg) was utilized for 72 hours as a post-operative analgesic. Behavioral experiments began 21 days after surgery.

Behavioral Testing

Mechanical Withdrawal Threshold: Testing was performed as described in (Solway et al., 2011). Mice were habituated to plexiglass chambers with opaque walls (15 × 4 × 4 cm) on a raised wire mesh platform for 30-60 minutes one day before and immediately prior to behavioral testing. Testing was performed using a calibrated set of logarithmically increasing von Frey monofilaments (Stoelting, Illinois) that range in gram force from 0.007 to 6.0 g. Beginning with a 0.4 g filament, these were applied perpendicular to the lateral hindpaw surface with sufficient force to cause a slight bending of the filament. A positive response was denoted as a rapid withdrawal

of the paw within 4 seconds of application. Using the Up-Down method (Chaplan et al., 1994), a positive response was followed by a lower filament and a negative response was followed by a higher filament to calculate the 50% withdrawal threshold for each mouse.

Cold Withdrawal Duration: Immediately following von Frey testing, acetone drop withdrawal testing was performed on mice in the same plexiglass chambers on a raised wire mesh platform. Using a syringe connected to PE-90 tubing, flared at the tip to a diameter of 3 1/2 mm, we applied a drop of acetone to the lateral side of the hind plantar paw. Surface tension maintained the volume of the drop to ~10 μL. The length of time the animal lifted or shook its paw was recorded for 30 s. Three observations were averaged.

Conditioned Place Preference/Avoidance: A three-day conditioning protocol using a biased chamber assignment was used for conditioned place preference (CPP). On the acclimation day (Day 1), mice had free access to explore all chambers of a 3-chamber conditioned place testing apparatus (side chambers: 170 x 150 mm; center chamber: 70 x 150 mm; height: 200 mm; San Diego Instruments) for 30 mins. Mice were able to discriminate between chambers using visual (vertical versus horizontal black-and-white striped walls) and sensory (rough versus smooth textured floor) cues. For pre-conditioning (Days 2 and 3), mice were again allowed to freely explore for 15 mins whilst their position was recorded via a 4 x 16 infra-red photobeam array by associated software (San Diego Instruments). For conditioning (Days 4-6) each mouse's preferred chamber was paired with saline and the non-preferred chamber with clozapine n' Oxide (CNO). Each morning mice received an i.p. saline injection, were returned to their home cage for 5 min, and were then placed in the designated side chamber for 60 min. 4 hours later, mice received i.p.

CNO (3 mg/kg; Tocris), were returned to their home cage for 5 min, and were placed into the CNO-designated chamber for 60 min. On test day (Day 7), mice could freely explore all chambers as their position was recorded as during pre-conditioning for 15 min. Difference scores were calculated as the time spent in the chamber on test day minus the time spent during pre-conditioning.

Hindpaw Stimulation for Fos: To produce *Fos* activation, a light-touch or acetone stimulation protocol was initiated on the ipsilateral hindpaw of SNI mice 14 days after nerve injury. Mice were anesthetized with isoflurane (5% induction, 2% maintenance) and the lateral surface of the left hindpaw was gently stroked in the longitudinal plane with a cotton tipped applicator for 3 seconds of every 5 seconds, for 5 minutes, or a 10uL droplet of acetone was applied every 30 seconds for 5 minutes. After an additional 60-minute awake and freely moving wait time in their home cage, mice received an intraperitoneal injection of sodium pentobarbital (.100 mg/kg, 0.2 mL, Fatal-Plus) and were transcardially perfused.

Fluorescence *in situ* Hybridization (FISH) (RNAscope)

Mice were transcardially perfused with ice cold 1x PBS followed by 10% buffered formalin and brains were extracted via blunt dissection, postfixed in 10% formalin (2-4 hrs), and then placed in 30% sucrose at 4°C until the tissue sank (~48-72 hrs). 20 μm thick floating PBN sections were obtained on a cryostat and mounted on Superfrost Plus Microscope slides and air dried overnight at room temperature. Slides underwent pretreatment for fluorescence *in situ* hybridization consisting of 10 min Xylene bath, 4 min 100% ethanol bath, and 2 min RNAscope® H2O2 treatment. Next, the FISH protocol for RNAscope Fluorescent v2 Assay (Advanced Cell

Diagnostics) was followed for hybridization to marker probes. Signal amplification was carried out using the TSA Fluorescein, Cyanine 3, and Cyanine 5 reagents (1:1000; Perkin Elmer or Akoya Biosciences). Slides were then coverslipped with VECTASHIELD HardSet Antifade Mounting Medium with DAPI.

Microscopy and Quantification

All images were captured on a Nikon Eclipse Ti2 microscope using a 20x or 40x objective and analyzed using NIS-Elements Advanced Research software v5.02. Cells with at least 3 puncta associated with a DAPI nucleus were considered positive.

Blinding procedures

In all experiments rigorous experimenter blinding was employed to promote research reproducibility. The experimenter was blinded to drug treatments in all behavioral pharmacology experiments as intraparabrachial injections were performed by a laboratory colleague thus providing complete anonymity of agent for each animal. For viral experiments a laboratory mate color-coded the virus tubes for the experimenter at the time of surgery as well as clozapine N' oxide (Tocris Bisociences) vs. saline at the time of behavior. The key for coding was kept hidden in a notebook until the completion of all experiments. The experimenter then obtained the key for data analysis.

Statistical Analyses and Data Representation

All data are presented as means ± SEM. Statistical significance was determined as $*P < 0.05$. All statistical analyses were performed in GraphPad Prism 9.0. Graphs and Images were created in GraphPad Prism 9.0., Adobe Illustrator 26.3.1., and Biorender.com.

Appendix D.3 Results

First, using brush- and acetone-evoked Fos analysis we found that SNI increased stimulus-evoked Fos expression as well as Fos co-expression in *Npy1r*-expressing neurons in the PBN (**Figure 40**). Thus, we hypothesized that pharmacological inhibition of the *Npy1r*-expressing neurons in the PBN would alleviate SNI-induced mechanical and cold hypersensitivity. Sure enough, in a brief pilot study (caveat is a low n and no baseline behavior) we found that infusion of the Y1 agonist [Leu^{31}, Pro^{34}]-NPY, reduced left hindlimb-elicited mechanical and cold hypersensitivity (**Figure 41**).

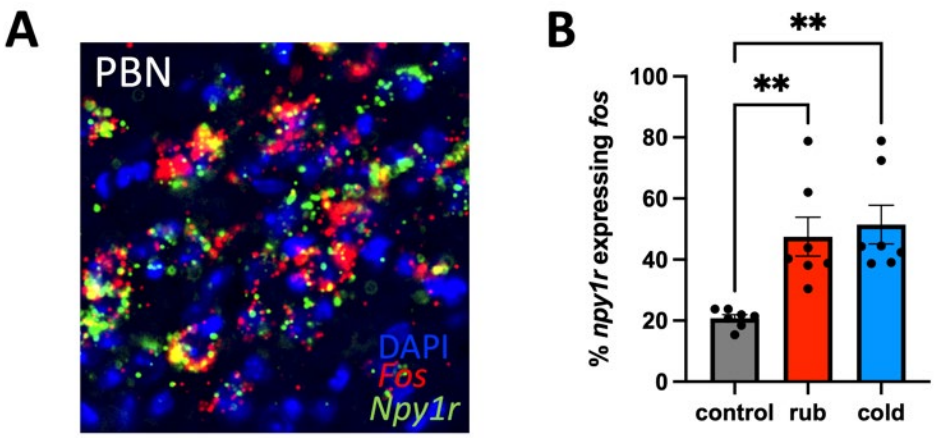

Figure 40. *Npy1r* PBN cells express Fos after mechanical and cold stimulation in nerve injured animals.

(**A, B**) Fluorescence *in situ* labeling reveals that the percent of PBN *Npy1r*-expressing cells co-expressing *Fos* in nerve injured animals is higher after mechanical (light brush) or cold stimulation (acetone droplet) compared to no stimulation controls (anesthesia alone). One-way ANVOA with Dunnett's post test, **p<0.01, n=7 mice per group.

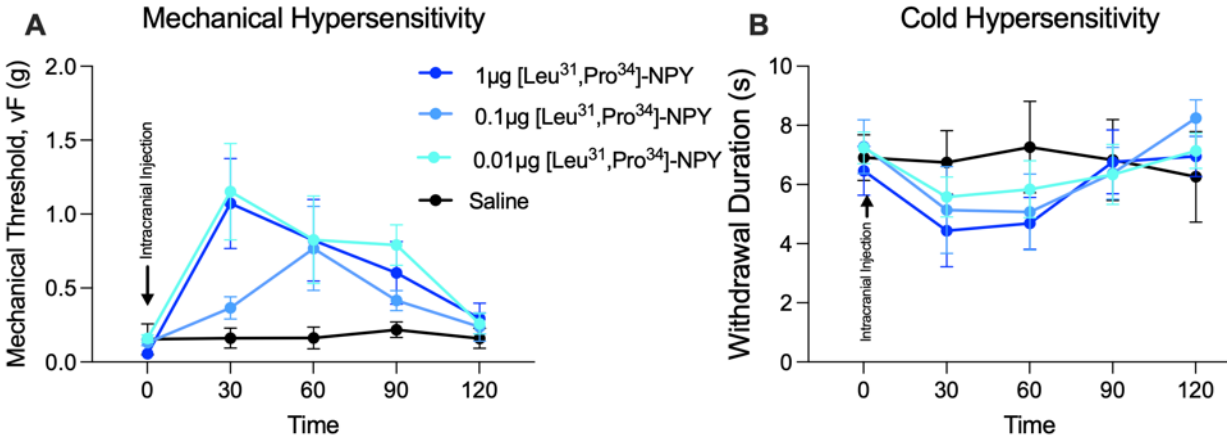

Figure 41. Intra-parabrachial administration of a Y1 agonist slightly alleviates nerve injury-induced mechanical and cold hypersensitivity.

Infusion of the Y1 selective agonist, [Leu^{31}, Pro^{34}]-NPY, into the right parabrachial nucleus slightly reduces ;eft leg SNI-induced mechanical and cold hypersensitivity. Two-way RM ANVOA with Dunnett's post test. n=5-7 mice/group.

These promising results led us to chemogenetically inhibit the bilateral *Npy1r*-expressing PBN neuron populations in sham and SNI mice. We found that inhibition of *Npy1r*-expressing PBN neurons with CNO alleviated mechanical and cold hypersensitivity in SNI mice but not sham surgery controls. Saline vehicle injections had no effect on pain-like behaviors (**Figure 42**). In addition to sensory-evoked/reflexive behavioral pain assessments we also performed conditioned place preference testing to assess the role of the *Npy1r*-expressing cells in the PBN on the affective component of neuropathic pain. To our surprise, chemogenetic inhibition of *Npy1r*-expressing cells in the PBN does not influence the affective component of neuropathic pain (**Figure 44**).

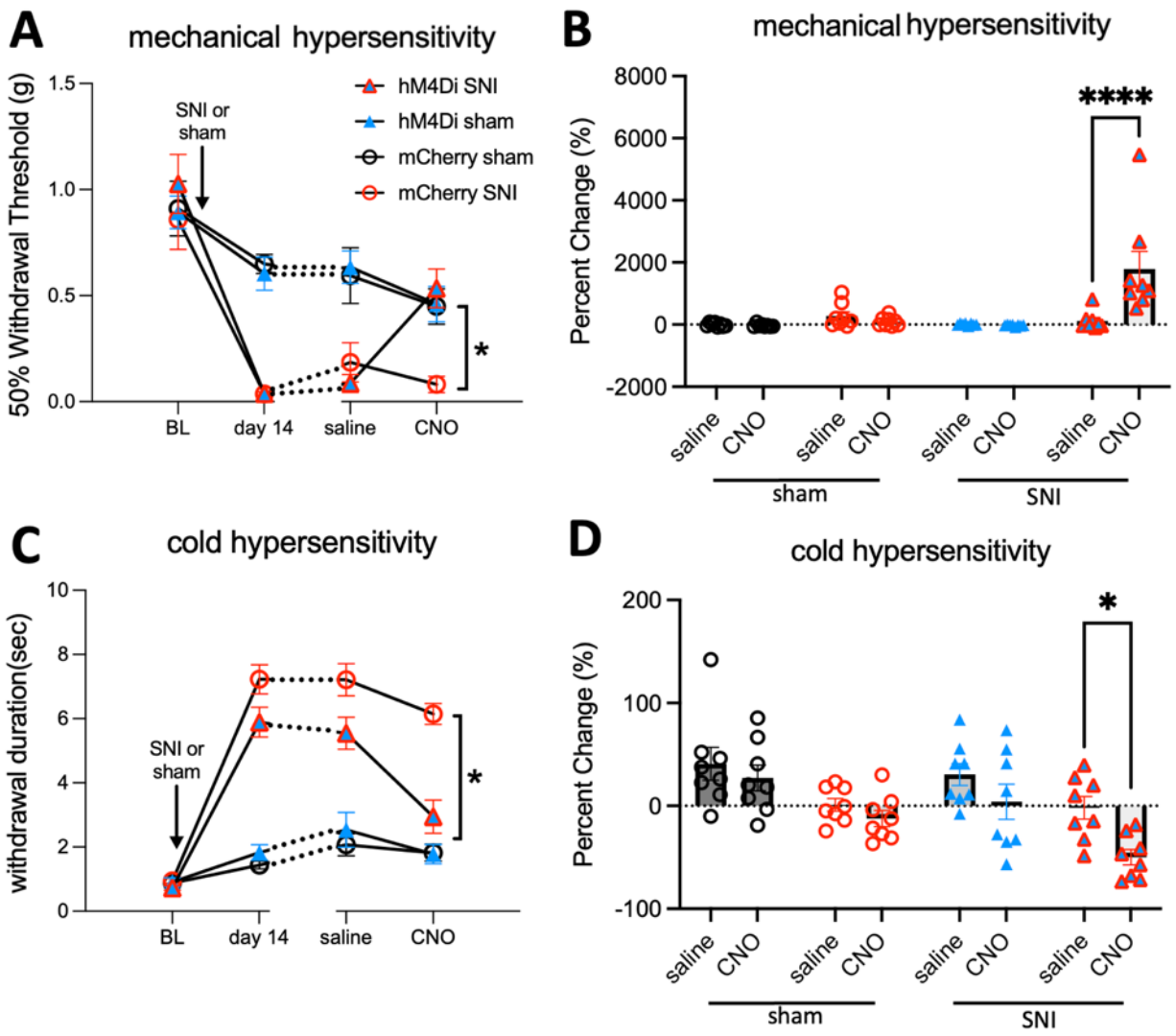

Figure 42. Silencing PBN *Npy1r*-expressing cells reduced nerve injury-induced reflexive behaviors.

Chemogenetic inhibition of *Npy1r*-expressing cells in the PBN reduced (**A, B**) mechanical and (**C, D**) cold hypersensitivity. n=8 mice/group. 2-way RM ANOVA, *p< 0.05, Dunnett post-hoc tests.

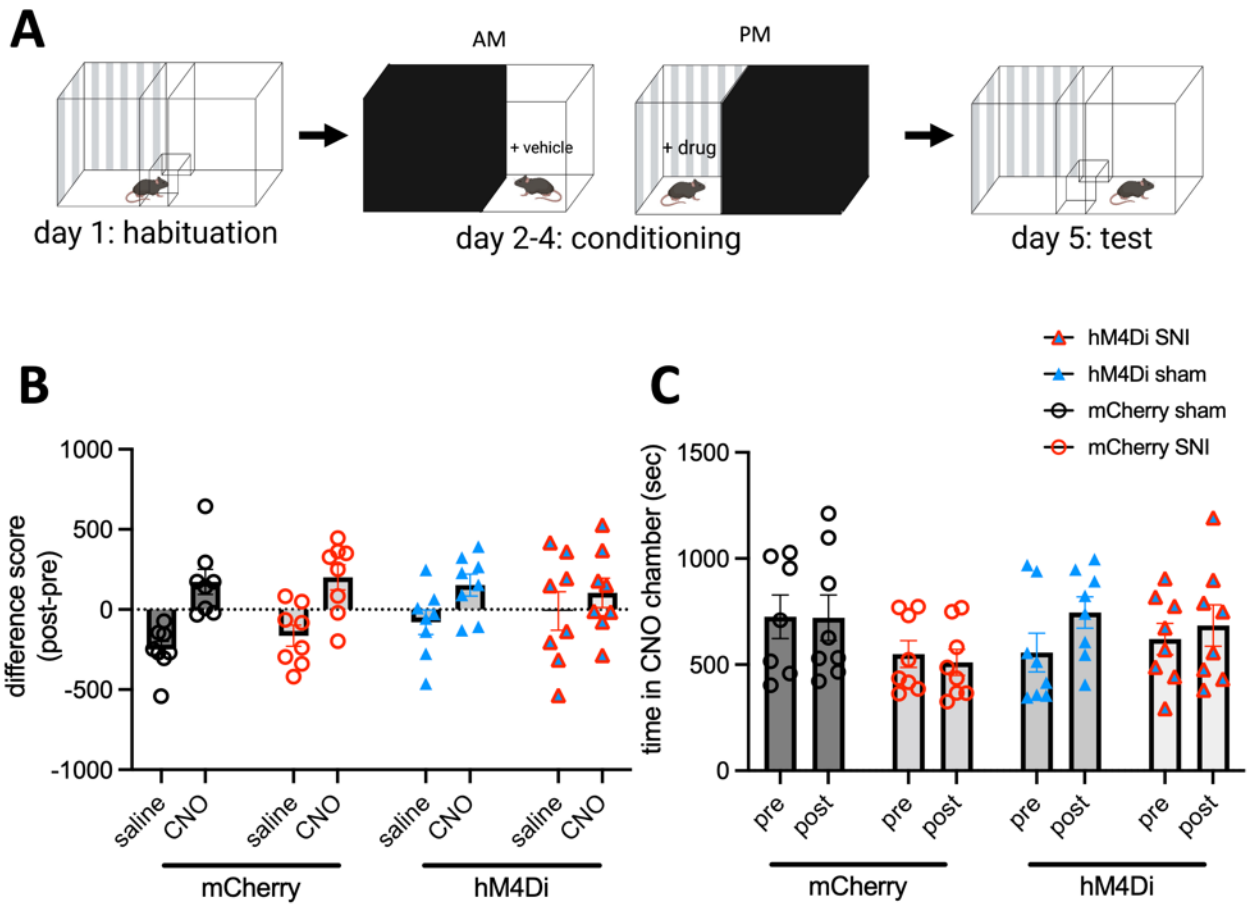

Figure 43. Silencing *Npy1r*-expressing PBN cells does not influence negative affect.

(**A**) Schematic of conditioned place preference. (**B, C**) Inhibition of *Npy1r*-expressing cells in the PBN via CNO does not alter preference for the drug-associated chamber. 2-way RM ANOVA, $p>0.05$, n=8 mice per group.

Appendix D.4 Discussion

In-situ hybridization and immunohistochemistry find many PBN neural subpopulations (demarcated via receptors, transcription factors, or neuropeptides) for which multiple Cre-driver lines readily exist to begin to understand their respective functions (Maeda et al., 2009; Palmiter, 2018). Several groups have begun to explore the PBN. For example, PBN neurons containing calcitonin gene-related peptide (CGRP) exhibit Fos immunoreactivity after a footshock stimulus and *in vivo* calcium transients in response to noxious cutaneous (shock, heat, pinch, itch) and visceral stimuli (lipopolysaccharide) (Campos et al., 2018; Han et al., 2015). In addition to the PBN CGRP-expressing neural population, investigators have probed other PBN neural subtypes. PBN neurons that express the tachykinin receptor 1 (TACR1) are the primary target of direct spinal cord dorsal horn projections (Barik et al., 2021; Deng et al., 2020). TACR1-expressing neurons in the PBN exhibit calcium transients in response to sustained noxious (mechanical pinch, heat, cold, topical chemical irritants, footshock) but not innocuous or transient noxious stimuli (Barik et al., 2021; Deng et al., 2020). Furthermore, chemogenetic activation of TACR1-expressing neurons is sufficient to induce spontaneous pain-related licking behaviors (Deng et al., 2020) and/or a general heightened arousal state with exaggerated responses to noxious stimuli (Barik et al., 2021). PBN neurons expressing tachykinin 1 (TAC1) trigger escape responses to heat stimuli via projections to the dorsal reticular formation in the medulla (MdD) (Barik et al., 2018). Neurons in the PBN expressing the mu opiate receptor (MOR) exhibit calcium transients in response to noxious mechanical and heat stimuli that can be largely diminished with systemic administration of opioids (Zhang et al., 2020). Interneurons within the lPBN that express prodynorphin (Pdyn) exhibit Fos immunoreactivity in response to capsaicin and their optogenetic activation induces real time place aversion (Chiang et al., 2020).

Surprisingly, few studies have activated and inhibited distinct neural populations within the lPBN in models of chronic or persistent pain. In marked contrast to these studies, we employed inhibitory chemogenetics to selectively manipulate the *Npy1r*-expressing cells in the PBN in the context of established chronic neuropathic pain. Our Fos results demonstrate that SNI sensitizes *Npy1r* cells in the PBN to non-noxious mechanical stimulation. Furthermore, we found that chemogenetic inhibition of these cells reverses evoked but not non-evoked/ongoing pain-like behaviors in a mouse model of chronic neuropathic pain. Perhaps, the reason for this dichotomy is that the PBN Y1 cells responsible for this effect do not project to the CeA or other affective processing centers. Future projection terminal analyses can begin to address such hypotheses.

In the future, more studies will need to be performed in established chronic pain models to fully understand the role of the PBN in chronic pain modalities. We predict that our understanding of PBN neuron subtypes will be further revolutionized via single-cell RNA-sequencing technologies. In particular, single cell RNA-sequencing will further unravel the diversity and heterogeneity of cell types within the healthy PBN, but then can be expanded to uncover dynamic changes in RNA expression profiles in PBN neurons in specific chronic pain modalities (ie. neuropathic, inflammatory) that will drive new experimental hypotheses with therapeutic implications.

Bibliography

Abraira, V.E., Ginty, D.D., 2013. The sensory neurons of touch. Neuron 79, 618–639. https://doi.org/10.1016/j.neuron.2013.07.051

Achour, L., Labbé-Jullié, C., Scott, M.G.H., Marullo, S., 2008. An escort for GPCRs: implications for regulation of receptor density at the cell surface. Trends Pharmacol. Sci. 29, 528–535. https://doi.org/10.1016/j.tips.2008.07.009

Acton, D., Ren, X., Di Costanzo, S., Dalet, A., Bourane, S., Bertocchi, I., Eva, C., Goulding, M., 2019. Spinal Neuropeptide Y1 Receptor-Expressing Neurons Form an Essential Excitatory Pathway for Mechanical Itch. Cell Rep. 28, 625–639. https://doi.org/10.1016/j.celrep.2019.06.033

Aira, Z., Barrenetxea, T., Buesa, I., Gómez-Esteban, J.C., Azkue, J.J., 2014. Synaptic upregulation and superadditive interaction of dopamine D2- and μ-opioid receptors after peripheral nerve injury. Pain 155, 2526–2533. https://doi.org/10.1016/j.pain.2014.09.012

Alba-Delgado, C., El Khoueiry, C., Peirs, C., Dallel, R., Artola, A., Antri, M., 2015. Subpopulations of PKCγ interneurons within the medullary dorsal horn revealed by electrophysiologic and morphologic approach. Pain 156, 1714–1728. https://doi.org/10.1097/j.pain.0000000000000221

Alba-Delgado, C., Mountadem, S., Mermet-Joret, N., Monconduit, L., Dallel, R., Artola, A., Antri, M., 2018. 5-HT 2A Receptor-Induced Morphological Reorganization of PKCγ-Expressing Interneurons Gates Inflammatory Mechanical Allodynia in Rat . J. Neurosci. 38, 10489–10504. https://doi.org/10.1523/jneurosci.1294-18.2018

Albisetti, G.W., Pagani, M., Platonova, E., Hösli, L., Johannssen, H.C., Fritschy, J.-M., Wildner, H., Zeilhofer, H.U., 2019. Dorsal Horn Gastrin-Releasing Peptide Expressing Neurons Transmit Spinal Itch But Not Pain Signals. J. Neurosci. 39, 2238–2250. https://doi.org/10.1523/JNEUROSCI.2559-18.2019

Alhadeff, A.L., Su, Z., Hernandez, E., Klima, M.L., Phillips, S.Z., Holland, R.A., Guo, C., Hantman, A.W., De Jonghe, B.C., Betley, J.N., 2018. A Neural Circuit for the Suppression of Pain by a Competing Need State. Cell 173, 140-152.e15. https://doi.org/10.1016/j.cell.2018.02.057

Allen, J.M., Gibson, S.J., Adrian, T.E., Polak, J.M., Bloom, S.R., 1984. Neuropeptide Y in human spinal cord. Brain Res. 308, 145–148. https://doi.org/10.1016/0006-8993(84)90926-0

Alles, S.R.A., Bandet, M. V., Eppler, K., Noh, M.C., Winship, I.R., Baker, G., Ballanyi, K., Smith, P.A., 2017. Acute anti-allodynic action of gabapentin in dorsal horn and primary somatosensory cortex: Correlation of behavioural and physiological data.

Neuropharmacology 113, 576–590. https://doi.org/10.1016/j.neuropharm.2016.11.011

Almarestani, L., Waters, S.M., Krause, J.E., Bennett, G.J., Ribeiro-Da-Silva, A., 2007. Morphological characterization of spinal cord dorsal horn lamina I neurons projecting to the parabrachial nucleus in the rat. J. Comp. Neurol. 504, 287–297. https://doi.org/10.1002/cne.21410

Aloisi, A.M., Albonetti, M.E., Muscettola, M., Facchinetti, F., Tanganelli, C., Carli, G., 1995. Effects of formalin-induced pain on ACTH, beta-endorphin, corticosterone and interleukin-6 plasma levels in rats. Neuroendocrinology 62, 13–18. https://doi.org/10.1159/000126983

Alt, A., Clark, M.J., Woods, J.H., Traynor, J.R., 2002. Mu and delta opioid receptors activate the same G proteins in human neuroblastoma SH-SY5Y cells. Br. J. Pharmacol. 135, 217–225. https://doi.org/10.1038/sj.bjp.0704430

Ang, S.T., Lee, A.T.H., Foo, F.C., Ng, L., Low, C.M., Khanna, S., 2015. GABAergic neurons of the medial septum play a nodal role in facilitation of nociception-induced affect. Sci. Rep. 5, 1–21. https://doi.org/10.1038/srep15419

Arcourt, A., Gorham, L., Dhandapani, R., Birchmeier, C., Heppenstall, P.A., Lechner, S.G., Arcourt, A., Gorham, L., Dhandapani, R., Prato, V., Taberner, F.J., Wende, H., 2017. Touch Receptor-Derived Sensory Information Alleviates Acute Pain Signaling and Fine-Tunes Nociceptive Reflex Coordination Article Touch Receptor-Derived Sensory Information Alleviates Acute Pain Signaling and Fine-Tunes Nociceptive Reflex Coordination. Neuron 93, 179–193. https://doi.org/10.1016/j.neuron.2016.11.027

Artola, A., Voisin, D., Dallel, R., 2020. PKCγ interneurons , a gateway to pathological pain in the dorsal horn. J. Neural Transm. https://doi.org/10.1007/s00702-020-02162-6

Balasubramanyan, S., Stemkowski, P.L., Stebbing, M.J., Smith, P.A., 2006. Sciatic chronic constriction injury produces cell-type-specific changes in the electrophysiological properties of rat substantia gelatinosa neurons. J. Neurophysiol. 96, 579–590. https://doi.org/10.1152/jn.00087.2006

Bantel, C., Childers, S.R., Eisenach, J.C., 2002. Role of adenosine receptors in spinal G-protein activation after peripheral nerve injury. Anesthesiology 96, 1443–1449. https://doi.org/10.1097/00000542-200206000-00025

Barik, A., Sathyamurthy, A., Thompson, J., Seltzer, M., Levine, A., Chesler, A., 2021. A spinoparabrachial circuit defined by tacr1 expression drives pain. Elife 10, 1–42. https://doi.org/10.7554/eLife.61135

Barik, A., Thompson, J.H., Seltzer, M., Ghitani, N., Chesler, A.T., 2018. A Brainstem-Spinal Circuit Controlling Nocifensive Behavior. Neuron 100, 1491-1503.e3. https://doi.org/10.1016/j.neuron.2018.10.037

Barry, D.M., Liu, X.T., Liu, B., Liu, X.Y., Gao, F., Zeng, X., Liu, J., Yang, Q., Wilhelm, S., Yin, J., Tao, A., Chen, Z.F., 2020. Exploration of sensory and spinal neurons expressing gastrin-

releasing peptide in itch and pain related behaviors. Nat. Commun. 11, 1–14. https://doi.org/10.1038/s41467-020-15230-y

Basu, P., Custodio-Patsey, L., Prasoon, P., Smith, B.N., Taylor, B.K., 2021. Sex differences in protein kinase A signaling of the latent postoperative pain sensitization that is masked by kappa opioid receptors in the spinal cord. J. Neurosci. 41, 9827–9843. https://doi.org/10.1523/JNEUROSCI.2622-20.2021

Bell, A.M., Mecinas, M.G., Stevenson, A., Benito, A.C., Wildner, H., West, S.J., Watanabe, M., Todd, A.J., 2020. Expression of green fluorescent protein defines a specific population of lamina II excitatory interneurons in the GRP :: eGFP mouse. Sci. Rep. 1–14. https://doi.org/10.1038/s41598-020-69711-7

Benarroch, E.E., 2016. Dorsal horn circuitry Complexity and implications for mechanisms of neuropathic pain. Neurology 86, 1060–1069.

Boadas-Vaello, P., Castany, S., Homs, J., Álvarez-Pérez, B., Deulofeu, M., Verdú, E., 2016. Neuroplasticity of ascending and descending pathways after somatosensory system injury: Reviewing knowledge to identify neuropathic pain therapeutic targets. Spinal Cord 54, 330–340. https://doi.org/10.1038/sc.2015.225

Bourane, S., Duan, B., Koch, S.C., Dalet, A., Britz, O., Garcia-Campmany, L., Kim, E., Cheng, L., Ghosh, A., Ma, Q., Goulding, M., 2015. Gate control of mechanical itch by a subpopulation of spinal cord interneurons. Science (80-.). 350, 550–554. https://doi.org/10.1126/science.aac8653

Bourne, H.R., Nicoll, R., 1993. Molecular machines integrate coincident synaptic signals. Cell 72, 65–75. https://doi.org/10.1016/S0092-8674(05)80029-7

Boyle, K.A., Gradwell, M.A., Yasaka, T., Dickie, A.C., Polgár, E., Ganley, R.P., Orr, D.P., Watanabe, M., Abraira, V.E., Kuehn, E.D., Zimmermann, A.L., Ginty, D.D., Callister, R.J., Graham, B.A., Hughes, D.I., 2019. Defining a Spinal Microcircuit that Gates Myelinated Afferent Input: Implications for Tactile Allodynia. SSRN Electron. J. 28, 526–540. https://doi.org/10.2139/ssrn.3377640

Boyle, K.A., Gutierrez-Mecinas, M., Polgár, E., Mooney, N., O'Connor, E., Furuta, T., Watanabe, M., Todd, A.J., 2017. A quantitative study of neurochemically defined populations of inhibitory interneurons in the superficial dorsal horn of the mouse spinal cord. Neuroscience 363, 120–133. https://doi.org/10.1016/j.neuroscience.2017.08.044

Braz, J., Solorzano, C., Wang, X., Basbaum, A., 2014. Transmitting Pain and Itch Messages: A Contemporary View of the Spinal Cord Circuits that Generate Gate Control. Neuron 82, 522–536. https://doi.org/10.1016/j.neuron.2014.01.018

Bröhl, D., Strehle, M., Wende, H., Hori, K., Bormuth, I., Nave, K.A., Müller, T., Birchmeier, C., 2008. A transcriptional network coordinately determines transmitter and peptidergic fate in the dorsal spinal cord. Dev. Biol. 322, 381–393. https://doi.org/10.1016/j.ydbio.2008.08.002

Brothers, S.P., Wahlestedt, C., 2010. Therapeutic potential of neuropeptide y (NPY) receptor ligands. EMBO Mol. Med. 2, 429–439. https://doi.org/10.1002/emmm.201000100

Brumovsky, P., Hofstetter, C., Olson, L., Ohning, G., Villar, M., Hökfelt, T., 2006. The neuropeptide tyrosine Y1R is expressed in interneurons and projection neurons in the dorsal horn and area X of the rat spinal cord. Neuroscience 138, 1361–1376. https://doi.org/10.1016/j.neuroscience.2005.11.069

Brumovsky, P., Shi, T.S., Landry, M., Villar, M.J., Hökfelt, T., 2007. Neuropeptide tyrosine and pain. Trends Pharmacol. Sci. 28, 93–102. https://doi.org/10.1016/j.tips.2006.12.003

Brumovsky, P., Stanic, D., Shuster, S., Herzog, H., Villar, M., Hökfelt, T., 2005. Neuropeptide Y2 receptor protein is present in peptidergic and nonpeptidergic primary sensory neurons of the mouse. J. Comp. Neurol. 489, 328–348. https://doi.org/10.1002/cne.20639

Brumovsky, P.R., Bergman, E., Liu, H.X., Hökfelt, T., Villar, M.J., 2004. Effect of a graded single constriction of the rat sciatic nerve on pain behavior and expression of immunoreactive NPY and NPY Y1 receptor in DRG neurons and spinal cord. Brain Res. 1006, 87–99. https://doi.org/10.1016/j.brainres.2003.09.085

Brumovsky, P.R., Shi, T.J., Matsuda, H., Kopp, J., Villar, M.J., Hökfelt, T., 2002. NPY Y1 receptors are present in axonal processes of DRG neurons. Exp. Neurol. 174, 1–10. https://doi.org/10.1006/exnr.2001.7845

Brust, T.F., Conley, J.M., Watts, V.J., 2015. Gαi/o-coupled receptor-mediated sensitization of adenylyl cyclase: 40 years later. Eur. J. Pharmacol. 763, 223–232. https://doi.org/10.1016/j.ejphar.2015.05.014

Cahill, C.M., Holdridge, S. V., Morinville, A., 2007. Trafficking of δ-opioid receptors and other G-protein-coupled receptors: implications for pain and analgesia. Trends Pharmacol. Sci. 28, 23–31. https://doi.org/10.1016/j.tips.2006.11.003

Campos, C.A., Bowen, A.J., Roman, C.W., Palmiter, R.D., 2018. Encoding of danger by parabrachial CGRP neurons. Nature 555, 617–620. https://doi.org/10.1038/nature25511

Cao, C.Q., Yu, X.H., Dray, A., Filosa, A., Perkins, M.N., 2003. A pro-nociceptive role of neuromedin U in adult mice. Pain 104, 609–616. https://doi.org/10.1016/S0304-3959(03)00118-0

Caterina, M.J., Schumacher, M.A., Tominaga, M., Rosen, T.A., Levine, J.D., Julius, D., 1997. The capsaicin receptor: A heat-activated ion channel in the pain pathway. Nature 389, 816–824. https://doi.org/10.1038/39807

Cavanaugh, D.J., Chesler, A.T., Bráz, J.M., Shah, N.M., Julius, D., Basbaum, A.I., 2011. Restriction of transient receptor potential vanilloid-1 to the peptidergic subset of primary afferent neurons follows its developmental downregulation in nonpeptidergic neurons. J. Neurosci. 31, 10119–10127. https://doi.org/10.1523/JNEUROSCI.1299-11.2011

Chabot-Doré, A.J., Schuster, D.J., Stone, L.S., Wilcox, G.L., 2015. Analgesic synergy between opioid and α2-adrenoceptors. Br. J. Pharmacol. 172, 388–402. https://doi.org/10.1111/bph.12695

Challa, S.R., 2015. Surgical animal models of neuropathic pain: Pros and Cons. Int. J. Neurosci. 125, 170–174. https://doi.org/10.3109/00207454.2014.922559

Chamessian, A., Young, M., Qadri, Y., Berta, T., Ji, R.R., Van De Ven, T., 2018. Transcriptional Profiling of Somatostatin Interneurons in the Spinal Dorsal Horn. Sci. Rep. 8, 1–16. https://doi.org/10.1038/s41598-018-25110-7

Chaplan, S.R., Bach, F.W., Pogrel, J.W., Chung, J.M., Yaksh, T.L., 1994. Quantitative assessment of tactile allodynia in the rat paw. J. Neurosci. Methods 53, 55–63. https://doi.org/10.1016/0165-0270(94)90144-9

Che, T., 2021. Advances in the treatment of chronic pain by targeting GPCRs. Biochemistry 60, 1401–1412. https://doi.org/10.1021/acs.biochem.0c00644

Chen, C.H., Stephens, R.L., Rogers, R.C., 1997. PYY and NPY: Control of gastric motility via action on Y1 and Y2 receptors in the DVC. Neurogastroenterol. Motil. 9, 109–116. https://doi.org/10.1046/j.1365-2982.1997.d01-26.x

Chen, L., Huang, J., Zhao, P., Persson, A.K., Dib-Hajj, F.B., Cheng, X., Tan, A., Waxman, S.G., Dib-Hajj, S.D., 2018. Conditional knockout of NaV1.6 in adult mice ameliorates neuropathic pain. Sci. Rep. 8, 1–17. https://doi.org/10.1038/s41598-018-22216-w

Chen, Q.L., Heinricher, M.M., 2019. Descending Control Mechanisms and Chronic Pain. Curr. Rheumatol. Rep. 21, 1–7. https://doi.org/10.1007/s11926-019-0813-1

Chen, S., Liu, X.Y., Jiao, Y., Chen, Z.F., Yu, W., 2019. NPY2R signaling gates spontaneous and mechanical, but not thermal, pain transmission. Mol. Pain 15, 1–7. https://doi.org/10.1177/1744806919887830

Chen, S.R., Sweigart, K.L., Lakoski, J.M., Pan, H.L., 2002. Functional μ opioid receptors are reduced in the spinal cord dorsal horn of diabetic rats. Anesthesiology 97, 1602–1608. https://doi.org/10.1097/00000542-200212000-00037

Chen, X., Henderson, K., Beinfeld, M.C., Westfall, T.C., 1988. Alterations in blood pressure of normotensive and hypertensive rats following intrathecal injections of neuropeptide Y. J. Cardiovasc. Pharmacol. https://doi.org/10.1097/00005344-198810000-00014

Chen, X., Knuepfer, M.M., Westfall, T.C., 1990. Hemodynamic and sympathetic effects of spinal administration of neuropeptide Y in rats. Am. J. Physiol. - Hear. Circ. Physiol. 259. https://doi.org/10.1152/ajpheart.1990.259.6.h1674

Chen, X., Westfall, T.C., 1993. Depressor effect of intrathecal neuropeptide Y (NPY) is mediated by Y2 subtype of NPY receptors. J. Cardiovasc. Pharmacol. https://doi.org/10.1097/00005344-199305000-00005

Chen, Y., Balasubramanyan, S., Lai, A.Y., Todd, K.G., Smith, P.A., 2009. Effects of sciatic nerve axotomy on excitatory synaptic transmission in rat substantia gelatinosa. J. Neurophysiol. 102, 3203–3215. https://doi.org/10.1152/jn.00296.2009

Chen, Z.-F., 2021. A neuropeptide code for itch. Nat. Rev. Neurosci. https://doi.org/10.1038/s41583-021-00526-9

Cheng, L., Duan, B., Huang, T., Zhang, Y., Chen, Y., Britz, O., Garcia-Campmany, L., Ren, X., Vong, L., Lowell, B.B., Goulding, M., Wang, Y., Ma, Q., 2017. Identification of spinal circuits involved in touch-evoked dynamic mechanical pain. Nat. Neurosci. 20, 804–814. https://doi.org/10.1038/nn.4549

Cheng, L., Samad, O.A., Xu, Y., Mizuguchi, R., Luo, P., Shirasawa, S., Goulding, M., Ma, Q., 2005. Lbx1 and Tlx3 are opposing switches in determining GABAergic versus glutamatergic transmitter phenotypes. Nat. Neurosci. 8, 1510–1515. https://doi.org/10.1038/nn1569

Cheriyan, J., Sheets, P.L., 2020. Peripheral nerve injury reduces the excitation-inhibition balance of basolateral amygdala inputs to prelimbic pyramidal neurons projecting to the periaqueductal gray. Mol. Brain 13, 1–4. https://doi.org/10.1186/s13041-020-00638-w

Chiang, M.C., Bowen, A., Schier, L.A., Tupone, D., Uddin, O., Heinricher, M.M., 2019. Parabrachial Complex: A Hub for Pain and Aversion. J. Neurosci. 39, 8225–8230. https://doi.org/10.1523/JNEUROSCI.1162-19.2019

Chiang, M.C., Nguyen, E.K., Canto-Bustos, M., Papale, A.E., Oswald, A.-M.M., Ross, S.E., 2020. Divergent Neural Pathways Emanating from the Lateral Parabrachial Nucleus Mediate Distinct Components of the Pain Response. Neuron 1–13. https://doi.org/10.1016/j.neuron.2020.03.014

Christensen, A.J., Iyer, S.M., François, A., Vyas, S., Ramakrishnan, C., Vesuna, S., Deisseroth, K., Scherrer, G., Delp, S.L., 2016. In Vivo Interrogation of Spinal Mechanosensory Circuits. Cell Rep. 17, 1699–1710. https://doi.org/10.1016/j.celrep.2016.10.010

Cichewicz, D.L., 2004. Synergistic interactions between cannabinoid and opioid analgesics. Life Sci. 74, 1317–1324. https://doi.org/10.1016/j.lfs.2003.09.038

Cleary, D.R., Roeder, Z., Elkhatib, R., Heinricher, M.M., 2014. Neuropeptide Y in the rostral ventromedial medulla reverses inflammatory and nerve injury hyperalgesia in rats via non-selective excitation of local neurons. Neuroscience 271, 149–159. https://doi.org/10.1016/j.neuroscience.2014.04.035

Colburn, R.W., Lubin, M. Lou, Stone, D.J., Wang, Y., Lawrence, D., D'Andrea, M.R.R., Brandt, M.R., Liu, Y., Flores, C.M., Qin, N., 2007. Attenuated Cold Sensitivity in TRPM8 Null Mice. Neuron 54, 379–386. https://doi.org/10.1016/j.neuron.2007.04.017

Colloca, L., Ludman, T., Bouhassira, D., Baron, R., Dickenson, A.H., Yarnitsky, D., Freeman, R., Truini, A., Attal, N., Finnerup, N.B., Eccleston, C., Kalso, E., Bennett, D.L., Dworkin,

R.H., Raja, S.N., 2017. Neuropathic pain. Nat. Rev. Dis. Prim. 3, 1–20. https://doi.org/10.1038/nrdp.2017.2

Colvin, L.A., Duggan, A.W., 2001. The effect of conduction block on the spinal release of immunoreactive-neuropeptide Y (ir-NPY) in the neuropathic rat. Pain 91, 235–240. https://doi.org/10.1016/S0304-3959(00)00438-3

Cordeaux, Y., Hill, S.J., 2002. Mechanisms of Cross-Talk between G-Protein-Coupled Receptors. Neurosignals 11, 45–57.

Corder, G., Doolen, S., Donahue, R.R., Winter, M.K., Jutras, B.L., He, Y., Hu, X., Wieskopf, J.S., Mogil, J.S., Storm, D.R., Wang, Z.J., McCarson, K.E., Taylor, B.K., 2013. Constitutive μ-opioid receptor activity leads to long-term endogenous analgesia and dependence. Science (80-.). 341, 1394–1399. https://doi.org/10.1126/science.1239403

Costigan, M., Scholz, J., Woolf, C.J., 2009. Neuropathic pain: A maladaptive response of the nervous system to damage. Annu. Rev. Neurosci. 32, 1–32. https://doi.org/10.1146/annurev.neuro.051508.135531

Craig, A.D., Zhang, E.T., Blomqvist, A., 2002. Association of spinothalamic lamina I neurons and their ascending axons with calbindin-immunoreactivity in monkey and human. Pain 97, 105–115. https://doi.org/10.1016/S0304-3959(02)00009-X

Crook, R.J., Dickson, K., Hanlon, R.T., Walters, E.T., 2014. Nociceptive sensitization reduces predation risk. Curr. Biol. 24, 1121–1125. https://doi.org/10.1016/j.cub.2014.03.043

Cui, H., Su, W., Cao, Y., Ma, L., Xu, G., Mou, W., Zhang, H., Yu, J., Ma, C., Zhang, X., Huang, Y., 2021. Lack of Spinal Neuropeptide Y Is Involved in Mechanical Itch in Aged Mice. Front. Aging Neurosci. 13, 1–8. https://doi.org/10.3389/fnagi.2021.654761

De Felice, M., Sanoja, R., Wang, R., Vera-Portocarrero, L., Oyarzo, J., King, T., Ossipov, M.H., Vanderah, T.W., Lai, J., Dussor, G.O., Fields, H.L., Price, T.J., Porreca, F., 2011. Engagement of descending inhibition from the rostral ventromedial medulla protects against chronic neuropathic pain. Pain 152, 2701–2709. https://doi.org/10.1016/j.pain.2011.06.008

Decosterd, I., Woolf, C.J., 2000. Spared nerve injury: an animal model of persistent peripheral neuropathic pain. Pain 87, 149–158.

Decressac, M., Barker, R.A., 2012. Neuropeptide Y and its role in CNS disease and repair. Exp. Neurol. 238, 265–272. https://doi.org/10.1016/j.expneurol.2012.09.004

Del Barrio, M.G., Bourane, S., Grossmann, K., Schüle, R., Britsch, S., O'Leary, D.D.M., Goulding, M., 2013. A transcription factor code defines nine sensory interneuron subtypes in the mechanosensory area of the spinal cord. PLoS One 8, e77928. https://doi.org/10.1371/journal.pone.0077928

Deng, J., Zhou, H., Lin, J.K., Shen, Z.X., Chen, W.Z., Wang, L.H., Li, Q., Mu, D., Wei, Y.C., Xu, X.H., Sun, Y.G., 2020. The Parabrachial Nucleus Directly Channels Spinal Nociceptive

Signals to the Intralaminar Thalamic Nuclei, but Not the Amygdala. Neuron 107, 909-923.e6. https://doi.org/10.1016/j.neuron.2020.06.017

Dhaka, A., Earley, T.J., Watson, J., Patapoutian, A., 2008. Visualizing cold spots: TRPM8-expressing sensory neurons and their projections. J. Neurosci. 28, 566–575. https://doi.org/10.1523/JNEUROSCI.3976-07.2008

Diaz-delCastillo, M., Woldbye, P.D., Marie, A., 2018. Neuropeptide Y and its Involvement in Chronic Pain. Neuroscience 387, 162–169. https://doi.org/10.1016/j.neuroscience.2017.08.050

Dickie, A.C., Bell, A.M., Iwagaki, N., Polgár, E., Gutierrez-Mecinas, M., Kelly, R., Lyon, H., Turnbull, K., West, S.J., Etlin, A., Braz, J., Watanabe, M., Bennett, D.L.H., Basbaum, A.I., Riddell, J.S., Todd, A.J., 2019. Morphological and functional properties distinguish the substance P and gastrin-releasing peptide subsets of excitatory interneuron in the spinal cord dorsal horn. Pain 160, 442–462. https://doi.org/10.1097/j.pain.0000000000001406

Djellas, Y., Antonakis, K., Le Breton, G.C., 2000. Shifts in the affinity distribution of one class of seven-transmembrane receptors by activation of a separate class of seven-transmembrane receptors. Biochem. Pharmacol. 59, 1521–1529. https://doi.org/10.1016/S0006-2952(00)00296-3

Dougherty, P.M., Chen, J., 2016. Relationship of membrane properties, spike burst responses, laminar location, and functional class of dorsal horn neurons recorded in vitro. J. Neurophysiol. 116, 1137–1151. https://doi.org/10.1152/jn.00187.2016

Drakulich, D.A., Walls, A.M., Toews, M.L., Hexum, T.D., 2003. Neuropeptide Y Receptor-Mediated Sensitization of ATP-Stimulated Inositol Phosphate Formation. J. Pharmacol. Exp. Ther. 307, 559–565. https://doi.org/10.1124/jpet.103.053082

Duan, B., Cheng, L., Bourane, S., Britz, O., Padilla, C., Garcia-campmany, L., Krashes, M., Knowlton, W., Velasquez, T., Ren, X., Ross, S.E., Lowell, B.B., Wang, Y., Goulding, M., Ma, Q., 2014. Identification of Spinal Circuits Transmitting and Gating Mechanical Pain. Cell 159, 1417–1432. https://doi.org/10.1016/j.cell.2014.11.003

Duan, B., Cheng, L., Ma, Q., 2018. Spinal Circuits Transmitting Mechanical Pain and Itch. Neurosci. Bull. 34, 186–193. https://doi.org/10.1007/s12264-017-0136-z

Duggan, A., Hope, P.J., Lang, C.W., 1991. Microinjection of neuropeptide y into the superficial dorsal horn reduces stimulus-evoked release of immunoreactive substance p in the anaesthetized cat. Neuroscience 44, 733–740. https://doi.org/10.1016/0306-4522(91)90092-3

Finnerup, N.B., Attal, N., Haroutounian, S., McNicol, E., Baron, R., Dworkin, R.H., Gilron, I., Haanpää, M., Hansson, P., Jensen, T.S., Kamerman, P.R., Lund, K., Moore, A., Raja, S.N., Rice, A.S.C., Rowbotham, M., Sena, E., Siddall, P., Smith, B.H., Wallace, M., 2015. Pharmacotherapy for neuropathic pain in adults: A systematic review and meta-analysis. Lancet Neurol. 14, 162–173. https://doi.org/10.1016/S1474-4422(14)70251-0

Finnerup, N.B., Kuner, R., Jensen, T.S., 2021. Neuropathic pain: From Mechanisms to Treatment. Physiol. Rev. 101, 259–301. https://doi.org/10.1152/physrev.00045.2019

Foster, E., Wildner, H., Tudeau, L., Haueter, S., Ralvenius, W.T., Jegen, M., Johannssen, H., Hösli, L., Haenraets, K., Ghanem, A., Conzelmann, K.K., Bösl, M., Zeilhofer, H.U., 2015. Targeted ablation, silencing, and activation establish glycinergic dorsal horn neurons as key components of a spinal gate for pain and itch. Neuron 85, 1289–1304. https://doi.org/10.1016/j.neuron.2015.02.028

Fu, W., Nelson, T.S., Santos, D.F., Doolen, S., Gutierrez, J.J.P., Ye, N., Zhou, J., K Taylor, B., 2019a. An NPY Y1 receptor antagonist unmasks latent sensitization and reveals the contribution of protein kinase A and Epac to chronic inflammatory pain. Pain 160, 1754–1765. https://doi.org/10.1097/j.pain.0000000000001557

Fu, W., Nelson, T.S., Santos, D.F., Doolen, S., Gutierrez, J.J.P., Ye, N., Zhou, J., Taylora, B.K., 2019b. An NPY Y1 receptor antagonist unmasks latent sensitization and reveals the contribution of protein kinase A and Epac to chronic inflammatory pain. Pain 160, 1754–1765. https://doi.org/10.1097/j.pain.0000000000001557

Fu, W., Wessel, C.R., Taylor, B.K., 2020. Neuropeptide Y tonically inhibits an NMDAR➔AC1➔TRPA1/TRPV1 mechanism of the affective dimension of chronic neuropathic pain. Neuropeptides 80, 102024. https://doi.org/10.1016/j.npep.2020.102024

Fukuoka, T., Noguchi, K., 2015. A potential anti-allodynic mechanism of GDNF following L5 spinal nerve ligation; Mitigation of NPY up-regulation in the touch sense pathway. Neuroscience 304, 240–249. https://doi.org/10.1016/j.neuroscience.2015.07.059

Gangadharan, V., Kuner, R., 2015. Unravelling Spinal Circuits of Pain and Mechanical Allodynia. Neuron 87, 673–675. https://doi.org/10.1016/j.neuron.2015.08.013

Gao, J., Ghibaudi, L., Hwa, J.J., 2004. Selective activation of central NPY Y1 vs. Y5 receptor elicits hyperinsulinemia via distinct mechanisms. Am. J. Physiol. - Endocrinol. Metab. 287, 706–711. https://doi.org/10.1152/ajpendo.00530.2003

Gao, T., Ma, H., Xu, B., Bergman, J., Larhammar, D., Lagerström, M.C., 2018. The Neuropeptide Y System Regulates Both Mechanical and Histaminergic Itch. J. Invest. Dermatol. 138, 2405–2411. https://doi.org/10.1016/j.jid.2018.05.008

Gao, Y.-J., Ji, R.-R., 2009. c-Fos and pERK, Which is a Better Marker for Neuronal Activation and Central Sensitization After Noxious Stimulation and Tissue Injury? Open Pain J. 2, 11–17. https://doi.org/10.2174/1876386300902010011

Gaskin, D.J., Richard, P., 2012. The economic costs of pain in the United States. J. Pain 13, 715–724. https://doi.org/10.1016/j.jpain.2012.03.009

Geppetti, P., Veldhuis, N.A., Lieu, T.M., Bunnett, N.W., 2015. G Protein-Coupled Receptors: Dynamic Machines for Signaling Pain and Itch. Neuron 88, 635–649. https://doi.org/10.1016/j.neuron.2015.11.001

Gerum, M., Simonin, F., 2021. Behavioral characterization, potential clinical relevance and mechanisms of latent pain sensitization. Pharmacol. Ther. 108032. https://doi.org/10.1016/j.pharmthera.2021.108032

Gibbs, J., Flores, C.M., Hargreaves, K.M., 2004. Neuropeptide Y inhibits capsaicin-sensitive nociceptors via a Y1-receptor-mediated mechanism. Neuroscience 125, 703–709. https://doi.org/10.1016/j.neuroscience.2004.01.044

Gibson, S.J., Polak, J.M., Allen, J.M., Adrian, T.E., Kelly, J.S., Bloom, S.R., 1984. The distribution and origin of a novel brain peptide, neuropeptide Y, in the spinal cord of several mammals. J. Comp. Neurol. 227, 78–91. https://doi.org/doi:10.1002/cne.902270109

Gierthmühlen, J., Baron, R., 2016. Neuropathic Pain. Semin. Neurol. 36, 462–468. https://doi.org/10.1055/s-0036-1584950

Gilding, E.K., Jami, S., Deuis, J.R., Israel, M.R., Harvey, P.J., Poth, A.G., Rehm, F.B.H., Stow, J.L., Robinson, S.D., Yap, K., Brown, D.L., Hamilton, B.R., Andersson, D., Craik, D.J., Vetter, I., Durek, T., 2020. Neurotoxic peptides from the venom of the giant Australian stinging tree. Sci. Adv. 6, 1–10. https://doi.org/10.1126/sciadv.abb8828

Glare, P., Aubrey, K.R., Myles, P.S., 2019. Transition from acute to chronic pain after surgery. Lancet 393, 1537–1546. https://doi.org/10.1016/S0140-6736(19)30352-6

Gold, M.S., Gebhart, G.F., 2010. Nociceptor sensitization in pain pathogenesis. Nat. Med. 16, 1248–1257. https://doi.org/10.1038/nm.2235

Gong, N., Hagopian, G., Holmes, T.C., Luo, Z.D., Xu, X., 2019. Functional reorganization of local circuit connectivity in superficial spinal dorsal horn with neuropathic pain states. eNeuro 6. https://doi.org/10.1523/ENEURO.0272-19.2019

Gradwell, M.A., Callister, R.J., Graham, B.A., 2020. Reviewing the case for compromised spinal inhibition in neuropathic pain. J. Neural Transm. 127, 481–503. https://doi.org/10.1007/s00702-019-02090-0

Grajales-Reyes, J.G., Copits, B.A., Lie, F., Yu, Y., Avila, R., Vogt, S.K., Huang, Y., Banks, A.R., Rogers, J.A., Gereau, R.W., Golden, J.P., 2021. Surgical implantation of wireless, battery-free optoelectronic epidural implants for optogenetic manipulation of spinal cord circuits in mice. Nat. Protoc. 16, 3072–3088. https://doi.org/10.1038/s41596-021-00532-2

Grenald, S.A., Young, M.A., Wang, Y., Ossipov, M.H., Ibrahim, M.M., Largent-Milnes, T.M., Vanderah, T.W., 2017. Synergistic attenuation of chronic pain using mu opioid and cannabinoid receptor 2 agonists. Neuropharmacology 116, 59–70. https://doi.org/10.1016/j.neuropharm.2016.12.008

Gross, M.K., Dottori, M., Goulding, M., 2002. Lbx1 specifies somatosensory association interneurons in the dorsal spinal cord. Neuron 34, 535–549. https://doi.org/10.1016/S0896-6273(02)00690-6

Grudt, T.J., Perl, E.R., 2002. Correlations between neuronal morphology and electro-physiological features in the rodent superficial dorsal horn. J. Physiol. 540, 189–207. https://doi.org/10.1113/jphysiol.2001.012890

Guo, Z., Zhao, C., Huang, M., Huang, T., Fan, M., Xie, Z., Chen, Y., Zhao, X., Xia, G., Geng, J., Cheng, L., 2012. Tlx1/3 and Ptf1a Control the Expression of Distinct Sets of Transmitter and Peptide Receptor Genes in the Developing Dorsal Spinal Cord. J. Neurosci. 32, 8509–8520. https://doi.org/10.1523/JNEUROSCI.6301-11.2012

Gupta, S., Gautam, M., Prasoon, P., Kumar, R., Ray, S.B., Kaler Jhajhria, S., 2019. Involvement of Neuropeptide y in Post-Incisional Nociception in Rats. Ann. Neurosci. 25, 268–276. https://doi.org/10.1159/000495130

Gupte, T.M., Malik, R.U., Sommese, R.F., Ritt, M., Sivaramakrishnan, S., 2017. Priming GPCR signaling through the synergistic effect of two G proteins. Proc. Natl. Acad. Sci. U. S. A. 114, 3756–3761. https://doi.org/10.1073/pnas.1617232114

Gurevich, V. V., Gurevich, E. V., 2020. Biased GPCR signaling: Possible mechanisms and inherent limitations. Pharmacol. Ther. 211, 107540. https://doi.org/10.1016/j.pharmthera.2020.107540

Gutierrez-Mecinas, M., Bell, A., Polgár, E., Watanabe, M., Todd, A.J., 2019. Expression of Neuropeptide FF Defines a Population of Excitatory Interneurons in the Superficial Dorsal Horn of the Mouse Spinal Cord that Respond to Noxious and Pruritic Stimuli. Neuroscience 416, 281–293. https://doi.org/10.1016/j.neuroscience.2019.08.013

Gutierrez-Mecinas, M., Furuta, T., Watanabe, M., Todd, A.J., 2016. A quantitative study of neurochemically defined excitatory interneuron populations in laminae I–III of the mouse spinal cord. Mol. Pain 12, 1–18. https://doi.org/10.1177/1744806916629065

Hachisuka, J., Chiang, M.C., Ross, S.E., 2018. Itch and neuropathic itch. Pain 159, 603–609. https://doi.org/10.1097/j.pain.0000000000001141

Haenraets, K., Albisetti, G.W., Foster, E., Wildner, H., 2018. Adeno-associated Virus-mediated Transgene Expression in Genetically Defined Neurons of the Spinal Cord. J. Vis. Exp. 1–11. https://doi.org/10.3791/57382

Haenraets, K., Foster, E., Johannssen, H., Kandra, V., Frezel, N., Steffen, T., Jaramillo, V., Paterna, J.C., Zeilhofer, H.U., Wildner, H., 2017. Spinal nociceptive circuit analysis with recombinant adeno-associated viruses: the impact of serotypes and promoters. J. Neurochem. 142, 721–733. https://doi.org/10.1111/jnc.14124

Hama, A., Yano, M., Sotogawa, W., Fujii, R., Awaga, Y., Natsume, T., Hayashi, I., Takamatsu, H., 2021. Pharmacological modulation of brain activation to non-noxious stimulation in a cynomolgus macaque model of peripheral nerve injury. Mol. Pain 17, 1–3. https://doi.org/10.1177/17448069211008697

Han, S., Soleiman, M., Soden, M., Zweifel, L., Palmiter, R.D., 2015. Elucidating an Affective

Pain Circuit that Creates a Threat Memory. Cell 162, 363–374. https://doi.org/10.1016/j.cell.2015.05.057

Häring, M., Zeisel, A., Hochgerner, H., Rinwa, P., Jakobsson, J.E.T., Lönnerberg, P., La Manno, G., Sharma, N., Borgius, L., Kiehn, O., Lagerström, M.C., Linnarsson, S., Ernfors, P., 2018. Neuronal atlas of the dorsal horn defines its architecture and links sensory input to transcriptional cell types. Nat. Neurosci. 21, 869–880. https://doi.org/10.1038/s41593-018-0141-1

Harrison, C., Traynor, J.R., 2003. The [35S]GTPγS binding assay: Approaches and applications in pharmacology. Life Sci. 74, 489–508. https://doi.org/10.1016/j.lfs.2003.07.005

Hellman, A., Maietta, T., Clum, A., Byraju, K., Raviv, N., Staudt, M.D., Jeannotte, E., Ghoshal, G., Shin, D., Neubauer, P., Williams, E., Heffter, T., Burdette, C., Qian, J., Nalwalk, J., Pilitsis, J.G., 2021a. Pilot study on the effects of low intensity focused ultrasound in a swine model of neuropathic pain. J. Neurosurg. 1–8. https://doi.org/10.3171/2020.9.jns202962

Hellman, A., Maietta, T., Clum, A., Byraju, K., Raviv, N., Staudt, M.D., Jeannotte, E., Nalwalk, J., Belin, S., Poitelon, Y., Pilitsis, J.G., 2021b. Development of a common peroneal nerve injury model in domestic swine for the study of translational neuropathic pain treatments. J. Neurosurg. 1–8. https://doi.org/10.3171/2020.9.jns202961

Henschke, N., Kamper, S.J., Maher, C.G., 2015. The epidemiology and economic consequences of pain. Mayo Clin. Proc. 90, 139–147. https://doi.org/10.1016/j.mayocp.2014.09.010

Hernandez-Miranda, L.R., Müller, T., Birchmeier, C., 2017. The dorsal spinal cord and hindbrain: From developmental mechanisms to functional circuits. Dev. Biol. 432, 34–42. https://doi.org/10.1016/j.ydbio.2016.10.008

Hökfelt, T., Brumovsky, P., Shi, T., Pedrazzini, T., Villar, M., 2007. NPY and pain as seen from the histochemical side. Peptides 28, 365–372. https://doi.org/10.1016/j.peptides.2006.07.024

Hökfelt, T., Zhang, X., Wiesenfeld-Hallin, Z., 1994. Messenger plasticity in primary sensory neurons following axotomy and its functional implications. Trends Neurosci. 17, 22–30. https://doi.org/10.1016/0166-2236(94)90031-0

Holtbäck, U., Brismar, H., DiBona, G.F., Fu, M., Greengard, P., Aperia, A., 1999. Receptor recruitment: A mechanism for interactions between G protein-coupled receptors. Proc. Natl. Acad. Sci. U. S. A. 96, 7271–7275. https://doi.org/10.1073/pnas.96.13.7271

Holzer, P., Reichmann, F., Farzi, A., 2012. Neuropeptide Y, peptide YY and pancreatic polypeptide in the gut-brain axis. Neuropeptides 46, 261–274. https://doi.org/10.1016/j.npep.2012.08.005

Hoot, M.R., Sim-Selley, L.J., Poklis, J.L., Abdullah, R.A., Scoggins, K.L., Selley, D.E., Dewey, W.L., 2010. Chronic constriction injury reduces cannabinoid receptor 1 activity in the rostral anterior cingulate cortex of mice. Brain Res. 1339, 18–25.

https://doi.org/10.1016/j.brainres.2010.03.105

Horioka, M., Ceraudo, E., Lorenzen, E., Sakmar, T.P., Huber, T., 2021. Purinergic Receptors Crosstalk with CCR5 to Amplify Ca2+ Signaling. Cell. Mol. Neurobiol. 41, 1085–1101. https://doi.org/10.1007/s10571-020-01002-1

Horwitz, L.R., Lee, H., Hor, C.C., Shen, F.Y., Cai, W., Li, C., Pai, E.L.-L., Fung, T.L.R., Rovcanin, I., Pipe, K.P., Xu, X.Z.S., Cai, D., Duan, B., 2022. A Spinal Circuit That Transmits Innocuous Cool Sensations. bioRxiv 2022.03.23.485555. https://doi.org/https://doi.org/10.1101/2022.03.23.485555

Howell, O.W., Scharfman, H.E., Herzog, H., Sundstrom, L.E., Beck-Sickinger, A., Gray, W.P., 2003. Neuropeptide Y is neuroproliferative for post-natal hippocampal precursor cells. J. Neurochem. 86, 646–659. https://doi.org/10.1046/j.1471-4159.2003.01895.x

Hu, J., Huang, T., Li, T., Guo, Z., Cheng, L., 2012. C-Maf is required for the development of dorsal horn laminae III/IV neurons and mechanoreceptive DRG axon projections. J. Neurosci. 32, 5362–5373. https://doi.org/10.1523/JNEUROSCI.6239-11.2012

Hua, X.Y., Boublik, J.H., Spicer, M.A., Rivier, J.E., Brown, M.R., Yaksh, T.L., 1991. The antinociceptive effects of spinally administered neuropeptide Y in the rat: systematic studies on structure-activity relationship. J. Pharmacol. Exp. Ther. 258, 243–8.

Huang, J., Polgár, E., Solinski, H.J., Mishra, S.K., Tseng, P.Y., Iwagaki, N., Boyle, K.A., Dickie, A.C., Kriegbaum, M.C., Wildner, H., Zeilhofer, H.U., Watanabe, M., Riddell, J.S., Todd, A.J., Hoon, M.A., 2018. Circuit dissection of the role of somatostatin in itch and pain. Nat. Neurosci. 21, 707–716. https://doi.org/10.1038/s41593-018-0119-z

Huang, M., Huang, T., Xiang, Y., Xie, Z., Chen, Y., Yan, R., Xu, J., Cheng, L., 2008. Ptf1a, Lbx1 and Pax2 coordinate glycinergic and peptidergic transmitter phenotypes in dorsal spinal inhibitory neurons. Dev. Biol. 322, 394–405. https://doi.org/10.1016/j.ydbio.2008.06.031

Hughes, D.I., Scott, D.T., Todd, A.J., Riddell, J.S., 2003. Lack of Evidence for Sprouting of Aβ Afferents into the Superficial Laminas of the Spinal Cord Dorsal Horn after Nerve Section. J. Neurosci. 23, 9491–9499. https://doi.org/10.1523/jneurosci.23-29-09491.2003

Hur, E.M., Kim, K.T., 2002. G protein-coupled receptor signalling and cross-talk: Achieving rapidity and specificity. Cell. Signal. 14, 397–405. https://doi.org/10.1016/S0898-6568(01)00258-3

Ibrahim, K.M., Ariffin, M.Z., Khanna, S., 2021. Modulation of Septo-Hippocampal Neural Responses in Anesthetized and Behaving Rats by Septal AMPA Receptor Mechanisms. Front. Neural Circuits 15, 1–22. https://doi.org/10.3389/fncir.2021.663633

Inquimbert, P., Bartels, K., Babaniyi, O.B., Barrett, L.B., Tegeder, I., Scholz, J., 2012. Peripheral nerve injury produces a sustained shift in the balance between glutamate release and uptake in the dorsal horn of the spinal cord. Pain 153, 2422–2431.

https://doi.org/10.1016/j.pain.2012.08.011

Inquimbert, P., Moll, M., Latremoliere, A., Tong, C.K., Whang, J., Sheehan, G.F., Smith, B.M., Korb, E., Athié, M.C.P., Babaniyi, O., Ghasemlou, N., Yanagawa, Y., Allis, C.D., Hof, P.R., Scholz, J., 2018. NMDA Receptor Activation Underlies the Loss of Spinal Dorsal Horn Neurons and the Transition to Persistent Pain after Peripheral Nerve Injury. Cell Rep. 23, 2678–2689. https://doi.org/10.1016/j.celrep.2018.04.107

Intondi, A.B., Dahlgren, M.N., Eilers, M.A., Taylor, B.K., 2008. Intrathecal neuropeptide Y reduces behavioral and molecular markers of inflammatory or neuropathic pain. Pain 137, 352–365. https://doi.org/10.1016/j.pain.2007.09.016

Jakobsson, J.E.T., Ma, H., Lagerström, M.C., 2019. Neuropeptide Y in itch regulation. Neuropeptides 78, 101976. https://doi.org/10.1016/j.npep.2019.101976

Jendryka, M., Palchaudhuri, M., Ursu, D., van der Veen, B., Liss, B., Kätzel, D., Nissen, W., Pekcec, A., 2019. Pharmacokinetic and pharmacodynamic actions of clozapine-N-oxide, clozapine, and compound 21 in DREADD-based chemogenetics in mice. Sci. Rep. 9, 1–14. https://doi.org/10.1038/s41598-019-41088-2

Jensen, M.P., Chodroff, M.J., Dworkin, R.H., 2007. The impact of neuropathic pain on health-related quality of life: Review and implications. Neurology 68, 1178–1182. https://doi.org/10.1212/01.wnl.0000259085.61898.9e

Jensen, T.S., Finnerup, N.B., 2014. Allodynia and hyperalgesia in neuropathic pain: Clinical manifestations and mechanisms. Lancet Neurol. 13, 924–935. https://doi.org/10.1016/S1474-4422(14)70102-4

Ji, R., Zhang, X., Wiesenfeld-Hallin, Z., Hokfelt, T., 1994. Expression of neuropeptide Y and neuropeptide Y (Y1) receptor mRNA in rat spinal cord and dorsal root ganglia following peripheral tissue inflammation. J. Neurosci. 14, 6423–6434. https://doi.org/10.1523/jneurosci.14-11-06423.1994

Ji, R.R., Kohno, T., Moore, K.A., Woolf, C.J., 2003. Central sensitization and LTP: Do pain and memory share similar mechanisms? Trends Neurosci. 26, 696–705. https://doi.org/10.1016/j.tins.2003.09.017

Jiang, L.Y., Li, S.R., Zhao, F.Y., Spanswick, D., Lin, M.T., 2010. Norepinephrine can Act via α2-Adrenoceptors to Reduce the Hyper-excitability of Spinal Dorsal Horn Neurons Following Chronic Nerve Injury. J. Formos. Med. Assoc. 109, 438–445. https://doi.org/10.1016/S0929-6646(10)60075-7

Jiang, N., Furue, H., Katafuchi, T., Yoshimura, M., 2003. Somatostatin directly inhibits substantia gelatinosa neurons in adult rat spinal dorsal horn in vitro. Neurosci. Res. 47, 97–107. https://doi.org/10.1016/S0168-0102(03)00183-4

Jordan, B.A., Devi, L.A., 1999. G-protein-coupled receptor heterodimerization modulates receptor function. Nature 399, 697–700. https://doi.org/10.1038/21441

Jung, S.J., Chang, J.W., Won, R., Cha, M.H., Nam, T.S., Lee, H.J., Lee, B.H., 2009. Modulation of neuropathic pain by galanin and neuropeptide y at the level of the medulla in rats. Int. J. Neurosci. 119, 1941–1955. https://doi.org/10.1080/00207450903263661

Kambiz, S., Baas, M., Duraku, L.S., Kerver, A.L., Koning, A.H.J., Walbeehm, E.T., Ruigrok, T.J.H., 2014. Innervation mapping of the hind paw of the rat using Evans Blue extravasation, Optical Surface Mapping and CASAM. J. Neurosci. Methods 229, 15–27. https://doi.org/10.1016/j.jneumeth.2014.03.015

Kar, S., Quirion, R., 1992. Quantitative autoradiographic localization of [125I] neuropeptide Y receptor binding sites in rat spinal cord and the effects of neonatal capsaicin, dorsal rhizotomy and peripheral axotomy. Brain Res. 574, 333–337. https://doi.org/10.1016/0006-8993(92)90836-X

Kazantzis, N.P., Casey, S.L., Seow, P.W., Mitchell, V.A., Vaughan, C.W., 2016. Opioid and cannabinoid synergy in a mouse neuropathic pain model. Br. J. Pharmacol. 173, 2521–2531. https://doi.org/10.1111/bph.13534

Kehlet, H., Jensen, T.S., Woolf, C.J., 2006. Persistent postsurgical pain: risk factors and prevention. Lancet 367, 1618–1625. https://doi.org/10.1016/S0140-6736(06)68700-X

Kiguchi, N., Fukazawa, Y., Saika, A., Uta, D., Saika, F., Nakamura, T.Y., Ko, M.C., Kishioka, S., 2021. Chemogenetic activation of central gastrin-releasing peptide-expressing neurons elicits itch-related scratching behavior in male and female mice. Pharmacol. Res. Perspect. 9, 1–11. https://doi.org/10.1002/prp2.790

Kim, A.Y., Tang, Z., Liu, Q., Patel, K.N., Maag, D., Geng, Y., Dong, X., 2008. Pirt, a Phosphoinositide-Binding Protein, Functions as a Regulatory Subunit of TRPV1. Cell 133, 475–485. https://doi.org/10.1016/j.cell.2008.02.053

Kim, S.J., Chung, W.H., Rhim, H., Eun, S.Y., Jung, S.J., Kim, J., 2002. Postsynaptic action mechanism of somatostatin on the membrane excitability in spinal substantia gelatinosa neurons of juvenile rats. Neuroscience 114, 1139–1148. https://doi.org/10.1016/S0306-4522(02)00245-2

Kim, Y.S., Anderson, M., Park, K., Zheng, Q., Agarwal, A., Gong, C., Saijilafu, Young, L.A., He, S., LaVinka, P.C., Zhou, F., Bergles, D., Hanani, M., Guan, Y., Spray, D.C., Dong, X., 2016. Coupled Activation of Primary Sensory Neurons Contributes to Chronic Pain. Neuron 91, 1085–1096. https://doi.org/10.1016/j.neuron.2016.07.044

Klapoetke, N.C., Murata, Y., Kim, S.S., Pulver, S.R., Birdsey-Benson, A., Cho, Y.K., Morimoto, T.K., Chuong, A.S., Carpenter, E.J., Tian, Z., Wang, J., Xie, Y., Yan, Z., Zhang, Y., Chow, B.Y., Surek, B., Melkonian, M., Jayaraman, V., Constantine-Paton, M., Wong, G.K.S., Boyden, E.S., 2014. Independent optical excitation of distinct neural populations. Nat. Methods 11, 338–346. https://doi.org/10.1038/nmeth.2836

Kline IV, R.H., Wiley, R.G., 2008. Spinal μ-opioid receptor-expressing dorsal horn neurons: Role in nociception and morphine antinociception. J. Neurosci. 28, 904–913.

https://doi.org/10.1523/JNEUROSCI.4452-07.2008

Knight, K.H., Brand, F.M., Mchaourab, A.S., Veneziano, G., 2007. Implantable intrathecal pumps for chronic pain: Highlights and updates. Croat. Med. J. 48, 22–34.

Koch, S.C., Acton, D., Goulding, M., 2018. Spinal Circuits for Touch, Pain, and Itch. Annu. Rev. Physiol. 80, 189–217. https://doi.org/10.1146/annurev-physiol-022516-034303

Kohno, T., Ji, R.R., Ito, N., Allchorne, A.J., Befort, K., Karchewski, L.A., Woolf, C.J., 2005. Peripheral axonal injury results in reduced μ opioid receptor pre- and post-synaptic action in the spinal cord. Pain 117, 77–87. https://doi.org/10.1016/j.pain.2005.05.035

Kopach, O., Medvediev, V., Krotov, V., Borisyuk, A., Tsymbaliuk, V., Voitenko, N., 2017. Opposite, bidirectional shifts in excitation and inhibition in specific types of dorsal horn interneurons are associated with spasticity and pain post-SCI. Sci. Rep. 7, 1–15. https://doi.org/10.1038/s41598-017-06049-7

Kopp, J., Zhang, X., Pedrazzini, T., Herzog, H., Kresse, A., Wong, H., Walsh, J.H., Ho, T., 2010. Expression of the Neuropeptide Y Y1 Receptor in the CNS of Rat and of Wild-Type and Y1 Receptor Knock-out Mice. Focus on Immunohistochemical Localization. Neuroscience 111, 443–532.

Kuner, R., 2010. Central mechanisms of pathological pain. Nat. Med. 16, 1258–1266. https://doi.org/10.1038/nm.2231

Kuphal, K.E., Solway, B., Pedrazzini, T., Taylor, B.K., 2008. Y1 receptor knockout increases nociception and prevents the anti-allodynic actions of NPY. Nutrition 24, 885–891. https://doi.org/10.1016/j.nut.2008.06.022

Kusunose, N., Koyanagi, S., Hamamura, K., Matsunaga, N., Yoshida, M., Uchida, T., Tsuda, M., Inoue, K., Ohdo, S., 2010. Molecular basis for the dosing time-dependency of anti-allodynic effects of gabapentin in a mouse model of neuropathic pain. Mol. Pain 6, 2–9. https://doi.org/10.1186/1744-8069-6-83

Laird, J.M.A., Bennett, G.J., 1993. An electrophysiological study of dorsal horn neurons in the spinal cord of rats with an experimental peripheral neuropathy. J. Neurophysiol. 69, 2072–2085. https://doi.org/10.1152/jn.1993.69.6.2072

Lappi, D., Wiley, R., 2012. Immunotoxins and Neuropeptide-Toxin Conjugates Experimental Applications. Mini-Reviews Med. Chem. 4, 585–595. https://doi.org/10.2174/1389557043403882

Latremoliere, A., Woolf, C.J., 2009. Central Sensitization: A Generator of Pain Hypersensitivity by Central Neural Plasticity. J. Pain 10, 895–926. https://doi.org/10.1016/j.jpain.2009.06.012

Lee, K.Y., Ratté, S., Prescott, S.A., 2019. Excitatory neurons are more disinhibited than inhibitory neurons by chloride dysregulation in the spinal dorsal horn. Elife 8, 1–23.

https://doi.org/10.7554/eLife.49753

Leith, J.L., Koutsikou, S., Lumb, B.M., Apps, R., 2010. Spinal processing of noxious and innocuous cold information: Differential modulation by the periaqueductal gray. J. Neurosci. 30, 4933–4942. https://doi.org/10.1523/JNEUROSCI.0122-10.2010

Lemons, L.L., Wiley, R.G., 2012. Neuropeptide Y receptor-expressing dorsal horn neurons: Role in nocifensive reflex and operant responses to aversive cold after CFA inflammation. Neuroscience 216, 158–166. https://doi.org/10.1016/j.neuroscience.2012.04.006

Levac, B.A.R., O'Dowd, B.F., George, S.R., 2002. Oligomerization of opioid receptors: Generation of novel signaling units. Curr. Opin. Pharmacol. 2, 76–81. https://doi.org/10.1016/S1471-4892(02)00124-8

Levitt, E.S., Purington, L.C., Traynor, J.R., 2011. Gi/o-coupled receptors compete for signaling to adenylyl cyclase in SH-SY5Y cells and reduce opioid-mediated cAMP overshoot. Mol. Pharmacol. 79, 461–471. https://doi.org/10.1124/mol.110.064816

Li, L., Rutlin, M., Abraira, V.E., Cassidy, C., Kus, L., Gong, S., Jankowski, M.P., Luo, W., Heintz, N., Koerber, H.R., Woodbury, C.J., Ginty, D.D., 2011. The functional organization of cutaneous low-threshold mechanosensory neurons. Cell 147, 1615–1627. https://doi.org/10.1016/j.cell.2011.11.027

Liu, Y., Latremoliere, A., Li, X., Zhang, Z., Chen, M., Wang, X., Fang, C., Zhu, J., Alexandre, C., Gao, Z., Chen, B., Ding, X., Zhou, J.Y., Zhang, Y., Chen, C., Wang, K.H., Woolf, C.J., He, Z., 2018. Touch and tactile neuropathic pain sensitivity are set by corticospinal projections. Nature 561, 547–550. https://doi.org/10.1038/s41586-018-0515-2

Lolignier, S., Eijkelkamp, N., Wood, J.N., 2014. Mechanical allodynia. Pflugers Arch. Eur. J. Physiol. 467, 133–139. https://doi.org/10.1007/s00424-014-1532-0

Lu, V.B., Biggs, J.E., Stebbing, M.J., Balasubramanyan, S., Todd, K.G., Lai, A.Y., Colmers, W.F., Dawbarn, D., Ballanyi, K., Smith, P.A., 2009. Brain-derived neurotrophic factor drives the changes in excitatory synaptic transmission in the rat superficial dorsal horn that follow sciatic nerve injury. J. Physiol. 587, 1013–1032. https://doi.org/10.1113/jphysiol.2008.166306

Lu, Y., Ji, R., Xiong, L., Lu, Y., Dong, H., Gao, Y., Gong, Y., Ren, Y., Gu, N., 2013. A feed-forward spinal cord glycinergic neural circuit gates mechanical allodynia. J. Clin. Invest. 123, 4050–4062. https://doi.org/10.1172/JCI70026.4050

Lu, Y., Perl, E.R., 2005. Modular Organization of Excitatory Circuits between Neurons of the Spinal Superficial Dorsal Horn (Laminae I and II). J. Neurosci. 25, 3900–3907. https://doi.org/10.1523/JNEUROSCI.0102-05.2005

Ma, H., Gao, T., Jakobsson, J.E.T., Weman, H.M., Xu, B., Larhammar, D., Lagerström, M.C., 2020. The Neuropeptide Y Y2 Receptor Is Coexpressed with Nppb in Primary Afferent Neurons and Y2 Activation Reduces Histaminergic and IL-31-Induced Itch. J. Pharmacol.

Exp. Ther. 372, 73–82. https://doi.org/10.1124/jpet.119.262584

Ma, Q., 2010. Labeled lines meet and talk: Population coding of somatic sensations. J. Clin. Invest. 120, 3773–3778. https://doi.org/10.1172/JCI43426

MacDonald, D.I., Luiz, A.P., Iseppon, F., Millet, Q., Emery, E.C., Wood, J.N., 2021. Silent cold-sensing neurons contribute to cold allodynia in neuropathic pain. Brain 144, 1711–1726. https://doi.org/10.1093/brain/awab086

Maeda, N., Onimura, M., Ohmoto, M., Inui, T., Yamamoto, T., Matsumoto, I., Abe, K., 2009. Spatial differences in molecular characteristics of the pontine parabrachial nucleus. Brain Res. 1296, 24–34. https://doi.org/10.1016/j.brainres.2009.07.098

Magnussen, C., Hung, S.-P., Ribeiro-da-Silva, A., 2015. Novel Expression Pattern of Neuropeptide Y Immunoreactivity in the Peripheral Nervous System in a Rat Model of Neuropathic Pain. Mol. Pain 11, s12990-015–0029. https://doi.org/10.1186/s12990-015-0029-y

Mahinda, T.B., Taylor, B.K., 2004. Intrathecal neuropeptide Y inhibits behavioral and cardiovascular responses to noxious inflammatory stimuli in awake rats. Physiol. Behav. 80, 703–711. https://doi.org/10.1016/j.physbeh.2003.12.007

Maiarù, M., Leese, C., Certo, M., Echeverria-Altuna, I., Mangione, A.S., Arsenault, J., Davletov, B., Hunt, S.P., 2018. Selective neuronal silencing using synthetic botulinum molecules alleviates chronic pain in mice. Sci. Transl. Med. 10, 1–12. https://doi.org/10.1126/scitranslmed.aar7384

Malet, M., Leiguarda, C., Gastón, G., McCarthy, C., Brumovsky, P., 2017. Spinal activation of the NPY Y1 receptor reduces mechanical and cold allodynia in rats with chronic constriction injury. Peptides 92, 38–45. https://doi.org/10.1016/j.peptides.2017.04.005

Malmberg, A.B., Chen, C., Tonegawa, S., Basbaum, A.I., 1997. Preserved acute pain and reduced neuropathic pain in mice lacking PKCγ. Science (80-.). 278, 279–283. https://doi.org/10.1126/science.278.5336.279

Mark, M.A., Colvin, L.A., Duggan, A.W., 1998. Spontaneous release of immunoreactive neuropeptide y from the central terminals of large diameter primary afferents of rats with peripheral nerve injury. Neuroscience 83, 581–589. https://doi.org/10.1016/S0306-4522(97)00402-8

Mark, M.A., Jarrott, B., Colvin, L.A., MacMillan, S.J.A., Duggan, A.W., 1997. The release of immunoreactive neuropeptide Y in the spinal cord of the anaesthetized rat and cat. Brain Res. 754, 195–203. https://doi.org/10.1016/S0006-8993(97)00061-9

Martínez-Navarro, M., Maldonado, R., Baños, J.E., 2019. Why mu-opioid agonists have less analgesic efficacy in neuropathic pain? Eur. J. Pain (United Kingdom) 23, 435–454. https://doi.org/10.1002/ejp.1328

Marvizon, J.C., Chen, W., Fu, W., Taylor, B.K., 2019. Neuropeptide Y release in the rat spinal cord measured with Y1 receptor internalization is increased after nerve injury. Neuropharmacology 158, 107732. https://doi.org/10.1016/j.neuropharm.2019.107732

Mathé, A.A., Michaneck, M., Berg, E., Charney, D.S., Murrough, J.W., 2020. A randomized controlled trial of intranasal Neuropeptide Y in patients with major depressive disorder. Int. J. Neuropsychopharmacol. 23, 783–790. https://doi.org/10.1093/ijnp/pyaa054

McDermott, B., Bell, D., 2007. NPY and Cardiac Diseases. Curr. Top. Med. Chem. 7, 1692–1703. https://doi.org/10.2174/156802607782340939

Meixiong, J., Dong, X., Weng, H.J., 2020. Neuropathic Itch. Cells 9, 1–6. https://doi.org/10.3390/cells9102263

Mellado, M.L., Gibert-Rahola, J., Chover, A.J., Micó, J.A., 1996. Effect on nociception of intracerebroventricular administration of low doses of neuropeptide Y in mice. Life Sci. 58, 2409–2414. https://doi.org/10.1016/0024-3205(96)00244-5

Melnick, I. V., 2012. Cell type-specific postsynaptic effects of neuropeptide Y in substantia gelatinosa neurons of the rat spinal cord. Synapse 66, 640–649. https://doi.org/10.1002/syn.21550

Melzack, R., Wall, P.D., 1965. Pain mechanisms: A new theory. Science (80-.). 150, 971–979. https://doi.org/10.1126/science.150.3699.971

Merighi, A., 2018. The histology, physiology, neurochemistry and circuitry of the substantia gelatinosa Rolandi (lamina II) in mammalian spinal cord. Prog. Neurobiol. 169, 91–134. https://doi.org/10.1016/j.pneurobio.2018.06.012

Miracourt, L.S., Dallel, R., Voisin, D.L., 2007. Glycine inhibitory dysfunction turns touch into pain through PKCgamma interneurons. PLoS One 2, 1–15. https://doi.org/10.1371/journal.pone.0001116

Misery, L., Brenaut, E., Le Garrec, R., Abasq, C., Genestet, S., Marcorelles, P., Zagnoli, F., 2014. Neuropathic pruritus. Nat. Rev. Neurol. 10, 408–416. https://doi.org/10.1038/nrneurol.2014.99

Mishra, S.K., Hoon, M.A., 2013. The cells and circuitry for itch responses in mice. Science (80-.). 340, 968–971. https://doi.org/10.1126/science.1233765

Miyakawa, A., Furue, H., Katafuchi, T., Jiang, N., Yasaka, T., Kato, G., Yoshimura, M., 2005. Action of neuropeptide Y on nociceptive transmission in substantia gelatinosa of the adult rat spinal dorsal horn. Neuroscience 134, 595–604. https://doi.org/10.1016/j.neuroscience.2005.04.045

Moehring, F., Halder, P., Seal, R.P., Stucky, C.L., 2018. Uncovering the Cells and Circuits of Touch in Normal and Pathological Settings. Neuron 100, 349–360. https://doi.org/10.1016/j.neuron.2018.10.019

Mogil, J.S., 2019. The translatability of pain across species. Philos. Trans. R. Soc. B Biol. Sci. 374, 0–3. https://doi.org/10.1098/rstb.2019.0286

Moran, T.D., Colmers, W.F., Smith, P.A., 2004. Opioid-like actions of neuropeptide Y in rat substantia gelatinosa: Y1 suppression of inhibition and Y2 suppression of excitation. J. Neurophysiol. 92, 3266–3275. https://doi.org/10.1152/jn.00096.2004

Moreno-García, A., Kun, A., Calero, O., Medina, M., Calero, M., 2018. An overview of the role of lipofuscin in age-related neurodegeneration. Front. Neurosci. 12, 1–13. https://doi.org/10.3389/fnins.2018.00464

Müller, T., Brohmann, H., Pierani, A., Heppenstall, P.A., Lewin, G.R., Jessell, T.M., Birchmeier, C., 2002. The homeodomain factor Lbx1 distinguishes two major programs of neuronal differentiation in the dorsal spinal cord. Neuron 34, 551–562. https://doi.org/10.1016/S0896-6273(02)00689-X

Mullins, D., Kirby, D., Hwa, J., Guzzi, M., Rivier, J., Parker, E., 2001. Identification of potent and selective neuropeptide Y Y1 receptor agonists with orexigenic activity in vivo. Mol. Pharmacol. 60, 534–540.

Murase, K., Nedeljkov, V., Randić, M., 1982. The actions of neuropeptides on dorsal horn neurons in the rat spinal cord slice preparation: an intracellular study. Brain Res. 234, 170–176. https://doi.org/10.1016/0006-8993(82)90483-8

Naveilhan, P., Canals, J.M., Valjakka, A., Vartiainen, J., Arenas, E., Ernfors, P., 2001a. Neuropeptide Y alters sedation through a hypothalamic Y1-mediated mechanism. Eur. J. Neurosci. 13, 2241–2246. https://doi.org/10.1046/j.0953-816X.2001.01601.x

Naveilhan, P., Hassani, H., Lucas, G., Blakeman, K.H., Hao, J.X., Xu, X.J., Wiesenfeld-Hallin, Z., Thorén, P., Ernfors, P., 2001b. Reduced antinociception and plasma extravasation in mice lacking a neuropeptide Y receptor. Nature 409, 513–517. https://doi.org/10.1038/35054063

Navratilova, E., Xie, J.Y., King, T., Porreca, F., 2013. Evaluation of reward from pain relief. Ann. N. Y. Acad. Sci. 1282, 1–11. https://doi.org/10.1111/nyas.12095

Nazli, M., Morris, R., 2000. Expression of neuropeptide Y and neuropeptide Y Y1 receptors and neuronal markers following axotomy in the rat spinal cord and gracile nucleus. Anat. Histol. Embryol. 29, 97–101. https://doi.org/10.1046/j.1439-0264.2000.00242.x

Nelson, T.S., 2019. Dorsal Horn PKCγ Interneurons Mediate Mechanical Allodynia through 5-HT 2A R-Dependent Structural Reorganization. J. Neurosci. 39, 6221–6223. https://doi.org/https://doi.org/10.1523/JNEUROSCI.0291-19.2019

Nelson, T.S., Fu, W., Donahue, R.R., Corder, G.F., Hökfelt, T., Wiley, R.G., Taylor, B.K., 2019. Facilitation of neuropathic pain by the NPY Y1 receptor-expressing subpopulation of excitatory interneurons in the dorsal horn. Sci. Rep. 9, 7248. https://doi.org/10.1038/s41598-019-43493-z

Nelson, T.S., Sinha, G.P., Santos, D.F., Jukkola, P., Prasoon, P., Winter, M.K., McCarson, K.E., Smith, B.N., Taylor, B.K., 2022. Spinal neuropeptide Y Y1 receptor-expressing neurons are a pharmacotherapeutic target for the alleviation of neuropathic pain. Proc. Natl. Acad. Sci. In Revisio.

Nelson, T.S., Taylor, B.K., 2021. Targeting spinal neuropeptide Y1 receptor-expressing interneurons to alleviate chronic pain and itch. Prog. Neurobiol. 196, 101894. https://doi.org/10.1016/j.pneurobio.2020.101894

Neumann, S., Braz, J.M., Skinner, K., Llewellyn-Smith, I.J., Basbaum, A.I., 2008. Innocuous, Not Noxious, Input Activates PKC Interneurons of the Spinal Dorsal Horn via Myelinated Afferent Fibers. J. Neurosci. 28, 7936–7944. https://doi.org/10.1523/jneurosci.1259-08.2008

Okamoto, M., Baba, H., Goldstein, P.A., Higashi, H., Shimoji, K., Yoshimura, M., 2001. Functional reorganization of sensory pathways in the rat spinal dorsal horn following peripheral nerve injury. J. Physiol. 532, 241–250. https://doi.org/10.1111/j.1469-7793.2001.0241g.x

Ossipov, M.H., Morimura, K., Porreca, F., 2014. Descending pain modulation and chronification of pain. Curr. Opin. Support. Palliat. Care 8, 143–151. https://doi.org/10.1097/SPC.0000000000000055

Ossipov, M.H., Zhang, E.T., Carvajal, C., Gardell, L., Quirion, R., Dumont, Y., Lai, J., Porreca, F., 2002. Selective mediation of nerve injury-induced tactile hypersensitivity by neuropeptide Y. J. Neurosci. 22, 9858–9867. https://doi.org/10.1523/jneurosci.22-22-09858.2002

Overland, A.C., Kitto, K.F., Chabot-Doré, A.J., Rothwell, P.E., Fairbanks, C.A., Stone, L.S., Wilcox, G.L., 2009. Protein kinase C mediates the synergistic interaction between agonists acting at α2-adrenergic and delta-opioid receptors in spinal cord. J. Neurosci. 29, 13264–13273. https://doi.org/10.1523/JNEUROSCI.1907-09.2009

Pagani, M., Albisetti, G.W., Sivakumar, N., Wildner, H., Santello, M., Johannssen, H.C., Zeilhofer, H.U., 2019. How Gastrin-Releasing Peptide Opens the Spinal Gate for Itch. Neuron 103, 102-117.e5. https://doi.org/10.1016/j.neuron.2019.04.022

Palmiter, R.D., 2018. The Parabrachial Nucleus: CGRP Neurons Function as a General Alarm. Trends Neurosci. 41, 280–293. https://doi.org/10.1016/j.tins.2018.03.007

Pan, H., Fatima, M., Li, A., Lee, H., Cai, W., Horwitz, L., Hor, C.C., Zaher, N., Cin, M., Slade, H., Huang, T., Xu, X.Z.S., Duan, B., 2019. Identification of a Spinal Circuit for Mechanical and Persistent Spontaneous Itch. Neuron 103, 1135-1149.e6. https://doi.org/10.1016/j.neuron.2019.06.016

Parker, S.L., Parker, M.S., Sah, R., Balasubramaniam, A., Sallee, F.R., 2008. Pertussis toxin induces parallel loss of neuropeptide Y Y1 receptor dimers and Gi α subunit function in CHO cells. Eur. J. Pharmacol. 579, 13–25. https://doi.org/10.1016/j.ejphar.2007.10.002

Peier, A.M., Moqrich, A., Hergarden, A.C., Reeve, A.J., Andersson, D.A., Story, G.M., Earley, T.J., Dragoni, I., McIntyre, P., Bevan, S., Patapoutian, A., 2002. A TRP channel that senses cold stimuli and menthol. Cell 108, 705–715. https://doi.org/10.1016/S0092-8674(02)00652-9

Peirs, C., Dallel, R., Todd, A.J., 2020. Recent advances in our understanding of the organization of dorsal horn neuron populations and their contribution to cutaneous mechanical allodynia. J. Neural Transm. 127, 505–525. https://doi.org/10.1007/s00702-020-02159-1

Peirs, C., Seal, R.P., 2016. Neural circuits for pain: Recent advances and current views. Science (80-.). 354, 578–584. https://doi.org/10.7554/eLife.22866

Peirs, C., Williams, S.P.G., Zhao, X., Arokiaraj, C.M., Ferreira, D.W., Noh, M. chul, Smith, K.M., Halder, P., Corrigan, K.A., Gedeon, J.Y., Lee, S.J., Gatto, G., Chi, D., Ross, S.E., Goulding, M., Seal, R.P., 2021. Mechanical Allodynia Circuitry in the Dorsal Horn Is Defined by the Nature of the Injury. Neuron 109, 73-90.e7. https://doi.org/10.1016/j.neuron.2020.10.027

Peirs, C., Williams, S.P.G., Zhao, X., Walsh, C.E., Gedeon, J.Y., Cagle, N.E., Goldring, A.C., Hioki, H., Liu, Z., Marell, P.S., Seal, R.P., 2015. Dorsal Horn Circuits for Persistent Mechanical Pain. Neuron 87, 797–812. https://doi.org/10.1016/j.neuron.2015.07.029

Petitjean, H., B. Bourojeni, F., Tsao, D., Davidova, A., Sotocinal, S.G., Mogil, J.S., Kania, A., Sharif-Naeini, R., 2019. Recruitment of Spinoparabrachial Neurons by Dorsal Horn Calretinin Neurons. Cell Rep. 28, 1429-1438.e4. https://doi.org/10.1016/j.celrep.2019.07.048

Petitjean, H., Pawlowski, S.A., Fraine, S.L., Sharif, B., Hamad, D., Fatima, T., Berg, J., Brown, C.M., Jan, L.Y., Ribeiro-da-Silva, A., Braz, J.M., Basbaum, A.I., Sharif-Naeini, R., 2015. Dorsal Horn Parvalbumin Neurons Are Gate-Keepers of Touch-Evoked Pain after Nerve Injury. Cell Rep. 13, 1246–1257. https://doi.org/10.1016/j.celrep.2015.09.080

Petrou, M., Pop-Busui, R., Foerster, B.R., Edden, R.A., Callaghan, B.C., Harte, S.E., Harris, R.E., Clauw, D.J., Feldman, E.L., 2012. Altered Excitation-inhibition Balance in the Brain of Patients with Diabetic Neuropathy. Acad. Radiol. 19, 607–612. https://doi.org/10.1016/j.acra.2012.02.004

Philip, F., Kadamur, G., Silos, R.G., Woodson, J., Ross, E.M., 2010. Synergistic activation of phospholipase C-β3 by Gαq and Gβγ describes a simple two-state coincidence detector. Curr. Biol. 20, 1327–1335. https://doi.org/10.1016/j.cub.2010.06.013

Pogatzki, E.M., Raja, S.N., 2003. A mouse model of incisional pain. Anesthesiology 99, 1023–1027. https://doi.org/10.1097/00000542-200310000-00041

Polgár, E., Al-Khater, K.M., Shehab, S., Watanabe, M., Todd, A.J., 2008. Large projection neurons in lamina I of the rat spinal cord that lack the neurokinin 1 receptor are densely innervated by VGLUT2-containing axons and possess GluR4-containing AMPA receptors. J. Neurosci. 28, 13150–13160. https://doi.org/10.1523/JNEUROSCI.4053-08.2008

Polgár, E., Dickie, A.C., Gutierrez-Mecinas, M., Bell, A.M., Boyle, K.A., Quillet, R., Rashid, E.A., Clark, R.A., German, M.T., Watanabe, M., Riddell, J.S., Todd, A.J., 2022. Grpr expression defines a population of superficial dorsal horn vertical cells that have a role in both itch and pain. Pain Publish Ah. https://doi.org/10.1097/j.pain.0000000000002677

Polgár, E., Fowler, J.H., McGill, M.M., Todd, A.J., 1999. The types of neuron which contain protein kinase C gamma in rat spinal cord. Brain Res. 833, 71–80. https://doi.org/10.1016/S0006-8993(99)01500-0

Polgar, E., Sardella, T.C.P., Watanabe, M., Todd, A.J., 2011. Quantitative study of NPY-expressing GABAergic neurons and axons in rat spinal dorsal horn. J. Comp. Neurol. 519, 1007–1023. https://doi.org/10.1002/cne.22570

Potter, L.E., Paylor, J.W., Suh, J.S., Tenorio, G., Caliaperumal, J., Colbourne, F., Baker, G., Winship, I., Kerr, B.J., 2016. Altered excitatory-inhibitory balance within somatosensory cortex is associated with enhanced plasticity and pain sensitivity in a mouse model of multiple sclerosis. J. Neuroinflammation 13, 1–20. https://doi.org/10.1186/s12974-016-0609-4

Prut, L., Belzung, C., 2003. The open field as a paradigm to measure the effects of drugs on anxiety-like behaviors: A review. Eur. J. Pharmacol. 463, 3–33. https://doi.org/10.1016/S0014-2999(03)01272-X

Punnakkal, P., von Schoultz, C., Haenraets, K., Wildner, H., Zeilhofer, H.U., 2014. Morphological, biophysical and synaptic properties of glutamatergic neurons of the mouse spinal dorsal horn. J. Physiol. 592, 759–776. https://doi.org/10.1113/jphysiol.2013.264937

Reichling, D.B., Levine, J.D., 2009. Critical role of nociceptor plasticity in chronic pain. Trends Neurosci. 32, 611–618. https://doi.org/10.1016/j.tins.2009.07.007

Rexed, B., 1952. The cytoarchitectonic organization of the spinal cord in the cat. J. Comp. Neurol. 96, 415–495. https://doi.org/10.1002/cne.900960303

Richebé, P., Capdevila, X., Rivat, C., 2018. Persistent Postsurgical Pain: Pathophysiology and Preventative Pharmacologic Considerations. Anesthesiology 129, 590–607. https://doi.org/10.1097/ALN.0000000000002238

Richner, M., Bjerrum, O.J., Nykjaer, A., Vaegter, C.B., 2011. The spared nerve injury (SNI) model of induced mechanical allodynia in mice. J. Vis. Exp. https://doi.org/10.3791/3092

Robinson, S.D., Mueller, A., Clayton, D., Starobova, H., Hamilton, B.R., Payne, R.J., Vetter, I., King, G.F., Undheim, E.A.B., 2018. A comprehensive portrait of the venom of the giant red bull ant, Myrmecia gulosa, reveals a hyperdiverse hymenopteran toxin gene family. Sci. Adv. 4, 1–13. https://doi.org/10.1126/sciadv.aau4640

Russ, D.E., Cross, R.B.P., Li, L., Koch, S.C., Matson, K.J.E., Yadav, A., Alkaslasi, M.R., Lee, D.I., Le Pichon, C.E., Menon, V., Levine, A.J., 2021. A harmonized atlas of mouse spinal cord cell types and their spatial organization. Nat. Commun. 12, 1–20.

https://doi.org/10.1038/s41467-021-25125-1

Saccò, M., Meschi, M., Regolisti, G., Detrenis, S., Bianchi, L., Bertorelli, M., Pioli, S., Magnano, A., Spagnoli, F., Giuri, P.G., Fiaccadori, E., Caiazza, A., 2013. The relationship between blood pressure and pain. J. Clin. Hypertens. 15, 600–605. https://doi.org/10.1111/jch.12145

Saeki, A., Yamanaka, H., Kobayashi, K., Okubo, M., 2022. Analgesic effect of gastrin-releasing peptide in the dorsal horn. Mol. Pain 18, 1–11. https://doi.org/10.1177/17448069221108965

Samineni, V.K., Yoon, J., Crawford, K.E., Jeong, Y.R., McKenzie, K.C., Shin, G., Xie, Z., Sundaram, S.S., Li, Y., Yang, M.Y., Kim, J., Wu, D., Xue, Y., Feng, X., Huang, Y., Mickle, A.D., Banks, A., Ha, J.S., Golden, J.P., Rogers, J.A., Gereau, R.W., 2017. Fully implantable, battery-free wireless optoelectronic devices for spinal optogenetics. Pain 158, 2108–2116. https://doi.org/10.1097/j.pain.0000000000000968

Sapunar, D., Vukojević, K., Kostić, S., Puljak, L., 2011. Attenuation of pain-related behavior evoked by injury through blockade of neuropeptide y Y2 receptor. Pain 152, 1173–1181. https://doi.org/10.1016/j.pain.2011.01.045

Sathyamurthy, A., Johnson, K.R., Matson, K.J.E., Dobrott, C.I., Li, L., Ryba, A.R., Bergman, T.B., Kelly, M.C., Kelley, M.W., Levine, A.J., 2018. Massively Parallel Single Nucleus Transcriptional Profiling Defines Spinal Cord Neurons and Their Activity during Behavior. Cell Rep. 22, 2094–2106. https://doi.org/10.1016/j.celrep.2018.02.003

Sayed, S., Van Dam, N.T., Horn, S.R., Kautz, M.M., Parides, M., Costi, S., Collins, K.A., Iacoviello, B., Iosifescu, D. V., Mathé, A.A., Southwick, S.M., Feder, A., Charney, D.S., Murrough, J.W., 2018. A Randomized Dose-Ranging Study of Neuropeptide y in Patients with Posttraumatic Stress Disorder. Int. J. Neuropsychopharmacol. 21, 3–11. https://doi.org/10.1093/ijnp/pyx109

Schoffnegger, D., Heinke, B., Sommer, C., Sandkühler, J., 2006. Physiological properties of spinal lamina II GABAergic neurons in mice following peripheral nerve injury. J. Physiol. 577, 869–878. https://doi.org/10.1113/jphysiol.2006.118034

Schoffnegger, D., Ruscheweyh, R., Sandkühler, J., 2008. Spread of excitation across modality borders in spinal dorsal horn of neuropathic rats. Pain 135, 300–310. https://doi.org/10.1016/j.pain.2007.12.016

Schuster, D.J., Metcalf, M.D., Kitto, K.F., Messing, R.O., Fairbanks, C.A., Wilcox, G.L., 2015. Ligand requirements for involvement of PKCε in synergistic analgesic interactions between spinal μ and δ opioid receptors. Br. J. Pharmacol. 172, 642–653. https://doi.org/10.1111/bph.12774

Selbie, L.A., Hill, S.J., 1998. G protein-coupled-receptor cross-talk: The fine-tuning of multiple receptor-signalling pathways. Trends Pharmacol. Sci. 19, 87–93. https://doi.org/10.1016/S0165-6147(97)01166-8

Sharma, S.K., Klee, W.A., Nirenberg, M., 1975. Dual regulation of adenylate cyclase accounts for narcotic dependence and tolerance. Proc. Natl. Acad. Sci. U. S. A. 72, 3092–3096. https://doi.org/10.1073/pnas.72.8.3092

Sherrington, C.S., 1906. The integrative action of the nervous system. Yale University Press.

Shi, T.J.S., Li, J., Dahlström, A., Theodorsson, E., Ceccatelli, S., Decosterd, I., Pedrazzini, T., Hökfelt, T., 2006. Deletion of the neuropeptide Y Y1 receptor affects pain sensitivity, neuropeptide transport and expression, and dorsal root ganglion neuron numbers. Neuroscience 140, 293–304. https://doi.org/10.1016/j.neuroscience.2006.02.009

Sieber, M.A., Storm, R., Martinez-de-la-Torre, M., Müller, T., Wende, H., Reuter, K., Vasyutina, E., Birchmeier, C., 2007. Lbx1 acts as a selector gene in the fate determination of somatosensory and viscerosensory relay neurons in the hindbrain. J. Neurosci. 27, 4902–4909. https://doi.org/10.1523/JNEUROSCI.0717-07.2007

Simon, P., Dupuis, R., Costentin, J., 1994. Thigmotaxis as an index of anxiety in mice. Influence of dopaminergic transmissions. Behav. Brain Res. 61, 59–64. https://doi.org/10.1016/0166-4328(94)90008-6

Sinha, G.P., Prasoon, P., Smith, B.N., Taylor, B.K., 2021. Fast A-type currents shape a rapidly adapting form of delayed short latency firing of excitatory superficial dorsal horn neurons that express the neuropeptide Y Y1 receptor. J. Physiol. 599, 2723–2750. https://doi.org/10.1113/JP281033

Sivilotti, L., Woolf, C.J., 1994. The contribution of GABAA and glycine receptors to central sensitization: disinhibition and touch-evoked allodynia in the spinal cord. J. Neurophysiol. 72, 169–179. https://doi.org/10.1152/jn.1994.72.1.169

Smith, K.M., Boyle, K.A., Madden, J.F., Dickinson, S.A., Jobling, P., Callister, R.J., Hughes, D.I., Graham, B.A., 2015. Functional heterogeneity of calretinin-expressing neurons in the mouse superficial dorsal horn: Implications for spinal pain processing. J. Physiol. 593, 4319–4339. https://doi.org/10.1113/JP270855

Smith, K.M., Boyle, K.A., Mustapa, M., Jobling, P., Callister, R.J., Hughes, D.I., Graham, B.A., 2016. Distinct forms of synaptic inhibition and neuromodulation regulate calretinin-positive neuron excitability in the spinal cord dorsal horn. Neuroscience 326, 10–21. https://doi.org/10.1016/j.neuroscience.2016.03.058

Smith, K.M., Browne, T.J., Davis, O.C., Coyle, A., Boyle, K.A., Watanabe, M., Dickinson, S.A., Iredale, J.A., Gradwell, M.A., Jobling, P., Callister, R.J., Dayas, C. V., Hughes, D.I., Graham, B.A., 2019a. Calretinin positive neurons form an excitatory amplifier network in the spinal cord dorsal horn. Elife 8, 673533. https://doi.org/10.7554/eLife.49190

Smith, K.M., Browne, T.J., Davis, O.C., Coyle, A., Boyle, K.A., Watanabe, M., Dickinson, S.A., Iredale, J.A., Gradwell, M.A., Jobling, P., Callister, R.J., Dayas, C. V., Hughes, D.I., Graham, B.A., 2019b. Calretinin positive neurons form an excitatory amplifier network in the spinal cord dorsal horn. Elife 8, 1–32. https://doi.org/10.7554/eLife.49190

Smith, P.A., 2014. BDNF: No gain without pain? Neuroscience 283, 107–123. https://doi.org/10.1016/j.neuroscience.2014.05.044

Smith, P.A., Moran, T.D., Abdulla, F., Tumber, K.K., Taylor, B.K., 2007. Spinal mechanisms of NPY analgesia. Peptides 28, 464–474. https://doi.org/10.1016/j.peptides.2006.09.029

Solinski, H.J., Kriegbaum, M.C., Tseng, P.Y., Earnest, T.W., Gu, X., Barik, A., Chesler, A.T., Hoon, M.A., 2019. Nppb Neurons Are Sensors of Mast Cell-Induced Itch. Cell Rep. 26, 3561-3573.e4. https://doi.org/10.1016/j.celrep.2019.02.089

Solway, B., Bose, S.C., Corder, G., Donahue, R.R., Taylor, B.K., 2011. Tonic inhibition of chronic pain by neuropeptide Y. Proc. Natl. Acad. Sci. U. S. A. 108, 7224–7229. https://doi.org/10.1073/pnas.1017719108

Song, A.J., Palmiter, R.D., 2018. Detecting and Avoiding Problems When Using the Cre–lox System. Trends Genet. 34, 333–340. https://doi.org/10.1016/j.tig.2017.12.008

Souza-Silva, E., Stein, T., Mascarin, L.Z., Dornelles, F.N., Bicca, M.A., Tonussi, C.R., 2020. Intra-articular injection of 2-pyridylethylamine produces spinal NPY-mediated antinociception in the formalin-induced rat knee-joint pain model. Brain Res. 1735, 146757. https://doi.org/10.1016/j.brainres.2020.146757

Steiner, I., Spivack, J.G., Jackson, A., Lavi, E., Fraser, N.W., 1989. Effects of lipofuscin on in situ hybridization in human neuronal tissue. J. Virol. Methods 24, 1–9. https://doi.org/10.1016/0166-0934(89)90002-5

Steinhoff, M., Schmelz, M., Szabó, I.L., Oaklander, A.L., 2018. Clinical presentation, management, and pathophysiology of neuropathic itch. Lancet Neurol. 17, 709–720. https://doi.org/10.1016/S1474-4422(18)30217-5

Stone, L.S., MacMillan, L.B., Kitto, K.F., Limbird, L.E., Wilcox, G.L., 1997. The α(2a) adrenergic receptor subtype mediates spinal analgesia evoked by α2 agonists and is necessary for spinal adrenergic-opioid synergy. J. Neurosci. 17, 7157–7165. https://doi.org/10.1523/jneurosci.17-18-07157.1997

Sun, L., Liu, R., Guo, F., Wen, M. qing, Ma, X. lin, Li, K. yuan, Sun, H., Xu, C. lin, Li, Y. yuan, Wu, M. yin, Zhu, Z. gang, Li, Xin jian, Yu, Y. qin, Chen, Z., Li, Xiang yao, Duan, S., 2020. Parabrachial nucleus circuit governs neuropathic pain-like behavior. Nat. Commun. 11. https://doi.org/10.1038/s41467-020-19767-w

Sun, S., Xu, Q., Guo, C., Guan, Y., Liu, Q., Dong, X., 2017. Leaky Gate Model: Intensity-Dependent Coding of Pain and Itch in the Spinal Cord. Neuron 93, 840-853.e5. https://doi.org/10.1016/j.neuron.2017.01.012

Sutters, K.A., Miaskowski, C., Taiwo, Y.O., Levine, J.D., 1990. Analgesic synergy and improved motor function produced by combinations of μ-δ- and μ-κ-opioids. Brain Res. 530, 290–294. https://doi.org/10.1016/0006-8993(90)91297-T

Szabo, N.E., Da Silva, R. V., Sotocinal, S.G., Zeilhofer, H.U., Mogil, J.S., Kania, A., 2015. Hoxb8 intersection defines a role for Lmx1b in excitatory dorsal horn neuron development, spinofugal connectivity, and nociception. J. Neurosci. 35, 5233–5246. https://doi.org/10.1523/JNEUROSCI.4690-14.2015

Taiwo, O.B., Taylor, B.K., 2002. Antihyperalgesic effects of intrathecal neuropeptide Y during inflammation are mediated by Y1 receptors. Pain 96, 353–363. https://doi.org/10.1016/S0304-3959(01)00481-X

Tallarida, R.J., 2016. Drug combinations: Tests and analysis with isoboles. Curr. Protoc. Pharmacol. 2016, 9.19.1-9.19.19. https://doi.org/10.1002/0471141755.ph0919s72

Tallarida, R.J., 2002. The interaction index: A measure of drug synergism. Pain 98, 163–168. https://doi.org/10.1016/S0304-3959(02)00041-6

Tallarida, R.J., 1992. Statistical analysis of drug combinations for synergism. Pain 49, 93–97. https://doi.org/10.1016/0304-3959(92)90193-F

Tallarida, R.J., Porreca, F., Cowan, A., 1989. Statistical analysis of drug-drug and site-site interactions with isobolograms. Life Sci. 45, 947–961. https://doi.org/10.1016/0024-3205(89)90148-3

Tan, C.M.J., Green, P., Tapoulal, N., Lewandowski, A.J., Leeson, P., Herring, N., 2018. The role of neuropeptide Y in cardiovascular health and disease. Front. Physiol. 9, 1–13. https://doi.org/10.3389/fphys.2018.01281

Taniguchi, H., He, M., Wu, P., Kim, S., Paik, R., Sugino, K., Kvitsani, D., Fu, Y., Lu, J., Lin, Y., Miyoshi, G., Shima, Y., Fishell, G., Nelson, S.B., Huang, Z.J., 2011. A Resource of Cre Driver Lines for Genetic Targeting of GABAergic Neurons in Cerebral Cortex. Neuron 71, 995–1013. https://doi.org/10.1016/j.neuron.2011.07.026

Tashima, R., Koga, K., Yoshikawa, Y., Sekine, M., Watanabe, M., Tozaki-Saitoh, H., Furue, H., Yasaka, T., Tsuda, M., 2021. A subset of spinal dorsal horn interneurons crucial for gating touch-evoked pain-like behavior. Proc. Natl. Acad. Sci. U. S. A. 118. https://doi.org/10.1073/pnas.2021220118

Tatemoto, K., Carlquist, M., Mutt, V., 1982. Neuropeptide Y—a novel brain peptide with structural similarities to peptide YY and pancreatic polypeptide. Nature 296, 659–660. https://doi.org/10.1038/296659a0

Taylor, B.K., 2009. Spinal inhibitory neurotransmission in neuropathic pain. Curr. Pain Headache Rep. 13, 208–214. https://doi.org/10.1007/s11916-009-0035-8

Taylor, B.K., Abhyankar, S.S., Vo, N.T.T., Kriedt, C.L., Churi, S.B., Urban, J.H., 2007. Neuropeptide Y acts at Y1 receptors in the rostral ventral medulla to inhibit neuropathic pain. Pain 131, 83–95. https://doi.org/10.1016/j.pain.2006.12.018

Taylor, B.K., Corder, G., 2014. Endogenous analgesia, dependence, and latent pain sensitization,

Current Topics in Behavioral Neurosciences. https://doi.org/10.1007/7854_2014_351

Taylor, Bradley K., Corder, G., 2014. Endogenous Analgesia, Dependence, and Latent Pain Sensitization. Curr. Top. Behav. Neurosci. 20, 283–325. https://doi.org/10.1007/7854

Taylor, B.K., Fu, W., Kuphal, K.E., Stiller, C.O., Winter, M.K., Chen, W., Corder, G.F., Urban, J.H., McCarson, K.E., Marvizon, J.C., 2014. Inflammation enhances Y1 receptor signaling, neuropeptide Y-mediated inhibition of hyperalgesia, and substance P release from primary afferent neurons. Neuroscience 256, 178–194. https://doi.org/10.1016/j.neuroscience.2013.10.054

Thapa, P., Euasobhon, P., 2018. Chronic postsurgical pain: Current evidence for prevention and management. Korean J. Pain 31, 155–173. https://doi.org/10.3344/kjp.2018.31.3.155

Todd, A.J., 2017. Identifying functional populations among the interneurons in laminae I-III of the spinal dorsal horn. Mol. Pain 13, 1–19. https://doi.org/10.1177/1744806917693003

Todd, A.J., 2010. Neuronal circuitry for pain processing in the dorsal horn. Nat. Rev. Neurosci. 11, 823–836. https://doi.org/10.1038/nrn2947

Todd, A.J., Hughes, D.I., Polgár, E., Nagy, G.G., Mackie, M., Ottersen, O.P., Maxwell, D.J., 2003. The expression of vesicular glutamate transporters VGLUT1 and VGLUT2 in neurochemically defined axonal populations in the rat spinal cord with emphasis on the dorsal horn. Eur. J. Neurosci. 17, 13–27. https://doi.org/10.1046/j.1460-9568.2003.02406.x

Todd, A.J., McGill, M.M., Shehab, S.A.S., 2000. Neurokinin 1 receptor expression by neurons in laminae I, III and IV of the rat spinal dorsal horn that project to the brainstem. Eur. J. Neurosci. 12, 689–700. https://doi.org/10.1046/j.1460-9568.2000.00950.x

Todd, A.J., Spike, R.C., Polgár, E., 1998. A quantitative study of neurons which express neurokinin-1 or somatostatin sst(2a) receptor in rat spinal dorsal horn. Neuroscience 85, 459–473. https://doi.org/10.1016/S0306-4522(97)00669-6

Torres, R., Croll, S.D., Vercollone, J., Reinhardt, J., Griffiths, J., Zabski, S., Anderson, K.D., Adams, N.C., Gowen, L., Sleeman, M.W., Valenzuela, D.M., Wiegand, S.J., Yancopoulos, G.D., Murphy, A.J., 2007. Mice genetically deficient in neuromedin U receptor 2, but not neuromedin U receptor 1, have impaired nociceptive responses. Pain 130, 267–278. https://doi.org/10.1016/j.pain.2007.01.036

Tracey, D.J., Romm, M.A., Yao, N.N.L., 1995. Peripheral hyperalgesia in experimental neuropathy: exacerbation by neuropeptide Y. Brain Res. 669, 245–254. https://doi.org/10.1016/0006-8993(94)01265-J

Tsubaki, T., Yokota, T., 1983. Heat-evoked Responses of Dorsal Horn Nociceptive Neurons in the Monkey. Jpn. J. Physiol. 33, 249–267. https://doi.org/10.2170/jjphysiol.33.249

Van Hecke, O., Austin, S.K., Khan, R.A., Smith, B.H., Torrance, N., 2014. Neuropathic pain in the general population: A systematic review of epidemiological studies. Pain 155, 654–662.

https://doi.org/10.1016/j.pain.2013.11.013

Vissers, K., Meert, T., 2005. A behavioral and pharmacological validation of the acetone spray test in gerbils with a chronic constriction injury. Anesth. Analg. 101, 457–464. https://doi.org/10.1213/01.ANE.0000158471.41575.F0

Vlasov, K., Van Dort, C.J., Solt, K., 2018. Optogenetics and Chemogenetics, 1st ed, Methods in Enzymology. Elsevier Inc. https://doi.org/10.1016/bs.mie.2018.01.022

von Hehn, C.A., Baron, R., Woolf, C.J., 2012. Deconstructing the Neuropathic Pain Phenotype to Reveal Neural Mechanisms. Neuron 73, 638–652. https://doi.org/10.1016/j.neuron.2012.02.008

Wakisaka, S., Kajander, K.C., Bennett, G.J., 1991. Increased neuropeptide Y (NPY)-like immunoreactivity in rat sensory neurons following peripheral axotomy. Neurosci. Lett. 124, 200–203. https://doi.org/10.1016/0304-3940(91)90093-9

Walwyn, W.M., Chen, W., Kim, H., Minasyan, A., Ennes, H.S., McRoberts, J.A., Marvizón, J.C.G., 2016. Sustained suppression of hyperalgesia during latent sensitization by μ-, δ-, and κ-opioid receptors and α2a adrenergic receptors: Role of constitutive activity. J. Neurosci. 36, 204–221. https://doi.org/10.1523/JNEUROSCI.1751-15.2016

Wang, D., Tawfik, V.L., Corder, G., Low, S.A., François, A., Basbaum, A.I., Scherrer, G., 2018. Functional Divergence of Delta and Mu Opioid Receptor Organization in CNS Pain Circuits. Neuron 98, 90-108.e5. https://doi.org/10.1016/j.neuron.2018.03.002

Wang, H., Chen, W., Dong, Z., Xing, G., Cui, W., Yao, L., Zou, W.-J., Robinson, H.L., Bian, Y., Liu, Z., Zhao, K., Luo, B., Gao, N., Zhang, H., Ren, X., Yu, Z., Meixiong, J., Xiong, W.-C., Mei, L., 2022. A novel spinal neuron connection for heat sensation. Neuron 1–19. https://doi.org/10.1016/j.neuron.2022.04.021

Wang, Q., Zhang, X., He, X., Du, S., Jiang, Z., Liu, P., Qi, L., Liang, C., Gu, N., Lu, Y., 2020. Synaptic Dynamics of the Feed-forward Inhibitory Circuitry Gating Mechanical Allodynia in Mice. Anesthesiology 132, 1212–1228. https://doi.org/10.1097/ALN.0000000000003194

Wang, W., Qiao, Y., Li, Z., 2018. New Insights into Modes of GPCR Activation. Trends Pharmacol. Sci. 39, 367–386. https://doi.org/10.1016/j.tips.2018.01.001

Wang, X., Zhang, J., Eberhart, D., Urban, R., Meda, K., Solorzano, C., Yamanaka, H., Rice, D., Basbaum, A.I., 2013. Excitatory superficial dorsal horn interneurons are functionally heterogeneous and required for the full behavioral expression of Pain and Itch. Neuron 78, 312–324. https://doi.org/10.1016/j.neuron.2013.03.001

Wang, Z., Jiang, C., Yao, H., Chen, O., Rahman, S., Gu, Y., Zhao, J., Huh, Y., Ji, R.R., 2021. Central opioid receptors mediate morphine-induced itch and chronic itch via disinhibition. Brain 144, 665–681. https://doi.org/10.1093/brain/awaa430

Watanabe, M., Dymecki, S.M., Chirila, A.M., Springel, M.W., Toliver, A.A., Zimmerman, A.L.,

Orefice, L.L., Bai, L., Song, B.J., Bashista, K.A., O'Neill, T.G., Zhuo, J., Tsan, C., Hoynoski, J., Ginty, D.D., 2017a. The Cellular and Synaptic Architecture of the Mechanosensory Dorsal Horn. Cell 168, 295-310.e19. https://doi.org/10.1016/j.cell.2016.12.010

Watanabe, M., Dymecki, S.M., Chirila, A.M., Springel, M.W., Toliver, A.A., Zimmerman, A.L., Orefice, L.L., Bai, L., Song, B.J., Bashista, K.A., O'Neill, T.G., Zhuo, J., Tsan, C., Hoynoski, J., Ginty, D.D., 2017b. The Cellular and Synaptic Architecture of the Mechanosensory Dorsal Horn. Cell 168, 295-310.e19. https://doi.org/10.1016/j.cell.2016.12.010

Watts, V.J., 2002. Molecular mechanisms for heterologous sensitization of adenylate cyclase. J. Pharmacol. Exp. Ther. 302, 1–7. https://doi.org/10.1124/jpet.302.1.1

West, S.J., Bannister, K., Dickenson, A.H., Bennett, D.L., 2015. Circuitry and plasticity of the dorsal horn - Toward a better understanding of neuropathic pain. Neuroscience 300, 254–275. https://doi.org/10.1016/j.neuroscience.2015.05.020

White, D.M., Mansfield, K., 1996. Vasoactive intestinal polypeptide and neuropeptide Y act indirectly to increase neurite outgrowth of dissociated dorsal root ganglion cells. Neuroscience 73, 881–887. https://doi.org/10.1016/0306-4522(96)00055-3

Wildner, H., Gupta, R. Das, Bröhl, D., Heppenstall, P.A., Zeilhofer, H.U., Birchmeier, C., 2013. Genome-wide expression analysis of Ptf1a- and Ascl1-deficient mice reveals new markers for distinct dorsal horn interneuron populations contributing to nociceptive reflex plasticity. J. Neurosci. 33, 7299–7307. https://doi.org/10.1523/JNEUROSCI.0491-13.2013

Wiley, R.G., Kline Iv, R.H., 2000. Neuronal lesioning with axonally transported toxins. J. Neurosci. Methods 103, 73–82. https://doi.org/10.1016/S0165-0270(00)00297-1

Wiley, R.G., Lemons, L.L., Kline IV, R.H., 2009. Neuropeptide Y receptor-expressing dorsal horn neurons: Role in nocifensive reflex responses to heat and formalin. Neuroscience 161, 139–147. https://doi.org/10.1016/j.neuroscience.2008.12.017

Winter, M.K., McCarson, K.E., 2005. G-protein activation by neurokinin-1 receptors is dynamically regulated during persistent nociception. J. Pharmacol. Exp. Ther. 315, 214–221. https://doi.org/10.1124/jpet.105.089565

Wolak, M.L., De Joseph, M.R., Cator, A.D., Mokashi, A.S., Brownfield, M.S., Urban, J.H., 2003. Comparative distribution of neuropeptide Y Y1 and Y5 receptors in the rat brain by using immunohistochemistry. J. Comp. Neurol. 464, 285–311. https://doi.org/10.1002/cne.10823

Woolf, C.J., 1983. Evidence for a central component of post-injury pain hypersensitivity. Nature 306, 686–688. https://doi.org/10.1038/306686a0

Woolf, C.J., Salter, M.W., 2000. Neuronal plasticity: Increasing the gain in pain. Science (80-.). 288, 1765–1768. https://doi.org/10.1126/science.288.5472.1765

Wrigley, P.J., Jeong, H.J., Vaughan, C.W., 2009. Primary afferents with TRPM8 and TRPA1 profiles target distinct subpopulations of rat superficial dorsal horn neurones. Br. J. Pharmacol. 157, 371–380. https://doi.org/10.1111/j.1476-5381.2009.00167.x

Xing, H., Chen, M., Ling, J., Tan, W., Gu, J.G., 2007. TRPM8 mechanism of cold allodynia after chronic nerve injury. J. Neurosci. 27, 13680–13690. https://doi.org/10.1523/JNEUROSCI.2203-07.2007

Xu, I.S., Hao, J.-X., Xu, X.-J., Hökfelt, T., Wiesenfeld-Hallin, Z., 1999. The effect of intrathecal selective agonists of Y1 and Y2 neuropeptide Y receptors on the flexor reflex in normal and axotomized rats. Brain Res. 833, 251–257. https://doi.org/10.1016/S0006-8993(99)01551-6

Xu, Y., Lopes, C., Qian, Y., Liu, Y., Cheng, L., Goulding, M., Turner, E.E., Lima, D., Ma, Q., 2008. Tlx1 and Tlx3 Coordinate Specification of Dorsal Horn Pain-Modulatory Peptidergic Neurons. J. Neurosci. 28, 4037–4046. https://doi.org/10.1523/JNEUROSCI.4126-07.2008

Xu, Z.Z., Kim, Y.H., Bang, S., Zhang, Y., Berta, T., Wang, F., Oh, S.B., Ji, R.R., 2015. Inhibition of mechanical allodynia in neuropathic pain by TLR5-mediated A-fiber blockade. Nat. Med. 21, 1326–1331. https://doi.org/10.1038/nm.3978

Yalamuri, S.M., Brennan, T.J., Spofford, C.M., 2013. Neuropeptide y is analgesic in rats after plantar incision. Eur. J. Pharmacol. 698, 206–212. https://doi.org/10.1016/j.ejphar.2012.10.036

Yao, L., Fan, P., Jiang, Z., Mailliard, W.S., Gordon, A.S., Diamond, I., 2003. Addicting drugs utilize a synergistic molecular mechanism in common requiring adenosine and Gi-βγ dimers. Proc. Natl. Acad. Sci. U. S. A. 100, 14379–14384. https://doi.org/10.1073/pnas.2336093100

Yao, L., McFarland, K., Fan, P., Jiang, Z., Ueda, T., Diamond, I., 2006. Adenosine A2a blockade prevents synergy between μ-opiate and cannabinoid CB1 receptors and eliminates heroin-seeking behavior in addicted rats. Proc. Natl. Acad. Sci. U. S. A. 103, 7877–7882. https://doi.org/10.1073/pnas.0602661103

Yasaka, T., Tiong, S.Y.X., Hughes, D.I., Riddell, J.S., Todd, A.J., 2010. Populations of inhibitory and excitatory interneurons in lamina II of the adult rat spinal dorsal horn revealed by a combined electrophysiological and anatomical approach. Pain 151, 475–488. https://doi.org/10.1016/j.pain.2010.08.008

Yu, X.H., Cao, C.Q., Mennicken, F., Puma, C., Dray, A., O'Donnell, D., Ahmad, S., Perkins, M., 2003. Pro-nociceptive effects of neuromedin U in rat. Neuroscience 120, 467–474. https://doi.org/10.1016/S0306-4522(03)00300-2

Yudin, Y., Rohacs, T., 2018. Inhibitory Gi/O-coupled receptors in somatosensory neurons: Potential therapeutic targets for novel analgesics. Mol. Pain 14. https://doi.org/10.1177/1744806918763646

Zeilhofer, H.U., Benke, D., Yevenes, G.E., 2012a. Chronic pain states: Pharmacological

strategies to restore diminished inhibitory Spinal pain control. Annu. Rev. Pharmacol. Toxicol. 52, 111–133. https://doi.org/10.1146/annurev-pharmtox-010611-134636

Zeilhofer, H.U., Wildner, H., Yévenes, G.E., 2012b. Fast synaptic inhibition in spinal sensory processing and pain control. Physiol. Rev. 92, 193–235. https://doi.org/10.1152/physrev.00043.2010

Zhang, H., Lecker, I., Collymore, C., Dokova, A., Pham, M.C., Rosen, S.F., Crawhall-Duk, H., Zain, M., Valencia, M., Filippini, H.F., Li, J., D'Souza, A.J., Cho, C., Michailidis, V., Whissell, P.D., Patel, I., Steenland, H.W., Virginia Lee, W.J., Moayedi, M., Sterley, T.L., Bains, J.S., Stratton, J.A., Matyas, J.R., Biernaskie, J., Dubins, D., Vukobradovic, I., Bezginov, A., Flenniken, A.M., Martin, L.J., Mogil, J.S., Bonin, R.P., 2021. Cage-lid hanging behavior as a translationally relevant measure of pain in mice. Pain 162, 1416–1425. https://doi.org/10.1097/j.pain.0000000000002127

Zhang, H., Li, Y., Yang, Q., Liu, X.-G., Dougherty, P.M., 2018. Morphological and Physiological Plasticity of Spinal Lamina II GABA Neurons Is Induced by Sciatic Nerve Chronic Constriction Injury in Mice. Front. Cell. Neurosci. 12, 1–8. https://doi.org/10.3389/fncel.2018.00143

Zhang, X., Bao, L., Shi, T.J., Ju, G., Elde, R., Hökfelt, T., 1997. Down-regulation of μ-opioid receptors in rat and monkey dorsal root ganglion neurons and spinal cord after peripheral axotomy. Neuroscience 82, 223–240. https://doi.org/10.1016/S0306-4522(97)00240-6

Zhang, X., Bao, L., Xu, Z.Q., Kopp, J., Arvidsson, U., Elde, R., Hökfelt, T., 1994. Localization of neuropeptide Y Y1 receptors in the rat nervous system with special reference to somatic receptors on small dorsal root ganglion neurons. Proc. Natl. Acad. Sci. U. S. A. 91, 11738–11742. https://doi.org/10.1073/pnas.91.24.11738

Zhang, X., Ji, R. -R, Nilsson, S., War, M., Ubink, R., Ju, G., Wiesenfeld-Hallin, Z., Hökfelt, T., 1995. Neuropeptide Y and Galanin Binding Sites in Rat and Monkev Lumbar Dorsal Root Ganalia and Spinal Cord and Effect of Peripheral Axotomy. Eur. J. Neurosci. 7, 367–380. https://doi.org/10.1111/j.1460-9568.1995.tb00332.x

Zhang, X., Tong, Y.G., Bao, L., Hokfelt, T., 1999. The neuropeptide Y Y1 receptor is a somatic receptor on dorsal root ganglion neurons and a postsynaptic receptor on somatostatin dorsal horn neurons. Eur. J. Neurosci. 11, 2211–2225. https://doi.org/10.1046/j.1460-9568.1999.00638.x

Zhang, X.Y., Dou, Y.N., Yuan, L., Li, Q., Zhu, Y.J., Wang, M., Sun, Y.G., 2020. Different neuronal populations mediate inflammatory pain analgesia by exogenous and endogenous opioids. Elife 9, 1–28. https://doi.org/10.7554/eLife.55289